Model Building and Phenomenology in Grand Unified Theories

Tomás E. Gonzalo Velasco

University College London

Submitted to University College London in fulfillment of
the requirements for the award of the degree of Doctor of Philosophy

August 2015

Declaration

I, Tomás E. Gonzalo Velasco,
confirm that the work presented in this thesis is my own.
Where information has been derived from other sources,
I confirm that this has been indicated in the thesis.

Tomás E. Gonzalo Velasco
August 2015

Abstract

The Standard Model (SM) of particle physics is known to suffer from several flaws, and the upcoming generation of experiments may shed some light onto their solution. Whether there is evidence of new physics or not, theories Beyond the SM (BSM) must be able to accommodate and explain the coming data. The lack of signs of BSM physics so far, calls for a exhaustive exploration beyond the minimal models, in particular Grand Unified theories, for they are able to solve some of the issues of the SM and can make testable predictions. Therefore, we attempt to develop a framework to build Grand Unified models, capable of generating and analysing general non-minimal models. In order to do so, first we create a computational tool to handle the group theoretical component, calculating properties of Lie Groups and their representations. Among them, those of interest to the model building process are the calculation of breaking chains from a group to a subgroup, the decomposition of representations of a group into those of a subgroup and the construction of group invariants. Using some of the capabilities of the group tool, and starting with a set of representations and a breaking chain, we generate all the conceivable models, classifying them to satisfy conditions such as anomaly cancellation and symmetry breaking. We then move on to study the unification of gauge couplings on the models and its consequences on the scale of unification and the scale of supersymmetry breaking, to later constrain them to match phenomenological observables, such as proton decay or current collider searches. We conclude by focusing the analysis on two specific models, a minimal supersymmetric $SO(10)$ model, with some interesting predictions for future colliders, and a flipped $SU(5) \otimes U(1)$ model, which serves as the triggering mechanism for the end of the inflationary epoch in the early universe.

Acknowledgements

First and foremost, I would like to thank my supervisor, Frank Deppisch, for his support during the very long journey that has been my Ph.D. His expert guidance and sound advice have proven essential for my research and the writing of this thesis. In addition, I would like to thank John Ellis who provided the means and opportunity, and whose vast knowledge helped me greatly along the way.

Also, I would like to express my gratitude to all my colleagues and friends at UCL, past and present, for the good times and fun these past years. My sincere gratitude to Lukáš Gráf, Julia Harz and Wei Chih Huang, with whom it was a pleasure to work. Without their help and contribution this thesis would not be finished.

I must also thank my family: my parents, Conchita and Tomás, and my sisters, Conchi and Ester, who have always inspired and supported me, even from the distance. Lastly, I would like to thank Ángela, for the unwavering support and infinite patience, and for giving me the necessary strength to see this through to the end.

The history of science shows
that theories are perishable.
With every new truth that is
revealed we get a better
understanding of Nature
and our conceptions
and views are modified.

- Nikola Tesla

Contents

List of Figures

List of Tables

1

Introduction

The Standard Model (SM) of particle physics, first proposed by Sheldon Glashow, Steven Weinberg and Abdus Salam in the late 1960's [1–3] is the most successful description of natural phenomena, for almost all of its theoretical predictions have been experimentally verified with an outstanding precision [4]. The last of the SM predictions to be confirmed was the existence of the Higgs boson, which was discovered in 2012 by the ATLAS and CMS collaborations at the LHC [5, 6], at a mass of $m_H = 125.7 \pm 0.4$ GeV [4].

In spite of its success, there are several experimental and theoretical problems that cannot be resolved in the SM. Such are, arguably among others, the electric charge quantization observed in nature, the tiny but finite masses of the neutrinos, the gauge hierarchy problem, the matter-antimatter asymmetry of the universe, or the identity of dark matter and dark energy. These issues indicate that the SM is not the ultimate theory of particle physics but rather an effective theory, very successful at low scales but incomplete and insufficient beyond. Therefore, at energy scales larger than the SM scale, $M_Z \sim 100$ GeV, one expects another theory to take control, a Beyond the Standard Model (BSM) theory that contains the SM and breaks down to it at a sufficiently low scale.

Grand Unified Theories (GUTs) are one such type of BSM theories, which postulate that the fundamental interactions described in the SM are different facets of a single force. In such a paradigm, the SM group of symmetries, $SU(3)_C \otimes SU(2)_L \otimes U(1)_Y$ is contained in a larger group $\mathcal{G}$, and the three independent gauge couplings of the SM, g_3, g_2 and g', merge into a single coupling g_{GUT} at some high scale M_{GUT}. This picture is motivated by the apparent convergence of the running of the gauge couplings in the SM, as can be seen in figure 1.1, which, despite being far from an accurate unification, hints to a larger organising structure.

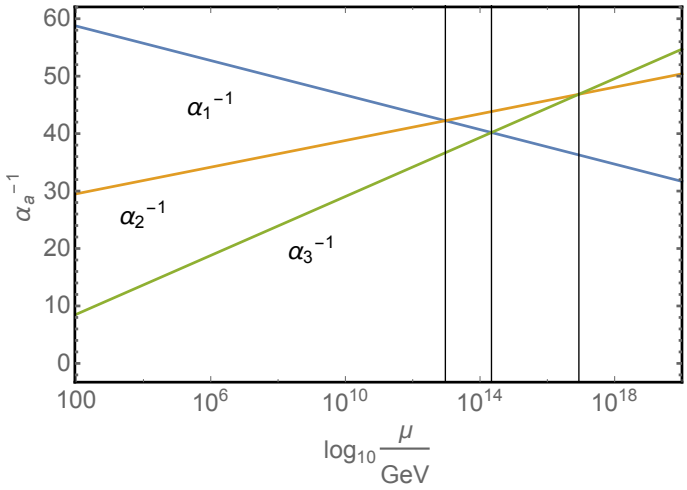

Figure 1.1: *Running of the Standard Model gauge couplings* $\alpha_a^{-1} = 4\pi/g_a^2$ *at one loop.*

Many of the issues of the SM can be solved within a grand unified framework. For instance, charge quantization of the electric charges, or hypercharges in the SM, can be easily explained by embedding the abelian group of hypercharge in a higher dimensional group [7]. Neutrino masses can also have an explanation in GUTs, as many of them include a right-handed neutrino within their particle spectrum, which can lead to very small neutrino masses via some type of see-saw mechanism [8]. Additionally, unified theories make specific predictions of their own beyond those of the SM, such as proton decay [9] and magnetic monopoles [10], which can be used to phenomenologically test GUT models.

A very popular realisation of GUTs include the addition of spacetime supersymmetry. The theory of supersymmetry (SUSY) [11] imposes a symmetric relation between fermions and bosons, which predicts that every particle in the SM has a supersymmetric partner, with a spin that differs from their SM counterpart by half a unit. The most common realisation of supersymmetry, the minimal supersymmetric extension of the SM (MSSM), assumes a mass for these supersymmetric particles of a few TeV, which allows a sufficient cancellation of the large loop contributions to the Higgs boson mass, thus solving the gauge hierarchy problem [12]. A major hint for the addition of SUSY to unified theories is the unification of gauge couplings, which is improved with respect to the approximated convergence of the SM in figure 1.1. The extended particle spectrum of the MSSM modifies the renormalisation group equations (RGEs) in such a way that all three gauge couplings may unify at a scale $M_{GUT} \sim 10^{16}$ GeV [13], even at one loop, as can be seen in figure 1.2.

At the time of writing, however, no evidence of supersymmetry has been found

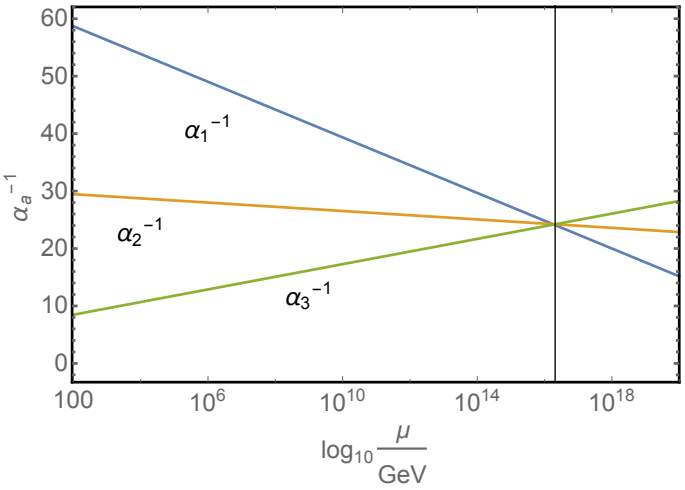

Figure 1.2: *Running of the MSSM gauge couplings* $\alpha_a^{-1} = 4\pi/g_a^2$*, and unification at* $M_{GUT} \sim 2 \times 10^{16}$ *GeV.*

at the TeV scale, which puts some of the most minimal models under tension (see for example [14, 15]). Non-minimal models may be challenged in the upcoming experiments, and this could lead to the exclusion of low energy supersymmetry.

Supersymmetric or not, GUTs are very powerful and one of the most likely candidates for BSM theories to be realised in nature. The main ingredients in the building of a GUT model are the choice of the unified gauge group, for example $SU(5)$ or $SO(10)$, the symmetry breaking chain from the GUT group to the SM group $SU(3)_C \otimes SU(2)_L \otimes U(1)_Y$ and a set of exotic fields present at various scales in the breaking chain. As a result, the range of possible unified models is enormous, thus most of the research on the topic to date has focused on minimal models, usually with a direct breaking of the unified group to the SM.

Given the fast rate at which experimental research in particle physics is advancing, minimal models might be proven insufficient shortly, for their predictions could be disproven in the current or next generation of experiments. More general GUT models thus need to be considered, which could have more degrees of freedom to match the prospected measurements or avoid the exclusion bounds. Therefore, it will be the subject of this thesis to develop a framework to consider and analyse general non-minimal GUT models. The structure of unified theories depends heavily on the mathematical properties of the unified group chosen, because the set of fields of the theory have to be embedded in representations of the group and the symmetry breaking chain goes through its collection of subgroups. Hence, starting with the theoretical description of the unified group, we will attempt to obtain GUT

models that can be constructed from such group, by scanning over all the possible combinations of fields at the several steps of the breaking chain. We will impose the unification of gauge couplings as a key assumption, while allowing the scale of unification to be determined dynamically, as well as other intermediate scales, including the scale of supersymmetry breaking. Lastly, we will classify the models obtained according to constraints, both of theoretical (e.g. anomaly cancellation) and phenomenological nature (e.g. proton decay).

In addition, two aspects of GUT theories are of particular interest recently, namely the impact of SUSY searches on GUT models [14, 15] and the hints for an inflationary scale of cosmology near the GUT scale [16, 17]. We will then provide a rough overview of the meaning of these topics and propose models that satisfy the latest limits on supersymmetric particle masses and cosmological observables, respectively [18, 19]. As opposed to the broad scanning mentioned above, these two aspects will be discussed within the framework of specific SUSY GUT models. They are intended to illustrate the phenomenological consequences when extending minimal models (such as the constrained minimal supersymmetric SM) with GUT ingredients. It will further elaborate our attempts to use currently important observables in order to gain an understanding of physics at very high energies.

The outline of the thesis will be as follows: we first start by reviewing the state of the art of gauge theories, in chapter 2, where we describe the SM, as the current successful gauge theory of particle physics; we will also introduce the most popular GUT theories studied to date, in a historical overview, and we will outline the main features of the theory of supersymmetry, including the MSSM as its phenomenological realisation. Chapter 3 is devoted to the mathematical description of Lie groups, the algorithms used to calculate their properties and their implementation in a computational tool. The physics application of the tool will be outlined in chapter 4, where we specify how the model building is performed and which constraints are imposed on the models, analysing one particular class of models, based on an $SO(10)$ unified group with an intermediate $SU(3)_C \otimes SU(2)_L \otimes SU(2)_R \otimes U(1)_{B-L}$ step in the breaking chain. In chapter 5 we will focus on a more detailed and phenomenological analysis of two specific models: namely a minimal supersymmetric $SO(10)$ model, with direct breaking to the SM group, and its predictions for the next run of the LHC; and a flipped $SU(5) \otimes U(1)$ model, which will be used to construct a hybrid inflationary scenario that will be compared with current cosmological observations. Lastly, in chapter 6, we will summarise the most interesting ideas of the thesis and suggest possible lines for their future development.

2

Gauge Models in Particle Physics

Gauge theories have played a crucial role in the conception and development of particle physics, for they have proven to be the most successful theoretical description of high energy phenomena [4]. They describe interactions among particles in the context of quantum field theory (QFT), mediated by vector fields known as gauge bosons, and they are built by imposing an internal and local group of symmetries, gauge symmetries, acting on the Lagrangian of the quantum theory [20].

The first complete gauge theory was formulated in the 1920s by Paul Dirac [21], known as Quantum Electrodynamics (QED). It was an abelian gauge theory, i.e. a Quantum Field Theory with a $U(1)$ symmetry. It describes free moving electrons and their interactions with photons, as gauge bosons or mediators of the electromagnetic force. The development of non-abelian gauge theories, by Chen Ning Yang and Robert Mills in 1954 [22], opened up the spectrum of theories to larger groups of symmetries, such as the unitary groups $SU(n)$. Unfortunately, this type of theory was dismissed shortly after their proposal, for they necessarily predict all of the particle fields to be massless, in disagreement with the measurements of the time. It was not until the 1960's when the model that we nowadays know as the Standard Model of particle physics was born [1–3], revamping the idea of non-abelian gauge theories but circumventing the mass problem through the mechanism of spontaneous symmetry breaking (SSB) [23–27].

As the first fully formulated gauge theory, QED is very useful as an example of how gauge symmetries enter the formalism of quantum field theories. Let $\mathcal{U}$ be an element of the $U(1)$ group of transformations, which infinitesimally near the identity can be expressed as $\mathcal{U} \approx \mathbb{1} + i\alpha$, with α a real continuous parameter. A fermionic field ψ transforms under this internal symmetry as $\delta\psi = i\alpha\psi$, and its conjugate as $\delta\bar{\psi} = -i\alpha\bar{\psi}$. If the parameter α is constant, then the $U(1)$ is a global symmetry

and the Lagrangian density of a massive free fermion,

$$\mathcal{L}_\psi = i\bar{\psi}\gamma^\mu\partial_\mu\psi - m\bar{\psi}\psi, \tag{2.0.1}$$

is invariant under the transformation. The Lagrangian is said to be globally $U(1)$ symmetric.

On the other hand, if α depends on the coordinates of spacetime, $\alpha = \alpha(x)$, $U(1)$ is a local or gauge symmetry, and the Lagrangian in equation (2.0.1) is not invariant under the symmetry, it transforms as $\delta\mathcal{L}_\psi = -\bar{\psi}\gamma^\mu\psi\partial_\mu\alpha$. In order to restore invariance to the Lagrangian one must introduce a gauge field A_μ, whose coupling to the fermion field and transformation under the symmetry are given by

$$\mathcal{L}_A = g\bar{\psi}\gamma^\mu\psi A_\mu, \qquad \delta A_\mu = \frac{1}{g}\partial_\mu\alpha, \tag{2.0.2}$$

with g being the gauge coupling. Defining a covariant derivative as $D_\mu = \partial_\mu - igA_\mu$, we can write $\mathcal{L}_\psi + \mathcal{L}_A$ as

$$\mathcal{L}_{QED} = i\bar{\psi}\gamma^\mu D_\mu\psi - m\bar{\psi}\psi, \tag{2.0.3}$$

which is the full gauge invariant Lagrangian of QED.

Since $U(1)$ is a continuous symmetry and $\mathcal{L}_{QED}$ is invariant under its action, Noether's theorem [28] states that there is a conserved current j^μ and a conserved charge Q, such that

$$\begin{aligned} j^\mu &= g\bar{\psi}\gamma^\mu\psi, & \partial_\mu j^\mu &= 0, \\ Q &= \int \mathrm{d}^3x j^0 = g\int \mathrm{d}^3x\psi^\dagger\psi, & \frac{\mathrm{d}Q}{\mathrm{d}t} &= 0, \end{aligned} \tag{2.0.4}$$

corresponding to the electromagnetic current j^μ_{em} and the total electric charge.

Throughout this section we will introduce more complicated gauge theories and describe their relevance and significance in particle physics. In section 2.1 we will describe the Standard Model (SM), the current successful theory of fundamental particle physics. Later, in section 2.2 we will discuss Grand Unified Theories (GUTs), which extend the SM internal symmetries, and, finally, in the last section, 2.3, we will describe supersymmetry (SUSY), as another extension of the SM, in this case with a larger group of spacetime symmetries.

2.1 The Standard Model

In the late 1960's, independent works by Sheldon Glashow [1], Steven Weinberg [2] and Abdus Salam [3], unified the existing theories for the electromagnetic inter-

action, Quantum Electrodynamics [21], and the weak interaction, the Fermi theory [29], into a theory with a single fundamental force, the electroweak theory. Their proposal, together with the later developed model for the strong force, the GIM model [30], form what is now known as the Standard Model of particle physics. Therefore, the SM describes the unified electroweak force and the strong force into a single formalism.

The Standard Model, as described by Glashow, Weinberg and Salam, proposes the symmetry group for the quantum interactions to be the Lie group $SU(3)_C \otimes SU(2)_L \otimes U(1)_Y$; where the first factor accounts for the strong (coloured) interactions and the remaining two for the electroweak interactions. Due to the measurement of parity violation in the weak sector by C. Wu and collaborators [31], we know that left-handed and right-handed components of fermions behave differently in processes involving electroweak interactions, where the former couple to the electroweak gauge bosons associated with both the $SU(2)_L$ and $U(1)_Y$ groups, whereas the latter only couple to the $U(1)_Y$ gauge bosons. This is theoretically realised by explicitly embedding left-handed and right-handed fermions in different representations of the electroweak symmetry, left-handed fields belonging to the doublet representation of $SU(2)_L$ and right-handed fields to the singlet representation. The fermionic content is, therefore, split into several representations of $SU(3)_C \otimes SU(2)_L \otimes U(1)_Y$, which are, for each generation ($i = 1, 2, 3$)[1],

$$
\begin{aligned}
&\{\mathbf{3}, \mathbf{2}, \tfrac{1}{6}\} \leftrightarrow \begin{pmatrix} u_1 & u_2 & u_3 \\ d_1 & d_2 & d_3 \end{pmatrix}^i \equiv Q^i, \qquad \{\mathbf{1}, \mathbf{2}, \text{-}\tfrac{1}{2}\} \leftrightarrow \begin{pmatrix} \nu_l \\ l \end{pmatrix}^i \equiv L^i, \\
&\{\overline{\mathbf{3}}, \mathbf{1}, \text{-}\tfrac{2}{3}\} \leftrightarrow \begin{pmatrix} u_1^c & u_2^c & u_3^c \end{pmatrix}^i \equiv (u^c)^i, \qquad \{\overline{\mathbf{3}}, \mathbf{1}, \tfrac{1}{3}\} \leftrightarrow \begin{pmatrix} d_1^c & d_2^c & d_3^c \end{pmatrix}^i \equiv (d^c)^i, \\
&\{\mathbf{1}, \mathbf{1}, 1\} \leftrightarrow (l^c)^i,
\end{aligned}
\tag{2.1.1}
$$

where the subindices $1, 2, 3$ represent the colour charges of the quarks, $\mathbf{3}$, $\overline{\mathbf{3}}$ and $\mathbf{1}$ are the fundamental triplet, conjugate triplet and singlet representations for $SU(3)_C$; $\mathbf{2}$ and $\mathbf{1}$ are the fundamental doublet and singlet representations of $SU(2)_L$, and the third number is the weak hypercharge Y of the representation, which is chosen so that the electric charge obeys $Q = T_3 + Y$, with T_3 the third component of the isospin generator of $SU(2)_L$.

The interactions among the Standard Model particles are mediated by vector bosons, associated with the symmetry group $SU(3)_C \otimes SU(2)_L \otimes U(1)_Y$. As was described above, in order to make a quantum field theory invariant under a local

[1]The quarks: $u^1 = u$, $u^2 = c$, $u^3 = t$; $d^1 = d$, $d^2 = s$, $d^3 = b$; and leptons: $l^1 = e$, $l^2 = \mu$, $l^3 = \tau$.

(gauge) symmetry, one needs to introduce vector fields that transform non-trivially under the symmetry. In the Standard Model these vector gauge bosons are: 8 gluons G^a_μ ($a = 1, \ldots, 8$) associated with the $SU(3)_C$ group, 3 weak gauge bosons W^i_μ ($i = 1, 2, 3$) associated with the $SU(2)_L$ group, and one hypercharge gauge boson B_μ, associated with $U(1)_Y$. The transformations of these vector fields under the gauge symmetries are

$$\begin{aligned} \delta G^a_\mu &= \frac{1}{g_3}\partial_\mu \gamma^a + i f^{abc}\gamma^b G^c_\mu \\ \delta W^i_\mu &= \frac{1}{g_2}\partial_\mu \omega^i + i\epsilon^{ijk}\omega^j W^k_\mu \\ \delta B_\mu &= \frac{1}{g'}\partial_\mu \beta \end{aligned} \tag{2.1.2}$$

where γ^a, ω^i and β are $SU(3)_C$, $SU(2)_L$ and $U(1)_Y$ transformations, respectively; g_3 and f^{abc} are the gauge coupling and structure constants of the $SU(3)_C$ group, g_2 and ϵ^{ijk} the gauge coupling and structure constants of $SU(2)_L$ and g' the gauge coupling of $U(1)_Y$.

All these fields in the Standard Model have to be massless in order to preserve the symmetry. A mass term for the fermions will be of the type $\overline{\psi}^i_L M_{ij}\psi^j_R$ will explicitly break the gauge symmetry since left and right-handed fermions have different $SU(2)_L$ and $U(1)_Y$ charges[2]. Similarly, a mass term for the gauge bosons of the type $A^a_\mu M_{ab} A^{\mu b}$ (with $A_\mu = G_\mu, W_\mu, B_\mu$) will violate the gauge symmetry, given the transformations in (2.1.2). This is inconsistent with experimental observations, for we have measured the masses of all SM fermions and some of the gauge bosons ($W^\pm$ and Z^0) with outstanding accuracy [4].

Therefore, at low energies the symmetries of the model must be spontaneously broken, through the so called Brout-Englert-Higgs (BEH) mechanism [25–27], to the remaining symmetry group $SU(3)_C \times U(1)_{\text{em}}$. Introducing a Higgs doublet, ϕ, in the Lagrangian, transforming under the $\{\mathbf{1}, \mathbf{2}, \frac{1}{2}\}$ representation of the SM gauge group and the scalar potential

$$V(\phi) = -\frac{1}{2}\,\mu^2\,\phi^\dagger\phi + \frac{\lambda}{4}\,(\phi^\dagger\phi)^2, \tag{2.1.3}$$

the ground state is not invariant under the SM symmetry, since ϕ acquires a non-zero vacuum expectation value, $\langle\phi\rangle = \mu/\sqrt{\lambda} = v/\sqrt{2} \simeq 174$ GeV. Thus, the Standard

[2]In the notation used in the representations, $\psi = \psi_L$ and $\psi^c = C\overline{\psi}^T_R$, the mass term would be $\psi^T C M \psi^c$, with $\psi = u$, d, l, or ν_l and C the charge conjugation matrix.

Model symmetry will be broken to a smaller symmetry, described by the group of strong and electromagnetic interactions, $SU(3)_C \otimes U(1)_{\rm em}$,

$$SU(3)_C \otimes SU(2)_L \otimes U(1)_Y \quad \rightarrow \quad SU(3)_C \otimes U(1)_{\rm em}. \tag{2.1.4}$$

One can then expand the scalar field around that vacuum expectation value (v.e.v.) as

$$\phi = \begin{pmatrix} \phi^+ \\ \frac{1}{\sqrt{2}}(v + h + i\sigma) \end{pmatrix}, \tag{2.1.5}$$

where h is the real Higgs field, and $\phi^\pm$ and σ are the massless Nambu-Goldstone bosons [23, 24], which will become the longitudinal components of the gauge bosons $W^\pm$ and Z. This can be seen as performing a $SU(2)$ transformation on ϕ so as to eliminate the degrees of freedom $\phi^+ = \sigma = 0$, which will reappear in the transformation of the gauge bosons. The Lagrangian of the Higgs sector before symmetry breaking is

$$\mathcal{L}_\phi = (D_\mu \phi)^\dagger \ (D^\mu \phi) + \frac{1}{2} \ \mu^2 \ \phi^\dagger \phi - \frac{1}{4!} \ \lambda \ (\phi^\dagger \phi)^2, \tag{2.1.6}$$

where $D_\mu \phi$ is the covariant derivative in the representation of ϕ given by

$$D_\mu \phi = \partial_\mu \phi - ig \frac{\tau^i}{2} W^i_\mu \phi - ig' Y B_\mu \phi. \tag{2.1.7}$$

Here g and g' are the gauge couplings of $SU(2)_L$ and $U(1)_Y$, respectively, τ^i are the generators of the $SU(2)_L$ group, proportional to the Pauli matrices, Y represents the hypercharge of ϕ and W^i_μ and B_μ are the vector bosons of $SU(2)_L$ and $U(1)_Y$, respectively. After symmetry breaking one can find mass terms in equation (2.1.6), of the form

$$\mathcal{L} \supset v^2 \ \frac{g^2}{8} W^1_\mu W^{1\mu} + v^2 \ \frac{g^2}{8} W^2_\mu W^{2\mu} + v^2 \ \frac{1}{8} (g W^3_\mu - g' B_\mu)(g W^{3\mu} - g' B^\mu).$$

Diagonalising these terms, the massive vector bosons obtained after symmetry breaking are

$$W^\pm_\mu = \frac{1}{\sqrt{2}} (W^1_\mu \mp i W^2_\mu), \qquad Z_\mu = \frac{1}{\sqrt{g^2 + g'^2}} (g W^3_\mu - g' B_\mu), \tag{2.1.8}$$

with non-vanishing masses at tree level,

$$M_W = g \ \frac{v}{2}, \qquad M_Z = \sqrt{g^2 + g'^2} \ \frac{v}{2}. \tag{2.1.9}$$

The remaining gauge boson is the orthogonal combination to Z_μ,

$$A_\mu = \frac{1}{\sqrt{g^2 + g'^2}} (g' W^3_\mu + g B_\mu), \tag{2.1.10}$$

which corresponds to the photon, gauge boson of $U(1)_{\text{em}}$, that will stay massless. The colour group $SU(3)_C$ is unaffected by the symmetry breaking and thus the gluons are also massless.

As previously mentioned, the SM symmetry does not allow fermionic mass terms of the form $\overline{\psi}_L M \psi_R$. However, similarly to the case of the gauge bosons, mass terms can be generated after electroweak symmetry breaking. The SM fermions may couple to the Higgs field as

$$\mathcal{L} \supset \overline{L}\mathbf{Y}_l l_R \phi + \overline{Q}\mathbf{Y}_d d_R \phi + \overline{Q}\mathbf{Y}_u u_R \phi^c + h.c., \tag{2.1.11}$$

where $\phi^c = i\tau_2 \phi^\dagger$ is the conjugate field of ϕ, with a hypercharge of $Y = -1/2$, and $\mathbf{Y}_i$ are the 3×3 Yukawa matrices in generation space. In the original formulation of the Standard Model, neutrinos are massless by definition, as a way to explain the absence of right handed neutrinos from the experiments.

After the Higgs fields acquires a non-vanishing vacuum expectation value v, the Yukawa couplings of equation (2.1.11) give rise to mass terms,

$$\mathcal{L} \supset \frac{v}{\sqrt{2}} \bar{l}_L \mathbf{Y}_l l_R + \frac{v}{\sqrt{2}} \bar{d}_L \mathbf{Y}_d d_R + \frac{v}{\sqrt{2}} \bar{u}_L \mathbf{Y}_u u_R + h.c., \tag{2.1.12}$$

which yield that $\mathbf{M}_{l,d,u} = \frac{v}{\sqrt{2}} \mathbf{Y}_{l,d,u}$ are the 3×3 mass matrices of the fermions.

The quark mass matrices $\mathbf{M}_d$ and $\mathbf{M}_d$ are not diagonal in generation space. Upon diagonalisation of the matrices, one obtains the mass eigenstates, which are the known flavours of quarks u, d, c, s, b and t. As was first discovered by Nicola Cabibbo [32] for two generations of quarks, and later extended by Makoto Kobayashi and Toshihide Maskawa [33] to include all three generations, these quark mass eigenstates q differ from the weak interaction eigenstates, q', by a rotation

$$\begin{aligned} q'_{u_L} &= V_{u_L}\ q_{u_L}, \quad q'_{d_L} = V_{d_L}\ q_{d_L}, \\ q'_{u_R} &= V_{u_R}\ q_{u_R}, \quad q'_{d_R} = V_{d_R}\ q_{d_R}, \end{aligned} \tag{2.1.13}$$

for up-type $q_{u_{L,R}} = (u_{L,R},\ c_{L,R},\ t_{L,R})$ and down-type $q_{d_{L,R}} = (d_{L,R},\ s_{L,R},\ b_{L,R})$ quarks, respectively. The CKM matrix V_{CKM}, defined as $V_{CKM} = V_{u_L}^\dagger V_{d_L}$ appears in the charged weak currents as

$$J_W^\mu = \bar{q}'_{u_L} \bar{\sigma}^\mu q'_{d_L} = \bar{q}_{u_L} \bar{\sigma}^\mu V_{CKM}\ q_{d_L}. \tag{2.1.14}$$

After eliminating five relative phases through a global $U(1)$ transformation, the CKM matrix has four free parameters left, three mixing angles and a CP-violating complex phase, which is consistent with the observation of CP-violating processes [34].

The SM is an incredibly successful theory, with some of its predictions being confirmed by experiment with astonishing accuracy. Since its inception in the late 60's and early 70's, the SM has successfully predicted the existence of several fundamental particles before their discovery, starting with the charm quark in the J/ψ resonance by both SLAC and BNL independently in 1974 [35, 36], the gluon by the PLUTO experiment at DESY in 1979 [37, 38], the W and Z bosons by the UA1 and UA2 experiments at CERN in 1983 [39–42], the top quark by CDF and D0 experiments at Tevatron in 1995 [43, 44] and most recently the Higgs boson by the ATLAS and CMS experiments at CERN [5, 6].

Despite the Standard Model's roaring success as a quantum theory of fields and particles, it has several shortcomings. Perhaps the most obvious of them is that it does not take into account gravitational interactions. Gravity cannot be described as a quantum field theory, the same way that the other interactions are, because it leads to an inconsistent theory, and as such it cannot make any testable predictions. Even disregarding gravity, there are still several issues with the Standard Model that need to be addressed:

The SM group and field content is very specific, chosen to match the experimental observations, but there is no hint to the origin of these structures. Furthermore, the hypercharge assignments in the Standard Model seem completely arbitrary, chosen to meet the observations[3]. A solution to this problem consists in embedding the SM into a GUT, which is the main topic of this work and which will be discussed extensively below, in sections 2.2, 4 and 5.

The SM seems to suffer from a **fine-tuning problem**. The so called hierarchy problem of the Standard Model [12, 45, 46] refers to an energy gap between the Standard Model scale (e.g. the measured Higgs mass, $m_H \sim 125$ GeV) and the only other known energy scale, the Planck scale, $M_P = 1.22 \times 10^{19}$ GeV. A more quantifiable version of this problem refers the strong dependence of the SM Higgs mass on the mass of any intermediate state appearing between the SM and the Plank scale. Both versions of this problem can be avoided by introducing spacetime supersymmetry, as explained in section 2.3.

There are a few problems related to recent **experimental observations**. First and foremost is the discovery of neutrino oscillations [47–49], which require the neutrinos to be massive, but very light ($\sum m_\nu < 0.23$ eV [50, 51]), contrary

[3]Though there is no theoretical motivation for the values of the hypercharges in the SM, some of them are not entirely arbitrary since they need to be such that cancel the gauge anomaly. See chapter 4 for a description of anomalies.

to their role in the Standard Model. Other measurements, such as the anomalous magnetic momentum, $g-2$, of the muon [52] or some flavour observables (e.g. $B \to \mu^+\mu^-$) [53], show slight or severe deviations from the Standard Model predictions. An extension of the SM is then required to reconcile the theoretical prediction for these observables with experiment, such as see-saw mechanisms to generate neutrino masses or additional exotic states that have loop contributions towards some flavour observables. Some of these topics are addressed within the context of GUTs or supersymmetry in sections 2.2 and 2.3.

Finally, there are some problems with the SM that are of **cosmological origin**. One such problem is that there is nothing in the Standard Model particle content that would take into account the observed presence of dark matter. Although the current experiments looking for dark matter signals have advanced significantly [54–59], at the time of writing no clear sign of its origin has been discovered, allowing for a very broad spectrum of interpretations. Whether dark matter is made of axions [60–63], sterile neutrinos [64], neutralinos [65, 66], or another type of exotic matter is still to be determined. Moreover, there are several other cosmological phenomena and measurements that are not explained by the SM, such as the baryon-antibaryon asymmetry [67], the cosmological constant problem [68, 69] and the horizon and flatness problem [70], the latter of which will be described in section 5.2.

Due to these issues the Standard Model cannot be the ultimate theory of particle physics. One needs to find extensions of the SM that address one or several of the items listed above. It is not, however, a trivial endeavour, for the predictions of the SM are surprisingly accurate, so any model or theory attempting to extend it must make sure that it contains the Standard Model as a subset and that it does not disturb its precise predictions.

2.2 Grand Unified Theories

The symmetries in the SM are realised by the Lie group $\mathcal{G}_{SM} = SU(3)_C \otimes SU(2)_L \otimes U(1)_Y$. The choice of group and representation content is done on the basis of experimental observation, but there is no underlying principle for that. As was mentioned before, these, seemingly arbitrary, choices may actually turn out to be not so random at all and thus hint to a larger theory that might have been spontaneously broken to the SM at some early stage of the evolution of the universe. This is the

case for GUTs which are extensions of the gauge symmetries of the SM that involve fewer, or no, arbitrary choices for groups and representations.

We therefore consider theories with a symmetry implemented by a Lie Group $\mathcal{G}$, that must contain the Standard Model group as a subgroup. $\mathcal{G}_{SM}$ is a semisimple Lie Group of rank 4 [4], hence $\mathcal{G}$ must have the same or higher rank. Furthermore, $\mathcal{G}$ should respect the chiral structure of the SM, where we have left-handed and right-handed particles that are in different representations of the group. For instance, left-handed up quarks and anti right-handed up quarks, that are both left-handed particles, are in a representation of the group, whereas the right-handed up quarks and the anti left-handed up quarks, that are both right-handed, are in the conjugate. Hence we will only be interested in GUTs with Lie groups that can admit this structure, i.e. that have complex representations.

The only rank 4 simple group that satisfies these conditions is the unitary group $SU(5)$. Other possible candidates are $SO(8)$, $SO(9)$, $Sp(8)$ or F_4, but none of these have complex representations. The $SU(5)$ unified group was introduced by H. Georgi and S. Glashow [7], and it is the first recognized attempt to construct a GUT. There are no other candidate groups of rank 4, simple or non-simple, since the only semisimple groups that contain $\mathcal{G}_{SM}$ and have complex representations are $SU(3) \otimes SU(3)$, $SU(3) \otimes SU(2) \otimes SU(2)$ and $SU(4) \otimes SU(2)$, but none of these reproduce the correct hypercharges for the SM fields [71].

Moving on to rank 5, other potential candidates arise. Most of them are not valid because they do not satisfy the condition of having complex representations, such as $SO(11)$ or $Sp(10)$. Other groups such as $SU(6)$ introduce exotic fields in the same representations as the SM fermions, which are difficult to decouple. Hence there is only one simple group candidate, $SO(10)$, which, despite being an orthogonal group, happens to have complex representations. $SO(10)$, first introduced by H. Fritzsch and P. Minkowski [71] and independently by H. Georgi [72], is a very appealing candidate because it unifies all SM fermions in the same representation of the group, including right-handed neutrinos. Further, there are a few non-simple candidates, $SU(5) \otimes U(1)$, as an extension of the $SU(5)$ model or in its "flipped" version [73–77], $SU(4) \otimes SU(2) \otimes SU(2)$, known as the Pati-Salam group [78], which embeds the leptons as a fourth colour, and $SU(3) \otimes SU(2) \otimes SU(2) \otimes U(1)$, known as the left-right symmetry group [79–82], which is actually a subgroup of the Pati-Salam group, and where right-handed fields couple to right-handed gauge bosons in a similar way that left-handed fields do in the SM. Interestingly, $SO(10)$ includes

[4] See chapter 3 for definitions of Lie groups and properties.

both $SU(5) \otimes U(1)$ and $SU(4)_C \otimes SU(2)_L \otimes SU(2)_R$ as maximal subgroups, and hence includes all the advantages of both cases.

Larger groups can also be considered as candidates for unification, though in general they can be seen as extensions of the models described above. For example, a rank 6 unified theory with E_6 as the gauge group [83,84], which contains $SO(10) \otimes U(1)$ as a maximal subgroup [85].

2.2.1 Georgi-Glashow Model: $SU(5)$

The unitary[5] $SU(5)$ unified group was first introduced in 1974 by H. Georgi and S. Glashow [7], and it is the first recognized attempt for a GUT. In this model, the left-handed fermions for each family are embedded into two representations of the group, $\overline{\mathbf{5}} \oplus \mathbf{10}$, in the following way[6]

$$\overline{\mathbf{5}} \leftrightarrow \begin{pmatrix} d_1^c \\ d_2^c \\ d_3^c \\ e \\ -\nu \end{pmatrix}_L , \quad \mathbf{10} \leftrightarrow \begin{pmatrix} 0 & u_3^c & -u_2^c & u_1 & d_1 \\ -u_3^c & 0 & u_1^c & u_2 & d_2 \\ u_2^c & -u_1^c & 0 & u_3 & d_3 \\ -u_1 & -u_2 & -u_3 & 0 & e^c \\ -d_1 & -d_2 & -d_3 & -e^c & 0 \end{pmatrix}_L , \tag{2.2.1}$$

where x^c is the charge conjugate of x with the same chirality (if x is a left-handed electron, x^c will be the anti right-handed electron, i.e. left-handed positron). Similarly, the right-handed sector is embedded in the conjugate representations, $\mathbf{5} \oplus \overline{\mathbf{10}}$. With this embedding, charge quantization is a straightforward consequence; keeping $SU(3)_C$ gauge invariance, the traceless charge generator is in general given by

$$Q = \mathrm{diag}(\alpha, \alpha, \alpha, \beta, -3\alpha - \beta). \tag{2.2.2}$$

With Q acting on the representations of (2.2.1), we obtain

$$\begin{aligned} &Q(d^c) = -\alpha, \quad Q(e) = -\beta, \qquad Q(\nu) = 3\alpha + \beta, \\ &Q(u^c) = \ 2\alpha, \quad Q(u) = \alpha + \beta, \quad Q(d) = -(2\alpha + \beta), \quad Q(e^c) = -3\alpha, \end{aligned} \tag{2.2.3}$$

and the charge assignment of the SM particles can be reproduced with $Q(\nu) = 0$ and $Q(e) = -1$.

[5] Unitary groups $U(N)$ are defined as the set of $N \times N$ unitary matrices $\mathcal{U}$, that satisfy $\mathcal{U}^\dagger \mathcal{U} = \mathbb{1}$, and have dimension N^2. Special unitary groups $SU(N)$ also satisfy $\det \mathcal{U} = 1$ and have dimension $N^2 - 1$.

[6] The lepton doublet is actually embedded as $\mathbf{2}^*$, the conjugate of $\mathbf{2}$, which in terms of the fields can be calculated as $\psi^* = i\sigma_2 \psi$, as shown in equation (2.2.1).

Anomaly[7] cancellation [86,87] in this model follows from similar arguments as the charge quantization [88]. Due to the particular $SU(3)_C$ embedding in $SU(5)$, the decomposition of the matter representations is

$$\begin{aligned}\bar{\mathbf{5}} &\to \{\bar{\mathbf{3}}, \mathbf{1}, \tfrac{1}{3}\} \oplus \{\mathbf{1}, \mathbf{2}^*, -\tfrac{1}{2}\},\\ \mathbf{10} &\to \{\mathbf{3}, \mathbf{2}, \tfrac{1}{6}\} \oplus \{\bar{\mathbf{3}}, \mathbf{1}, -\tfrac{2}{3}\} \oplus \{\mathbf{1}, \mathbf{1}, 1\}.\end{aligned} \tag{2.2.4}$$

Since $SU(2)$ is a safe algebra [89], the anomaly of each representation is driven by the anomaly of the $SU(3)$ subgroup:

$$\begin{aligned}A(\bar{\mathbf{5}}) &= A(\bar{\mathbf{3}}),\\ A(\mathbf{10}) &= 2A(\mathbf{3}) + A(\bar{\mathbf{3}}),\end{aligned} \tag{2.2.5}$$

which obviously makes the representation $\bar{\mathbf{5}} \oplus \mathbf{10}$ anomaly free, since the anomaly contribution of conjugate representations is opposite in sign.

The gauge bosons of the $SU(5)$ model are in the adjoint **24** representation, which decomposes into representations of $SU(3) \otimes SU(2) \otimes U(1)$ as

$$\mathbf{24} \to \{\mathbf{8}, \mathbf{1}, 0\} \oplus \{\mathbf{1}, \mathbf{3}, 0\} \oplus \{\mathbf{1}, \mathbf{1}, 0\} \oplus \{\mathbf{3}, \mathbf{2}, \tfrac{1}{6}\} \oplus \{\bar{\mathbf{3}}, \mathbf{2}, -\tfrac{1}{6}\}. \tag{2.2.6}$$

It naturally includes the gauge bosons of $SU(3)$, $\{\mathbf{8}, \mathbf{1}, 0\}$, those of $SU(2)$, $\{\mathbf{1}, \mathbf{3}, 0\}$ and of $U(1)$, $\{\mathbf{1}, \mathbf{1}, 0\}$, plus exotic coloured states.

The Higgs sector of the $SU(5)$ model must include a scalar field Σ that breaks $SU(5)$ to $\mathcal{G}_{SM}$ and another scalar (or two, in supersymmetric models) that triggers electroweak symmetry breaking. The field Σ must be in the adjoint representation of $SU(5)$, which is the **24**, since the breaking to the SM must preserve the rank[8]. The $SU(5)$ breaking Higgs Σ must acquire a vacuum expectation value in the direction

$$\langle \Sigma \rangle = v \ (2, 2, 2-3, -3), \tag{2.2.7}$$

[7] See chapter 4 for a description of anomalies.

[8] Higgs bosons living in the adjoint representation of a group do not reduce the rank of the group when they get a vacuum expectation value. This is because the vacuum expectation value (v.e.v.) still holds the symmetry induced by the Cartan subalgebra of the group. If T_{Cartan} are the generators of the Cartan subalgebra, a Higgs in the adjoint representation will transform as $\delta H = T^{ad}_{Cartan} H = [T_{Cartan}, H]$. The generators T_{Cartan} are diagonal by definition, and the v.e.v. $\langle H \rangle$ can be diagonalised by a transformation of the group, hence the commutator $[T_{Cartan}, \langle H \rangle]$ gives zero and we conclude that the vacuum conserves the Cartan subalgebra, i.e. the rank of the group. The converse is not necessarily true, i.e. if a Higgs boson preserves the rank, it does not need to be in the adjoint representation but the adjoint is always the one with the smallest dimension.

in order to break to $SU(3) \otimes SU(2) \otimes U(1)$ (instead of the other maximal subgroup $SU(4) \otimes U(1)$).

The second scalar field must contain the electroweak Higgs, which lies in the $\{\mathbf{1}, \mathbf{2}, \text{-}\frac{1}{2}\}$ representation of $\mathcal{G}_{SM}$. The simplest choice would be the $\mathbf{5}$ representation, so that it decomposes under $\mathcal{G}_{SM}$ as

$$\mathbf{5} \to \{\mathbf{3}, \mathbf{1}, \text{-}\tfrac{1}{3}\} \oplus \{\mathbf{1}, \mathbf{2}, \ \tfrac{1}{2}\}. \tag{2.2.8}$$

In some cases two Higgs fields are needed for electroweak symmetry breaking (EWSB), one of them will be on the $\mathbf{5}$ and the other on the $\bar{\mathbf{5}}$, e.g. the MSSM[9] or the 2 Higgs Doublet Model (2HDM) [90].

The $SU(5)$ model is very appealing and solves some of the problems and shortcomings of the SM, however it also produces a few of its own:

1. The $SU(5)$ model requires precise gauge coupling unification, at some high scale M_{GUT}. Let g_3 be the gauge coupling of the $SU(3)_C$ group, g_2 of $SU(2)_L$ and g_1 of $U(1)_Y$ (c.f. $g_2 = g$ and $g_1 = \sqrt{\frac{5}{3}}g'$, in section 2.1), and $\alpha_i = g_i^2/4\pi$, then
$$\alpha_{GUT} = \alpha_3(M_{GUT}) = \alpha_2(M_{GUT}) = \alpha_1(M_{GUT}). \tag{2.2.9}$$
Unfortunately, this unification does not happen exactly in the SM, where the running of the couplings at one loop[10] can be seen in figure 1.1. A common solution to this involves adding exotic matter at some intermediate scale to change the running, as happens, for example, in the supersymmetric version of the $SU(5)$ GUT [92], whose couplings can be seen to unify rather accurately in figure 1.2.

2. Because of its Higgs structure, it requires a so-called doublet-triplet splitting, which accounts for the fact that in order to get a light Higgs doublet ($m_H \sim$ 125 GeV) compared to the heavy triplet ($m_T \sim M_{GUT}$ in order to suppress proton decay), one needs a fine tuning of one part in $\mathcal{O}(M_{GUT}^2/M_Z^2) \sim 10^{26}$, in the simplest case. There are known solutions to this problem [93–97], which usually involve adding extra fields to the model or extra symmetries.

3. Similarly to gauge coupling unification, the $SU(5)$ model also requires Yukawa coupling unification. From a top to bottom approach, this condition imposes

[9] See section 2.3.3.

[10] Unification in the SM does not happen at any loop order or including threshold corrections [91].

a relation between the masses of the fermions at the GUT scale, $m_b(M_{GUT}) = m_\tau(M_{GUT})$, $m_s(M_{GUT}) = m_\mu(M_{GUT})$ and $m_d(M_{GUT}) = m_e(M_{GUT})$. Though the first relation can be realised in the MSSM with an uncertainty of $20-30\%$ [98], the last two conditions are off by almost one order of magnitude [99]. Known ways to solve this issue rely on adding other Higgs representations and/or non-renormalisable operators to the model to expand the parameter space allowing for more freedom to fit the fermion masses [100, 101].

4. There are several ways to generate neutrino masses in the $SU(5)$ model, both in the supersymmetric and non-supersymmetric version. Most often one needs to add extra representations to generate a see-saw mechanism, typically a **15** or a **24** representation [102,103]. Additionally, in supersymmetric models, one could have R-parity and lepton number violating interactions that generate neutrino masses [104].

5. Lastly, a general problem of GUTs, not just of $SU(5)$, is that they usually predict rapid proton decay. GUT models usually have either gauge or scalar bosons charged under the strong and electroweak forces simultaneously, and thus trigger the decay $p \to \pi e$. The decay width of this process can be estimated as
$$\Gamma(p \to \pi e) \sim \frac{\alpha_{GUT}^2 \, m_p^5}{M_X^4}, \tag{2.2.10}$$
where X is the mediator boson of the decay. Current experiments set the lower limit on the half life of the proton to 1.29×10^{34} years [105]. This is quite constraining on GUTs, for this means that the GUT scale must be generally higher than $M_{GUT} \sim 10^{16}$ GeV.

For the $SU(5)$ model all these issues mean that it is excluded in its non-supersymmetric form, since there is not real unification and coloured states appear at scales lower than the experimental limit [106–108], thus producing rapid proton decay. The supersymmetric $SU(5)$ model, however, does not suffer from these afflictions [109–114].

2.2.2 Flipped $SU(5) \otimes U(1)$

There are two ways to realise the $SU(5) \otimes U(1)$ model. The first is a trivial extension of the Georgi-Glashow $SU(5)$ model of section 2.2.1, by assigning $U(1)$ charges to its $SU(5)$ fields, subject only to the condition of traceless generators. The second,

more interesting option, is the flipped $SU(5) \otimes U(1)$ model [73–77], also denoted as $SU(5)' \otimes U(1)$, where $SU(5)'$ does not contain the Standard Model as a subgroup, unlike the usual $SU(5)$ case.

The key feature of the flipped $SU(5) \otimes U(1)$ is that the hypercharge of the Standard Model comes from a linear combination of a diagonal generator of $SU(5)$ and the generator of $U(1)$. If T_{24} is the generator of the abelian subgroup of $SU(5)$ ($T_{24} \propto \mathrm{diag}(2,2,2,-3,-3)$) and X is the generator of the external $U(1)$, then

$$Y = aT_{24} + bX, \tag{2.2.11}$$

which turns out to have two solutions to generate the SM hypercharges. The first is $a = 1$, $b = 0$, which corresponds to the trivial extension of $SU(5)$, and the second turns out to be $a = -1/5$, $b = 1/5$, which is the flipped $SU(5) \otimes U(1)$. The first consequence of this flipped version is a different embedding of the SM fermions in the group representations,

$$\overline{\mathbf{5}}_{-3} \leftrightarrow \begin{pmatrix} u_1^c \\ u_2^c \\ u_3^c \\ e \\ -\nu \end{pmatrix}_L , \quad \mathbf{10}_1 \leftrightarrow \begin{pmatrix} 0 & d_3^c & -d_2^c & u_1 & d_1 \\ -d_3^c & 0 & d_1^c & u_2 & d_2 \\ d_2^c & -d_1^c & 0 & u_3 & d_3 \\ -u_1 & -u_2 & -u_3 & 0 & \nu^c \\ -d_1 & -d_2 & -d_3 & -\nu^c & 0 \end{pmatrix}_L , \quad \mathbf{1}_5 \leftrightarrow (e^c)_L. \tag{2.2.12}$$

where $\mathbf{n}_\alpha$ represents the n-dimensional representation of $SU(5)$ with α the external $U(1)$ charge. It can be noticed that the embedding of the up-type right-handed quarks u^c has been swapped with that of the down-type right-handed quarks d^c, and the right-handed neutrino ν^c with the right-handed charge lepton e^c.

Symmetry breaking in this case, $SU(5) \otimes U(1) \to SU(3) \otimes SU(2) \otimes U(1)$, reduces the rank of the group, and thus it does not happen through the **24** representation as before, but rather through the $\mathbf{10}_1$ representation of scalar fields. This can easily be seen from (2.2.12) where the $\mathbf{10}_1$ representation includes the right-handed neutrino, which is a SM singlet, and thus if the same component of a Higgs field in that representation acquires a v.e.v., the symmetry would be broken to the SM. In its supersymmetric version [76, 77], it also requires the representation $\overline{\mathbf{10}}_{-1}$ to avoid gauge and gravitational anomalies.

Other properties of the flipped $SU(5) \otimes U(1)$ model mimic those of the standard $SU(5)$ model. The gauge bosons fall into the same $\mathbf{24}_0$ representations, as in equation (2.2.6), with trivial abelian charge. Similarly, the electroweak Higgs boson

is in the $\mathbf{5}_{-2}$ representation (and the $\bar{\mathbf{5}}_2$ in the supersymmetric case). Gauge coupling unification, however, occurs rather differently because at the GUT scale only α_2 and α_3 unify,

$$\alpha_2(M_{GUT}) = \alpha_3(M_{GUT}) = \alpha_5(M_{GUT}), \tag{2.2.13}$$

whereas α_1 is obtained as a combination of α_5 and the gauge coupling of the external abelian part α_X,

$$\alpha_1^{-1}(M_{GUT}) = 25(\alpha_5^{-1}(M_{GUT}) + \alpha_X^{-1}(M_{GUT})). \tag{2.2.14}$$

This allows more freedom in the unification scenario since the value of α_X at M_{GUT} is unconstrained. Given this fact, both the partial and total unification in figures 1.1 and 1.2 are allowed for this model, since the only requirement at this stage is the unification of α_2 and α_3, which happens in both models for $M_{GUT} > 10^{16}$, thereby potentially evading the experimental proton decay limit.

Furthermore, the supersymmetric version of this model does not suffer from double-triplet splitting [115]. The couplings $\mathbf{10}_1\mathbf{10}_1\mathbf{5}_{-2}$ and $\overline{\mathbf{10}}_{-1}\overline{\mathbf{10}}_{-1}\bar{\mathbf{5}}_2$ of Higgs fields do not induce bilinear couplings of the electroweak Higgs, but it does so for the coloured triplets. It is then enough to assume that the coupling $\mathbf{5}_{-2}\bar{\mathbf{5}}_2$ has a coupling of the order of the electroweak scale, to satisfy the splitting. This assumption can also be realised by the vacuum expectation value of a singlet field $\mathbf{1}_0$, with a coupling $\mathbf{5}_{-2}\bar{\mathbf{5}}_2\mathbf{1}_0$.

Regarding neutrino masses, the flipped $SU(5) \otimes U(1)$ model does also much better than its standard counterpart. Adding three sterile neutrinos $\mathbf{1}_0^j$, the couplings with the tenplet of SM fermions $\mathbf{10}_F$ and the conjugate tenplet of symmetry breaking higgses $\overline{\mathbf{10}}_H$, are

$$\lambda_j \mathbf{10}_F \overline{\mathbf{10}}_H \mathbf{1}_0^j \tag{2.2.15}$$

These couplings give large Dirac-type masses to the right-handed neutrinos, of the order of the GUT breaking v.e.v., which via a double see-saw mechanism produces light neutrino masses [77].

Lastly, it is worth mentioning that the flipped $SU(5) \otimes U(1)$ model has properties very attractive for superstring theory, because it does not require adjoint or larger representations of the groups, so it can be obtained from a weakly-coupled fermionic formulation of string theory [116–119].

2.2.3 Pati-Salam Model

The Pati-Salam (PS) model [78], with group $SU(4)_C \otimes SU(2)_L \otimes SU(2)_R$, is, together with the Georgi-Glashow model, among the first attempts to build extensions of the Standard Model through gauge symmetries. Though not really a GUT, it does go halfway towards unification by extending the colour group to $SU(4)_C$, thereby considering leptons as a "fourth colour". Thus, the quark doublet and the lepton doublet of each generation are embedded into the same representation as

$$\{\mathbf{4}, \mathbf{2}, \mathbf{1}\} \leftrightarrow \begin{pmatrix} u_1 & u_2 & u_3 & \nu \\ d_1 & d_2 & d_3 & e \end{pmatrix}. \tag{2.2.16}$$

where $\mathbf{4}$ is a representation of $SU(4)_C$, $\mathbf{2}$ of $SU(2)_L$ and $\mathbf{1}$ of $SU(2)_R$.

Moreover, the PS group includes another copy of $SU(2)_R$ acting on the right-handed sector, analogous to the $SU(2)_L$[11]. Due to the presence of the $SU(2)_R$ factor, the PS model includes automatically a right-handed neutrino ν^c which, together with the right-handed charged lepton, forms a $SU(2)_R$ doublet. The right-handed up-type and down-type quarks also become a doublet under $SU(2)_R$, and under PS are embedded as

$$\{\overline{\mathbf{4}}, \mathbf{1}, \mathbf{2}^*\} \leftrightarrow \begin{pmatrix} d_1^c & d_2^c & d_3^c & e^c \\ -u_1^c & -u_2^c & -u_3^c & -\nu^c \end{pmatrix}. \tag{2.2.17}$$

The gauge sector of the Pati-Salam model will contain the adjoint representations of $SU(4)_C$, $SU(2)_L$ and $SU(2)_R$, which are $\{\mathbf{15}, \mathbf{1}, \mathbf{1}\}$, $\{\mathbf{1}, \mathbf{3}, \mathbf{1}\}$ and $\{\mathbf{1}, \mathbf{1}, \mathbf{3}\}$, respectively, and will decompose into the SM gauge bosons as

$$\begin{aligned} \{\mathbf{15}, \mathbf{1}, \mathbf{1}\} &\to \{\mathbf{8}, \mathbf{1}, 0\} \oplus \{\mathbf{1}, \mathbf{1}, 0\} \oplus \{\mathbf{3}, \mathbf{1}, \tfrac{1}{3}\} \oplus \{\overline{\mathbf{3}}, \mathbf{1}, \text{-}\tfrac{1}{3}\}, \\ \{\mathbf{1}, \mathbf{3}, \mathbf{1}\} &\to \{\mathbf{1}, \mathbf{3}, 0\}, \\ \{\mathbf{1}, \mathbf{1}, \mathbf{3}\} &\to \{\mathbf{1}, \mathbf{1}, 1\} \oplus \{\mathbf{1}, \mathbf{1}, 0\} \oplus \{\mathbf{1}, \mathbf{1}, \text{-}1\}, \end{aligned} \tag{2.2.18}$$

where the gauge bosons of $SU(3)_C$ and $SU(2)_L$ can be seen, and the gauge boson of $U(1)_Y$ will be a linear combination of the $\{\mathbf{1}, \mathbf{1}, 0\}$ in the first and third rows.

The Higgs sector of the PS model strongly depends on how the breaking of the $SU(4)_C \otimes SU(2)_L \otimes SU(2)_R$ group happens. There are several breaking patterns, depending on the intermediate steps involved.

As can be seen in figure 2.1, the options are [120]

[11] Typically an extra discrete Z_2 symmetry (also called D-parity) is introduced as part of the group, which makes the model symmetric under the exchange $SU(2)_L \leftrightarrow SU(2)_R$.

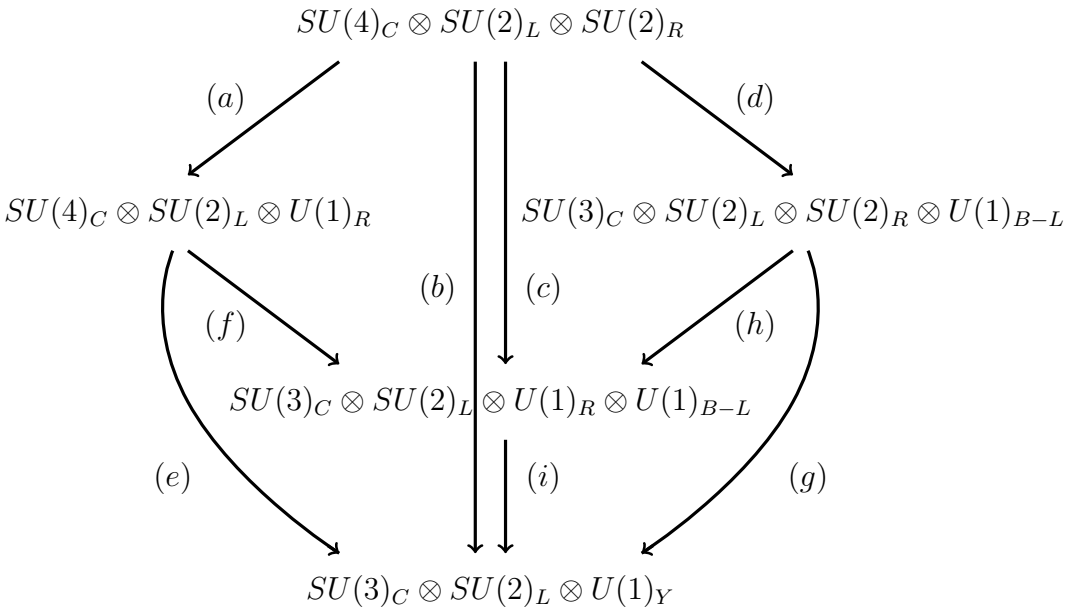

Figure 2.1: *Breaking patterns of the Pati-Salam model*

1. The "fourth colour" preserving path (a) can be triggered by a Higgs in the representation $\{\mathbf{1}, \mathbf{1}, \mathbf{3}\}$ of the PS group. Only the $SU(2)_R$ group will break and will leave the coloured and left-handed sector untouched. Further breaking to $\mathcal{G}_{SM}$ will happen through the path (e) or (f) followed by (i). The representations to satisfy this breaking are $\{\overline{\mathbf{10}}, \mathbf{1}, \alpha\}$ $(\alpha \neq 0)$ of $SU(4)_C \otimes SU(2)_L \otimes U(1)_R$, for the first case, and $\{\mathbf{15}, \mathbf{1}, 0\}$ followed by $\{\mathbf{1}, \mathbf{1}, \beta, \gamma\}$ (with at least one of $\beta, \gamma \neq 0$) of $SU(3)_C \otimes SU(2)_L \otimes U(1)_R \otimes U(1)_{B-L}$, for the second.

2. The simplest case is the direct breaking from the PS group to the SM group, path (b). To trigger this breaking, one would need a scalar field in, for example, the representation $\{\overline{\mathbf{10}}, \mathbf{1}, \mathbf{3}\}$ of the Pati-Salam group, for it has a $SU(3) \otimes SU(2) \otimes U(1)$ flat direction, but transforms non-trivially under any of the possible intermediate subgroups.

3. A similar breaking to the previous case is the path (c), where also both the "fourth colour" structure and the left-right symmetry are broken, but in this case there is no loss of rank. Thus the representation that breaks the symmetry is the $\{\mathbf{15}, \mathbf{1}, \mathbf{3}\}$ of the PS group, followed by $\{\mathbf{1}, \mathbf{1}, \beta, \gamma\}$ of $SU(3)_C \otimes SU(2)_L \otimes U(1)_R \otimes U(1)_{B-L}$ for path (i) (β and/or $\gamma \neq 0$), as before.

4. Lastly, the path (d) preserves the left-right symmetric structure. Symmetry breaking from the Pati-Salam group to this subgroup happens through a rep-

resentation $\{\mathbf{15},\mathbf{1},\mathbf{1}\}$ of PS. In order to break to the SM group, one then needs to give a v.e.v. to the $\{\mathbf{1},\mathbf{1},\mathbf{3},\alpha\}$ representation of $SU(3)_C \otimes SU(2)_L \otimes SU(2)_R \otimes U(1)_{B-L}$, where the breaking happens through path (h) if $\alpha = 0$ or through path (g) otherwise. Same as before, breaking through path (i) happens with $\{\mathbf{1},\mathbf{1},\beta,\gamma\}$ $(\beta,\gamma \neq 0)$ of $SU(3)_C \otimes SU(2)_L \otimes U(1)_R \otimes U(1)_{B-L}$.

Additionally to the Higgs fields mentioned before, required to satisfy the particular breaking paths, one needs the electroweak Higgs field. There are a few ways to embed the SM Higgs doublet into the Pati-Salam group, two candidate representations used are $\{\mathbf{1},\mathbf{2},\mathbf{2}\}$ and $\{\mathbf{15},\mathbf{2},\mathbf{2}\}$. Furthermore, these representations will potentially provide a second Higgs doublet, as it is needed in supersymmetric models and 2HDMs. At the Standard Model scale, these representations decompose as

$$\begin{aligned}
\{\mathbf{1},\mathbf{2},\mathbf{2}\} \;&\rightarrow\; \{\mathbf{1},\mathbf{2},\tfrac{1}{2}\} \oplus \{\mathbf{1},\mathbf{2},\text{-}\tfrac{1}{2}\},\\
\{\mathbf{15},\mathbf{2},\mathbf{2}\} \rightarrow\; &\{\mathbf{8},\mathbf{2},\tfrac{1}{2}\} \oplus \{\mathbf{8},\mathbf{2},\text{-}\tfrac{1}{2}\} \oplus \{\mathbf{3},\mathbf{2},\tfrac{7}{6}\} \oplus \{\mathbf{3},\mathbf{2},\tfrac{1}{6}\}\\
&\oplus \{\bar{\mathbf{3}},\mathbf{2},\text{-}\tfrac{1}{6}\} \oplus \{\bar{\mathbf{3}},\mathbf{2},\text{-}\tfrac{7}{6}\} \oplus \{\mathbf{1},\mathbf{2},\tfrac{1}{2}\} \oplus \{\mathbf{1},\mathbf{2},\text{-}\tfrac{1}{2}\}.
\end{aligned} \tag{2.2.19}$$

Regardless of the symmetry breaking path, the hypercharge of the Standard Model is derived from the breaking of the PS group to $\mathcal{G}_{SM}$, which provides an explanation for the charge quantization in the Standard Model. In general it will be a linear combination of the $B-L$ generator, embedded in $SU(4)$ in PS, and the right-handed diagonal generator T_R^3. With the usual normalisation for $B-L$ and $SU(2)_R$ charges [88], we get

$$Y = T_R^3 + \frac{1}{2}(B-L). \tag{2.2.20}$$

Since the Pati-Salam model include automatically a right-handed neutrino, it is possible to provide the neutrinos with small masses, as found in experiments [50]. In the Standard Model, as an effective field theory, one would expect to generate those masses through a dimension 5 operator [121] of the type

$$\frac{1}{\Lambda_\nu} C(L^T\phi)(\phi^T L), \tag{2.2.21}$$

where ϕ and L are the Higgs and lepton fields, C is the charge conjugation matrix and Λ_ν is the $B-L$ breaking scale. This effective operator can be obtained as the result of integrating out a heavy field from a renormalisable operator at the scale Λ_ν. If that heavy field is a right handed neutrino, ν^c, this procedure is known as type-I see-saw mechanism [8,122,123], or if it comes from exotic triplet fields, scalar or fermionic, we have type-II [124–126] and type-III [127], respectively.

An interesting consequence of the Pati-Salam model, in contrast to $SU(5)$, is that the proton is often stable [88, 128]. Gauge bosons with both colour and electroweak charge can, a priori, mediate transitions between quarks and leptons, however, it has been proven that the Lagrangian of the PS gauge sector is invariant under baryon number B and lepton number L individually, thus forbidding the transition [88]. Furthermore, minimal PS models do not include scalars capable of mediating proton decay transitions either. The effective dimension 6 operator that could arise is

$$\frac{\lambda}{\Lambda}\epsilon_{ijkl}Q^iQ^jQ^kQ^l, \tag{2.2.22}$$

with Q the fermion representation in (2.2.16) or (2.2.17). Therefore, only anti-symmetric scalar fields could mediate this decay, but these states rarely appear in PS models; most minimal models only include singlets or symmetric states under $SU(4)$, thus avoiding the issue of rapid proton decay.

2.2.4 Left-Right Symmetry

A submodel of Pati-Salam is the left-right symmetry model, which has the gauge group $SU(3)_C \otimes SU(2)_L \otimes SU(2)_R \otimes U(1)_{B-L}$. As a subset of PS, it can be an intermediate step on the breaking chain, path (d) in figure 2.1. Alternatively, since the LR symmetry preserves some of the many advantages of the PS model, it can be considered on its own, and that is often the approach taken [79–81].

The representations of the SM fermions in the left-right symmetric model are those obtained from the decomposition of the PS model,

$$\begin{aligned}\{\mathbf{4},\mathbf{2},\mathbf{1}\} &\to \{\mathbf{3},\mathbf{2},\mathbf{1},\ \tfrac{1}{3}\} \oplus \{\mathbf{1},\mathbf{2},\mathbf{1},\text{-}1\},\\ \{\bar{\mathbf{4}},\mathbf{1},\mathbf{2}\} &\to \{\bar{\mathbf{3}},\mathbf{1},\mathbf{2},\text{-}\tfrac{1}{3}\} \oplus \{\mathbf{1},\mathbf{1},\mathbf{2},\ 1\}.\end{aligned} \tag{2.2.23}$$

Symmetry breaking from the left-right symmetric model follows the directives discussed for the Pati-Salam breaking path (d) in figure 2.1. One needs a Higgs field in a representation $\{\mathbf{1},\mathbf{1},\mathbf{3},\alpha\}$, where if $\alpha \neq 0$ the final group is the SM group $SU(3)_C \otimes SU(2)_L \otimes U(1)_Y$, with the value of the hypercharge as in eq. (2.2.20). If $\alpha = 0$, there is an intermediate step with group $SU(3)_C \otimes SU(2)_L \otimes U(1)_R \otimes U(1)_{B-L}$. Analogous to the PS model, the EW Higgs is embedded in $\{\mathbf{1},\mathbf{2},\mathbf{2},0\}$ under $SU(3)_C \otimes SU(2)_L \otimes SU(2)_R \otimes U(1)_{B-L}$.

Unlike the Pati-Salam model, left-right symmetric models allow for the existence of baryon number violating operators, thus producing rapid proton decay.

Though it might not be the case in some specific field configurations, in the general case one needs to consider the possible contribution of any coloured state to the half-life of the proton [129].

Left-right symmetry models are very popular and have been extensively studied in the literature, both as a subgroup of PS or on its own [79–82, 130–134]. They are very attractive in non-supersymmetric theories because they are consistent with the running of the gauge couplings (c.f. figure 1.1) [129, 135–138], and also because it has very high predicting power, specially in the neutrino sector [139–143]. Finally, it can predict the existence of light states, light enough to be within the reach of the upcoming experiments [144–148].

2.2.5 $SO(10)$

In 1975, Harald Fritzsch and Peter Minkowski [71] realised that, since the group $SU(4) \otimes SU(2) \otimes SU(2)$ is locally isomorphic to $SO(6) \otimes SO(4)$, and the latter is naturally embedded in $SO(10)$, one could have a fully unified theory with $SO(10)$ as the gauge group, and the PS group as an intermediate step. Furthermore, it also contains $SU(5) \otimes U(1)$ as a maximal subgroup, hence it potentially benefits from the properties of both the PS and the Georgi-Glashow (GG) scenario. Because of this, $SO(10)$ is considered as the minimal viable fully unified theory, with the PS and GG models as possible subgroups.

In contrast to the unitary groups described before, $SO(10)$ is an orthogonal group [12]. In the unitary case, the elements of the group are complex matrices, and thus there are many complex representations satisfying the required chiral structure, present in the Standard Model, c.f. eqs. (2.1.1), (2.2.1), (2.2.16) and (2.2.17). On the other hand, elements of orthogonal groups are real matrices, so a priori one could not construct complex representations out of them with the necessary properties, e.g. the fundamental 10-plet representation of $SO(10)$ is real.

However, the structure of orthogonal groups allows for an elegant solution to this issue, by the way of spinor representations. In a general $SO(N)$ group, one can find a set of N matrices Γ_i, $i = 1, \ldots, N$, of dimensions $2^n \times 2^n$, with $N = 2n$ if even or $N = 2n + 1$ if odd, such that

$$\{\Gamma_i, \Gamma_j\} = 2\delta_{ij}, \tag{2.2.24}$$

[12] Orthogonal groups $O(N)$ are defined as the set of orthogonal $N \times N$ matrices $\mathcal{O}$, satisfying $\mathcal{O}^T\mathcal{O} = \mathbb{1}$, and with dimension $\frac{1}{2}N(N-1)$. Special orthogonal groups $SO(N)$ also satisfy $\det \mathcal{O} = 1$.

i.e. they satisfy the Grassmann algebra. These matrices can be used to construct

$$\Sigma_{ij} = \frac{i}{8\sqrt{2}}[\Gamma_i, \Gamma_j], \tag{2.2.25}$$

which satisfy the commutation relations of the generators of $SO(N)$. Therefore, the matrices Γ_i, through the generators Σ_{ij}, span a 2^n-dimensional representation of the group, which is the spinor representation. For N even, $SO(2n)$, this spinor representation is reducible. This can be seen from the fact that for $SO(2n)$, there is another matrix Γ_{2n+1}, that anticommutes with all other Γ_i, $i = 1, \ldots, 2n$, that can be obtained as

$$\Gamma_{2n+1} = (-i)^n \, \Gamma_1 \Gamma_2 \ldots \Gamma_{2n-1} \Gamma_{2n}. \tag{2.2.26}$$

From a spinor ψ transforming under the reducible $\mathbf{2^n}$ representation of $SO(2n)$, we can then define the spinors

$$\begin{aligned} \psi^+ &= \frac{1}{2}(1 + \Gamma_{2n+1})\psi, \\ \psi^- &= \frac{1}{2}(1 - \Gamma_{2n+1})\psi, \end{aligned} \tag{2.2.27}$$

which transform under the irreducible $\mathbf{2^{n-1}}$ and $\bar{\mathbf{2}}^{\mathbf{n-1}}$ representations, respectively. Furthermore, if n is even, the representations $\mathbf{2^{n-1}}$ and $\bar{\mathbf{2}}^{\mathbf{n-1}}$ are equivalent, and thus real. On the other hand, if n is odd, they are complex, which is exactly what we need to satisfy the chirality condition.

Therefore, in $SO(10)$ we will have two representations, $\mathbf{16}$ and $\overline{\mathbf{16}}$, that are not equivalent, and complex conjugate to each other. Hence we can embed all the SM fermions of one generation into a single representation of $SO(10)$, including right-handed neutrinos. The Γ_i matrices can be constructed in different bases [149], one convenient choice renders the fermions to be embedded as

$$\mathbf{16} = \{u_1^c, d_1^c, d_1 u_1, \nu^c, e^c, d_2, u_2, u_2^c, d_2^c, d_3, u_3, u_3^c, d_3^c, e, \nu\}_L, \tag{2.2.28}$$

which, under the maximal subgroups, $SU(5) \otimes U(1)$ and $SU(4)_C \otimes SU(2)_L \otimes SU(2)_R$ described above, decomposes as

$$\begin{aligned} \mathbf{16} &\to \mathbf{10}_1 \oplus \bar{\mathbf{5}}_{-1} \oplus \mathbf{1}_5, \\ \mathbf{16} &\to \{\mathbf{4}, \mathbf{2}, \mathbf{1}\} \oplus \{\bar{\mathbf{4}}, \mathbf{1}, \mathbf{2}^*\}. \end{aligned} \tag{2.2.29}$$

The adjoint representation $\mathbf{45}$ of $SO(10)$ contains the gauge bosons of $SO(10)$, including the SM gauge bosons: the 8-plet of gluons G_μ^a ($a = 1, \ldots, 8$), the triplet of electroweak bosons W_μ^i ($i = 1, \ldots, 3$), and the hypercharge field B_μ. In addition,

there are 33 extra gauge bosons that will carry both colour and weak charge, which mediate quark-lepton transitions, leading to proton decay, so they must be kept heavy. The decomposition of **45** in the SM group is

$$
\begin{aligned}
\mathbf{45} \rightarrow\ & \{\mathbf{8},\mathbf{1},\ 0\} \oplus \{\mathbf{1},\mathbf{3},\ 0\} \oplus \{\mathbf{1},\mathbf{1},\ 0\} && \leftarrow \text{SM gauge bosons} \\
& \oplus \{\mathbf{3},\mathbf{2},\ \tfrac{1}{6}\} \oplus \{\overline{\mathbf{3}},\mathbf{2},\text{-}\tfrac{1}{6}\} \oplus \{\mathbf{3},\mathbf{2},\ \tfrac{1}{6}\} \\
& \oplus \{\overline{\mathbf{3}},\mathbf{2},\text{-}\tfrac{1}{6}\} \oplus \{\overline{\mathbf{3}},\mathbf{1},\text{-}\tfrac{2}{3}\} \oplus \{\mathbf{3},\mathbf{1},\ \tfrac{2}{3}\} && \leftarrow \text{additional gauge bosons} \\
& \oplus \{\mathbf{1},\mathbf{1},\ 1\} \oplus \{\mathbf{1},\mathbf{1},\text{-}1\} \oplus \{\mathbf{1},\mathbf{1},\ 0\}.
\end{aligned}
$$

where all the coloured additional gauge bosons mediate proton decay.

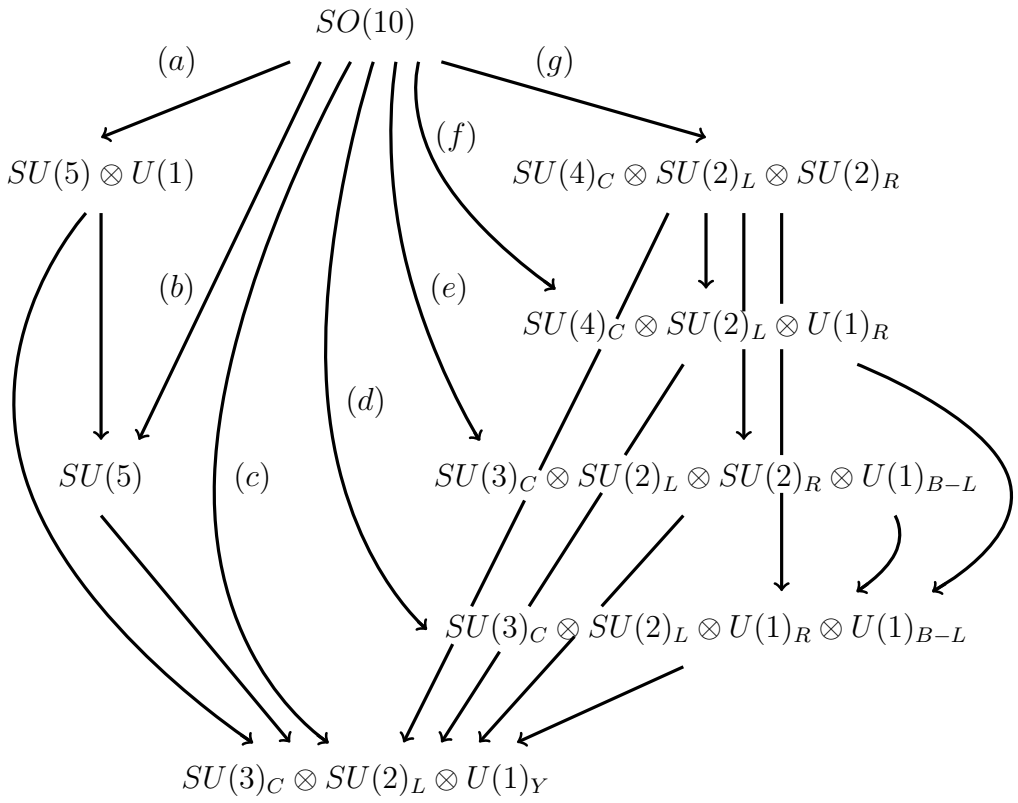

Figure 2.2: *Patterns of symmetry breaking from $SO(10)$ to the SM group.*

Symmetry breaking from $SO(10)$ to $\mathcal{G}_{SM}$ can happen in a number of ways, determined by the vacuum expectation values of the scalar fields in the theory. The Higgs sector of the $SO(10)$ model must be complex enough to satisfy the requirements of the chosen breaking path, all the way to the SM. According to figure 2.2, there are seven paths to break $SO(10)$ into one of its subgroups. The most interesting of them are

1. The path (a) first breaks into the maximal subgroup $SU(5) \otimes U(1)$. At this stage there is no indication of whether we have the standard or the flipped realisation of $SU(5) \otimes U(1)$; this would depend on the consistency with following steps. This path of symmetry breaking can be realised with Higgs fields in the **45** or **210** representations, acquiring a v.e.v. at a very high scale M_{GUT}, along the singlet directions

$$\begin{aligned} \mathbf{45} &\to \mathbf{24}_0 \oplus \mathbf{10}_1 \oplus \overline{\mathbf{10}}_{-1} \oplus \mathbf{1}_0, \\ \mathbf{210} &\to \mathbf{75}_0 \oplus \mathbf{40}_{-1} \oplus \overline{\mathbf{40}}_1 \oplus \mathbf{24}_0 \oplus \mathbf{10}_1 \oplus \overline{\mathbf{10}}_{-1} \oplus \mathbf{5}_{-2} \oplus \bar{\mathbf{5}}_2 \oplus \mathbf{1}_0. \end{aligned}$$

   Further breaking to $\mathcal{G}_{SM}$, at an intermediate scale M_I, requires other Higgs fields, depending on whether it is the standard or flipped version of $SU(5) \otimes U(1)$. As described in section 2.2.2, to break the flipped $SU(5) \otimes U(1)$, Higgses in the $\mathbf{10}_1$ and $\overline{\mathbf{10}}_{-1}$ representations are needed, which could originate from many different representations of $SO(10)$, e.g. **16**. To break the standard version of $SU(5) \otimes U(1)$ one would need either a two-step process, breaking the $SU(5)$ and $U(1)$ independently, or a one-step process, with a $\mathbf{24}_\alpha$ $(\alpha \neq 0)$ representation, probably coming from an $SO(10)$ **144**.

2. Breaking to the subgroup $SU(5)$ via path (b) reduces the rank by one and thus requires a non-adjoint representation such as **16**, $\overline{\mathbf{16}}$, **126** or $\overline{\mathbf{126}}$. Decomposition of **16** follows equation (2.2.29), and

$$\begin{aligned} \overline{\mathbf{16}} &\to \overline{\mathbf{10}} \oplus \mathbf{5} \oplus \mathbf{1}, \\ \mathbf{126} &\to \mathbf{50} \oplus \mathbf{45} \oplus \overline{\mathbf{15}} \oplus \mathbf{10} \oplus \bar{\mathbf{5}} \oplus \mathbf{1}. \end{aligned} \tag{2.2.30}$$

   An extra Higgs in the adjoint **24** of $SU(5)$ is needed in order to break to the SM at an intermediate scale M_I, as described in section 2.2.1. This Higgs field may come from the adjoint **45** of $SO(10)$ or from a larger adjoint-like representation like **54** or **210**.

3. Direct breaking to $\mathcal{G}_{SM}$ via path (c) is triggered by a Higgs in a representation that does not have singlets in the directions of any of the intermediate subgroups. The minimal case is given by the **144** representation of $SO(10)$, which decomposes under the intermediate maximal subgroups as,

   $SU(5) \otimes U(1)$:

$$\mathbf{144} \to \mathbf{45}_{-3} \oplus \mathbf{40}_1 \oplus \mathbf{24}_5 \oplus \overline{\mathbf{15}}_1 \oplus \overline{\mathbf{10}}_1 \oplus \bar{\mathbf{5}}_{-7} \oplus \mathbf{5}_{-7}, \tag{2.2.31}$$

   $SU(4)_C \otimes SU(2)_L \otimes SU(2)_R$:

$$\mathbf{144} \to \{\mathbf{20}, \mathbf{2}, \mathbf{1}\} \oplus \{\overline{\mathbf{20}}, \mathbf{1}, \mathbf{2}\} \oplus \{\mathbf{4}, \mathbf{2}, \mathbf{3}\} \oplus \{\bar{\mathbf{4}}, \mathbf{3}, \mathbf{2}\} \oplus \{\mathbf{4}, \mathbf{2}, \mathbf{1}\} \oplus \{\bar{\mathbf{4}}, \mathbf{1}, \mathbf{2}\},$$

and similarly with other subgroups. It does have a SM singlet, coming from the $\mathbf{24}_5$ or the $\mathbf{10}_1$ in the standard and flipped realization of $SU(5) \otimes U(1)$, respectively; or from the $\{\bar{\mathbf{4}}, \mathbf{1}, \mathbf{2}\}$ of $SU(4) \otimes SU(2) \otimes SU(2)$.

4. The Pati-Salam group and its subgroups, paths (d) through (g), are among the most popular breaking paths. Similarly to the $SU(5)$-type chains above, it is also possible to have a two-step breaking chain, first breaking to a subgroup of $SO(10)$ at a high scale M_{GUT} and then to the Standard Model at an intermediate scale M_I.

   A very interesting option within the Pati-Salam subset is the direct breaking from $SO(10)$ to the left-right symmetric group, $SU(3)_C \otimes SU(2)_L \otimes SU(2)_R \otimes U(1)_{B-L}$. This breaking cannot happen with a **54** representation since it already has a singlet direction along the PS little group, whereas the **210** has another singlet direction that does not preserve Pati-Salam. Hence, one would need either a **45** or a **210**, similarly as the $SU(5) \otimes U(1)$ case, to realise the breaking. The **45** representation decomposes as

$$\begin{aligned}\mathbf{45} \to &\{\mathbf{8},\mathbf{1},\mathbf{1},\ 0\} \oplus \{\mathbf{3},\mathbf{2},\mathbf{2},\ 1\} \oplus \{\bar{\mathbf{3}},\mathbf{2},\mathbf{2},\text{-}1\} \oplus \{\mathbf{1},\mathbf{3},\mathbf{1},\ 0\} \oplus \{\mathbf{1},\mathbf{1},\mathbf{3},\ 0\} \\ &\oplus\ \{\mathbf{3},\mathbf{1},\mathbf{1},\text{-}2\} \oplus \{\bar{\mathbf{3}},\mathbf{1},\mathbf{1},\ 2\} \oplus \{\mathbf{1},\mathbf{1},\mathbf{1},\ 0\},\end{aligned}$$

   and the new singlet direction of **210** can be obtained from the $\{\mathbf{15},\mathbf{1},\mathbf{1}\}$ representation in eq. (2.2.32).

   However, the most interesting scenarios arise when the breaking happens in multiple steps. Breaking to the PS group first at M_{GUT} and then, following the arguments in section 2.2.3, to the Standard Model in several steps at intermediate scales $M_{I_1}, \ldots, M_{I_3}$. To satisfy this case, one would need a Higgs field in a **54** or **210** representations of $SO(10)$, because both of them have singlets in the directions of the intermediate group. The decomposition of these representations into PS is

$$\begin{aligned}\mathbf{54} &\to \{\mathbf{20},\mathbf{1},\mathbf{1}\} \oplus \{\mathbf{1},\mathbf{3},\mathbf{1}\} \oplus \{\mathbf{1},\mathbf{1},\mathbf{3}\} \oplus \{\mathbf{6},\mathbf{2},\mathbf{2}\}, \\ \mathbf{210} &\to \{\mathbf{15},\mathbf{3},\mathbf{1}\} \oplus \{\mathbf{15},\mathbf{1},\mathbf{3}\} \oplus \{\mathbf{10},\mathbf{2},\mathbf{2}\} \oplus \{\overline{\mathbf{10}},\mathbf{2},\mathbf{2}\} \\ &\quad \oplus\ \{\mathbf{6},\mathbf{2},\mathbf{2}\} \oplus \{\mathbf{15},\mathbf{1},\mathbf{1}\} \oplus \{\mathbf{1},\mathbf{1},\mathbf{1}\}. \end{aligned} \tag{2.2.32}$$

   The next step, the breaking of $SU(4)_C \otimes SU(2)_L \otimes SU(2)_R$, happening at M_I, may occur in different ways, as it was covered in section 2.2.3. Typically one would need to include representations such as **16**, $\overline{\mathbf{16}}$, **126** or $\overline{\mathbf{126}}$, since they produce the rank breaking required to reach the Standard Model group.

Lastly, one needs to specify the mechanism of EWSB. The Higgs representation is constricted by the fact that in order to provide masses to the SM particles, one needs to construct Yukawa-type couplings between the matter fields and the Higgs. Due to the spinorial character of the matter fields in the **16** representation, the most general Yukawa term is of the form [88]

$$\mathcal{L}_{Yuk} = \mathbf{Y} \cdot \mathbf{16}^T C_L C_{10} \Gamma_{i_1 \dots i_k} \mathbf{16} \Phi^{i_1 \dots i_k}, \tag{2.2.33}$$

where $\mathbf{Y}$ is a matrix in family space, C_L and C_{10} are the charge conjugation matrices in the Poincaré and $SO(10)$ groups, $\Gamma_{i_1 \dots i_k}$ is a product of k gamma matrices Γ_i used for the construction of the spinor representations, and $\Phi^{i_1 \dots i_k}$ is a Higgs field. Luckily there are severe constraints on the product of gamma matrices that will reduce the number of possible representations for the Higgs field Φ. First, from the properties of gamma matrices, the product must be antisymmetric in the indices $i_1 \dots i_k$ which allows us to introduce a $\epsilon_{ijklmnopqr}$ symbol whenever $k > 5$ and then reduce to the case with $10 - k$ indices. Moreover, due to the anticommutation properties of the C_{10} matrix and the Γ_i matrices, the only way to obtain an $SO(10)$ invariant product is with an odd number of Γ matrices. Hence there are only 3 possible cases with $k = 1, 3, 5$,

$$\mathcal{L}_{Yuk} = \mathbf{Y} \cdot \mathbf{16}^T C_L C_{10} (\Gamma_i \Phi^i + \Gamma_{[i} \Gamma_j \Gamma_{k]} \Phi^{ijk} + \Gamma_{[i} \Gamma_j \Gamma_k \Gamma_l \Gamma_{m]} \Phi^{ijklm}) \mathbf{16}, \tag{2.2.34}$$

which precisely corresponds to the scalar fields Φ^i, Φ^{ijk} and Φ^{ijklm} in the representations **10**, **120** and **126**, respectively. This may also be seen from the direct product of two spinor representations,

$$\mathbf{16} \otimes \mathbf{16} = \mathbf{10} \oplus \mathbf{120} \oplus \overline{\mathbf{126}}. \tag{2.2.35}$$

These representations will decompose into the electroweak Higgs fields that we have seen previously in section 2.2.1, 2.2.2 and 2.2.3, that is the two fiveplets of $SU(5)$, **5** and $\bar{\mathbf{5}}$ (with the corresponding charges in $SU(5) \otimes U(1)$), and the bidoublet of $SU(4) \otimes SU(2) \otimes SU(2)$, $\{\mathbf{1}, \mathbf{2}, \mathbf{2}\}$. The full decomposition of **10**, **120** and **126**

under the maximal subgroups of $SO(10)$ is

$$
\begin{aligned}
&SU(5)\otimes U(1):\\
&\quad \mathbf{10} \;\to \mathbf{5}_2 \oplus \overline{\mathbf{5}}_{-2},\\
&\quad \mathbf{120} \to \mathbf{45}_{-1} \oplus \overline{\mathbf{45}}_1 \oplus \mathbf{10}_{-3} \oplus \overline{\mathbf{10}}_3 \oplus \mathbf{5}_1 \oplus \overline{\mathbf{5}}_{-1},\\
&\quad \mathbf{126} \to \mathbf{50}_{-1} \oplus \mathbf{45}_1 \oplus \overline{\mathbf{15}}_3 \oplus \mathbf{10}_{-3} \oplus \overline{\mathbf{5}}_{-1} \oplus \mathbf{1}_{-5}.\\
&SU(4)_C \otimes SU(2)_L \otimes SU(2)_R:\\
&\quad \mathbf{10} \;\to \{\mathbf{6},\mathbf{1},\mathbf{1}\} \oplus \{\mathbf{1},\mathbf{2},\mathbf{2}\},\\
&\quad \mathbf{120} \to \{\mathbf{15},\mathbf{2},\mathbf{2}\} \oplus \{\mathbf{6},\mathbf{3},\mathbf{1}\} \oplus \{\mathbf{6},\mathbf{1},\mathbf{3}\} \oplus \{\mathbf{10},\mathbf{1},\mathbf{1}\} \oplus \{\overline{\mathbf{10}},\mathbf{1},\mathbf{1}\} \oplus \{\mathbf{1},\mathbf{2},\mathbf{2}\},\\
&\quad \mathbf{126} \to \{\mathbf{15},\mathbf{2},\mathbf{2}\} \oplus \{\mathbf{10},\mathbf{1},\mathbf{3}\} \oplus \{\overline{\mathbf{10}},\mathbf{1},\mathbf{3}\} \oplus \{\mathbf{6},\mathbf{1},\mathbf{1}\}.
\end{aligned}
\tag{2.2.36}
$$

Typically, one needs more than one of these representations at a time to be able to fit fermion masses [88, 150]. As an example, working in the Pati-Salam scenario, let the Yukawa matrices for **10**, **120** and **126** be $\mathbf{Y}_{10}$, $\mathbf{Y}_{120}$ and $\mathbf{Y}_{126}$, and assume that after electroweak symmetry breaking (EWSB) the $\{\mathbf{1},\mathbf{2},\mathbf{2}\}$ representations in **10** and **120**, and the $\{\mathbf{15},\mathbf{2},\mathbf{2}\}$ representations in **120** and **126** acquire up and down-type expectation values

$$
\begin{aligned}
v_{u,d} &= \langle \mathbf{10} \rangle \quad\;\; = \langle \{\mathbf{1},\mathbf{2},\mathbf{2}\}_{u,d} \rangle,\\
\sigma_{u,d} &= \langle \mathbf{126} \rangle = \langle \{\mathbf{15},\mathbf{2},\mathbf{2}\}_{u,d} \rangle,\\
\omega^{\alpha}_{u,d} &= \langle \mathbf{120}^{\alpha} \rangle \;\; = \langle \{\mathbf{1},\mathbf{2},\mathbf{2}\}_{u,d} \rangle,\\
\omega^{\beta}_{u,d} &= \langle \mathbf{120}^{\beta} \rangle = \langle \{\mathbf{15},\mathbf{2},\mathbf{2}\}_{u,d} \rangle,
\end{aligned}
\tag{2.2.37}
$$

where α and β denote whether the v.e.v. comes from the $\{\mathbf{1},\mathbf{2},\mathbf{2}\}$ or $\{\mathbf{15},\mathbf{2},\mathbf{2}\}$ of **120**, respectively.

The masses of the fermions are then obtained as [88]

$$
\begin{aligned}
\mathbf{m}_u &= \mathbf{Y}_{10}\; v_u + \;\; \mathbf{Y}_{126}\; \sigma_u + \mathbf{Y}_{120}\; (\omega^{\alpha}_u + \;\; \omega^{\beta}_u),\\
\mathbf{m}_d &= \mathbf{Y}_{10}\; v_d + \;\; \mathbf{Y}_{126}\; \sigma_d + \mathbf{Y}_{120}\; (\omega^{\alpha}_d + \;\; \omega^{\beta}_d),\\
\mathbf{m}_e &= \mathbf{Y}_{10}\; v_d - 3\mathbf{Y}_{126}\; \sigma_d + \mathbf{Y}_{120}\; (\omega^{\alpha}_d - 3\;\omega^{\beta}_d),\\
\mathbf{m}_\nu &= \mathbf{Y}_{10}\; v_u - 3\mathbf{Y}_{126}\; \sigma_u + \mathbf{Y}_{120}\; (\omega^{\alpha}_u - 3\;\omega^{\beta}_u)
\end{aligned}
\tag{2.2.38}
$$

where $\mathbf{m}_\nu$ is the Dirac mass of the neutrino. In order to fit the small neutrino masses, one need a see-saw mechanism [8, 122–127]. Majorana masses for the neutrinos $\mathbf{m}_L$

and $\mathbf{m}_R$ can be generated from the expectation values of the **126** representation

$$\begin{aligned} v_L = \langle\{\overline{\mathbf{10}}, \mathbf{3}, \mathbf{1}\}\rangle, \quad v_R = \langle\{\mathbf{10}, \mathbf{1}, \mathbf{3}\}\rangle, \\ \mathbf{m}_L = \mathbf{Y}_{126} v_L, \\ \mathbf{m}_R = \mathbf{Y}_{126} v_R, \end{aligned} \tag{2.2.39}$$

for the same $\mathbf{Y}_{126}$ as above.

Most of the appeal of $SO(10)$ models comes from the plethora of different breaking options it has. It feeds from the successes of its subgroups, through the Pati-Salam breaking path [151, 152], the $SU(5)$-like path [153] or through direct breaking [154].

2.3 Supersymmetry

As was mentioned in section 2.1, the Standard Model suffers from the so called hierarchy problem [12, 45, 46]. Effectively this has the consequence that the mass of the Higgs boson (or any scalar, for that matter) is unstable to radiative corrections coming from new physics states. These corrections come from diagrams similar to those in figure 2.3, where both scalars (left) and Weyl fermions (right) contribute to the mass.

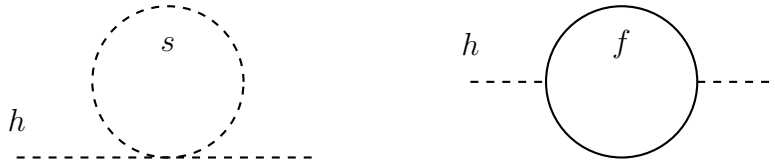

Figure 2.3: *One-loop contributions to the Higgs mass.*

The contributions from these diagrams can be sizeable and, they are, in general, proportional to the mass scale Λ of the new physics states in the loop ($m_s \sim m_f \sim \Lambda$). They can be estimated as [155]

$$\Delta m_h^2 = -\frac{|\lambda_f|^2}{16\pi^2}\Lambda^2 + \frac{\lambda_s}{16\pi^2}\Lambda^2 + \dots \tag{2.3.1}$$

where λ_f and λ_s are the couplings of h to the fermions and scalars respectively. Even if there are no such couplings in the Lagrangian, similar contributions can be generated at the 2-loop level involving gauge bosons that couple to both sectors [155]. The ellipsis in the equation above refer to contributions from diagrams with higher loops or which are logarithmic in Λ. The leading and most dangerous contribution,

however, comes from the terms proportional to Λ^2, which give large contributions to the Higgs mass, since Λ can potentially be as large as the Planck scale M_P.

This strong dependence on the mass of heavy states can be seen already in the SM, where there are fermion loop contributions to the Higgs mass like those in the right hand diagram of figure 2.3. The dominant contribution in that case comes from top loops, with a mass of $m_t = 173.2 \pm 1.2$ [4], which drives the mass of the Higgs to its current measured value of $m_h = 125.7 \pm 0.4$ [4].

In parallel to what we did in section 2.2, where we attempted to solve the problems of the Standard Model by increasing its symmetries, we will try to cancel this potentially fatal phenomenon by the use of symmetries. Imposing the symmetry condition that for every fermionic degree of freedom there is a complex scalar degree of freedom with coupling $\lambda_s = |\lambda_f|^2$, we cancel exactly the dangerous contributions to the Higgs mass in equation (2.3.1), thus allowing for a light Higgs. This symmetry is known as *supersymmetry* [11, 156–160].

2.3.1 Introduction to Supersymmetry

From the theoretical point of view, supersymmetry (SUSY) is an extension of the spacetime symmetry, described by the Poincaré group. The Haag-Lopuszanski-Sohnius extension [161] of the Coleman-Mandula theorem [162] states that the only possible way to extend the spacetime symmetry is with fermionic operators. These operators Q^α also known as supercharges, together with the generators of the Poincaré group, form what is called the Super-Poincaré group [163]. Because of the fermionic nature of the supercharges, they generate transformations that interchange fermionic and bosonic degrees of freedom,

$$Q^\alpha|B\rangle = |F\rangle^\alpha, \qquad Q^\alpha|F\rangle_\alpha = |B\rangle, \tag{2.3.2}$$

where $|B\rangle$ is a bosonic state, $|F\rangle$ a fermionic state and α labels the fermionic components of $|F\rangle$ and Q.

Therefore, supersymmetry collects fermionic and bosonic degrees of freedom into a single multiplet, which in this context is called a superfield Φ. A priori, one could have any number $\mathcal{N} \geq 1$ of supercharges, Q_A^α with $A = 1 \ldots \mathcal{N}$, known as "extended supersymmetry". However, in reality there is no way to build a renormalisable supersymmetric field theory unless $\mathcal{N} \leq 4$ [164, 165][13]. The superfield Φ will contain $\mathcal{N} + 1$ on-shell fields and a few examples of possible realisations are:

[13] Relaxing the renormalisability condition, the maximum number of supersymmetries is $\mathcal{N} = 8$,

- $\mathcal{N}=1$ (anti) chiral multiplet: includes a boson of spin $s=0$ and a fermion of spin $s=\frac{1}{2}$ ($s=-\frac{1}{2}$),
- $\mathcal{N}=1$ vector multiplet: a fermion of spin $s=\frac{1}{2}$ and a boson with $s=1$,
- $\mathcal{N}=2$ hypermultiplet: two fermions, spin $s=\pm\frac{1}{2}$ and a two bosons $s=0$,
- $\mathcal{N}=4$ vector multiplet: 8 bosons, $s=\pm1$, $6\times s=0$, and 8 fermions, $4\times s=\pm\frac{1}{2}$.

However, despite the freedom of extended supersymmetry, only $\mathcal{N}=1$ is phenomenologically viable [163]. All the multiplets for $\mathcal{N}>1$, except the hypermultiplet, necessarily include a $s=1$ boson, which needs to be in the adjoint representation of the gauge group in order to make a consistent gauge theory. However, this would imply that all other components, bosons or fermions, of the multiplet will also be in the same representation, contradicting the chirality condition of the Standard Model. Not even the $\mathcal{N}=2$ hypermultiplet satisfies this condition for it has $s=\frac{1}{2}$ and $s=-\frac{1}{2}$ in the same gauge multiplet. In the following we will concentrate on $\mathcal{N}=1$ supersymmetry, which is the dominant choice for low energy SUSY phenomenology[14].

In order to build an $\mathcal{N}=1$ supersymmetric theory out of chiral Φ_i, anti-chiral Φ^{*j} and vector V^a superfields, one needs to construct the Super-Poincaré invariant action, or "Superaction" [155, 163]. Let θ^α and $\theta^\dagger_{\dot\alpha}$ be the anticommuting spinorial coordinates in superspace upon which the generators Q^α and $Q^\dagger_{\dot\alpha}$ act[15]. One can then expand the chiral, anti-chiral and vector superfields in powers of θ and $\theta^\dagger$ as [155]

$$\begin{aligned}
\Phi_i &= \phi_i + \sqrt{2}\theta\psi_i + i\theta^\dagger\bar\sigma^\mu\theta\partial_\mu\phi_i + \theta\theta F_i - \frac{i}{\sqrt{2}}\theta\theta\theta^\dagger\bar\sigma^\mu\partial_\mu\psi_i \\
&\quad + \frac{1}{4}\theta\theta\theta^\dagger\theta^\dagger\partial^\mu\partial_\mu\phi_i, \\
\Phi^{*j} &= \phi^{*j} + \sqrt{2}\theta^\dagger\psi^{\dagger j} - i\theta^\dagger\bar\sigma^\mu\theta\partial_\mu\phi^{*j} + \theta^\dagger\theta^\dagger F^{*j} - \frac{i}{\sqrt{2}}\theta^\dagger\theta^\dagger\theta\sigma^\mu\partial_\mu\psi^{\dagger j} \\
&\quad + \frac{1}{4}\theta\theta\theta^\dagger\theta^\dagger\partial^\mu\partial_\mu\phi^{*j}, \\
V^a_{WZ} &= \theta^\dagger\bar\sigma^\mu\theta A^a_\mu + \theta^\dagger\theta^\dagger\theta\lambda^a + \theta\theta\theta^\dagger\lambda^a + \frac{1}{2}\theta\theta\theta^\dagger\theta^\dagger D^a,
\end{aligned} \tag{2.3.3}$$

since there are no known particles with spin $s>2$ and if there were, they would have no conserved currents or couplings at low energies [164, 165].

[14] $\mathcal{N}>1$ realisations of SUSY could exist at higher scales, broken into $\mathcal{N}=1$ SUSY at low scales, thus circumventing these issues.

[15] For an extended review of calculus with θ and $\theta^\dagger$ and the Grassmann algebra, see [163].

where ϕ is a complex scalar, ψ and λ^a are Weyl fermions, A^a_μ is a vector field and F_i and D^a are auxiliary non-dynamical (off-shell) fields. V^a_{WZ} is written in the Wess-Zumino gauge, which eliminates several components by a supergauge transformation [155].

It can be shown [155,163] that the supersymmetry transformation of the F and D terms is a total derivative, so they can be used to write supersymmetry invariant actions. Therefore the most general, not necessarily renormalisable, Superaction can be written from F and D terms of chiral and vector superfields, respectively, as [155]

$$\mathcal{S} = \int d^4x \int d^2\theta d^2\theta^\dagger \left\{ K(\Phi_i, \Phi^{*j}) + \left(\delta^{(2)}(\theta^\dagger)[\frac{1}{4} f_{ab}(\Phi_i)\mathcal{W}^a\mathcal{W}^b + W(\Phi)] + \text{c.c.} \right) \right\}, \tag{2.3.4}$$

where K, f_{ab}, $\mathcal{W}$ and W are functions of the superfields, defined as

- K, known as the Kähler potential [155,163], is a vector superfield, of dimension (mass)^2. In the renormalisable limit the Kähler potential takes the gauge invariant form $K = \Phi^{*j}(e^{2T^aV^a})^i_j\Phi_i$, with T^a the generators of the gauge group. In non-renormalisable theories, however, it can take any form, as long as K is kept real and gauge invariant. Integrating the Kähler potential with the measure $d^2\theta d^2\theta^\dagger$ extracts its D-term, i.e., the term in K proportional to $\theta^2\theta^{\dagger 2}$, which makes this term of the Superaction invariant under supersymmetry transformations.

- W is a chiral superfield of dimension (mass)^3 called the Superpotential. It is holomorphic[16] in Φ. The general form of this function is

$$W(\Phi) = \sum_n \frac{1}{n!} \frac{y^{i_1\dots i_n}}{M^{n-3}} \Phi_{i_1} \dots \Phi_{i_n}, \tag{2.3.5}$$

  with $y^{i_1\dots i_n}$ dimensionless couplings and M has a mass scale. In the renormalisable limit $n \leq 3$ and we can write it as

$$W(\Phi) = l^i\Phi_i + \frac{1}{2}\mu_{ij}\Phi_i\Phi_j + \frac{1}{6}y^{ijk}\Phi_i\Phi_j\Phi_k. \tag{2.3.6}$$

  The superaction gets the F-terms of the superpotential, i.e., those proportional to θ^2, because of the integration measure $d^2\theta d^2\theta^\dagger \delta^{(2)}(\theta^\dagger)$, plus the equivalent of

[16] A holomorphic function $g(z)$ with z a complex variable, is a function that depends only on z, but not on its complex onjugate, z^*.

its complex conjugate, proportional to $\theta^{\dagger 2}$, both of which are invariant under supersymmetry transformations.

- Finally, f_{ab} and $\mathcal{W}$ are the gauge kinetic function and gauge field strength, respectively, which will produce the kinetic and self-interaction terms for the gauge sector. The gauge field strength of the vector superfield V^a is defined as [155, 163]

$$\mathcal{W}_\alpha^a = -\frac{g_a}{4} D^\dagger D^\dagger \left(e^{-2g_a T^a V^a} D_\alpha e^{2g_a T^a V^a} \right), \tag{2.3.7}$$

where D and $D^\dagger$ are the supersymmetric covariant derivatives on θ and $\theta^\dagger$. respectively. The kinetic function f_{ab} depends on Φ in the general case and will produce coupling terms between the vector and chiral superfields. In the renormalisable limit, however, it is independent of Φ and takes the form [155, 163]

$$f_{ab} = \delta_{ab} \left(\frac{1}{g_a^2} - i \frac{\Theta_a}{8\pi^2} \right), \tag{2.3.8}$$

where Θ_a is an arbitrary new parameter that introduces CP-violation in the strong sector [61]. Similarly to the superpotential, only the θ^2 and $\theta^{\dagger 2}$ components of the kinetic term, the F-terms, will contribute to the superaction, since they are invariant under supersymmetry transformations.

From the Superaction in eq. (2.3.4) one can extract the scalar potential of the theory, obtained after eliminating the off-shell F_i and D^a fields from the action and can be written as [163].

$$V = \sum_i \left| \frac{\partial W}{\partial \Phi_i} \right|^2_{\Phi=\phi} + g_a^2 (\phi^{*i} T^a \phi_i)^2, \tag{2.3.9}$$

where the first term is obtained from the superpotential and the last one, known as the D-term of the scalar potential, comes from the Kähler potential and gauge kinetic term.

2.3.2 Supersymmetry Breaking

Since supersymmetry is a symmetry between fermions and bosons, it naturally predicts equal masses for all members of each supermultiplet. However, this is not observed in nature. There is no evidence of scalar partners of the SM fermions with the same mass, nor fermionic partners of the Higgs or gauge bosons[17]. Therefore,

[17]The vector or scalar bosons of the SM cannot be the superpartners of the SM fermions, since they belong to different representations of the gauge group.

supersymmetry must be broken at the SM scale and the supersymmetric partners of the SM particles must have masses above the current experimental limits.

Unlike the usual mechanism for spontaneous symmetry breaking, as seen for gauge symmetries in sections 2.1 and 2.2, the method of SUSY breaking must be such that it preserves the solution to the hierarchy problem, described at the beginning of the section. The most popular way for this to happen is to have SUSY be broken in a hidden sector, a sector of the theory not accessible via SM interactions, and then transported to the visible (SM) sector via non-SM interactions. The way the symmetry breaking is transferred to the SM results in different mechanisms:

- Supergravity mediation (SUGRA): the breaking is mediated by gravitational or other Planck scale interactions [166–172].
- Gauge mediation (GMSB): some new chiral supermultiplets acts as messengers of the breaking through gauge interactions [173–178].
- Anomaly mediation (AMSB): the breaking is produced by the presence of anomalies, where the violation of superconformal invariance generates the breaking [179, 180].

One can, however, ignore the actual mechanism of SUSY breaking and simply parametrize the effects that it has on the visible sector. A typical way of doing so is by adding to the SUSY Lagrangian the so called soft SUSY breaking terms, which explicitly break supersymmetry. The soft SUSY breaking Lagrangian can be written as [155]

$$\begin{aligned}\mathcal{L}_{\text{soft}} = &-\left(\frac{1}{2}M_a\lambda^a\lambda^a + \frac{1}{6}a^{ijk}\phi_i\phi_j\phi_k + \frac{1}{2}b^{ij}\phi_i\phi_j + c^i\phi_i\right) + \text{c.c.} \\ &- (m^2)^i_j\phi^{*j}\phi_i,\end{aligned} \tag{2.3.10}$$

where ϕ_i are the sfermions (scalar superpartners of the SM fermions) and Higgses, and λ^a are the fermion superpartners of the gauge bosons (gauginos), and c.c. refers to the complex conjugate of the terms in front. These terms explicitly break SUSY as they provide masses and couplings for the supersymmetric partners, but not for the SM fields. The mass terms in $\mathcal{L}_{\text{soft}}$, $(m^2)^i_j$ and M_a, spoil the exact cancellation of the diagrams in figure 2.3, but for low masses, $1 - 10$ TeV, one can have a sufficient cancellation to preserve the solution of the hierarchy problem.

A minimal form for these soft terms, known as mSUGRA [166] for gravity mediated models, assumes that the masses of the scalar and fermionic superpartners

are universal at some high scale, Λ_{UV},

$$M_a(\Lambda_{UV}) = m_{1/2}, \quad (m^2)^i_j(\Lambda_{UV}) = m_0^2\ \delta^i_j, \tag{2.3.11}$$

and, the trilinear terms a^{ijk} are assumed to be proportional to the corresponding Yukawa term in the superpotential, $a^{ijk} = A_0 y^{ijk}$ and similarly for the bilinear terms, proportional to the μ term in the superpotential, $b^{ij} = B\mu^{ij}$, with universal couplings A_0 and B.

2.3.3 The MSSM

The Minimal Supersymmetric Standard Model (MSSM) is, as the name suggests, the most minimal extension of the SM including supersymmetry. According to the definitions of chiral and vector superfields above, we start by considering all SM fermions as the fermionic part of chiral superfields, the Higgs as the scalar part of another chiral superfield and the gauge bosons as the vector part of vector superfields. In the MSSM we need to have two chiral superfields for the Higgs, one with hypercharge $-\frac{1}{2}$ and another with hypercharge $\frac{1}{2}$. This is due to two reasons: first, since the superpotential is holomorphic in the superfields, we cannot use ϕ^* for the Yukawa coupling to up-type quarks, as we did in the SM in section 2.1, and second because one needs to introduce a chiral superfield with hypercharge $\frac{1}{2}$ to cancel triangle diagrams that can be source of gauge anomalies [86, 87]. Hence, the MSSM field content discussed can be seen summarised in table 2.1, where $i = 1, \ldots, 3$ is the flavour index, representing the three generations of quarks and leptons.

It can be noticed that for every Weyl fermion in the Standard Model, there is a complex scalar, to match the number of components. A Dirac fermion, however, has four components, so it corresponds to two complex scalars, e.g. if e is the electron, a Dirac fermion, then it has two complex scalars $\tilde{e}_L \in \tilde{L}_1$ and $\tilde{e}_R \equiv (\tilde{e}^c_1)^*$ as superpartners. For the same reason, the superpartners of the Higgs and gauge bosons are Majorana fermions, e.g. the hypercharge vector boson B_μ has two independent components, same as the complex Majorana spinor $\tilde{B}$.

At first glance, this field content in the MSSM could lead to disastrous consequences. There is nothing in the theory that forbids couplings of the type $u^c d^c \tilde{d^c}$ or $QL\tilde{d^c}$, which will induce rapid proton decay at tree level, since they violate both baryon and lepton number [181]. A solution to this is to impose a Z_2 symmetry that does not allow for such terms. This discrete symmetry is typically known as

Superfield	$s=0$	$s=\frac{1}{2}$	$s=1$	$SU(3)_C \otimes SU(2)_L \otimes U(1)_Y$
$\hat{Q}_i$	$\tilde{Q}_i$	Q_i	-	$\{\mathbf{3}, \mathbf{2}, \frac{1}{6}\}$
$\hat{u}_i^c$	$\tilde{u}_i^c$	u_i^c	-	$\{\bar{\mathbf{3}}, \mathbf{1}, -\frac{2}{3}\}$
$\hat{d}_i^c$	$\tilde{d}_i^c$	d_i^c	-	$\{\bar{\mathbf{3}}, \mathbf{1}, \frac{1}{3}\}$
$\hat{L}_i$	$\tilde{L}_i$	L_i	-	$\{\mathbf{1}, \mathbf{2}, -\frac{1}{2}\}$
$\hat{e}_i^c$	$\tilde{e}_i^c$	e_i^c	-	$\{\mathbf{1}, \mathbf{1}, 1\}$
$\hat{H}_u$	H_u	$\tilde{H}_u$	-	$\{\mathbf{1}, \mathbf{2}, \frac{1}{2}\}$
$\hat{H}_d$	H_d	$\tilde{H}_d$	-	$\{\mathbf{1}, \mathbf{2}, -\frac{1}{2}\}$
$\hat{G}$	-	$\tilde{G}$	G_μ	$\{\mathbf{8}, \mathbf{1}, 0\}$
$\hat{W}$	-	$\tilde{W}$	W_μ	$\{\mathbf{1}, \mathbf{3}, 0\}$
$\hat{B}$	-	$\tilde{B}$	B_μ	$\{\mathbf{1}, \mathbf{1}, 0\}$

Table 2.1: *Superfield content in the MSSM. Only chiral superfields are depicted, corresponding to left-handed fermionic components. An analogous table for anti-chiral superfields (right-handed fermions) is omitted.*

R-parity and it is defined as

$$P_R = (-1)^{3B+L+2s}, \tag{2.3.12}$$

with B, L and s the baryon and lepton numbers, and spin, respectively. Effectively, this definition assigns a positive R-parity $P_R = 1$ to the SM particles and $P_R = -1$ to their superpartners which, besides solving the proton decay problem, has the consequence of making the lightest supersymmetric particle (LSP) stable. Hence supersymmetry has a candidate for dark matter, which is often a linear combination of $\tilde{B}$, $\tilde{W}^3$, $\tilde{H}_u$ and $\tilde{H}_d$.

The R-parity conserving superpotential of the MSSM is

$$W_{MSSM} = \mathbf{y}_u \hat{u}^c \hat{Q} \hat{H}_u - \mathbf{y}_d \hat{d}^c \hat{Q} \hat{H}_d - \mathbf{y}_e \hat{e}^c \hat{L} \hat{H}_d + \mu \hat{H}_u \hat{H}_d, \tag{2.3.13}$$

where $\mathbf{y}_u$, $\mathbf{y}_d$ and $\mathbf{y}_e$ are, 3×3 Yukawa matrices in family space, and μ is a dimensionful parameter which determines the Higgs self-coupling, as well as the mass of the superpartners of the Higgs bosons (higgsinos).

The soft SUSY breaking terms for the MSSM, obtained from equation (2.3.10)

with the content of table 2.1, are

$$\begin{aligned}\mathcal{L}_{\text{soft}} = &-\frac{1}{2}\left(M_3\tilde{g}\tilde{g} + M_2\tilde{W}\tilde{W} + M_1\tilde{B}\tilde{B} + \text{c.c.}\right)\\ &-\left(A_u\tilde{u}^c\mathbf{y}_u\tilde{Q}H_u - A_d\tilde{d}^c\mathbf{y}_d\tilde{Q}H_d - A_e\tilde{e}^c\mathbf{y}_e\tilde{L}H_d + \text{c.c.}\right)\\ &-\tilde{Q}^*\mathbf{m}_Q^2\tilde{Q} - \tilde{L}^*\mathbf{m}_L^2\tilde{L} - \tilde{u}^{c*}\mathbf{m}_u^2\tilde{u}^c - \tilde{d}^{c*}\mathbf{m}_d^2\tilde{d}^c - \tilde{e}^{c*}\mathbf{m}_e^2\tilde{e}^c\\ &-m_{H_u}^2H_u^*H_u - m_{H_d}^2H_d^*H_d - (B_0\mu H_uH_d + \text{c.c.})\,. \end{aligned} \tag{2.3.14}$$

Another advantage of the MSSM over the Standard Model is that it provides a mechanism for electroweak symmetry breaking, in a dynamical way [170,171,182]. The scalar potential of the MSSM for the neutral components of the Higgs multiplets can be obtained from the full scalar potential in eq. (2.3.9). The relevant part of the Higgs scalar potential will then look like [155]

$$\begin{aligned}V = \;&(|\mu|^2 + m_{H_u}^2)|H_u^0|^2 + (|\mu|^2 + m_{H_d}^2)|H_d^0|^2 - (B\mu H_u^0H_d^0 + \text{c.c.})\\ &+\frac{1}{8}(g^2 + g'^2)(|H_u^0|^2 - |H_d^0|^2)^2. \end{aligned} \tag{2.3.15}$$

The conditions for this scalar potential to have a non-trivial minimum, consistent with the SM minimum, are [155]

$$\begin{aligned}m_{H_u}^2 + |\mu|^2 - B\mu\cot\beta - \frac{1}{2}M_Z^2\cos(2\beta) = 0,\\ m_{H_d}^2 + |\mu|^2 - B\mu\tan\beta + \frac{1}{2}M_Z^2\cos(2\beta) = 0, \end{aligned} \tag{2.3.16}$$

where M_Z is the mass of the Z boson, $M_Z^2 = \frac{1}{2}v^2(g^2 + g'^2)$, and β is defined through the ratio of the vacuum expectation values of H_u^0 and H_d^0

$$\tan\beta = \frac{v_u}{v_d}, \tag{2.3.17}$$

with $v_u = \langle H_u^0\rangle$ and $v_d = \langle H_d^0\rangle$.

Hence, the conditions in (2.3.16) imply that there is a minimum in the potential that breaks the electroweak symmetry, and that minimum depends on the value of the soft SUSY breaking parameters $m_{H_u}^2$ and $m_{H_d}^2$. One or both of these parameters can be driven to be negative around the EW scale [170], mainly due to the large Yukawa coupling of the top quark during the evolution of the Renormalisation Group Equations (RGEs), thus providing a dynamical mechanism of symmetry breaking.

After electroweak symmetry breaking, three out of the eight components of the Higgs doublets will become Nambu-Goldstone bosons, acting as the longitudinal

degrees of freedom of the gauge fields. The other five components will be massive states, two CP-even, h and H, one CP-odd, A, and two charged Higgses, $H^{\pm}$, which will have the tree level masses [155]

$$\begin{aligned} m_A^2 &= 2|\mu|^2 + m_{H_u}^2 + m_{H_d}^2, \\ m_{H^\pm}^2 &= m_A^2 + M_W^2, \\ m_{h,H}^2 &= \frac{1}{2}\left(m_A^2 + M_Z^2 \mp \sqrt{(m_A^2 - M_Z^2)^2 + 4M_Z^2 m_A^2 \sin^2(2\beta)} \right). \end{aligned} \tag{2.3.18}$$

The lightest higgs boson h will have SM-like properties, provided the mixing between h and H is small.

Many of the other supersymmetric particles will also have mass eigenstates that differ from the interacting states The sfermions mix due to the Yukawa couplings of the superpotential, eq. (2.3.13) and the A-terms in the soft SUSY breaking Lagrangian, eq. (2.3.14), whereas the gauginos mix due to the electroweak symmetry breaking D-terms. Their mass terms in the lagrangian will look like

$$\mathcal{L} \supset -\frac{1}{2}(\tilde{F}^\dagger)^i \left(\mathbf{M}_{\tilde{f}}^2\right)_i^j (\tilde{F})_j - \frac{1}{2}(\tilde{N})^T \mathbf{M}_{\tilde{N}} (\tilde{N}) - \frac{1}{2}(\tilde{C}^\pm)^T \mathbf{M}_{\tilde{C}} (\tilde{C}^\pm), \tag{2.3.19}$$

where $\tilde{F}_j = (\tilde{f}_L, \tilde{f}_R)_j^T$ are the jth generation of sfermions, $\tilde{N} = (\tilde{B}, \tilde{W}^3, \tilde{H}_d^0, \tilde{H}_u^0)^T$ are the neutral gauginos and higgsinos, and $\tilde{C}^\pm = (\tilde{W}^\pm, \tilde{H}^\pm)^T$ are the charged gauginos and higgsinos. The mass matrix of the sfermions can be written as [183, 184]

$$\mathbf{M}_{\tilde{f}}^2 = \begin{pmatrix} \mathbf{m}_{\tilde{f}_L}^2 + \mathbf{m}_f^2 + D_{\tilde{f}_L}\mathbf{1} & \mathbf{m}_f(A_f - \mu\ (\tan\beta)^\varepsilon) \\ \mathbf{m}_f(A_f - \mu\ (\tan\beta)^\varepsilon) & \mathbf{m}_{\tilde{f}_R}^2 + \mathbf{m}_f^2 + D_{\tilde{f}_R}\mathbf{1} \end{pmatrix}, \tag{2.3.20}$$

where the quantities in bold face are 3×3 matrices in flavour space and $\mathbf{1} = \delta_j^i$; $\mathbf{m}_{\tilde{f}_L}^2$ and $\mathbf{m}_{\tilde{f}_R}^2$ are the soft SUSY breaking masses for the left-handed ($\tilde{Q}$, $\tilde{L}$) and right-handed ($\tilde{u}^c$, $\tilde{d}^c$, $\tilde{e}^c$) sfermions in equation (2.3.14); $\mathbf{m}_f$ is the Yukawa-type mass of the corresponding fermions; A_f is the soft SUSY breaking trilinear coupling of the sfermion $\tilde{f}$; the exponent ε is -1 for up-type ($\tilde{u}$) and $+1$ for down-type sfermions ($\tilde{d}$, $\tilde{e}$); and $D_{\tilde{f}_L}$ and $D_{\tilde{f}_R}$ are the electroweak D-terms, derived from eq. (2.3.9) after electroweak symmetry breaking (EWSB), with values

$$\begin{aligned} D_{\tilde{f}_L} &= M_Z^2 \cos(2\beta)(T_f^3 - Q_f \sin^2\theta_W), \\ D_{\tilde{f}_R} &= M_Z^2 \cos(2\beta) Q_f \sin^2\theta_W, \end{aligned} \tag{2.3.21}$$

with T_f^3 and Q_f the third component of isospin and electric charge of the fermion f. Diagonalisation of this mass matrix will result in the mass eigenstates $\tilde{f}_1$ and $\tilde{f}_2$ and the unitary diagonalisation matrix describes the mixing.

The mass eigenstates of neutral gauginos and higgsinos are known as neutralinos and are labelled as $\tilde{\chi}_i^0$ with $i = 1, \ldots, 4$, ordered from lightest to heaviest. They are obtained through diagonalisation of the mass matrix

$$\mathbf{M}_{\tilde{N}} = \begin{pmatrix} M_1 & 0 & -M_Z \sin\theta_W \cos\beta & M_Z \sin\theta_W \sin\beta \\ 0 & M_2 & M_Z \cos\theta_W \cos\beta & M_Z \cos\theta_W \sin\beta \\ -M_Z \sin\theta_W \cos\beta & M_Z \cos\theta_W \cos\beta & 0 & -\mu \\ M_Z \sin\theta_W \sin\beta & M_Z \cos\theta_W \sin\beta & -\mu & 0 \end{pmatrix}, \tag{2.3.22}$$

where M_1 and M_2 are the soft masses of the $U(1)_Y$ and $SU(2)_L$ gauginos respectively, c.f eq. (2.3.14), and μ is the coupling of the bilinear term in the superpotential, c.f. eq. (2.3.13).

Similarly, the mass eigenstates of charged gauginos and higgsinos are called charginos and are labelled as $\tilde{\chi}_i^{\pm}$ for $i = 1, 2$. Their mass matrix is given by

$$\mathbf{M}_{\tilde{C}} = \begin{pmatrix} M_2 & \sqrt{2} M_W \sin\beta \\ \sqrt{2} M_W \cos\beta & \mu \end{pmatrix}. \tag{2.3.23}$$

It was mentioned before, in section 2.3.2, that it is commonplace to have universal soft SUSY breaking parameters at some high scale, typically around or at the unification scale. Phenomenologically this corresponds to the scenario known as "constrained" MSSM (CMSSM) and it is realised by applying the following boundary conditions at the universality scale

$$\begin{aligned} M_1 = M_2 = \ M_3 &= m_{1/2}, \\ \mathbf{m}_Q^2 = \mathbf{m}_L^2 = \mathbf{m}_u^2 = \mathbf{m}_d^2 = \ \mathbf{m}_e^2 &= m_0^2 \mathbf{1}, \\ m_{H_u}^2 = m_{H_d}^2 &= m_0^2, \\ A_u = \ A_d = \ A_e &= A_0. \end{aligned} \tag{2.3.24}$$

Their electroweak values will be obtained from the RGE running of the parameters to the electroweak scale. The full two-loop [185] set of RGEs for the MSSM can be found in Appendix A. As highlighted before, a consequence of the MSSM RGEs is that the gauge couplings unify at $M_{GUT} \simeq 2 \times 10^{16}$ GeV. The gauge RGEs and their conditions for unification will be discussed in chapter 4.

Despite the many advantages of supersymmetry and the MSSM in particular, no proof of its existence has been found so far. There are stringent constraints form low energy and direct searches. In particular, the ATLAS and CMS experiments at the LHC have found no signal for supersymmetry and the current exclusion limits

are pushing the parameter space to the heavier regions [14, 15]. As can be seen in figures 2.4 and 2.5, the limits for the masses for gluinos and first generation squarks lie around the $m_{\tilde{g}}, m_{\tilde{q}} \gtrsim 1$ TeV, whereas the limit on stops and sbottoms is around $m_{\tilde{t}}, m_{\tilde{b}} \gtrsim 500$ GeV. In the electroweak sector, the lower limit on the sleptons is $m_{\tilde{l}} \gtrsim 325$ GeV and a very broad limit for the heavy neutralinos and charginos $m_{\tilde{\chi}_2^0, \tilde{\chi}_1^\pm} \gtrsim 100 - 700$ GeV.

There have been several attempts to fit these results to the simplest versions of the MSSM, namely the CMSSM mentioned before, and non-universal Higgs models, which extend the CMSSM by allowing the masses of the Higgs doublets to be different than m_0, either equal among themselves (NUMH1) or different (NUHM2) [186–189].

Heavy masses for supersymmetric particles, in particular the stops, put pressure on the hierarchy solution, because the partial cancellations of the diagrams in figure 2.3 depend on the mass difference between the top quark and the lightest stop [155]. The experimental exclusion limits are based on specific minimal models, like the CMSSM, but there are still non-minimal models that are consistent with the searches, while still keeping a reasonably low particle spectrum, such as "effective" supersymmetry [190], "focus point" supersymmetry [191], "compressed" supersymmetry [192] or R-parity violating supersymmetry [193].

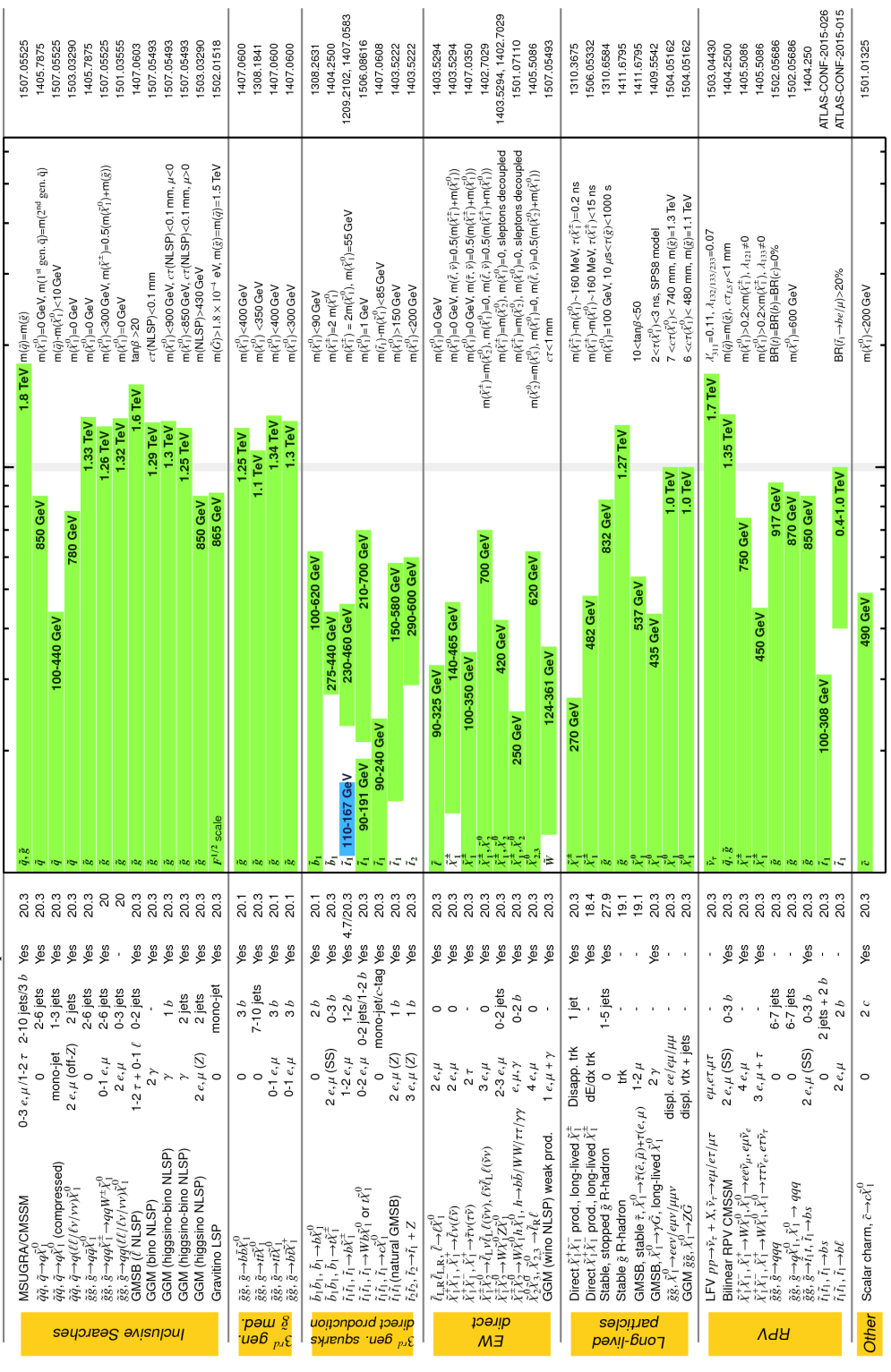

Figure 2.4: *Searches for supersymmetry and current limits from the ATLAS collaboratios, taken from [194].*

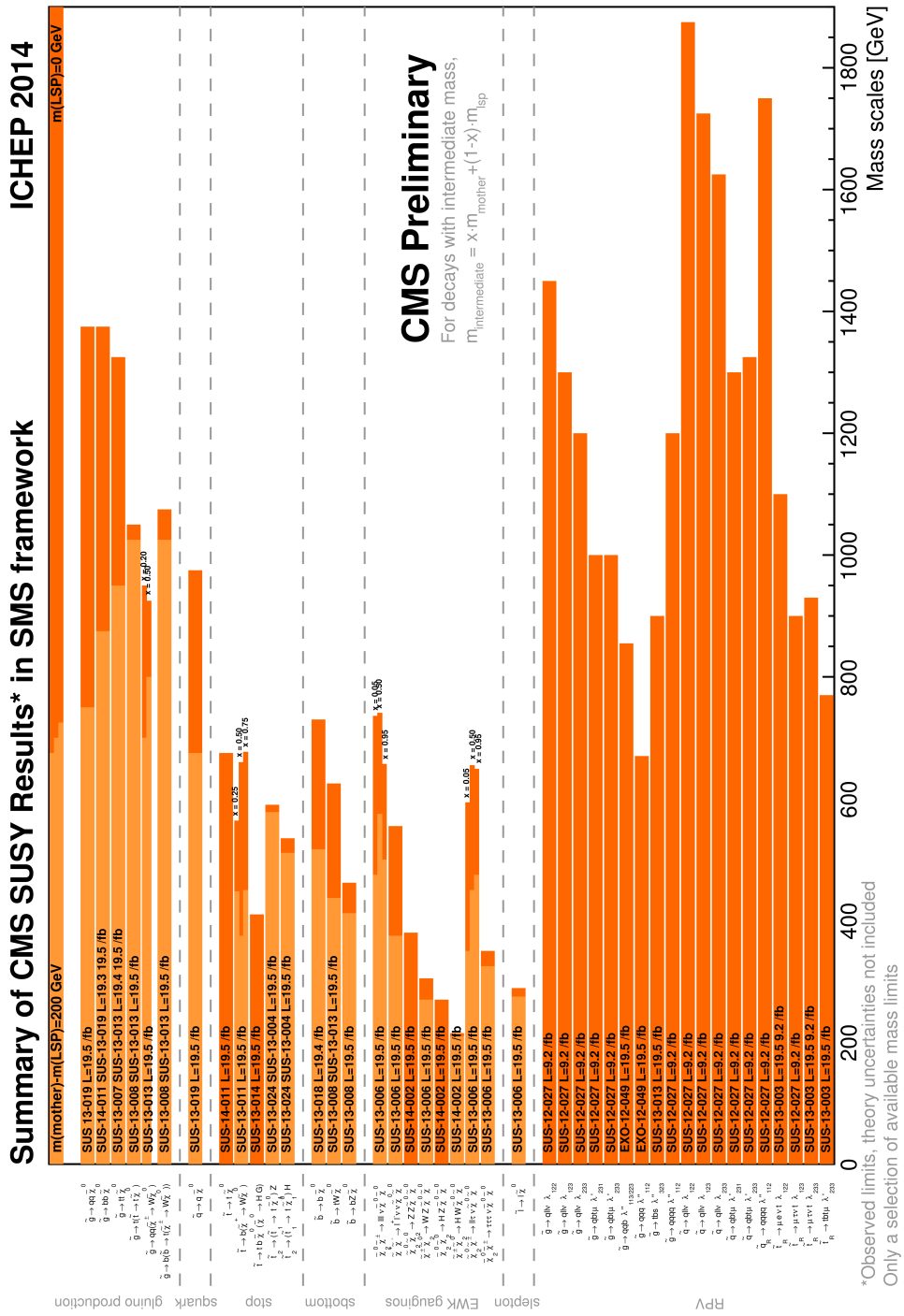

Figure 2.5: *Searches for supersymmetry and current limits from the CMS collaboration, taken from [195].*

3

Symmetries and Lie Groups

In every area of physics, symmetries play an essential role for they provide a useful tool to solve complicated systems and classify elements of a theory. These symmetries are precisely the result of system's invariance under certain transformations, and the set of these transformations is a mathematical object called a *Group*. In particular, in quantum mechanics, groups serve to classify the states, vectors in the Hilbert space, according to objects called *representations* of the group. They also provide conserved quantities that simplify the theory and, in most cases, can be tested experimentally. Furthermore, a specific type of groups, called *Lie Groups*, are particularly useful, because they are parametrized by a finite set of continuous parameters and can thus describe continuous transformations to the quantum states.

Historically, the first Lie Group to become relevant in quantum theory was the group of three-dimensional rotations, or $SO(3)$, associated with the quantum mechanical treatment of angular momentum, used to describe atomic energy levels [196]; but a lot of effort has gone into applying the theory of Lie Groups to internal symmetries of the fundamental particles, where groups such as $SU(3)$ or $SU(2)$ provide a classification according to colour charges and weak isospins, respectively [1–3].

Throughout this chapter we will provide the **Definition** of groups and Lie groups, as well as their **Lie algebras** and **Representations**. We will describe what is the **Cartan Classification of Simple Lie Algebras** which will motivate the creation of a **Group Theory Tool**, whose features and algorithms will be described in detail. Finally we will give an overview of the **Implementation** of the group tool and conclude with an **Example Run** of the program for a sample group.

3.1 Definition

A *Group* [197–199], $\mathcal{G}$, is defined as the aggregate of a set of elements $\{g_i\}$, finite or infinite, and an operation, $g_1 \cdot g_2 = g_1\ g_2$, with $g_1, g_2 \in \mathcal{G}$. The group operation satisfies four fundamental properties, which are

- Closure: let g_1 and g_2 be two elements of $\mathcal{G}$, then the element $h = g_1\ g_2$ is also an element of the group.
- Associativity: let g_1, g_2 and g_3 be elements of the group, then $(g_1\ g_2)\ g_3 = g_1\ (g_2\ g_3)$.
- Identity: there is an element in $\mathcal{G}$, e, such that $g_i\ e = g_i$, for all g_i in the group.
- Invertibility: for every g_i in the group, there is an element h_i in $\mathcal{G}$, such that $g_i\ h_i = e$.

A *Lie Group* [197–199] $\mathcal{G}$ is an infinite group (a group with an infinite number of elements) that has the structure of a differentiable manifold[1]. The elements of the group will depend on a set of continuous parameters α, where $\alpha \in \mathcal{M}_\mathcal{G}$, for $\mathcal{M}_\mathcal{G}$ the n-dimensional (n a positive integer) differentiable manifold associated with the Lie group. If ψ is a coordinate chart on $\mathcal{M}_\mathcal{G}$ then $(\alpha^1, \ldots, \alpha^n) \in \mathbb{R}^n$ are local coordinates of α defined as $\alpha^j = \psi(\alpha)^j$. Henceforth we will represent an element of the Lie Group as $g(\alpha)$, defined as a map $g : \mathcal{M}_\mathcal{G} \to \mathcal{G}$.

Since $\mathcal{G}$ is a group, it must satisfy the group properties described above, closure, associativity, identity and invertibility. In a Lie group the group operation is

$$g(\alpha)\ g(\beta) = g(\gamma) \Rightarrow \gamma^j = \phi^j(\alpha, \beta), \quad j = 1, \ldots, n. \tag{3.1.1}$$

where β and γ are different points on $\mathcal{M}_\mathcal{G}$ with coordinates $\beta^j = \psi(\beta)^j$ and $\gamma^j = \psi(\gamma)^j$, and ϕ^j are local coordinates through the coordinate chart ψ of a smooth map $\phi : \mathcal{M}_\mathcal{G} \times \mathcal{M}_\mathcal{G} \to \mathcal{M}_\mathcal{G}$, as is required by the closure property of the group. The identity e of the group can be chosen as the origin of the coordinate chart for convenience, so that,

$$\begin{aligned} g(0) = e \Rightarrow g(0)\ g(\alpha) = g(\alpha)\ g(0) = g(\alpha) \\ \Rightarrow \phi^j(0, \alpha) = \phi^j(\alpha, 0) = \alpha^j. \end{aligned} \tag{3.1.2}$$

[1] An *n-dimensional manifold* is a topological space that is locally homeomorphic to $\mathbb{R}^n$. A *differentiable manifold* is a manifold together with a collection of smooth maps or coordinate charts, ψ, that cover all the manifold and are such that the change of coordinate charts in overlapping regions is smooth.

With this identity we can define the inverse $g(\alpha)^{-1}$ or $g(\bar{\alpha})$ of the element $g(\alpha)$ so that

$$\begin{aligned} & g(\alpha)^{-1}\ g(\alpha) = g(\bar{\alpha})\ g(\alpha) = g(\alpha)\ g(\alpha)^{-1} = g(\alpha)\ g(\bar{\alpha}) = e \\ & \Rightarrow \phi^j(\bar{\alpha}, \alpha) = \phi^j(\alpha, \bar{\alpha}) = 0. \end{aligned} \tag{3.1.3}$$

The associativity of the group elements is realised as

$$\begin{aligned} & (g(\alpha)\ g(\beta))\ \ g(\gamma) = g(\alpha)\ \ (g(\beta)\ g(\gamma)) \\ & \Rightarrow \phi^j(\phi(\alpha, \beta), \gamma) = \phi^j(\alpha, \phi(\beta, \gamma)). \end{aligned} \tag{3.1.4}$$

Some groups also satisfy commutativity relations, these are called *abelian Groups*, so that,

$$g(\alpha)\ g(\beta) = g(\beta)\ g(\alpha) \quad \Rightarrow \quad \phi(\alpha, \beta) = \phi(\beta, \alpha). \tag{3.1.5}$$

A subset of elements of the Lie group $\mathcal{G}$ defines a *subgroup* if it is closed under the operation of the group, i.e. if $\mathcal{H}$ is a subgroup of $\mathcal{G}$ and $h(\alpha)$ and $h(\beta)$ are elements of $\mathcal{H}$, then the element $h(\gamma) = h(\alpha)\ h(\beta)$ is also an element of $\mathcal{H}$. Furthermore, a *normal* or *invariant subgroup* of a Lie group $\mathcal{G}$ refers to the subgroup $\mathcal{H}$, whose elements $h(\alpha)$ satisfy the property $g(\beta)\ h(\alpha)\ g(\beta)^{-1} \in \mathcal{H}$ for all elements $g(\beta) \in \mathcal{G}$.

3.2 Lie algebras

If we consider an element close to the identity $g(\epsilon)$, so that when multiplied by an arbitrary group element $g(\alpha)$,

$$\begin{aligned} & g(\alpha)g(\epsilon) = g(\alpha + \delta\alpha) \\ \Rightarrow \quad & \alpha^j + \delta\alpha^j = \phi^j(\alpha, \epsilon) = \alpha^j + \epsilon^a\ \frac{\partial \phi^j(\alpha, \epsilon)}{\partial \epsilon^a}\bigg|_{\epsilon=0}, \end{aligned} \tag{3.2.1}$$

where repeated indices are summed over and $a = 1, \ldots, n$ labels a direction in the tangent space of $\mathcal{M}_\mathcal{G}$ around the identity, $T_e(\mathcal{M}_\mathcal{G})$[2]. We can then define the generators of the group $\mathcal{G}$, using the basis induced by the coordinate system α^i in the tangent space, as

$$T_a = \frac{\partial \phi^j(\alpha, \epsilon)}{\partial \epsilon^a}\bigg|_{\epsilon=0} \frac{\partial}{\partial \alpha^j}. \tag{3.2.2}$$

[2]The tangent space, $T_p(\mathcal{M}_\mathcal{G})$ of a manifold $\mathcal{M}_\mathcal{G}$ around the point p is the vector space of all possible directions tangent to p.

where sum over the index j is assumed.

However, the coordinate basis $\frac{\partial}{\partial \alpha^j}$ is chart-dependent, so it is not a good basis for the tangent space. Fortunately, the generators T_a are independent of the chart, as we will show next, so they will be a good basis for the tangent space. In order to prove this, consider a different chart on α, $\psi'(\alpha)^i = \alpha'^i$, and expanding similarly we obtain[3],

$$\delta\alpha'^j = \epsilon^a \left.\frac{\partial \phi'^j(\alpha,\epsilon)}{\partial \epsilon^a}\right|_{\epsilon=0}, \tag{3.2.4}$$

then, using that since $\phi(\alpha,\epsilon)$ is a smooth function its derivative is invertible, from (3.2.1) we have that

$$\begin{aligned} \delta\alpha'^j &= \delta\alpha^l \left[\left.\frac{\partial \phi^l(\alpha,\epsilon)}{\partial \epsilon^a}\right|_{\epsilon=0}\right]^{-1} \left.\frac{\partial \phi'^j(\alpha,\epsilon)}{\partial \epsilon^a}\right|_{\epsilon=0} \\ \Rightarrow \frac{\partial \alpha'^j}{\partial \alpha^l} &= \left[\left.\frac{\partial \phi^l(\alpha,\epsilon)}{\partial \epsilon^a}\right|_{\epsilon=0}\right]^{-1} \left.\frac{\partial \phi'^j(\alpha,\epsilon)}{\partial \epsilon^a}\right|_{\epsilon=0}. \end{aligned} \tag{3.2.5}$$

Then the definition of the generators,

$$T_a = \left.\frac{\partial \phi^k(\alpha,\epsilon)}{\partial \epsilon^a}\right|_{\epsilon=0} \frac{\partial \alpha'^j}{\partial \alpha^k}\frac{\partial}{\partial \alpha'^j} = \left.\frac{\partial \phi'^k(\alpha,\epsilon)}{\partial \epsilon^a}\right|_{\epsilon=0} \frac{\partial}{\partial \alpha'^k}, \tag{3.2.6}$$

is the same in every coordinate chart, and is therefore a good basis for $T_e(\mathcal{M}_\mathcal{G})$.

We will now define the *Lie algebra* $\mathfrak{g}$ of the Lie Group $\mathcal{G}$ as the vector tangent space $T_e(\mathcal{M}_\mathcal{G})$, i.e. the vector space spanned by the generators T_a of the Lie group, $\mathfrak{g} = \{\epsilon^a T_a\}$.

For any element $\epsilon^a T_a \in \mathfrak{g}$ there is a *one-parameter subgroup* of the associated Lie Group $\mathcal{G}$ corresponding to a path in $\mathcal{M}_\mathcal{G}$ whose tangent at the identity is $\epsilon^a T_a$ [197–199]. Using coordinates α^j, the path can be defined as $\alpha^j(s)$ with $s \in \mathbb{R}$ and defining T_a^j as the components of T_a in the coordinate basis of $T_e(\mathcal{M}_\mathcal{G})$, we have that

$$\frac{d}{ds}\alpha_s^j = \epsilon^a T_a^j(\alpha_s), \tag{3.2.7}$$

[3]The expression is independent of the chart used for the ϵ since the actual expression for $\delta\alpha^j$ should be

$$\delta\alpha^j = \epsilon(\phi^j(\alpha,\epsilon))\big|_{\epsilon=0}, \tag{3.2.3}$$

where, in an abuse of notation, ϵ refers to a vector field tangent at the identity to the curve that passes through ϵ (the point in $\mathcal{M}_\mathcal{G}$). Hence, since the vector field ϵ is used without referring to a particular basis, is chart-independent and then expression (3.2.4) is independent of the chart used to define ϵ^a.

or written in terms of the group elements $g(\alpha_s)$:

$$\frac{d}{ds}g(\alpha_s) = \epsilon^a T_a(\alpha_s)g(\alpha_s). \tag{3.2.8}$$

It can be proven that one-parameter subgroups, as abelian subgroups, have the properties [198]

$$\begin{aligned} g(\alpha_s)g(\alpha_t) &= g(\alpha_{s+t}), \\ g(\alpha_0) &= e, \\ g(\alpha_s)^{-1} &= g(\alpha_{-s}), \end{aligned} \tag{3.2.9}$$

with $\alpha_0 = (0, \ldots, 0)$. Solving (3.2.8) for the group element $g(\alpha_s)$ together with the identity condition in (3.2.9), we can define an *exponential map*, so that

$$\begin{aligned} \exp: \quad \mathfrak{g} \quad &\to \quad \mathcal{G}, \\ \epsilon^a T_a \to g(\alpha_s) &= \exp(s\epsilon^a T_a). \end{aligned} \tag{3.2.10}$$

where the exponential is defined in terms of its power series[4]

$$\exp(s\epsilon^a T_a) = \sum_{n=0}^{\infty} \frac{1}{n!}(s\epsilon^a T_a)^n. \tag{3.2.12}$$

From differential geometry we know that any tangent space of a manifold $\mathcal{M}$ at a point x, $T_x(\mathcal{M})$ is equipped with a *Lie bracket* or *commutator* that is closed within the tangent space, i.e., for two vector fields $X, Y \in T_x(\mathcal{M})$, the commutator $[X, Y] \in T_x(\mathcal{M})$ defines a further vector field [197]. In our case, this means that $X, Y \in \mathfrak{g} \Rightarrow [X, Y] \in \mathfrak{g}$ that also follows from closure on $\mathcal{G}$, or using the basis of the Lie algebra $\mathfrak{g}$, i.e. the generators of $\mathcal{G}$,

$$[T_a, T_b] = f_{ab}^c T_c, \tag{3.2.13}$$

where f_{ab}^c are constants known as *structure constants* and from the definition we have that $f_{ab}^c = -f_{ba}^c$. These structure constants actually classify the Lie algebras, as we will see later. Lie algebras with the same structure constants are isomorphic, e.g. $\mathfrak{su}(2) \cong \mathfrak{so}(3)$.

[4]This exponential is not the same as the exponential of scalars, since $e^{tX}e^{tY} \neq e^{tX+tY}$, but

$$e^{tX}e^{tY} = e^{tX+tY+\frac{1}{2}t^2[X,Y]+\frac{1}{12}t^3([X,[X,Y]]-[Y,[X,Y]])+O(t^4)}. \tag{3.2.11}$$

This expression is known as the Baker-Campbell-Hausdorff formula (see [197] for further details).

Since the commutators satisfy the Jacobi identity, $[X,[Y,Z]]+[Y,[Z,X]]+[Z,[X,Y]]=0$, there is a analogous Jacobi identity for the structure constants that reads:

$$f^e_{ad}f^d_{bc}+f^e_{bd}f^d_{ca}+f^e_{cd}f^d_{ab}=0. \tag{3.2.14}$$

Through the exponential map, eq. (3.2.13) can be obtained simply by imposing closure for the Lie Group $\mathcal{G}$,

$$\begin{aligned} g(\alpha_s) &= g(\alpha_t)g(\alpha_r), \\ \exp(s\epsilon^a T_a) &= \exp(t\epsilon^a T_a)\exp(r\epsilon^a T_a). \end{aligned} \tag{3.2.15}$$

Taking the logarithm on both sides and absorbing the parameters s, r and t into ϵ^a, θ^a and η^a, we can express this as[5]:

$$\begin{aligned} \epsilon^a T_a &= \log\left[(\exp(\theta^a T_a)\exp(\eta^a T_a)\right] \\ &= \log\left[1+\theta^a T_a+\eta^a T_a+\theta^a\eta^b T_aT_b+\dots\right] \\ &= \theta^a T_a+\eta^a T_a+\theta^a\eta^b T_aT_b-\frac{1}{2}\theta^a\eta^b T_aT_b-\frac{1}{2}\eta^a\theta^b T_aT_b+\dots \\ &= \theta^a T_a+\eta^a T_a+\tfrac{1}{2}\theta^a\eta^b[T_a,T_b]+\dots, \end{aligned} \tag{3.2.17}$$

where we have neglected terms of order θ^2 and η^2. Therefore, at that order, we have

$$\theta^a\eta^b[T_a,T_b]=2(\epsilon^c-\theta^c-\eta^c)T_c, \tag{3.2.18}$$

and since this is true for all values of θ^a and η^a, we can define the structure constants as $\theta^a\eta^b f^c_{ab}=2(\epsilon^c-\theta^c-\eta^c)$ so that

$$[T_a,T_b]=f^c_{ab}T_c. \tag{3.2.19}$$

Moreover, the exponential map allows us to define some of the concepts for the groups directly in the Lie algebra. For instance, we will define a Lie algebra as *abelian* if all the commutators are zero, $[X,Y]=0$ for all $X,Y\in\mathfrak{g}$. Using the Baker-Campbell-Hausdorff formula, for an abelian Lie algebra we have that $e^{tX}e^{tY}=e^{tX+tY}$ and then if $g(\alpha_t)=e^{tX}, g(\beta_t)=e^{tY}$,

$$g(\alpha_t)g(\beta_t)=e^{tX}e^{tY}=e^{tX+tY}=e^{tY}e^{tX}=g(\beta_t)g(\alpha_t). \tag{3.2.20}$$

[5]Same as with the exponential, the logarithm here is defined by its power series

$$\log(1+X)=\sum_{n=1}^{\infty}\frac{(-1)^{n+1}}{n}X^n. \tag{3.2.16}$$

Similarly as with groups we can define a *subalgebra* $\mathfrak{h} \subset \mathfrak{g}$ as the subset of $\mathfrak{g}$ that is closed under conmutation. If $\mathcal{H} \subset \mathcal{G}$ is a subgroup, then its Lie algebra $\mathfrak{h}$ is a subalgebra of $\mathfrak{g}$. A subalgebra $\mathfrak{h}$ is an *invariant subalgebra* or *ideal* if $\mathcal{H}$ is a normal subgroup of $\mathcal{G}$ and will satisfy,

$$[X, Y] \in \mathfrak{h} \quad \text{for all} \quad Y \in \mathfrak{h}, X \in \mathfrak{g}. \tag{3.2.21}$$

A Lie algebra is *simple* if it does not contain any invariant subalgebra. A Lie algebra is *semisimple* if it does not contain any invariant abelian subalgebra. Obviously if an algebra is simple it is also semisimple. Semisimple algebras are a very powerful tool since they can be decomposed as the direct product of simple subalgebras [198, 199].

3.3 Representations

A *representation* $\mathcal{R}$ of a group is a map $\mathcal{R} : \mathcal{G} \to GL(n)$[6], that maps every element of the group $g(\alpha)$, onto a square matrix $D(g(\alpha)) \equiv D(\alpha)$. The dimension of the representation is the dimension of the matrix $D(\alpha)$. A representation realises the group multiplication law as a usual matrix multiplication,

$$D(g(\alpha)g(\beta)) = D(g(\alpha))D(g(\beta)) = D(\alpha)D(\beta). \tag{3.3.1}$$

For group elements close to the identity with infinitesimal parameters ϵ^a we can write,

$$D(\epsilon) = \mathbb{1} + \epsilon^a t_a, \tag{3.3.2}$$

where t_a are a set of n matrices that form a basis of the representation. These matrices are the generators of the group in the representation $\mathcal{R}$. To verify this consider an infinitesimal variation of the point α,

$$\begin{aligned} D(\alpha + \delta\alpha) &= D(g(\alpha + \delta\alpha)) = D(g(\alpha)g(\epsilon)) = D(g(\alpha))D(g(\epsilon)) \\ &= D(\alpha)D(\epsilon) = D(\alpha)(\mathbb{1} + \epsilon^a t_a) = D(\alpha) + D(\alpha)\epsilon^a t_a. \end{aligned} \tag{3.3.3}$$

On the other hand, using (3.2.1) and (3.2.2),

$$D(\alpha + \delta\alpha) = D(\alpha) + \delta\alpha^j \frac{\partial}{\partial \alpha^j} D(\alpha) = D(\alpha) + \epsilon^a T_a D(\alpha). \tag{3.3.4}$$

[6]The General Linear Group $GL(n)$ is the group of $n \times n$ invertible matrices with the matrix multiplication as its operation.

So $t_a = D(\alpha)^{-1} T_a D(\alpha)$ and then the matrices t_a obey the same commutation relation as do T_a, the generators of the Lie Group and, therefore, are the generators of the group in the representation $\mathcal{R}$,

$$\begin{aligned}[t_a, t_b] &= [D(\alpha)^{-1} T_a D(\alpha), D(\alpha)^{-1} T_b D(\alpha)] \\ &= D(\alpha)^{-1} [T_a, T_b] D(\alpha) \\ &= f_{ab}^c D(\alpha)^{-1} T_c D(\alpha) \\ &= f_{ab}^c t_c.\end{aligned} \tag{3.3.5}$$

This shows that the representation $\mathcal{R}$ not only maps group elements to matrices, but it also acts on the Lie algebra, $\mathcal{R} : \mathfrak{g} \to GL(n)$, so that for an element $X \in \mathfrak{g}$, the representation assigns a matrix $D(X)$. In particular, we can write $D(T_a) = t_a$ as a representation of the generators.

Let us consider the representation of an element of $\mathcal{G}$ close to the identity

$$D(g(\epsilon)) = \mathbb{1} + \epsilon^a t_a + O(\epsilon^2), \quad D(g(\epsilon))^{-1} = \mathbb{1} - \epsilon^a t_a + O(\epsilon^2). \tag{3.3.6}$$

If the matrices of the representation, $D(g)$, are unitary matrices, i.e. they obey $D(g)^{-1} = D(g)^\dagger$, then the matrix generators are anti-hermitian,

$$t_a^\dagger = -t_a. \tag{3.3.7}$$

Similarly if the $D(g)$ are orthogonal, i.e. $D(g)^{-1} = D(g)^T$, the generators are antisymmetric

$$t_a^T = -t_a. \tag{3.3.8}$$

Further, if the matrices $D(g)$ have unit determinant, $\det(D(g)) = 1$, then we may use the identity $\det(D(g)) = \det(\mathbb{1} + \epsilon^a t_a + O(\epsilon^2)) = 1 + \epsilon^a \mathrm{tr}(t_a) + O(\epsilon^2)$, to get that the generators are traceless

$$\mathrm{tr}(t_a) = 0. \tag{3.3.9}$$

A representation $D(g)$ is *reducible* if it has an invariant subspace, i.e. there exists a set of vectors in the representation space that is closed under the action of the elements on the representation. Conversely, a representation $D(g)$ is *irreducible*, usually called *irrep*, if it has no invariant subspaces.

The complex conjugate of a representation (complex conjugate of all the matrix elements of the representation) is also a representation of the algebra, for its

generators, often denoted as t_a^* or $\bar{t}_a$, satisfy the commutation relations of the algebra. In general a representation and its conjugate are not equivalent[7], and the representation t_a is said to be a *complex* representation, but for some cases, e.g. for $SU(2)$, they are equivalent, i.e., for some C,

$$t_a^* = -t_a^T = C t_a C^{-1}. \tag{3.3.10}$$

By the use of Schur's lemma, it is possible to deduce that $C^T = \pm C$ [198]. Whether the sign is plus or minus will classify the representations as *real* and *pseudo-real*, respectively.

In matrix Lie Groups, if the generators in a representation t_a are precisely the generators T_a, then the representation is said to be the *fundamental representation* of the algebra.

There is a representation of every Lie algebra that deserves special mention. The *adjoint representation* of a Lie algebra $\mathfrak{g}$ is the representation that spans over the vector space of the Lie algebra. The generators of the adjoint representation t_a^{ad} are defined in such a way that when they act on elements of the Lie algebra, $Y \in \mathfrak{g}, t_a^{\text{ad}} Y = [T_a, Y]$[8]. If we apply such generators of the adjoint representation to the generators T_a, we get

$$t_a^{\text{ad}} T_b = [T_a, T_b] = f_{ab}^c T_c \quad \Rightarrow (t_a^{\text{ad}})_b^c = f_{ab}^c. \tag{3.3.11}$$

The generators of the adjoint representation are therefore given by the structure constants. By virtue of the Jacobi identity for structure constants, eq. (3.2.14), we get that the generators of the adjoint representation satisfy the Lie algebra,

$$\begin{aligned} [t_a^{\text{ad}}, t_b^{\text{ad}}]_d^e &= (t_a^{\text{ad}} t_b^{\text{ad}})_d^e - (t_b^{\text{ad}} t_a^{\text{ad}})_d^e \\ &= (t_a^{\text{ad}})_c^e (t_b^{\text{ad}})_d^c - (t_b^{\text{ad}})_c^e (t_a^{\text{ad}})_d^c \\ &= f_{ac}^e f_{bd}^c - f_{bc}^e f_{ad}^c \\ &= f_{dc}^e f_{ba}^c = f_{ab}^c f_{cd}^e \\ &= f_{ab}^c (t_c^{\text{ad}})_d^e \\ \Rightarrow [t_a^{\text{ad}}, t_b^{\text{ad}}] &= f_{ab}^c t_c^{\text{ad}}. \end{aligned} \tag{3.3.12}$$

[7] Two representations of a group element $D(g)$ and $D'(g)$ are equivalent if $D'(g) = A^{-1} D(g) A$ for a similarity transformation A (linear and invertible) [199].

[8] As a matter of fact, the generators of the adjoint representations are defined by virtue of the *adjoint map*, $\text{ad} : \mathfrak{g} \to \mathfrak{g}$, that acts on every vector of the Lie algebra. For the generators $\text{ad}(T_a) = t_a^{\text{ad}}$, and for any $X \in \mathfrak{g}$, $\text{ad}(X) = X^{\text{ad}}$.

The adjoint representation can be used to construct an invariant symmetric bilinear form, characteristic of the Lie algebra, called the *Killing form*, which is defined as

$$\kappa(X,Y) = \mathrm{tr}(X^{\mathrm{ad}}Y^{\mathrm{ad}}) \quad \text{for all} \quad X,Y \in \mathfrak{g}, \tag{3.3.13}$$

where the trace is defined as the sum over the vector space of $\mathfrak{g}$. The Killing form can be written using a basis as,

$$\kappa_{ab} = \kappa(T_a, T_b), \tag{3.3.14}$$

so that $\kappa(X,Y) = \kappa_{ab}X^aY^b$. It is clearly symmetric, $\kappa_{ab} = \kappa_{ba}$, and obeys

$$\kappa([Z,X],Y) + \kappa(X,[Z,Y]) = 0, \tag{3.3.15}$$

which can be easily proven by the properties of the trace and the adjoint representation. This expression can be written in components as,

$$\kappa_{db}f^d_{ca} + \kappa_{ad}f^d_{cb} = 0, \tag{3.3.16}$$

or, by defining $f_{abc} \equiv f^d_{ab}\kappa_{dc}$, as

$$f_{cab} + f_{cba} = 0, \tag{3.3.17}$$

which makes f_{abc} a completely antisymmetric tensor, since it was already antisymmetric in the first two indices from the commutator properties.

It can be proven that the Killing form is non-degenerate if and only if the algebra is semisimple [198], which makes the Killing form especially useful in physics, because it can act as a metric for the manifold. This means that the Killing form $\kappa \equiv [\kappa_{ab}]$ has an inverse $\kappa^{-1} \equiv [\kappa^{ab}]$, so that $\kappa^{ab}\kappa_{bc} = \delta^a_c$, and then κ_{ab} and κ^{ab} can be used to raise and lower indices. With the inverse Killing form we can obtain an expression similar to eq. (3.3.16)

$$f^b_{ad}\kappa^{dc} + f^c_{ad}\kappa^{bd} = 0. \tag{3.3.18}$$

We can now define the *Casimir operator* of a semisimple Lie algebra in the representation spanned by $\{t_a\}$ as

$$C = \kappa^{ab}t_at_b. \tag{3.3.19}$$

This operator commutes with all the generators of the algebra,

$$\begin{aligned}[t_a, C] &= [t_a, \kappa^{bc}t_bt_c] = \kappa^{bc}([t_a,t_b]t_c + t_b[t_a,t_c]) \\ &= \kappa^{bc}(f^d_{ab}t_dt_c + f^d_{ac}t_bt_d) = (\kappa^{bc}f^d_{ab} + \kappa^{db}f^c_{ab})t_dt_c = 0.\end{aligned} \tag{3.3.20}$$

Some examples of Casimir operators for well known groups are the squared angular momentum operator, $J^2 = J_1^2 + J_2^2 + J_3^2$, that is the Casimir of the $SO(3)$ group, or for the Poincaré group, isomorphic to $SU(2) \otimes SU(2)$, the squared Pauli-Lubanski vector $W^2 = W_\mu W^\mu$, $W^\mu = \frac{1}{2}\epsilon^{\mu\nu\sigma\rho} P_\nu M_{\sigma\rho}$, with P_ν the generator of translations and $M_{\sigma\rho}$ the generator of the Lorentz transformations.

Lastly we define the symmetrized trace tensor d_{abc} of the representation $\mathcal{R}$, with generators $\{t_a\}$, as

$$d_{abc} = \mathrm{tr}[\{t_a, t_b\} t_c]. \tag{3.3.21}$$

3.4 Cartan Classification of Simple Lie Algebras

Simple algebras are a very special type of algebra since they do not have any invariant subalgebra other then the null algebra and itself. Furthermore, summing simple algebras it is possible to construct semisimple algebras, which makes simple algebras all the more useful, because semisimple algebras have non-trivial commutation relations among all its generators and they are good candidates to represent the symmetries of real physical systems. Over a 100 years ago, Élie Cartan classified all existing simple algebras into 4 series and 5 exceptional cases [200]. This classification is made on the basis of two features of the algebras: the rank and the simple roots.

The *Cartan subalgebra* $\mathfrak{h}$ of a simple algebra $\mathfrak{g}$ is the maximal set of commuting generators of the algebra, i.e.,

$$H_i, H_j \in \mathfrak{g} \quad \text{such that} \quad [H_i, H_j] = 0 \quad \text{with } H_i, H_j \in \mathfrak{h} \text{ and } i = 1, \ldots, r, \tag{3.4.1}$$

where r is the dimension of the Cartan subalgebra (the number of commuting generators), called the *rank* of the algebra. Here we have labelled the generators of the Cartan subalgebra with indices $i, j, \cdots = 1, \ldots, r$ and the rest of the generators we will label with indices $a, b, \cdots = r+1, \ldots, n$. Since the Cartan subalgebra cannot be an invariant subalgebra, as we are only working with simple algebras, then necessarily for $H_i \in \mathfrak{h}, T_a \in \mathfrak{g}$, $[H_i, T_a] \notin \mathfrak{h}$. Since all Cartan generators commute they can be simultanously diagonalised[9] so that for all $T_a \in \mathfrak{g}$ we have $[H_i, T_a] = f_{ia}^a T_a$ (no sum over a) for all i. Therefore, if we call $E_{\vec{\alpha}}$ the generators of $\mathfrak{g}$ that are not in $\mathfrak{h}$, then we have

$$[H_i, E_{\vec{\alpha}}] = \alpha_i E_{\vec{\alpha}}, \tag{3.4.2}$$

[9]That the generators can be simultaneously diagonalised means that in every representation of the Cartan generatros $D(H_i)$ there are eigenvectors v so that $D(H_i)v = \lambda_i v$, for all i.

where α_i are the components of the *roots* of the algebra. We will define the *root* or *root vector* $\vec{\alpha}$ as the vector of length r and components $\alpha_i, i = 1, \ldots, r$ that specifies the generator $E_{\vec{\alpha}}$ precisely, i.e. two generators cannot have the same root vector, a statement that will be proven later.

For a specific representation of the generators $D(H_i), D(E_{\vec{\alpha}})$, we can define the *weight*s as the eigenvalues of the generators of the Cartan subalgebra when acting on eigenvectors of the representation vector space. Since H_i can be simultaneously diagonalised, if we called v an eigenvector of all H_i in that representation, then

$$D(H_i)v = \omega_i v, \tag{3.4.3}$$

where ω_i is the component of the weight of the representation under the generator H_i. Similarly as with roots, we can define then the *weight* or *weight vector* $\vec{\omega}$, with the components ω_i.

If $\vec{\alpha}$ is a root then $-\vec{\alpha}$ is also a root, because if we take the hermitian conjugate of equation (3.4.2), we get

$$[H_i, E^\dagger_{\vec{\alpha}}] = -\alpha_i E^\dagger_{\vec{\alpha}}. \tag{3.4.4}$$

So $-\vec{\alpha}$ is the root associated with the generator $E^\dagger_{\vec{\alpha}}$, and we define $E_{-\vec{\alpha}} = E^\dagger_{\vec{\alpha}}$. Using the Jacobi identity we get

$$[H_i, [E_{\vec{\alpha}}, E_{\vec{\beta}}]] = [E_{\vec{\alpha}}, [H_i, E_{\vec{\beta}}]] + [[H_i, E_{\vec{\alpha}}], E_{\vec{\beta}}] = (\alpha_i + \beta_i)[E_{\vec{\alpha}}, E_{\vec{\beta}}]. \tag{3.4.5}$$

Since $[E_{\vec{\alpha}}, E_{\vec{\beta}}]$ cannot be zero for two different generators not belonging to the Cartan subalgebra, it must be another generator with root $\vec{\alpha} + \vec{\beta}$. However, if $\vec{\beta} = -\vec{\alpha}$, the right hand side is zero, so H_i and $[E_{\vec{\alpha}}, E_{\vec{\beta}}]$ commute. Hence $[E_{\vec{\alpha}}, E_{-\vec{\alpha}}]$ must be in the Cartan subalgebra, i.e., it must be a linear combination of the H_i

$$[E_{\vec{\alpha}}, E_{-\vec{\alpha}}] = \alpha'^i H_i. \tag{3.4.6}$$

We would like to prove that $\alpha'_i = \alpha_i$, so we will make use of the Killing form defined in (3.3.13). The Killing form acts on generators, as they are elements of the algebra, c.f. (3.3.14), so acting on two generators H_i and H_j

$$\begin{aligned} \alpha'^j \kappa(H_i, H_j) &= \kappa(H_i, [E_{\vec{\alpha}}, E_{-\vec{\alpha}}]) \\ &= \kappa([H_i, E_{\vec{\alpha}}], E_{-\vec{\alpha}}) \\ &= \alpha_i \kappa(E_{\vec{\alpha}}, E_{-\vec{\alpha}}), \end{aligned} \tag{3.4.7}$$

where we have used the symmetry property in equation (3.3.15). Since we can always rescale $E_{\vec{\alpha}}$ so that $\kappa(E_{\vec{\alpha}}, E_{-\vec{\alpha}}) = 1$ [201], we get

$$\kappa(H_i, H_j) = \alpha_i \alpha'_j. \tag{3.4.8}$$

But the quantity $\kappa(H_i, H_j)$ cannot depend on the specific root, because the result above could have been done for any root, i.e. $\kappa(H_i, H_j) = \alpha_i \alpha'_j = \beta_i \beta'_j$. So the only way to reconcile this with the independence of roots, is if $\alpha_i \alpha'_j = k\delta_{ij}$, for some constant k that we can rescale to 1 by an arbitrary redefinition of H_i or H_j. Therefore $\alpha'^j \delta_{ij} = \alpha_i$ implies that $\alpha'_i = \alpha_i$ and

$$[E_{\vec{\alpha}}, E_{-\vec{\alpha}}] = \alpha^i H_i. \tag{3.4.9}$$

We now prove that different root vectors belong to different generators. Let $F_{\vec{\alpha}}$ be a generator associated with the root $\vec{\alpha}$. Since the Killing form restricted to the Cartan subalgebra is non-degenerate [201], we can define $F_{\vec{\alpha}}$ as $\alpha_i = \kappa(H_i, F_{\vec{\alpha}})$, which can be solved uniquely for $F_{\vec{\alpha}}$. On the other hand, we have

$$\begin{aligned} \kappa(H_i, [E_{\vec{\alpha}}, E_{-\vec{\alpha}}]) &= \alpha_i \kappa(E_{\vec{\alpha}}, E_{-\vec{\alpha}}) \\ &= \kappa(H_i, F_{\vec{\alpha}}) \kappa(E_{\vec{\alpha}}, E_{-\vec{\alpha}}). \end{aligned} \tag{3.4.10}$$

Hence $\kappa(H_i, [E_{\vec{\alpha}}, E_{-\vec{\alpha}}] - \kappa(E_{\vec{\alpha}}, E_{-\vec{\alpha}}) F_{\vec{\alpha}}) = 0$, for all i. But κ is non-degenerate, so $[E_{\vec{\alpha}}, E_{-\vec{\alpha}}] = \kappa(E_{\vec{\alpha}}, E_{-\vec{\alpha}}) F_{\vec{\alpha}} = F_{\vec{\alpha}}$ by rescaling. Therefore, since $F_{\vec{\alpha}}$ is uniquely defined for each $\vec{\alpha}$, so is $E_{\vec{\alpha}}$.

We can then summarise all the commutation relations obtained previously as

$$\begin{aligned} [H_i, H_j] &= 0, \\ [H_i, E_{\vec{\alpha}}] &= \alpha_i E_{\vec{\alpha}}, \\ [E_{\vec{\alpha}}, E_{-\vec{\alpha}}] &= \alpha^i H_i, \\ [E_{\vec{\alpha}}, E_{\vec{\beta}}] &= N_{\vec{\alpha}+\vec{\beta}} E_{\vec{\alpha}+\vec{\beta}}. \end{aligned} \tag{3.4.11}$$

where $N_{\vec{\alpha}+\vec{\beta}}$ is a constant that will depend on the normalisation of $E_{\vec{\alpha}}$ and $E_{\vec{\beta}}$, and it will be zero if $\vec{\alpha} + \vec{\beta}$ is not a root of the algebra.

Through eq. (3.4.11), we can find the structure constants, that uniquely define the algebra. And we can easily notice that they only depend on the number of Cartan generators (the rank of the algebra) and the roots (modulo some normalisation constants). However, we will now see that we do not even need all the roots to specify the algebra, for they are not all independent. From the known roots $\vec{\alpha}$ and $\vec{\beta}$, we define the *$\vec{\alpha}$-string of roots through $\vec{\beta}$* as $\vec{\beta} + n\vec{\alpha}$ for $n \in \mathbb{Z}$, which can be proven to be roots as long as $\vec{\alpha}$ and $\vec{\beta}$ are roots and $p \leq n \leq q$ for some $p, q \in \mathbb{Z}$ with $p \leq 0 \leq q$ [197, 201]. Furthermore we have

$$p + q = -2 \, \frac{\vec{\beta} \cdot \vec{\alpha}}{\vec{\alpha} \cdot \vec{\alpha}}, \tag{3.4.12}$$

where the scalar product is defined as

$$\vec{\alpha} \cdot \vec{\beta} = \kappa(E_{\vec{\alpha}}, E_{\vec{\beta}}). \tag{3.4.13}$$

Conversely, we can define the $\vec{\beta}$-*string of roots through* $\vec{\alpha}$ as $\vec{\alpha} + n\vec{\beta}$ in the same way, with possible different values for p and q.

Hence with just a small number of roots, we can specify the algebra, since other roots can be obtained through the strings. We will call *simple roots* those roots that are positive and cannot be written as a sum of positive roots. This implies that if $\vec{\alpha}$ and $\vec{\beta}$ are different simple roots, then $\vec{\alpha} - \vec{\beta}$ is not a root[10] and $\vec{\alpha} \cdot \vec{\beta} \leq 0$[11]. We find that the set of simple roots of an algebra are linearly independent and, moreover, there are precisely r simple roots, hence they form a basis of the root space. It would therefore make sense, to classify the possible Lie algebras in terms of these simple roots. As a matter of fact, it is enough to consider the number of them (the rank of the algebra) and the angles between the roots which are defined as

$$\cos\theta = \frac{\vec{\alpha} \cdot \vec{\beta}}{|\vec{\alpha}||\vec{\beta}|}, \tag{3.4.14}$$

which only allows for four possible values: $\pi/2$, $2\pi/3$, $3\pi/4$ and $5\pi/6$ [199].

Then, it is possible to define, for $\vec{\alpha}_i$ the set of simple roots of an algebra, the *Cartan matrix* K as a $r \times r$ matrix with components given by,

$$K_{ij} = \frac{2\vec{\alpha}_i \cdot \vec{\alpha}_j}{\vec{\alpha}_j \cdot \vec{\alpha}_j}, \tag{3.4.15}$$

that will uniquely classify the algebra.

A Cartan matrix describes the root system of an algebra and thus defines it unambiguously. Their entries correspond to the angles among the simple roots of the group, normalised by the length of the roots, $|\vec{\alpha}|$, to integer numbers[12]. Following the original classification and nomenclature of E. Cartan [200], the Cartan matrices, and thus the algebras, are classified into six series: four regular series, A_r, B_r, C_r and D_r, for all values of the rank $r > 1$, and five exceptional algebras, E_r with $6 \leq r \leq 8$, F_4 and G_2.

[10] If $\vec{\beta} - \vec{\alpha}$ is a root, if $\vec{\beta} > \vec{\alpha}$ then $\vec{\beta} - \vec{\alpha}$ is positive and one can write $\vec{\beta} = (\vec{\beta} - \vec{\alpha}) + \vec{\alpha}$ which is a sum of positive roots, which is a contradiction as $\vec{\beta}$ is simple. Similarly, if $\vec{\alpha} > \vec{\beta}$ we will reach the same contradiction. Hence $\vec{\beta} - \vec{\alpha}$ is not a root.

[11] Since $\vec{\beta} - \vec{\alpha}$ is not a root, in the $\vec{\alpha}$ string of roots through $\vec{\beta}$, $\vec{\beta} + n\vec{\alpha}$, n must be positive or zero. Hence $p = 0$, and then from (3.4.12), $\vec{\alpha} \cdot \vec{\beta} = -q(\vec{\alpha} \cdot \vec{\alpha}) \leq 0$.

[12] Conventionally, longer roots are normalised so that $|\vec{\alpha}|^2 = \vec{\alpha} \cdot \vec{\alpha} = 2$.

The regular series of Cartan matrices will have a variable size depending on the rank, but the shape is consistent regardless of the size, with the last 2 or 3 rows and columns setting the differences among them. These matrices are

$$K(A_r) = \begin{pmatrix} 2 & -1 & 0 & \dots & 0 & 0 \\ -1 & 2 & -1 & \dots & 0 & 0 \\ 0 & -1 & 2 & \dots & 0 & 0 \\ \dots & \dots & \dots & \dots & \dots & \dots \\ 0 & 0 & \dots & 2 & -1 & 0 \\ 0 & 0 & \dots & -1 & 2 & -1 \\ 0 & 0 & \dots & 0 & -1 & 2 \end{pmatrix}, \quad K(B_r) = \begin{pmatrix} 2 & -1 & 0 & \dots & 0 & 0 \\ -1 & 2 & -1 & \dots & 0 & 0 \\ 0 & -1 & 2 & \dots & 0 & 0 \\ \dots & \dots & \dots & \dots & \dots & \dots \\ 0 & 0 & \dots & 2 & -1 & 0 \\ 0 & 0 & \dots & -1 & \mathbf{2} & \mathbf{-2} \\ 0 & 0 & \dots & 0 & \mathbf{-1} & \mathbf{2} \end{pmatrix},$$

$$K(C_r) = \begin{pmatrix} 2 & -1 & 0 & \dots & 0 & 0 \\ -1 & 2 & -1 & \dots & 0 & 0 \\ 0 & -1 & 2 & \dots & 0 & 0 \\ \dots & \dots & \dots & \dots & \dots & \dots \\ 0 & 0 & \dots & 2 & -1 & 0 \\ 0 & 0 & \dots & -1 & \mathbf{2} & \mathbf{-1} \\ 0 & 0 & \dots & 0 & \mathbf{-2} & \mathbf{2} \end{pmatrix}, \quad K(D_r) = \begin{pmatrix} 2 & -1 & 0 & \dots & 0 & 0 \\ -1 & 2 & -1 & \dots & 0 & 0 \\ 0 & -1 & 2 & \dots & 0 & 0 \\ \dots & \dots & \dots & \dots & \dots & \dots \\ 0 & 0 & \dots & \mathbf{2} & \mathbf{-1} & \mathbf{-1} \\ 0 & 0 & \dots & \mathbf{-1} & \mathbf{2} & \mathbf{0} \\ 0 & 0 & \dots & \mathbf{-1} & \mathbf{0} & \mathbf{2} \end{pmatrix}, \tag{3.4.16}$$

where the bold entries highlight the main differences of the series, while the other entries are universal with 2 on the diagonal and -1 above and below the diagonal.

The exceptional algebras are a finite series, they do not appear for every value of the rank. The E_r series only allows for ranks 6, 7 and 8, whereas the F_r and G_r series only have ranks 4 and 2, respectively. Their Cartan matrices, specific for each algebra, are

$$K(E_6) = \begin{pmatrix} 2 & -1 & 0 & 0 & 0 & 0 \\ -1 & 2 & -1 & 0 & 0 & 0 \\ 0 & -1 & \mathbf{2} & \mathbf{-1} & \mathbf{0} & \mathbf{-1} \\ 0 & 0 & \mathbf{-1} & 2 & -1 & \mathbf{0} \\ 0 & 0 & \mathbf{0} & -1 & 2 & \mathbf{0} \\ 0 & 0 & \mathbf{-1} & \mathbf{0} & \mathbf{0} & \mathbf{2} \end{pmatrix},$$

$$K(E_7) = \begin{pmatrix} 2 & -1 & 0 & 0 & 0 & 0 & 0 \\ -1 & 2 & -1 & 0 & 0 & 0 & 0 \\ 0 & -1 & \mathbf{2} & \mathbf{-1} & \mathbf{0} & \mathbf{0} & \mathbf{-1} \\ 0 & 0 & \mathbf{-1} & 2 & -1 & 0 & \mathbf{0} \\ 0 & 0 & \mathbf{0} & -1 & 2 & -1 & \mathbf{0} \\ 0 & 0 & \mathbf{0} & 0 & -1 & 2 & \mathbf{0} \\ 0 & 0 & \mathbf{-1} & \mathbf{0} & \mathbf{0} & \mathbf{0} & \mathbf{2} \end{pmatrix}, \quad K(F_4) = \begin{pmatrix} 2 & -1 & 0 & 0 \\ -1 & \mathbf{2} & \mathbf{-2} & 0 \\ 0 & \mathbf{-1} & \mathbf{2} & -1 \\ 0 & 0 & -1 & 2 \end{pmatrix},$$

$$K(E_8) = \begin{pmatrix} 2 & -1 & 0 & 0 & 0 & 0 & 0 & 0 \\ -1 & 2 & -1 & 0 & 0 & 0 & 0 & 0 \\ 0 & -1 & \mathbf{2} & \mathbf{-1} & \mathbf{0} & \mathbf{0} & \mathbf{0} & \mathbf{-1} \\ 0 & 0 & \mathbf{-1} & 2 & -1 & 0 & 0 & \mathbf{0} \\ 0 & 0 & \mathbf{0} & -1 & 2 & -1 & 0 & \mathbf{0} \\ 0 & 0 & \mathbf{0} & 0 & -1 & 2 & -1 & \mathbf{0} \\ 0 & 0 & \mathbf{0} & 0 & 0 & -1 & 2 & \mathbf{0} \\ 0 & 0 & \mathbf{-1} & \mathbf{0} & \mathbf{0} & \mathbf{0} & \mathbf{0} & \mathbf{2} \end{pmatrix}, \quad K(G_2) = \begin{pmatrix} \mathbf{2} & \mathbf{-3} \\ \mathbf{-1} & \mathbf{2} \end{pmatrix}, \tag{3.4.17}$$

where, again, we have highlighted in bold face the unusual rows and columns that do not follow the general cannon.

Therefore, it is enough to know the rank of an algebra and its series, since that specifies the Cartan matrix. According to that, the simple algebras can be classified as can be seen in table 3.1, where the rank r and dimension d of the algebras are specified. Additionally, the classical notation of the regular algebras, used extensively in physics, is provided.

Cartan's notation	Classical notation	Rank r	Dimension d
A_r	$\mathfrak{su}(r+1)$	$r \geq 1$	$r(r+2)$
B_r	$\mathfrak{so}(2r+1)$	$r \geq 1$	$r(2r+1)$
C_r	$\mathfrak{sp}(2r)$	$r \geq 1$	$r(2r+1)$
D_r	$\mathfrak{so}(2r)$	$r > 2$	$r(2r-1)$
E_6	-	6	78
E_7	-	7	133
E_8	-	8	248
G_2	-	2	14
F_4	-	4	52

Table 3.1: *Cartan classification of simple Lie algebras, with r the rank of group, i.e. number of commuting generators, and d the dimension of the group, i.e. total number of generators.*

An alternative way of representing the simple roots of a Lie algebra is through the use of the Dynkin diagrams [202]. These are graphs where the nodes represent simple roots and the links correspond to the angles among them, see eq. (3.4.14). Nodes with no link between them have an angle of $\pi/2$, a single link corresponds to an angle of $2\pi/3$, two links to $3\pi/4$ and three links (the maximum allowed) to $5\pi/6$. The Dynkin diagrams of all the series of table 3.1, equivalent to the Cartan matrices of (3.4.16) and (3.4.17), can be seen in figure 3.1. In those diagrams with roots of different lengths, shorter roots are represented with black filled nodes[13].

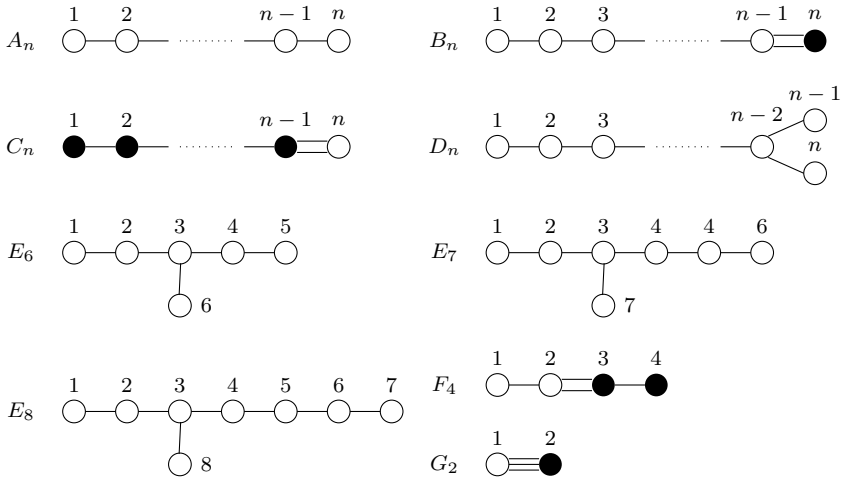

Figure 3.1: *Dynkin diagrams of simple Lie algebras.*

There are two different bases in which the simple roots of a Lie algebra can be written. The Dynkin or fundamental basis can be read off the Cartan matrix, where each row corresponds to a simple root and as such are always integer numbers. For example, the simple roots $\vec{\alpha}_i$ of the algebra D_4 ($\mathfrak{so}(8)$) have the following components in the Dynkin basis

$$\vec{\alpha} = \{(\ 2,\text{-}1,\ 0,\ 0),\ (\text{-}1,\ 2,\text{-}1,\text{-}1),\ (\ 0,\text{-}1,\ 2,\ 0),\ (\ 0,\text{-}1,\ 0,\ 2)\}\,. \tag{3.4.18}$$

The other type of basis, known as the dual basis, is defined as the components of any root $\vec{\beta}$, when written as a linear combination of the simple roots. By convention, these components are normalised according to the length of the simple roots, with a factor $\frac{2}{\vec{\alpha}_i \cdot \vec{\alpha}_i}$ up front. This is

$$\vec{\beta} = \sum_i \lambda_i \frac{2}{\vec{\alpha}_i \cdot \vec{\alpha}_i} \vec{\alpha}_i, \tag{3.4.19}$$

[13]Roots of different lengths have larger angles between them, equation (3.4.14), and this has a great impact in the construction of root and weight systems, as will be seen later.

so by definition, the components λ_i of the simple roots in the dual basis are just non-zero real numbers for the entries that correspond to themselves, one for long roots and $\frac{\vec{\alpha}\cdot\vec{\alpha}}{2}$ for short roots, and zero everywhere else. Following the example before, the simple roots $\vec{\alpha}_i$ of D_4 in the dual basis (subindex $*$ to distinguish it from the Dynkin basis) are

$$\vec{\alpha}_* = \{(\ 1,\ 0,\ 0,\ 0),\ (\ 0,\ 1,\ 0,\ 0),\ (\ 0,\ 0,\ 1,\ 0),\ (\ 0,\ 0,\ 0,\ 1)\}\,, \tag{3.4.20}$$

since all the simple roots of D_4 are the same length.

Converting from one basis to another is done with the metric tensor of the Lie algebra G_{ij} [203], defined by

$$G_{ij} = (K_{ij})^{-1}\frac{\vec{\alpha}_j\cdot\vec{\alpha}_j}{2}. \tag{3.4.21}$$

The metric tensor is the projection of the Killing form into root space, and as such the scalar product of roots, defined in eq. (3.4.13), can be written as

$$\vec{\alpha}\cdot\vec{\beta} = \sum_{ij} a_i G_{ij} b_j = \sum_j \lambda_j b_j = \sum_i a_i \tau_i, \tag{3.4.22}$$

where $\vec{\alpha} = (a_1, \ldots, a_r)$, $\vec{\beta} = (b_1, \ldots, b_r)$ in Dynkin components, and $\vec{\alpha} = (\lambda_1, \ldots, \lambda_r)$, $\vec{\beta} = (\tau_1, \ldots, \tau_r)$ in dual components.

Similar to the fact that roots describe simple algebras, weights describe irreducible representations of the algebra. It can be easily proven [201] that every representation $\mathcal{R}$ has a *highest vector*, v_{hw}, defined so that

$$D_{\mathcal{R}}(E_{-\vec{\alpha}})v_{hw} = 0, \tag{3.4.23}$$

for all $\vec{\alpha}_i$, simple roots of the algebra. The weight associated to the highest vector is known as the *highest weight*, defined as

$$D_{\mathcal{R}}(\vec{H})v_{hw} = \vec{\omega}v_{hw}. \tag{3.4.24}$$

Such highest weight defines a representation of an algebra unambiguously. Because of this, it is used to label and identify irreducible representations (irreps) in a simple algebra. The dimension of a irrep, $\mathcal{R}$, can be calculated easily from the highest weight $\vec{\omega}$ by using the Weyl formula [203]

$$\dim(\mathcal{R}) = \prod_{\vec{\alpha}>0}\frac{\vec{\alpha}\cdot(\vec{\omega}+\vec{\delta})}{\vec{\alpha}\cdot\vec{\delta}}, \tag{3.4.25}$$

where $\vec{\delta} = (\ 1, \ldots,\ 1)$ in the Dynkin basis and the product runs over the positive roots $\vec{\alpha} > 0$.

Weights, as roots, can be written in both the Dynkin and dual bases, and their relations mirror those of roots. As an example, the weights of the **5** dimensional representation of A_4 ($\mathfrak{su}(5)$), in Dynkin and dual bases respectively, are

$$\begin{aligned}\vec{\omega} &= \{(\ 1,\ 0,\ 0,\ 0),\ (\text{-}1,\ 1,\ 0,\ 0),\ (\ 0,\text{-}1,\ 1,\ 0),\ (\ 0,\ 0,\text{-}1,\ 1),\ (\ 0,\ 0,\ 0,\text{-}1)\},\\ \vec{\omega}_* &= \{(\ \tfrac{4}{5},\ \tfrac{3}{5},\ \tfrac{2}{5},\ \tfrac{1}{5}),\ (\text{-}\tfrac{1}{5},\ \tfrac{3}{5},\ \tfrac{2}{5},\ \tfrac{1}{5}),\ (\text{-}\tfrac{1}{5},\text{-}\tfrac{2}{5},\ \tfrac{2}{5},\ \tfrac{1}{5}),\ (\text{-}\tfrac{1}{5},\text{-}\tfrac{2}{5},\text{-}\tfrac{3}{5},\ \tfrac{1}{5}),\ (\text{-}\tfrac{1}{5},\text{-}\tfrac{2}{5},\text{-}\tfrac{3}{5},\text{-}\tfrac{4}{5})\}.\end{aligned} \tag{3.4.26}$$

where the first weight, $\omega = (1, 0, 0, 0)$ in Dynkin basis, is the highest weight.

The last properties of Lie algebras and its representations that we must discuss are the Casimir invariants and the Dynkin indices. The Casimir invariant was defined in eq. (3.3.19) in terms of the generators of the algebra, and it can be easily redefined in terms of the weights of irreducible representations. Let ω be the highest weight of a representations $\mathcal{R}$, then the Casimir invariant of that representation is [203]

$$C(\mathcal{R}) = \vec{\omega} \cdot (\vec{\omega} + 2\vec{\delta}). \tag{3.4.27}$$

The Casimir invariant of the algebra corresponds to that of the adjoint representation $C(\mathcal{G}) = C(\mathcal{R}_{\text{Adj}})$.

The Dynkin index (or simply index) of an irreducible representation can be calculated as

$$S(\mathcal{R}) = \frac{\dim(\mathcal{R})}{\text{ord}(\mathcal{G})} C(\mathcal{R}), \tag{3.4.28}$$

where $\text{ord}(\mathcal{G})$ is the order of the group, which corresponds to $\text{ord}(\mathcal{G}) = \dim(\mathcal{R}_{\text{Adj}})$.

Finally, it is worth mentioning that abelian algebras are not part of this description of simple algebras, in terms of roots and weights, since all their generators satisfy $[T_a, T_b] = 0$, hence they have no roots. In classical notation, a n dimensional abelian group is known as $U(1)^n$, with n commuting generators.

3.5 Group Theory Tool

The Cartan classification of simple algebras provides a description of Lie algebras in terms of roots and weights, and this opens the field for computational treatment. The development of an algorithmic implementation of the features of simple algebras

allows for a universal way of handling them, thus simplifying the calculation of the physical properties that would be needed in the model building phase.

Simple algebras, those that do not contain invariant subalgebras, are ever present in the world of quantum mechanics. For example, the rotations in space are described using the simple algebra $SO(3)$. On the other hand, in the quantum world one often finds that physical systems have disjoint sets of symmetries, and these cannot be considered as simple algebras. In this case, semisimple algebras come to the rescue. Semisimple algebras do contain, non-abelian, invariant subalgebras, so they can be expressed as direct products of simple algebras [199]. As an example, hadronic particles are often thought as states in representations of a $SU(3) \otimes SU(2)$ group, where $SU(3)$ is the Gell-Mann quark flavour symmetry and $SU(2)$ the spin group.

However, despite its usefulness, semisimple algebras cannot be used to describe the symmetries of all physical systems. Some symmetric systems have an abelian invariant subalgebra, e.g. the colour and electric charge symmetries of quarks at low energies, $SU(3)_C \otimes U(1)_{em}$. In those cases one needs non-semisimple algebras for the description, which can be expressed as the direct product of semisimple algebras and abelian $U(1)$ factors.

Therefore, we will try to build a computational tool to handle the properties of all Lie algebras (simple, semisimple or neither). This tool will be very useful from the physics point of view, because it would simplify the group theoretical part of the model building process, by bringing all the mathematical and analytical treatment of groups and algebras to computational grounds, thus gaining in speed and versatility.

In order to do so, we will specify the algorithms and processes that are required to obtain the main constituents of Lie algebras, **Roots and Weights**, which will be necessary for every other process to follow. Additionally, there are three main concepts that have a direct application to model building in Quantum Field Theory and we will detail the algorithms to obtain them. These are the calculation of the **Subgroups and Breaking Chains** of a Lie algebra, which will allow us to know the symmetry breaking path a theory undergoes; the **Decomposition of Representations** of a Lie algebra into representations of a subalgebra, which will provide knowledge about the fields that live at every step of the symmetry breaking chain; and the **Construction of Group Invariants**, required to build Lagrangians of gauge theories. Henceforth, we will drop the distinction between the labels of a group, e.g. $SU(N)$, and its algebra, e.g., $\mathfrak{su}(N)$, for simplicity, thus it will be implied that we refer to the properties of the algebras unless explicitly stated otherwise.

3.5.1 Roots and Weights

As mentioned before, in section 3.4, the minimum set of roots to unambiguously define a simple algebra is the set of simple roots, from where all other roots can be obtained. The way to do so is by following the argument above equation (3.4.12), where one could construct roots simply through strings of roots. Due to the condition in eq. (3.4.12), new roots can only be obtained from non-orthogonal roots, i.e. $\vec{\alpha} \cdot \vec{\beta} \neq 0$, and since the length of the chain of roots depends on the angle between them, eq. (3.4.14), roots with wider angles will have longer strings. Then, using the root chains we can derive an algorithm to calculate the whole set of roots of a simple algebra [203].

Let $\{\vec{\alpha}^s\}$ be the set of simple roots of the algebra, which are all positive, by definition, and $\{\vec{\alpha}\}$ the full set of roots, currently containing only the simple roots. When written in the Dynkin basis, a negative component of the root $\vec{\alpha}_i$, $a_{ij} < 0$, means that the simple root $\vec{\alpha}^s_j$ is not orthogonal to $\vec{\alpha}_i$. So, by the argument above, there are a_{ij} new roots, calculated via the chain $\vec{\beta}_{ij} = \vec{\alpha}_i + k\vec{\alpha}^s_j$ with $k = 1, \ldots, a_{ij}$, which we add to the set of roots $\{\vec{\alpha}\}$. We iterate this algorithm for all negative components of the root $\vec{\alpha}_i$, and for all roots $\{\vec{\alpha}\}$, plus all other roots obtained throughout this process, until there are no more roots with negative components. In the end, we end up with the set of all positive roots, the last of which is known as the highest or most positive root, whose components are all positive.

Since we know that if $\vec{\alpha}$ is a root, so is $-\vec{\alpha}$, the negative roots are easily obtained from the positive roots. Finally, every simple algebra has r, rank of the algebra, null roots, corresponding to the commutators of the generators of the Cartan subalgebra. Therefore, following the algorithm, illustrated in figure 3.2, we obtain the full set of roots $\{\vec{\alpha}\}$ of the algebra, including the positive, negative and null roots, whose dimension corresponds to the dimension of the group.

To illustrate this process we describe here an example case, B_3 ($SO(7)$), chosen because it has roots with different lengths. The Cartan matrix of B_3 can be found in equation (3.4.16), so the simple roots are

$$\vec{\alpha} = \{(\ 2, \text{-}1,\ 0),\ (\text{-}1,\ 2, \text{-}2),\ (\ 0, \text{-}1,\ 2)\}. \tag{3.5.1}$$

Following the algorithm above, if we start with $\vec{\alpha}_1 = (\ 2, \text{-}1,\ 0)$ we can see that the second component is negative, $a_{12} = -1$, thus $\vec{\alpha}_1 + \vec{\alpha}_2 = (\ 1,\ 1, \text{-}2)$ is a root. The first component of $\vec{\alpha}_2$ is also negative, $a_{21} = -1$, but that leads to the same root as before, so we there are no new roots there. Next, we notice that the third

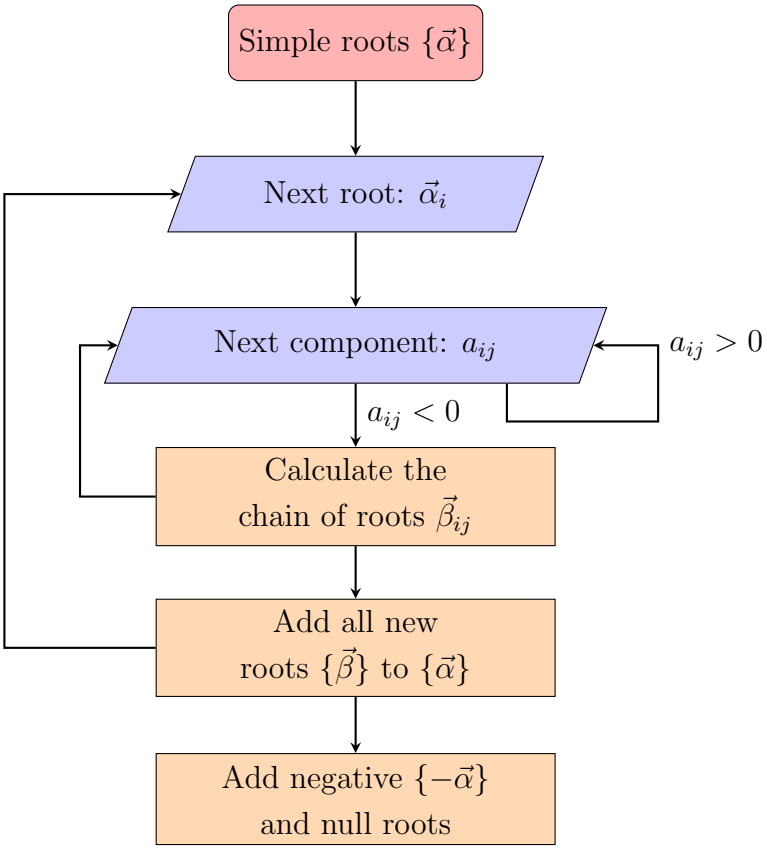

Figure 3.2: *Algorithm for obtaining the roots of a simple algebra.*

component of $\vec{\alpha}_2$ is not only negative, but smaller than -1. This means that both $\vec{\alpha}_2 + \vec{\alpha}_3 =$ (-1, 1, 0) and $\vec{\alpha}_2 + 2\alpha_3 =$ (-1, 0, 2) are roots. Adding all the obtained roots to the set and iterating for all roots we find

$$\vec{\alpha} = \left\{ \begin{array}{ccc} (0, 1, 0) & & \\ (1,\text{-}1, 2) & & \\ (1, 0, 0) & (\text{-}1, 0, 2) & \\ (1, 1,\text{-}2) & (\text{-}1, 1, 0) & \\ (2,\text{-}1, 0) & (\text{-}1, 2,\text{-}2) & (0,\text{-}1, 2) \end{array} \right\}, \tag{3.5.2}$$

which are the full set of positive roots, laid out in levels corresponding to the overall number of simple roots involved in the sum, e.g., the highest root is $\vec{\beta} = \vec{\alpha}_1 + 2\vec{\alpha}_2 + 2\vec{\alpha}_3$ and so it has level 5. Adding the negative and null roots, we find the full set of roots of B_3

$$\vec{\alpha} = \left\{ \begin{array}{ccc} & (0,\ 1,\ 0) & \\ & (1,\text{-}1,\ 2) & \\ (1,\ 0,\ 0) & & (\text{-}1,\ 0,\ 2) \\ (1,\ 1,\text{-}2) & & (\text{-}1,\ 1,\ 0) \\ (2,\text{-}1,\ 0) & (\text{-}1,\ 2,\text{-}2) & (0,\text{-}1,\ 2) \\ (0,\ 0,\ 0) & (0,\ 0,\ 0) & (0,\ 0,\ 0) \\ (\text{-}1,\text{-}1,\ 2) & & (1,\text{-}1,\ 0) \\ (\text{-}1,\ 0,\ 0) & & (1,\ 0,\text{-}2) \\ & (\text{-}1,\ 1,\text{-}2) & \\ & (0,\text{-}1,\ 0) & \end{array} \right\}, \tag{3.5.3}$$

which is the root diagram of the simple algebra.

Extending of the computation of roots to semisimple algebras is straightforward, following their decomposition into direct products of simple algebras. The set of roots of an algebra $\mathcal{G}_1 \otimes \cdots \otimes \mathcal{G}_N$ is taken as the disjoint set of roots $\{\{\vec{\alpha}\}_1, \ldots, \{\vec{\alpha}\}_N\}$, where $\{\vec{\alpha}\}_j$ are the roots of $\mathcal{G}_j$. Since abelian algebras do not have roots, there is no further extension for non-semisimple algebras.

A similar algorithm to the one above can be used to obtain the weights of a representation of the algebra. Since irreducible representations (irreps) are defined by their highest weight, we will build the weight diagram for the representation from it. Then, unlike the construction of the root system, where we started from the simple roots and built upwards by adding them together, we will now subtract the simple roots from the weights, starting from the highest weight, and build the diagram downwards [203].

Starting from the highest weight $\vec{\Omega}$, we obtain new weights by subtracting the simple root $\vec{\alpha}_j$ from it, where now w_j, the jth component of $\vec{\Omega}$ is a positive component, instead of negative. The new weights, $\vec{\omega}_j = \vec{\Omega} - k\vec{\alpha}_j$, with $k = 1, \ldots, w_j$, are then added to the list of weights, $\{\vec{\omega}\}$, originally only populated by $\vec{\Omega}$, and iterate. Unlike roots, weights can have different multiplicities, i.e. each weight can appear more than once, which can be calculated for a weight $\vec{\omega}$ as

$$\mathcal{M}_{\vec{\omega}} = 2 \sum_{\vec{\alpha}>0, k>0} \mathcal{M}_{\vec{\omega}+k\vec{\alpha}} \frac{(\vec{\omega} + k\vec{\alpha}) \cdot \vec{\alpha}}{|\vec{\Omega} + \vec{\delta}|^2 - |\vec{\omega} + \vec{\delta}|^2}, \tag{3.5.4}$$

where $\vec{\delta} = (1, \ldots, 1)$ in the Dynkin basis and the sum runs over all positive roots $\vec{\alpha}$ and all positive integers k, provided that $\omega + k\alpha$ is a weight, with given multiplicity $\mathcal{M}_{\vec{\omega}+k\vec{\alpha}}$. Therefore the weight system of the representation defined by $\vec{\Omega}$, with a

number of weights equal to the dimension of the representation, can be calculated this way, as illustrated in figure 3.3.

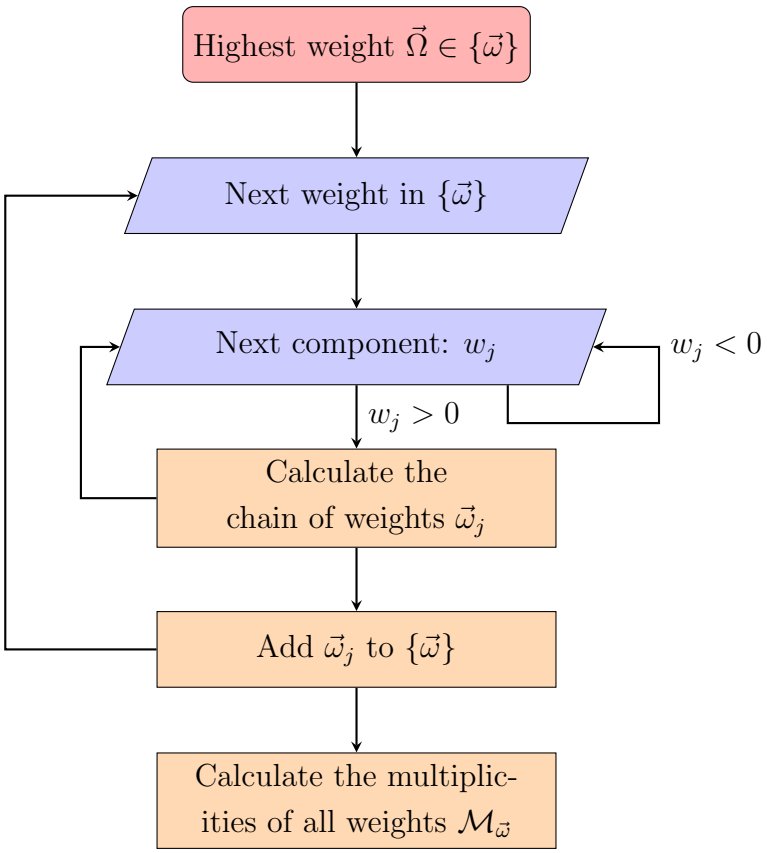

Figure 3.3: *Algorithm for calculating the weights of the representation defined by the highest weight* $\vec{\Omega}$.

As before, we give an example of a weight diagram for a representation. For the purpose of illustration, we choose a non-trivial irrep, with weights of different multiplicities. We take the representation with highest weight (1, 1, 0) of A_3 ($SU(4)$), whose dimension is **20**, calculated with equation (3.4.25). Following the algorithm, we find two positive components of the highest weight, first and second, so the next level of the diagram will have two weights $\vec{\omega}_1 = \vec{\Omega} - \vec{\alpha}_1 =$ (-1, 2, 0) and $\vec{\omega}_2 = \vec{\Omega} - \vec{\alpha}_2 =$ (2,-1, 1). In the next level we find the first case of a weight with non-trivial multiplicity, which is $\vec{\omega}_3 = \vec{\omega}_1 - \vec{\alpha}_2 =$ (0, 0, 1). If we compute its multiplicity, using equation (3.5.4), we find that $\mathcal{M}_{\vec{\omega}_3} = 2$, and we can see this is indeed true since ω_3 can be obtained in two different ways[14], the previously mentioned $\vec{\omega}_1 - \vec{\alpha}_2$

[14]It is true that a weight with multiplicity $\mathcal{M} = n$ must be reached trough at least n different paths. Conversely, a weight obtained through n different paths must have a multiplicity $\mathcal{M} \leq n$.

and $\vec{\omega}_2 - \vec{\alpha}_1$. Iterating the process for all weights we find the diagram

$$\vec{\omega} = \left\{ \begin{array}{cccc} & & (\ 1,\ 1,\ 0) & \\ & (\text{-}1,\ 2,\ 0) & & (\ 2,\text{-}1,\ 1) \\ (\ \mathbf{0},\ \mathbf{0},\ \mathbf{1}) & & (\ \mathbf{0},\ \mathbf{0},\ \mathbf{1}) & & (\ 2,\ 0,\text{-}1) \\ (\ 1,\text{-}2,\ 2) & (\text{-}2,\ 1,\ 1) & & (\ \mathbf{0},\ \mathbf{1},\text{-}\mathbf{1}) & (\ \mathbf{0},\ \mathbf{1},\text{-}\mathbf{1}) \\ (\text{-}1,\text{-}1,\ 2) & & (\ \mathbf{1},\text{-}\mathbf{1},\ \mathbf{0}) & & (\ \mathbf{1},\text{-}\mathbf{1},\ \mathbf{0}) & (\text{-}2,\ 2,\text{-}1) \\ (\ 1,\ 0,\text{-}2) & & (\text{-}\mathbf{1},\ \mathbf{0},\ \mathbf{0}) & & (\text{-}\mathbf{1},\ \mathbf{0},\ \mathbf{0}) \\ & (\text{-}1,\ 1,\text{-}2) & & (\ 0,\text{-}2,\ 1) & \\ & & (\ 0,\text{-}1,\text{-}1) & & \end{array} \right\}, \tag{3.5.5}$$

where it can be seen that there are four weights with multiplicity $\mathcal{M} = 2$, which are: (0, 0, 1), (0, 1,-1), (1,-1, 0) and (-1, 0, 0).

For semisimple algebras, the calculation of the weights needs an extra step. The weights of a product representation $\mathcal{R}_1 \otimes \cdots \otimes \mathcal{R}_N$ are taken as combinations of the weights from the simple reps. That is, if $\{\vec{\omega}^i\}_k$ are the weights of $\mathcal{R}_i$ and $\{\vec{\omega}^j\}_l$ are the weights of $\mathcal{R}_j$, with components w^i_{kr} and w^j_{ls} respectively, then the weights of the product rep $\mathcal{R}_i \otimes \mathcal{R}_j$, of dimension $\dim(\mathcal{R}_i) \times \dim(\mathcal{R}_j)$, have components $(w^i_{k1}, \ldots, w^i_{kr}, w^j_{l1}, \ldots, w^j_{ls})$ for $k = 1, \ldots, \dim(\mathcal{R}_i)$ and $l = 1, \ldots, \dim(\mathcal{R}_j)$. The weights of the full product representation $\mathcal{R}_1 \otimes \cdots \otimes \mathcal{R}_N$ are obtained the same way, and will result in a weight system of dimension $\dim(\mathcal{R}_1) \times \cdots \times \dim(\mathcal{R}_N)$.

An example case, for a semisimple $A_3 \otimes A_1$ algebra ($SU(4) \otimes SU(2)$). The rank 4 weights of the $\mathbf{20} \otimes \mathbf{2}$ representation, typically labelled $\{\mathbf{20}, \mathbf{2}\}$, are a combination of the weights of the **20**, in (3.5.5) and the weights of the **2**, $\{(\ 1), (\text{-}1)\}$. Effectively this doubles the number weights by adding a last entry to the weights of **20** with either a 1 or a -1. The first few weights will be (1, 1, 0, 1), (1, 1, 0,-1), (-1, 2, 0, 1), (-1, 2, 0,-1) (2,-1, 1, 1), (2,-1, 0,-1) and so on.

In the non-semisimple case, because abelian algebras do not have roots or weights, there is no need to combine the weights of the semisimple part with the abelian one. However, since the vector space of an abelian $U(1)$ algebra spans the set of real numbers, the components of the weights corresponding to the abelian factors will be filled with real numbers. For a non-semisimple algebra $\mathcal{G} \otimes U(1)_1 \otimes \cdots \otimes U(1)_k$ this means that the highest weight will have the components $(w_1, \ldots, w_r, n_1, \ldots, n_k)$ where $(w_1, \ldots, w_r)$ is the highest weight of $\mathcal{G}$ and $n_1, \ldots, n_k$ are real numbers.

3.5.2 Subgroups and Breaking Chains

Most physical systems undergo a phase transition at some point in their evolution, as does, for example, the universe when the Higgs field condensates, during electroweak symmetry breaking. When this happens, some of the symmetries of the system are broken and the new system will keep only a subset of those. If this process were to be repeated a number of times, the evolution of the system could be characterised by the chain of broken symmetries, i.e. a chain of Lie algebras.

There are two main features to compute here. First, we will need to obtain the set of subalgebras of a given algebra, which will give us the candidates for last step of a symmetry breaking transition, and second we need to calculate the breaking chains between a Lie algebra and one of its subalgebras, providing all possible symmetry breaking paths.

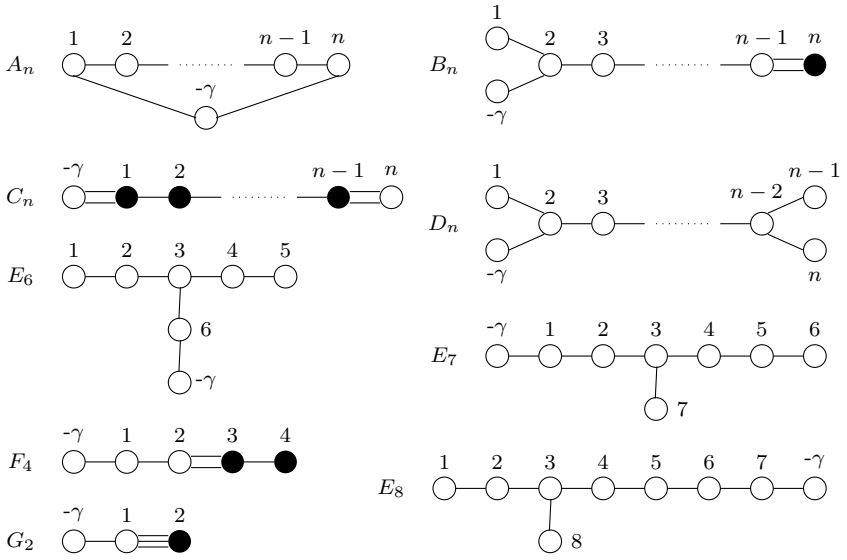

Figure 3.4: *Extended or affine Dynkin diagrams of simple Lie algebras.*

We start with the subalgebras. The first set of subalgebras that need to be calculated are the maximal subalgebras, those that are not subalgebras of any of the other maximal subalgebras. These can be obtained from the Dynkin diagrams (or equivalently from the Cartan matrices) and from what is known as the *extended* or *affine* Dynkin diagrams (or the extended or affine Cartan matrices). The extended diagrams, that can be seen in figure 3.4, are obtained by adding the most negative root in the root system, $-\gamma$, and its links to the simple roots will be given by its

angles with respect to them, i.e,

$$\cos\theta_i = -\frac{\alpha_i \cdot \gamma}{|\alpha_i||\gamma|}, \qquad i \in \{1, r\}. \tag{3.5.6}$$

Therefore, there are two ways to compute subalgebras, starting with the Dynkin diagrams, which will give non-semisimple subalgebras, or starting with extended Dynkin diagrams, which will result in semisimple subalgebras [203].

Starting with the Dynkin diagram of a Lie algebra, the way to obtain the non-semisimple subalgebras is to remove one of its nodes. After removing a node from the diagram, which corresponds to a simple root of the algebra, we end up with one that is disconnected, with two or more subdiagrams. After this, the subalgebra will then be identified as the direct product of the simple algebras that correspond to each of the subdiagrams left, with an abelian factor, $U(1)$, at the end. As an example of this algorithm, we can see in figure 3.5 that if we eliminate the second node of the diagram of $SO(9)$ (B_4), we get the subalgebra $SO(5) \otimes SU(2) \otimes U(1)$ ($B_2 \times A_1 \times U_1$).

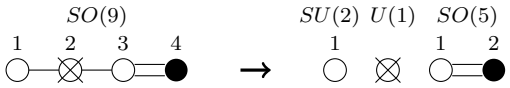

Figure 3.5: *Eliminate the second node (crossed) from the Dynkin diagram of $SO(9)$ to obtain the subalgebra $SO(5) \times SU(2) \times U(1)$.*

Alternatively, one could start with the Cartan matrix and remove a row and a column, corresponding to the eliminated node from the diagram, and then matching the remaining block diagonal matrix with the Cartan matrices of simple algebras. This way is actually easier from the computational point of view and therefore is the path chosen in the implementation, with its algorithm shown in the left hand diagram of figure 3.6, but it is harder to illustrate and thus, since it leads to the same conclusions (it is the same process, after all) we have chosen to present the examples in the former.

For semisimple maximal subalgebras, one must start with the extended Dynkin diagram, and then drop one of the nodes (the corresponding row and column from the extended Cartan matrix). The resulting disconnected diagram would be that of the product subalgebra. The algorithm for this process is shown in the right hand diagram of figure 3.6. It can be seen in figure 3.4, if one were to drop a node from the diagram for a A_n algebra, the subalgebra will always be the same A_n algebra, so unitary algebras do not have semisimple maximal subalgebras. As an example, we

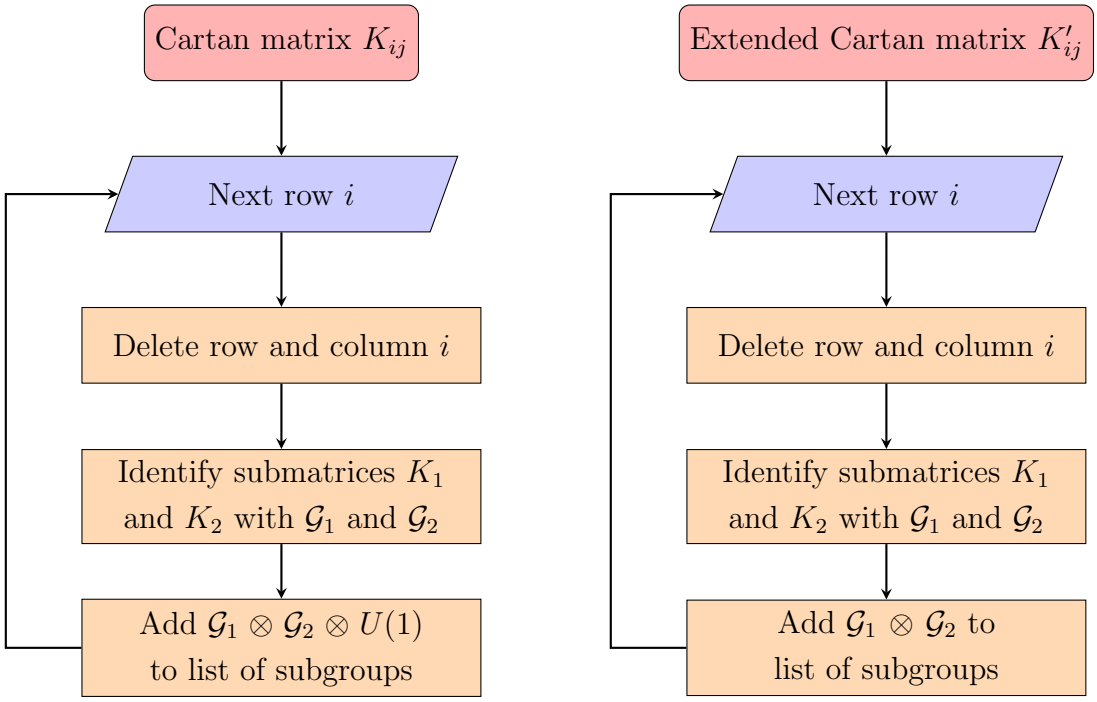

Figure 3.6: *Algorithms for obtaining the maximal subalgebras of a Lie algebra, non-semisimple (left) and semisimple (right).*

show in figure 3.7 the case when the third root from the diagram of $SO(10)$ (D_5) is removed, resulting in the subalgebra $SU(4) \times SU(2) \times SU(2)$.

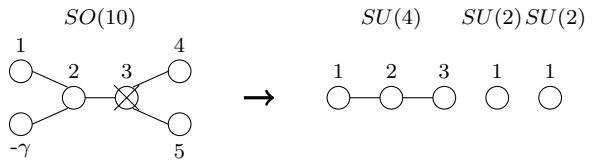

Figure 3.7: *Eliminate the third node from the extended Dynkin diagram of $SO(10)$ to obtain the subalgebra $SU(4) \times SU(2) \times SU(2)$.*

By repeating the above procedure for all dots of the diagrams (or, equivalently, for all rows of the Cartan matrix), one obtains the maximal subalgebras of a given Lie algebra. There is, however, another set of maximal subalgebras that is not obtained this way, but rather in a more heuristic fashion. These are known as *special* maximal subalgebras, as opposed to the former ones, which are dubbed *regular* maximal subalgebras. The unique property of these subalgebras is that the generating representation of the superalgebra, from which all other representations

can be obtained, decomposes into a single representation of the subalgebra, e.g.

$$\begin{aligned} SO(10) &\to SO(9) \\ \mathbf{16} &\to \mathbf{16} \end{aligned} \tag{3.5.7}$$

To my knowledge there is no algorithm to obtain these special maximal subalgebras. They are unique pairings of algebra and subalgebra, but they do not present any special attributes that might qualify them for an algorithmic approach. Therefore they must be read out from existing tables in the literature, rather than calculated [203].

These two sets, regular $\{M_{\mathcal{G}}\}$ and special $\{S_{\mathcal{G}}\}$ subalgebras, constitute all maximal subalgebras of a Lie algebra $\mathcal{G}$. In order to obtain all subalgebras, one has to iterate the above process for the maximal subalgebras, $\{M_{\mathcal{G}}\}$ and $\{S_{\mathcal{G}}\}$, thereby obtaining a list of subalgebras with the same rank as the superalgebra. Throughout this process one expects to find cases with two or more occurrences of the same subalgebras but very often they will have different embeddings into the superalgebra. Whenever this happens, these differences are highlighted by appending labels to the factors of the subalgebras to mark the simple algebra from which they originate. As an example, there are two ways in which the subalgebra $SU(3) \times U(1) \times U(1)$ is embedded into $SU(5)$, through its $SU(4) \times U(1)$ or its $SU(3) \times SU(2) \times U(1)$ subalgebras. The different labels in the $SU(2)$ factors for both cases will then indicate that they have different embeddings

$$\begin{array}{ccc} & SU(5) & \\ & \swarrow \quad \searrow & \\ SU(4)_A \otimes U(1)_B & & SU(3)_A \otimes SU(2)_B \otimes U(1)_C \\ \downarrow & & \downarrow \\ SU(3)_{AA} \otimes U(1)_{AB} \otimes U(1)_B & & SU(3)_A \otimes U(1)_B \otimes U(1)_C \end{array} \tag{3.5.8}$$

Subalgebras with smaller rank than the superalgebra can be obtained by breaking one or more of the abelian subalgebras previously calculated [203]. This is however a non trivial matter, for the abelian component of the subalgebra that gets broken, i.e. the generator of the Cartan subalgebra that breaks, may be any linear combination of the diagonal generators of the given Lie algebra. If the whole abelian sector of the Lie algebra is broken, then all combinations of generators are broken, but otherwise the specific combination is determined by the abelian charges of the order parameter of the phase transition. Deferring the actual combination of the charges to the model building section, when we will know the order parameter of

the transition, this apparently arbitrary combination will be represented using labels in the abelian sector. The well known example of electroweak symmetry breaking, where the actual combination of the diagonal charge of $SU(2)$ and $U(1)$ will be given by the Higgs charges, is

$$SU(3) \otimes SU(2) \otimes U(1) \Rightarrow SU(3)_A \otimes U(1)_{B+C} \tag{3.5.9}$$

Finally, once a full set of subalgebras of a given Lie algebra $\mathcal{G}$ is obtained, the breaking chains from that algebra to one of its subalgebras $\mathcal{F}$ can be calculated, i.e. $\mathcal{G} \to \cdots \to \mathcal{F}$. The first step is to identify the subalgebras $\{\mathcal{G}_i\}$ of $\mathcal{G}$ such that $\mathcal{G} \supset \mathcal{G}_i \supset \mathcal{F}$. Now, for all $\mathcal{G}_i \neq \mathcal{F}$, in a recursive manner, we calculate all its breaking chains to $\mathcal{F}$, $\mathcal{G}_i \to \cdots \to \mathcal{F}$, which we will then append to the original Lie algebra, so $\mathcal{G} \to \mathcal{G}_i \cdots \to \mathcal{F}$. The breaking point of the recursive algorithm is when an intermediate subalgebra $\mathcal{G}_j = \mathcal{F}$, in which case the chain is just $\mathcal{G}_i \to \mathcal{F}$. This algorithm can be seen in a flow chart in figure 3.8.

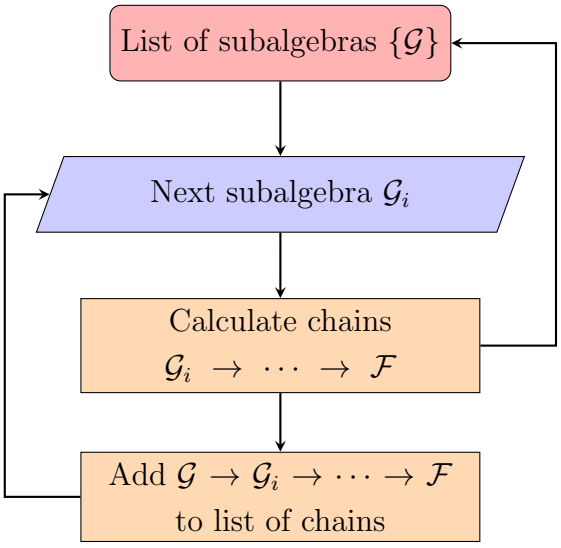

Figure 3.8: *Algorithm to obtain the breaking chains of a Lie algebra.*

In figure 3.9 one can see an example of three out of the 38 possible breaking chains from $SO(10)$ to the Standard Model algebra $SU(3) \times SU(2) \times U(1)$ through different intermediate steps. The first case has $SU(5)$ as an intermediate step, the second has $SU(5) \times U(1)$ with non-trivial $U(1)$ mixing when broken to the SM algebra, and the last one has two intermediate steps, the Pati-Salam algebra (see section 2.2) $SU(4) \times SU(2) \times SU(2)$ and a step in which $SU(4)$ is broken into $SU(3) \times U(1)$, which requires mixing between this abelian subalgebra and the diagonal generator embedded in the broken $SU(2)$.

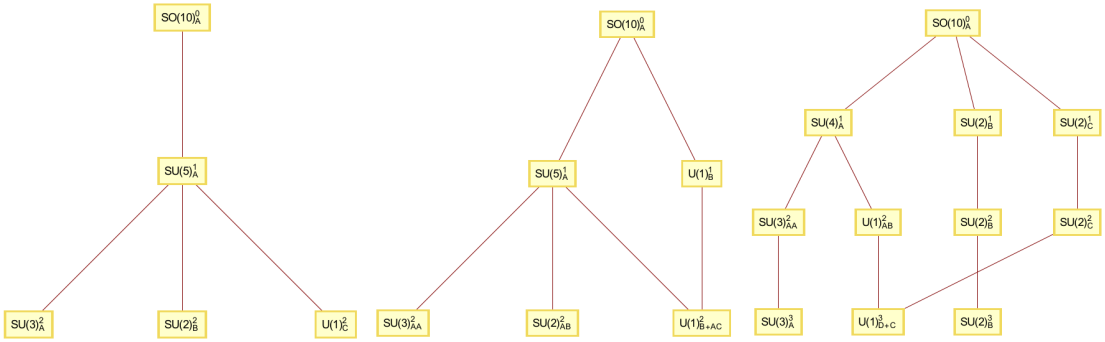

Figure 3.9: *Example of three breaking chains from $SO(10)$ to $SU(3) \times SU(2) \times U(1)$, with different intermediate steps. Superscripts refer to the level in the chain.*

The computation of subalgebras and breaking chains for product algebras, semisimple or not, is rather straightforward from the discussion above. Let $\mathcal{G} = \mathcal{G}_1 \otimes \cdots \otimes \mathcal{G}_N$ be a product algebra, whose factors can be abelian or not, and assume the subalgebras of $\mathcal{G}_i$ are $\{\mathcal{F}_{ij}\}$, calculated via the algorithms above. The subalgebras of $\mathcal{G}$ will be the full combination of the lists of subalgebras, but including the simple algebras $\mathcal{G}_i$ and the empty set element $\varnothing$ in those lists, i.e. $\{\mathcal{G}_i, \mathcal{F}_{i1}, \ldots, \mathcal{F}_{in_i}, \varnothing\}$. For the example case $N = 2$, the subalgebras of $\mathcal{G}_1 \otimes \mathcal{G}_2$ are

$$\left\{ \begin{array}{c} \mathcal{G}_1 \otimes \mathcal{F}_{21}, \ldots, \quad \mathcal{G}_1 \otimes \mathcal{F}_{2n_2}, \\ \mathcal{F}_{11} \otimes \mathcal{G}_2, \ldots, \mathcal{F}_{1n_2} \otimes \mathcal{G}_2, \\ \mathcal{F}_{11} \otimes \mathcal{F}_{21}, \ldots, \quad \mathcal{F}_{11} \otimes \mathcal{F}_{2n_2}, \\ \ldots, \\ \mathcal{F}_{1n_1} \otimes \mathcal{F}_{21}, \ldots, \mathcal{F}_{1n_1} \otimes \mathcal{F}_{2n_2}, \\ \mathcal{F}_{11}, \ldots, \mathcal{F}_{1n_1}, \\ \mathcal{F}_{21}, \ldots, \mathcal{F}_{2n_2}, \\ \mathcal{G}_1, \quad \mathcal{G}_2 \end{array} \right\}, \tag{3.5.10}$$

where $\varnothing \otimes \mathcal{F}_k = \mathcal{F}_k$.

Let us give a simple example, we will calculate the subalgebras of $SU(3) \otimes SU(2)$. We start by assuming we already know the subalgebras of $SU(3)$ and $SU(2)$, from the algorithms described above for simple algebras. These are

$$SU(3) \to \left\{ \begin{array}{l} SU(2) \otimes U(1), \\ SU(2), \\ U(1) \otimes U(1), \\ U(1) \end{array} \right\}, \tag{3.5.11}$$

$$SU(2) \to \{U(1)\}, \tag{3.5.12}$$

we can calculate the subalgebras of the semisimple algebra $SU(3) \otimes SU(2)$ by combining the lists, including $SU(3)$ and $SU(2)$ in their respective lists. The results will be

$$\left\{ \begin{array}{ll} SU(3) \otimes U(1), & SU(2) \otimes U(1) \otimes SU(2), \\ SU(2) \otimes SU(2), & U(1) \otimes U(1) \otimes SU(2), \\ U(1) \otimes SU(2), & SU(2) \otimes U(1) \otimes U(1), \\ SU(2) \otimes U(1), & U(1) \otimes U(1) \otimes U(1), \\ U(1) \otimes U(1), & SU(3) \\ SU(2), & U(1) \end{array} \right\}. \tag{3.5.13}$$

3.5.3 Decomposition of Representations

Along with its symmetries, a physical system can be characterised by a set of fields, of classical or quantum nature, which transform according to representations of the algebra. Hence, the fields form multiplets, of dimension the dimension of the irrep, and the states of the multiplet are eigenstates of the Cartan generators of the algebra with eigenvalues corresponding to the weights of the representation. If at any point during the evolution of the system its symmetries are broken, the representations will decompose into representations of the new Lie algebra, and thus the fields will transform under the irreducible representations of the subalgebra. If $\mathcal{R}$ is a representation of an algebra, there exists a decomposition such as

$$\mathcal{R} \to \sum_i \mathcal{R}_i \tag{3.5.14}$$

where $\mathcal{R}_i$ are irreps of the subalgebra.

As explained in section 3.4, representations of a Lie algebra are unequivocally defined by their sets of weights. Thus, in order to find the decomposition any $\mathcal{R}$ of the algebra it is enough to project its weights into subweights of the subalgebra, and by identifying those with the weights of the irreps $\mathcal{R}_i$ we are able to reconstruct the decomposition in equation (3.5.14) [203]. If we take W to be the matrix of weights of $\mathcal{R}$, with the weights as columns, and V the subweights matrix, then there is a matrix P known as the projection matrix, that satisfies the relation $P \cdot W = V$. The projection matrix P is independent of the representation that it is acting on, and it only depends on the embedding of the subalgebra into the original algebra.

For an arbitrary representation of the algebra, one could invert the relation $P \cdot W = V$ to obtain the projection matrix [204]. Since W is, in general, not a square matrix, it is not invertible in the usual sense, hence we would need to use the

"Pseudoinverse" matrix or Moore-Penrose inverse matrix of W [205,206], defined as W^+ such that

$$\begin{aligned} W \cdot W^+ \cdot W &= W, \\ (W \cdot W^+)^\dagger &= W \cdot W^+. \end{aligned} \tag{3.5.15}$$

It can be calculated from W as $W^+ = W^\dagger \cdot (W \cdot W^\dagger)^{-1}$, which for a real matrix, as W generally is, reduces to

$$W^+ = W^T \cdot (W \cdot W^T)^{-1}, \tag{3.5.16}$$

where $W \cdot W^T$ is guaranteed to be invertible, as long as W has full rank, which it does for any case of interest. If we were to know both weight matrices W and V, for given representations of the algebra and subalgebra respectively, we could calculate the projection matrix as

$$P = V \cdot W^+, \tag{3.5.17}$$

which follows from equation (3.5.15).

For simplicity and since the calculation of P is independent of the representation taken, we choose $\mathcal{R}$ to be the generating representation of the algebra, which gives us the matrix W. The matrix of subweights V can be calculated during the process of obtaining the set of subalgebras of a Lie algebra, and it depends on whether the subalgebra is semisimple or not. These two cases will be discussed below.

As was seen in section 3.5.2, the process of obtaining non-semisimple subalgebras involved eliminating a node from the Dynkin diagram (or row and column entry of the Cartan matrix) and later adding an abelian factor to the product. Assume the matrix of weights W is already known, then the matrix of subweights V can obtained by extracting the jth row of W, W_j, where jth is the node eliminated from the diagram. Then we move the extracted row to the bottom of the matrix and swap its entries for their values in the dual basis.

This algorithm, which is shown in the left hand diagram of figure 3.10, gives us the matrix of subweights V which, together with the pseudoinverse of the already known matrix of weights W (W^+ from equation (3.5.16)), is used to obtain the projection matrix via equation (3.5.17).

As an example we choose the same as in section 3.5.2, the breaking of $SU(5)$ to $SU(3) \times SU(2) \times U(1)$. The generating irrep of $SU(5)$ is the complex **5**, so we

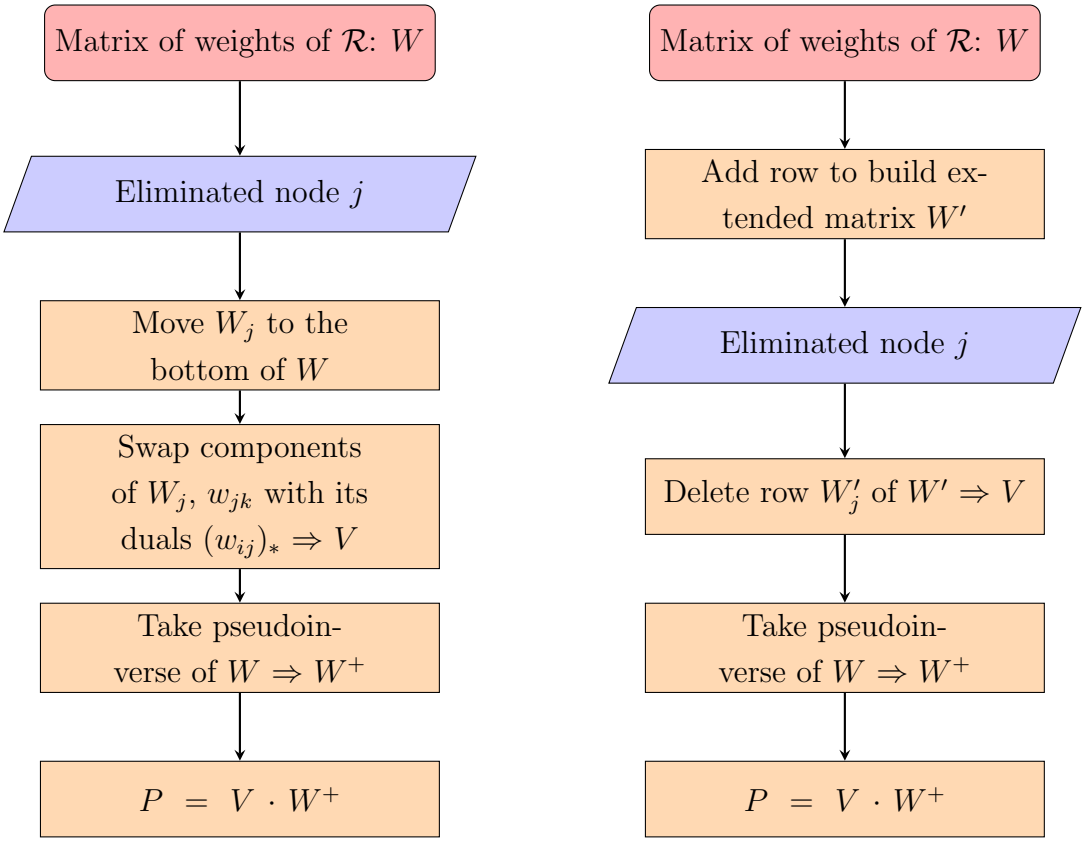

Figure 3.10: *Algorithms for calculating the projection matrix for a pair algebra-subalgebra, for the non-semisimple (left) and semisimple case (right).*

calculate the subweights as

$$W_{\mathbf{5}} = \begin{pmatrix} 1 & -1 & 0 & 0 & 0 \\ 0 & 1 & -1 & 0 & 0 \\ 0 & 0 & 1 & -1 & 0 \\ 0 & 0 & 0 & 1 & -1 \end{pmatrix} \to \begin{pmatrix} 1 & -1 & 0 & 0 & 0 \\ 0 & 1 & -1 & 0 & 0 \\ \mathbf{0} & \mathbf{0} & \mathbf{1} & \mathbf{-1} & \mathbf{0} \\ 0 & 0 & 0 & 1 & -1 \end{pmatrix} \to$$
$$\to \begin{pmatrix} 1 & -1 & 0 & 0 & 0 \\ 0 & 1 & -1 & 0 & 0 \\ 0 & 0 & 0 & 1 & -1 \\ \mathbf{0} & \mathbf{0} & \mathbf{1} & \mathbf{-1} & \mathbf{0} \end{pmatrix} \to \begin{pmatrix} 1 & -1 & 0 & 0 & 0 \\ 0 & 1 & -1 & 0 & 0 \\ 0 & 0 & 0 & 1 & -1 \\ \mathbf{\frac{2}{5}} & \mathbf{\frac{2}{5}} & \mathbf{\frac{2}{5}} & \mathbf{-\frac{3}{5}} & \mathbf{-\frac{3}{5}} \end{pmatrix} = V, \quad (3.5.18)$$

With both W_5 and V we can now construct the projection matrix P, which will be

$$P = \begin{pmatrix} 1 & 0 & 0 & 0 \\ 0 & 1 & 0 & 0 \\ 0 & 0 & 0 & -1 \\ \frac{2}{5} & \frac{4}{5} & \frac{6}{5} & \frac{3}{5} \end{pmatrix}. \quad (3.5.19)$$

In the case of semisimple subalgebras, we obtained the set of subalgebras by removing a node from the extended Dynkin diagram (or the extended Cartan matrix). Similarly as the previous case we will eliminate the row from the weight matrix corresponding to the removed node from the diagram, but in this case we will be using an extended weight matrix W'. These extended weights are obtained by adding an entry to the weight vector equal to the product with the extended root, i.e. $-\gamma \cdot w$, and position it in the weight vector in the same place it is according to the extended diagram. Then, removing the jth row of W', W'_j, corresponding to the removed node from the diagram, will give the subweight matrix V. Lastly, as before, with both V and W we can construct the projection matrix using (3.5.17). The full algorithm can be seen in the right hand side of figure 3.10.

Again, we use the same example as in section 3.5.2, the embedding of $SU(2) \otimes SU(2) \otimes SU(2)$ in $SO(7)$. The generating irrep for $SO(7)$ is **8** and we can calculate the subweights as

$$W = \begin{pmatrix} 0 & 0 & 1 & -1 & 1 & -1 & 0 & 0 \\ 0 & 1 & -1 & 0 & 0 & 1 & -1 & 0 \\ 1 & -1 & 1 & 1 & -1 & -1 & 1 & -1 \end{pmatrix} \rightarrow \begin{pmatrix} 0 & 0 & 1 & -1 & 1 & -1 & 0 & 0 \\ \mathbf{-1} & \mathbf{-1} & \mathbf{0} & \mathbf{0} & \mathbf{0} & \mathbf{0} & \mathbf{1} & \mathbf{1} \\ 0 & 1 & -1 & 0 & 0 & 1 & -1 & 0 \\ 1 & -1 & 1 & 1 & -1 & -1 & 1 & -1 \end{pmatrix} = W'$$

$$\rightarrow \begin{pmatrix} 0 & 0 & 1 & -1 & 1 & -1 & 0 & 0 \\ \mathbf{-1} & \mathbf{-1} & \mathbf{0} & \mathbf{0} & \mathbf{0} & \mathbf{0} & \mathbf{1} & \mathbf{1} \\ 1 & -1 & 1 & 1 & -1 & -1 & 1 & -1 \end{pmatrix} = V. \tag{3.5.20}$$

Then the projection matrix is

$$P = \begin{pmatrix} 1 & 0 & 0 \\ -1 & -2 & -1 \\ 0 & 0 & 1 \end{pmatrix}, \tag{3.5.21}$$

After having calculated the projection matrix P, via either of the algorithms described above, it can be used to obtain the decomposition of any representation of the algebra. For any representation $\mathcal{R}$, whose weight matrix W can be calculated using the algorithms in section 3.5.1, one can calculate the matrix of subweights V by $P \cdot W = V$. Lastly, the only step left is to identify V as the weights of the direct sum of representations $\mathcal{R}_i$, as in equation (3.5.14).

The algorithm to identify the representations, which can be seen in figure 3.11, goes as follows [203]. The first step is to identify the most positive weight $\vec{\omega}_i = (w_{i1}, \ldots, w_{ir})$ in V, i.e. the positive weight, $w_{ij} > 0$, with larger sum of

components $\sum_j w_{ij}$. The weight $\vec{\omega}_i$ will be the highest weight of a representation, $\mathcal{R}_i$. We then proceed to build the weight diagram for $\mathcal{R}_i$, W_i, and then pick out those weights from the matrix of subweights V. Next, find the new most positive weight in V and iterate, until there are no more weights in V.

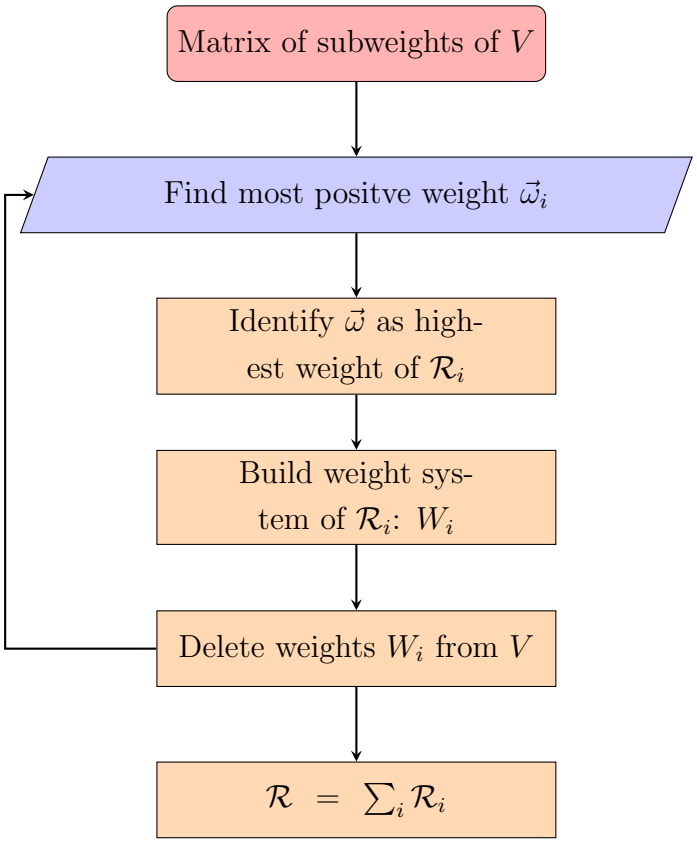

Figure 3.11: *Algorithm for identifying the representations from the subweights V.*

Following the examples given above, for semisimple subalgebras, $SU(5) \to SU(3) \otimes SU(2) \otimes U(1)$, and non-semisimple subalgebras, $SO(7) \to SU(2) \otimes SU(2) \otimes SU(2)$, with the projection matrices in (3.5.19) and (3.5.21), we can use this algorithm to find that the subweights in (3.5.18) and (3.5.20) correspond to the decompositions

$$\begin{aligned} \mathbf{5} &\to \sum_i \mathcal{R}_i = \{\mathbf{3}, \mathbf{1}, \tfrac{2}{5}\} + \{\mathbf{1}, \mathbf{2}, -\tfrac{3}{5}\}, \\ \mathbf{8} &\to \sum_i \mathcal{R}_i = \{\mathbf{1}, \mathbf{2}, \mathbf{2}\} + \{\mathbf{2}, \mathbf{1}, \mathbf{2}\}, \end{aligned} \tag{3.5.22}$$

respectively. Moreover, as we mentioned before, we can use these projection matrices to obtain the decomposition of every other representation of the algebra. For

example

$$
\begin{aligned}
SU(5) &\begin{cases} \bar{\mathbf{5}} & \to \{\bar{\mathbf{3}}, \mathbf{1}, -\frac{2}{5}\} + \{\mathbf{1}, \mathbf{2}, \frac{3}{5}\}, \\ \mathbf{10} & \to \{\mathbf{3}, \mathbf{2}, -\frac{1}{5}\} + \{\bar{\mathbf{3}}, \mathbf{1}, \frac{4}{5}\} + \{\mathbf{1}, \mathbf{1}, -\frac{6}{5}\}, \\ \mathbf{24} & \to \{\mathbf{8}, \mathbf{1}, 0\} + \{\mathbf{1}, \mathbf{3}, 0\} + \{\mathbf{3}, \mathbf{2}, 1\} + \{\bar{\mathbf{3}}, \mathbf{2}, -1\} + \{\mathbf{1}, \mathbf{1}, 0\}, \end{cases} \\
SO(7) &\begin{cases} \mathbf{7} & \to \{\mathbf{2}, \mathbf{2}, \mathbf{1}\} + \{\mathbf{1}, \mathbf{1}, \mathbf{3}\}, \\ \mathbf{21} & \to \{\mathbf{3}, \mathbf{1}, \mathbf{1}\} + \{\mathbf{1}, \mathbf{3}, \mathbf{1}\} + \{\mathbf{1}, \mathbf{1}, \mathbf{3}\} + \{\mathbf{2}, \mathbf{2}, \mathbf{3}\}. \end{cases}
\end{aligned}
\tag{3.5.23}
$$

Finally, we need to specify how the reducible representations[15] of product algebras decompose into subalgebras. Since the weights of a product representation are built by combining the weights of the simple factors, as we learnt in section 3.5.1, so will be the weight matrix W, because its columns are just the weights of the product. Therefore, the projection matrix P can be built be stacking together the projection matrices of the individual simple algebras as blocks in a block diagonal matrix. Let $\mathcal{G}_1 \otimes \mathcal{G}_1$ be a product algebra, that decomposes into $\mathcal{F}_1 \otimes \mathcal{F}_2$, themselves product algebras in general, and the projection matrices from $\mathcal{G}_1 \to \mathcal{F}_1$ and $\mathcal{G}_2 \to \mathcal{F}_2$ be P_1 and P_2. Then the projection matrix P from $\mathcal{G}_1 \otimes \mathcal{G}_2 \to \mathcal{F}_1 \otimes \mathcal{F}_2$ is

$$
P = \left(\begin{array}{ccc|ccc} & & & 0 & \dots & 0 \\ & P_1 & & \vdots & \ddots & \vdots \\ & & & 0 & \dots & 0 \\ \hline 0 & \dots & 0 & & & \\ \vdots & \ddots & \vdots & & P_2 & \\ 0 & \dots & 0 & & & \end{array}\right). \tag{3.5.24}
$$

Occasionally, when the rank of the broken algebra is larger than that of the subalgebra and the subalgebra has an abelian factor, there is mixing of the broken diagonal generators, as in equation (3.5.9). In those cases the remaining abelian charge will be a linear combination of the abelian charges of the broken generators. This means that if the algebra $\mathcal{G}_A \otimes \mathcal{G}_B$ decomposes into $\mathcal{F}_A \otimes \mathcal{F}_B \otimes U(1)_{A+B}$, the projection matrix of this embedding can be calculated using the projection matrices

$$
P_A \leftrightarrow \mathcal{G}_A \otimes \mathcal{G}_B \to \mathcal{F}_A \otimes \mathcal{F}_B \otimes U(1)_A, \tag{3.5.25}
$$

$$
P_B \leftrightarrow \mathcal{G}_A \otimes \mathcal{G}_B \to \mathcal{F}_A \otimes \mathcal{F}_B \otimes U(1)_B, \tag{3.5.26}
$$

[15] In product algebras, the representations are reducible, because they decompose naturally into the irreducible representations of the simple factors of the product.

which will only differ on their last row, and a mixing vector $M = (\alpha, \beta)$, that depends on the process of symmetry breaking, as

$$P = \begin{pmatrix} (P_A)_i \\ \alpha(P_A)_{-1} + \beta(P_B)_{-1} \end{pmatrix}, \tag{3.5.27}$$

where i labels the rows of P_A from $1, \ldots,$ rank$(\mathcal{F}_A \otimes \mathcal{F}_B)$ and the -1 index refers to the last row of both P_A and P_B.

3.5.4 Constructing Invariants

In the context of Quantum Field Theories, the fundamental object from which observables and measurable quantities can be obtained is the action. Because of this, the action must be invariant under the symmetry transformations of the Lie algebra of the system. Given a set of fields, embedded in representations of the algebra, one needs to find the combinations that will render the action invariant. The first step towards that goal is to calculate the direct products of the representations of the algebra, and from the outcome of that product, we will look for invariant or singlet combinations.

Let $\mathcal{R}_1$ and $\mathcal{R}_2$ be representations of the algebra, then their direct product would be a reducible representation, which can be decomposed as the direct sum of irreducible representations, i.e. $\mathcal{R}_1 \otimes \mathcal{R}_2 = \bigoplus_i \mathcal{R}_i$. The weight system of the product of representations W can be calculated as the sum of the weights of both $\mathcal{R}_i$ and $\mathcal{R}_2$, that is $W_{ij} = \vec{\omega}_i + \vec{\nu}_j$, where $\vec{\omega}_i$ and $\vec{\nu}_j$ are weights of $\mathcal{R}_1$ and $\mathcal{R}$ respectively. Within this weight system, the weights of the irreducible representations that it decomposes into can be easily found. The algorithm starts by locating the most positive weight in W, it then identifies the irrep it belongs to and constructs its weight system. Extracting out those weights from W and starting over to look for the most positive weight, iterating until there are no weights left in W, one finds the list of irreps $\mathcal{R}_i$. The diagram for this algorithm can be seen in fig. 3.12.

As an example, we will use representations of $SU(3)$, and we will calculate the direct product $\mathbf{3} \otimes \bar{\mathbf{3}}$. The weight systems of $\mathbf{3}$ and $\bar{\mathbf{3}}$ are,

$$\mathbf{3} \to \begin{pmatrix} 1 & 0 \\ -1 & 1 \\ 0 & -1 \end{pmatrix}, \quad \bar{\mathbf{3}} \to \begin{pmatrix} 0 & 1 \\ 1 & -1 \\ -1 & 0 \end{pmatrix}, \tag{3.5.28}$$

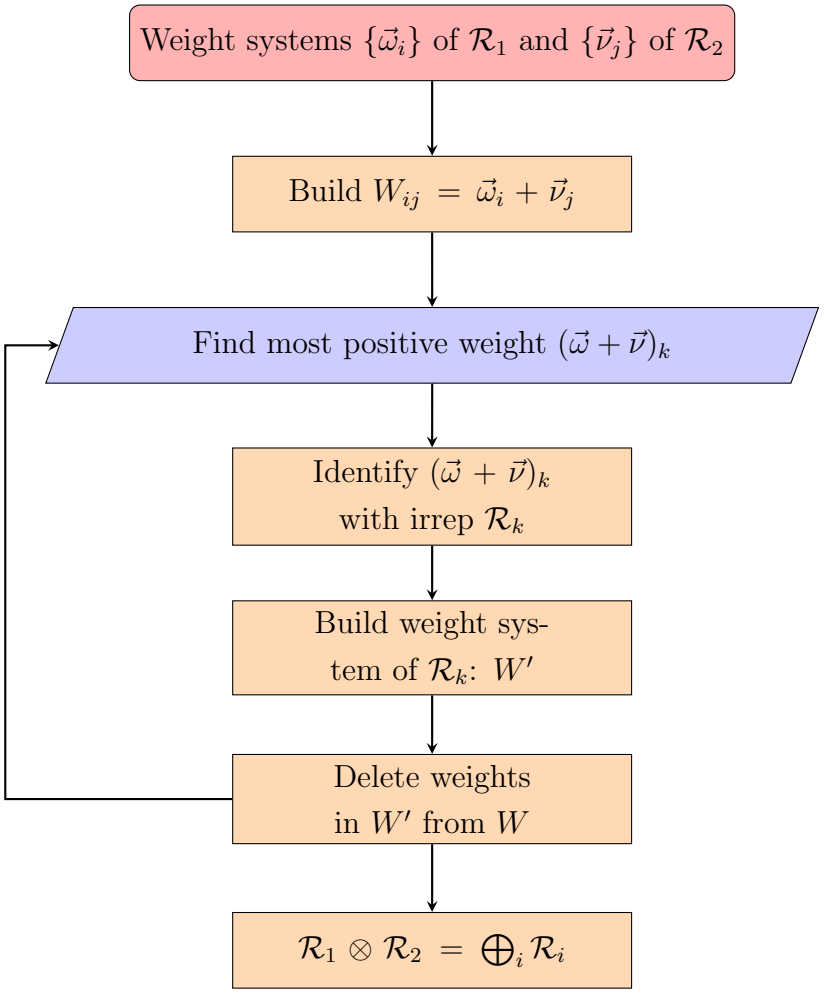

Figure 3.12: *Algorithm for calculating the direct product of representations of an algebra.*

so the weights of the direct product are

$$\mathbf{3} \otimes \bar{\mathbf{3}} \rightarrow \left(\begin{array}{cc} 1 & 1 \\ 2 & -1 \\ -1 & 2 \\ 0 & 0 \\ 0 & 0 \\ 1 & -2 \\ -2 & 1 \\ -1 & -1 \\ 0 & 0 \end{array} \right) \begin{array}{l} \Bigg\} \\ \\ \\ \\ \\ \\ \\ \\ \rightarrow \end{array} \begin{array}{l} \mathbf{8} \\ \\ \\ \\ \\ \\ \\ \\ \mathbf{1}, \end{array} \tag{3.5.29}$$

where the first eight rows correspond to the **8** representation of $SU(3)$ and the last

one to the singlet $\mathbf{1}$. Accordingly the decomposition would be

$$\mathbf{3} \otimes \bar{\mathbf{3}} = \mathbf{8} \oplus \mathbf{1}. \tag{3.5.30}$$

Incidentally, the product representations of equation (3.5.30) contain a singlet, and thus the combination of $\mathbf{3}$ and $\bar{\mathbf{3}}$ gives rise to a algebra invariant combination and as such, a viable term in the action.

Therefore, in order to construct the invariant combinations of a given set of representations, one needs to build the direct products of those representations that generate a singlet representation. Singlet representations are defined for simple algebras as those irreducible representations with dimension equal to the unity. This can also be extended to all Lie algebras by requiring that a singlet representation under a Lie algebra is a singlet under every embedded simple algebra, which for abelian algebras corresponds to having a zero charge. Thus a singlet representation of the Lie algebra $SU(3) \otimes SU(2) \otimes U(1)$ would be the $\{\mathbf{1}, \mathbf{1}, 0\}$.

Given a set of n irreducible representations of a Lie algebra, $\{\mathcal{R}_1, \ldots, \mathcal{R}_n\}$, we build all possible direct products of them $\mathcal{R}_{i_1} \otimes \cdots \otimes \mathcal{R}_{i_k}$ where $i_1, \ldots, i_k$ are chosen from $\{1, \ldots, n\}$ with possible repeated indices, and k ranges from 1 until the maximum number of representations allowed in a product. This number depends on the dimension of the fields involved and whether the theory is supersymmetric or not, e.g. if all fields are scalars in a non-supersymmetric theory and all couplings are renormalisable, then $k = 4$.

Following up the example above, with the set of representations given by $\{\mathbf{3}, \bar{\mathbf{3}}\}$, in a all-scalar non-supersymmetric renormalisable theory, the possible combinations are

$$\begin{array}{lll} \mathbf{3} \otimes \mathbf{3}, & \mathbf{3} \otimes \mathbf{3} \otimes \mathbf{3}, & \mathbf{3} \otimes \mathbf{3} \otimes \mathbf{3} \otimes \mathbf{3}, \\ \mathbf{3} \otimes \bar{\mathbf{3}}, & \mathbf{3} \otimes \mathbf{3} \otimes \bar{\mathbf{3}}, & \mathbf{3} \otimes \mathbf{3} \otimes \mathbf{3} \otimes \bar{\mathbf{3}}, \\ \bar{\mathbf{3}} \otimes \bar{\mathbf{3}}, & \mathbf{3} \otimes \bar{\mathbf{3}} \otimes \bar{\mathbf{3}}, & \mathbf{3} \otimes \mathbf{3} \otimes \bar{\mathbf{3}} \otimes \bar{\mathbf{3}}, \\ & \bar{\mathbf{3}} \otimes \bar{\mathbf{3}} \otimes \bar{\mathbf{3}}, & \mathbf{3} \otimes \bar{\mathbf{3}} \otimes \bar{\mathbf{3}} \otimes \bar{\mathbf{3}}, \\ & & \bar{\mathbf{3}} \otimes \bar{\mathbf{3}} \otimes \bar{\mathbf{3}} \otimes \bar{\mathbf{3}}, \end{array} \tag{3.5.31}$$

and with the result we obtained in equation (3.5.30) and the fact that $\mathbf{3} \otimes \mathbf{3} = \mathbf{6} \otimes \bar{\mathbf{3}}$, the only combinations that have a singlet in the product are

$$\mathbf{3} \otimes \bar{\mathbf{3}}, \quad \mathbf{3} \otimes \mathbf{3} \otimes \mathbf{3}, \quad \bar{\mathbf{3}} \otimes \bar{\mathbf{3}} \otimes \bar{\mathbf{3}}, \quad \mathbf{3} \otimes \mathbf{3} \otimes \bar{\mathbf{3}} \otimes \bar{\mathbf{3}}. \tag{3.5.32}$$

Given this result one could build a Lagrangian from a pair of real fields ϕ and $\bar{\phi}$ in the representations $\mathbf{3}$ and $\bar{\mathbf{3}}$ respectively. Assuming they are scalars fields, the

Lagrangian density is

$$\mathcal{L} = \mu^2 \ \bar{\phi}\phi + \lambda \ \phi^3 + \bar{\lambda} \ \bar{\phi}^3 + \rho \ \bar{\phi}^2\phi^2. \tag{3.5.33}$$

with arbitary real couplings μ, λ, $\bar{\lambda}$ and ρ.

While building Lagrangians in Quantum Field Theory, one must always take Poincaré invariance into account. This means that together with the internal gauge symmetries $\mathcal{G}$, such as $SU(3)$ in the example above, one must add the global Lorentz subgroup of symmetries. Luckily, in four dimensions the Lorentz algebra is isomorphic to $SU(2) \otimes SU(2)$, so it is enough to build invariant terms under the $\mathcal{G} \otimes SU(2) \otimes SU(2)$.

Carrying on with the example above, if ψ is a $SU(3)$ singlet spin-1/2 field it will be in the $\{\mathbf{2}, \mathbf{1}\}$ representation of the Lorentz group, while the scalar field ϕ from before is in the singlet $\{\mathbf{1}, \mathbf{1}\}$. Hence, we can add a $\psi\psi$ term to the Lagrangian above, while any other term will be forbidden by the Lorenz symmetry, ψ or ψ^3, or because of dimension counting (sticking to renormalisable Lagrangians), ψ^4 or $\psi\bar{\phi}\phi$.

3.6 Implementation and Example Run

All the algorithms described in section 3.5 are implemented in the group theory tool [207], using the object oriented programming language $C{+}{+}$ and it can be run through the command line. The details of which will be laid out in section 3.6.1. In order to add usability and pulchritude to the tool, an interface in Mathematica has been developed, which will call upon the $C{+}{+}$ backend through the library Mathlink [208], and its details are given in section 3.6.2. Finally, an example run of the tool is shown, in section 3.6.3, with typical input and sample output. The following description is intended as a brief overview of the practical implementation and usage, but should not be seen as a technical manual.

Similar approaches to building a computational tool capable of calculating Lie group properties have been done in the past, such as LieART [204] and Susyno [209]. Both of these tools use Mathematica as the main computational engine. However, neither of them go as far as this tool in calculating group properties. For example, LieART [204] does not calculate subgroups or breaking chains but rather depends on tabulated values, whereas Susyno [209] focuses mostly on properties of representations and it does not tackle any of the symmetry breaking elements, subgroups, chains or decomposition of representations.

3.6.1 *C++* Backend

Exploiting the object oriented paradigm of *C++*, all the main elements of the group tool are implemented in classes, with its properties and characteristics as the attributes and methods of such classes. The class diagram of the tool is depicted in figure 3.13, where one can see the main classes used in the implementation and their relations. The details of these classes are:

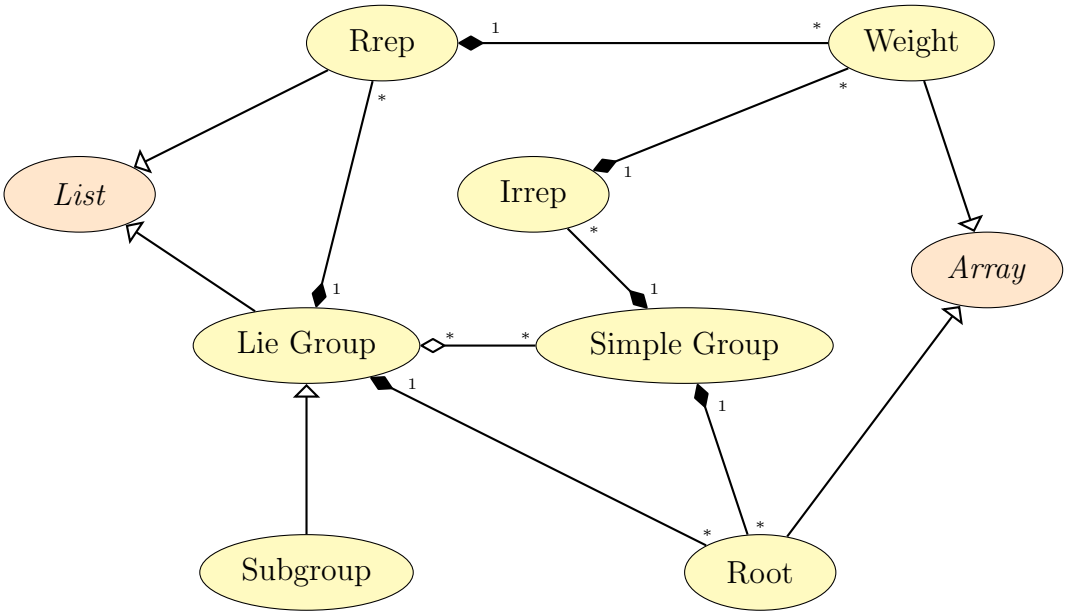

Figure 3.13: *Class diagram of the group theory tool. Yellow bubbles represent classes in the tool whereas orange bubbles are classes defined in C++ or other libraries. Triangle arrows denote generalization relations, hollow diamond arrows denote aggregation and full diamond arrows composition, whose multiplicities are indicated.*

- **Simple Group**: refers to a simple group or algebra, as defined previously, with attributes that span the properties of a simple algebra, such as type, rank, dimension, order, label, Cartan matrix, metric matrix, Casimir and information about the roots and representations.

- **Lie Group**: is a subclass of a List class, since it is stored as a list of simple groups. Its attributes mimic those of simple groups plus more specific ones such as number of abelian subalgebras or whether is simple, semisimple or neither.

- **Subgroup**: a subclass of the Lie group class, represents a subgroup and as

such along with the Lie group properties stores information about the supergroup, the projection matrix and a list of labels for the factors of the subgroup.

- **Irrep**: represents an irreducible representation of a simple group, and its attributes are the properties of a representation: dimension, highest weight, Casimir, Dynkin index, along with information about the group it belongs to and its weights.

- **Rrep**: represents a reducible representation of a Lie group and is a subclass of the class List. It is constructed as a list of irreps. Along with the properties of irreps, this class also stores the number of irreducible representations it contains.

- **Root**: is defined as a subclass of the class Array, together with information of the group it belongs to plus its length.

- **Weight**: similar to roots, is a subclass of Array and it also stores the multiplicity of the weight, its level and whether it is positive or not.

The methods of these classes will be those required to implement the algorithms previously described in section 3.5. Both the Simple Group and Lie Group classes will include methods to calculate their roots, where the Irrep and Rrep classes will have functions to obtain the weights. Similarly, the calculation of subgroups and breaking chains is implemented in methods of the Simple Group and Lie Group classes, as well as the construction of invariants. On the other hand, decomposition and direct product of representations are functions of Irrep and Rrep classes.

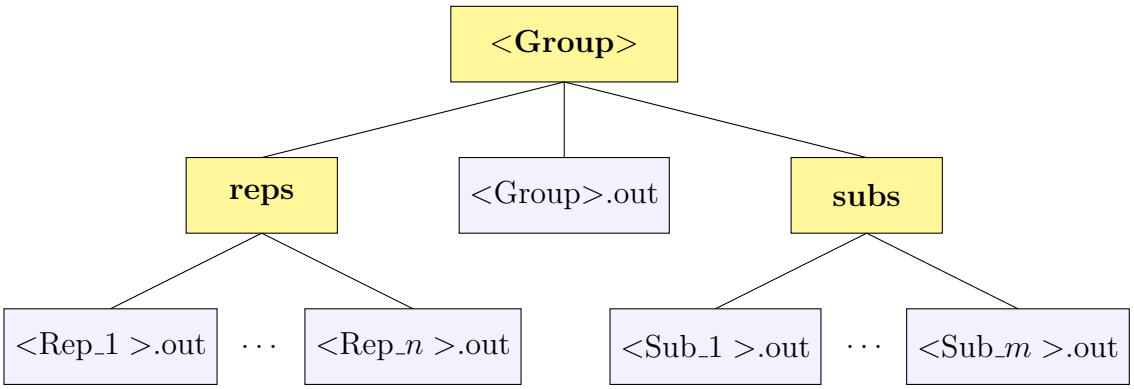

Figure 3.14: *File system for the group tool for a group of label <Group>. Yellow elements represent folder whereas grey elements represent files on the storage system.*

It is worth mentioning that, to speed up the calculation process, the tool stores information already calculated into files. The file system, shown in figure 3.14, will include information of the group in a file, encoded in JSON format [210], together with a list of representations and a list of subgroups, each of which with their properties in a file, also encoded in JSON format.

As an example, the file structure of the group A_2 ($SU(3)$) will include the file "A2.out", that will have the content:


```
{
    "id" :  "A2",
    "rank" :  2,
    "type" :  "A",
    "dim" :  8,
    "order" :  3,
    "label" :  "SU(3)",
    "abelian" :  false,
    "Cartan" :  [[2,-1],[-1,2]],
    "G" :  [[0.666667,0.333333],[0.333333,0.666667]],
    "Casimir" :  3,
    "Reps" :  [
        "(0,0)A2",
        "(1,0)A2",
        "(0,1)A2",
        "(2,0)A2",
        "(0,2)A2",
        "(1,1)A2"
    ],
    "Subgroups" :  [
        "A1(A)xU1(B)[A2]",
        "U1(A)xU1(B)[A2]",
        "A1(A)[A2]",
        "U1(A)[A2]",
        "U1(B)[A2]"
    ]
}
```


The representations folder, "reps" will have a file named "(1,0)A2.out", which will refer to the **3** representation and its contents:

```
{
     "id" :  "(1,0)A2",
     "Group" :  "A2",
     "HWeight" :  [[1,0]],
     "dim" :  3,
     "real" :  false,
     "label" :  "3",
     "Casimir" :  1.333334,
     "DynkinIndex" :  0.5,
     "conjugate" :  0,
     "congruency" :  [[1]],
     "Weights" :  [
          "(1,0)A2",
          "(-1,1)A2",
          "(0,-1)A2"
     ]
}
```


Finally, an example subgroup, in the subgroup folder "subs" there will be a file "A1(A)xU1(B)[A2].out" with the information of the $SU(2) \otimes U(1)$ subgroup, with contents:


```
{
     "rank" :  2,
     "dim" :  4,
     "label" :  "SU(2) x U(1)",
     "simple" :  false,
     "semisimple" :  false,
     "ngroups" :  2,
     "nabelians" :  1,
     "Casimir" :  [2,0],
     "Reps" :  [],
     "Subgroups" :  [],
     "id" :  "A1(A)xU1(B)[A2]",
     "SuperGroups" :  ["A2" :  ["A1(A)" :  [],"U1(B)" :  []]],
     "Projection" :  [[0,-1],[-0.666667,-0.333333]],
     "labels" :  ["A","B"],
     "maximal" :  true,
```

```
    "regular" :  true,
    "special" :  false
}
```

where the subgroups and representations have been omitted for convenience.

3.6.2 Mathematica Frontend

The Mathematica frontend extends and improves the usability of the group tool, since it brings together the analytical and interpreted Mathematica interface with the fast and powerful computation capabilities of C++. The connection between Mathematica and the C++ backend is implemented via the use of the library Mathlink [208].

In order to build a Mathlink between a Mathematica notebook and a piece of code in C++, one needs two basis ingredients: specific methods on the code for the different intended uses and a template file to translate those routines to Mathematica functions.

The methods required in the C++ code must be procedural, i.e. not object oriented, functions. They need to be written using only C native types and they can neither catch or handle exceptions. They are allowed to return a native type value, although it is usually convenient to return a void value and use the built-in Mathlink functions to return one or more values, e.g. `MLPutString(stdlink, const char *arg)`. This will be the approach taken here and all values returned will be JSON strings, so as to allow an easy and universal way to transfer large amounts of information in a format that Mathematica can easily decode.

As an example, we show a piece of code including a function that calculates the properties of a simple group given its rank and type and returns it through the Mathlink as a JSON string:

```
#include "liegroups.h"
#include "mathlink.h"

void getGroup(int rank, const char *type) {
    SimpleGroup G(rank, type[0]);
    G.Irreps();
    G.Subgroups();
    MLPutString(stdlink, G.json().write_formatted().c_str());
```

```
    return ;
}
```

Additionally the main function, that would be run through the MathLink (ML), needs only to call the main ML function, i.e., `MLMain(argc,argv)`[16].

The template file, required to translate the $C++$ methods as described above into Mathematica functions, needs to be written in a ML specific format. The same function as on the example above will need the following template

```
:Begin:
:Function:       getGroup
:Pattern:        GetGroup[rank_Integer, type_String]
:Arguments:      rank, type
:ArgumentTypes:  Integer, String
:ReturnType:     Manual
:End:
:Evaluate:       GetGroup::usage = "GetGroup[rank, type] gets the
                 information of the group defined by rank and type".
```

where the `:Function:` tag specifies the $C++$ method that is to be called, the `:Pattern:` tag defines the Mathematica function, with the arguments in `:Arguments:` and types in `:ArgumentTypes:`. As mentioned before, with a manual `:ReturnType:` one needs the $C++$ method to return void but information can be passed via ML functions such as `MLPutString(stdlink, arg)`. Lastly the tag `:Evaluate:` is optional and will contain a description of the function to the Mathematica frontend.

Therefore, once properly compiled and built, it is enough to install the program, called "mathgroup" in our case, in the Mathematica frontend via

```
Link = Install["mathgroup"].
```

Then all the functions defined in the template file as above can be used, and a list of those functions can be obtained by `LinkPatterns[Link]`, which in our case prompts the output:

Finally, in the Mathematica frontend we will make use of these functions to obtain the information of the groups, irreps, etc. However, in order to maintain a similar level of object orientation as we had in the $C++$ backend, we define functions that will implement a "pseudo" object oriented paradigm. These functions will

[16]In Windows systems, the call to the Mathlink main function is a bit more involved, but since we expect to run this only on Unix systems, we will not expand into this.

```
GetGroup[rank_Integer,type_String]
GetGroup[id_String]
GetReps[id_String,maxdim_Integer]
GetSubgroups[id_String]
GetRep[id_String]
GetRep[dimId_String,groupId_String]
GetSubgroup[id_String]
GetSubgroup[id_String,MixingId_String]
GetBreakingChains[SuperId_String,SubId_String]
GetDecomposeRep[RepId_String,SubgroupId_String,MixingId_String]
GetWeights[RepId_String]
GetDirectProduct[RepId1_String,RepId2_String]
GetInvariants[RepsId_String,dim_Integer]
```

gather the information from the particular object, store it in an internal variable in the Mathematica Kernel, under a unique identifier, `DBData[id]`, typically the label of the group, irrep, etc., and return that identifier as if it were a handle of an object. Along with the advantage of a modular and object oriented way of treating objects in Mathematica, one also benefits from faster access to the information, since all the data stored in the internal variable `DBData` will be reused when needed, without having to recalculate it through the MathLink.

3.6.3 Sample Session

To illustrate the practical use of our tool, a sample case for the semisimple algebra $A_3 \otimes A_1 \otimes A_1$ ($SU(4) \otimes SU(2) \otimes SU(2)$) will be provided. Though it is possible to get the same information through the command line, running directly the executable program obtained from the $C{+}{+}$ code, the output is in a dense format and it is hard to identify the properties. Hence, we will give the example using the Mathematica frontend, since it is more suitable for illustration.

The first step is to install the program using the MathLink library. Provided the Mathematica notebook and the executable file are in the same directory, this can be done by

```
In[1]:= Link = Install["./mathgroup"];
```

Next we create the "object" for the group, which we will use for the rest of the program, so we store the identifier, the label, in a variable `G` for later use.

```
In[2]:= G = NewGroup["A3xA1xA1"]
Out[2]:= A3xA1xA1
```

In order to access the properties of the group, stored in the internal variables, we use the function `Attribute`, e.g. to get the rank, dimension and Casimir of `G` we use

```
In[3] := Attribute[G]["rank"]
         Attribute[G]["dim"]
         Attribute[G]["Casimir"]
Out[3]:= 5
Out[4]:= 21
Out[5]:= {4, 2, 2}
```

or we can use the reserved word `All` to get all the properties

```
In[6]:= Attribute[G][All] // TableForm
Out[6]//TableForm:=
         rank → 5
         dim → 21
         id → A3xA1xA1
         nabelians → 0
         label → SU(4) x SU(2) x SU(2)
         simple → False
         ngroups → 3
         semisimple → True
         Casimir → {4, 2, 2}
         Reps → {(0,0,0,0,0)A3xA1xA1,(0,0,0,0,1)A3xA1xA1,...}
         Subgroups → {A3(A)xA1(B)xU1(C)[A3xA1xA1],...}
```

where we have omitted the extensive list of representations and subgroups for illustrative purposes.

To calculate the breaking chains for this group `G` to another one, say the Standard Model group, $A2 \otimes A1 \otimes U1$ ($SU(3) \otimes SU(2) \otimes U(1)$), we need first to create such a group, and then call a function `BreakingChains`, which uses `GetBreakingChains` to get the list through the MathLink connection and formats the output, as well as printing trees for every breaking chain:

```
In[7] := SM = NewGroup["A2xA1xU1"]
Out[7]:= A2xA1xU1
In[8] := BreakingChains[G,SM];
```

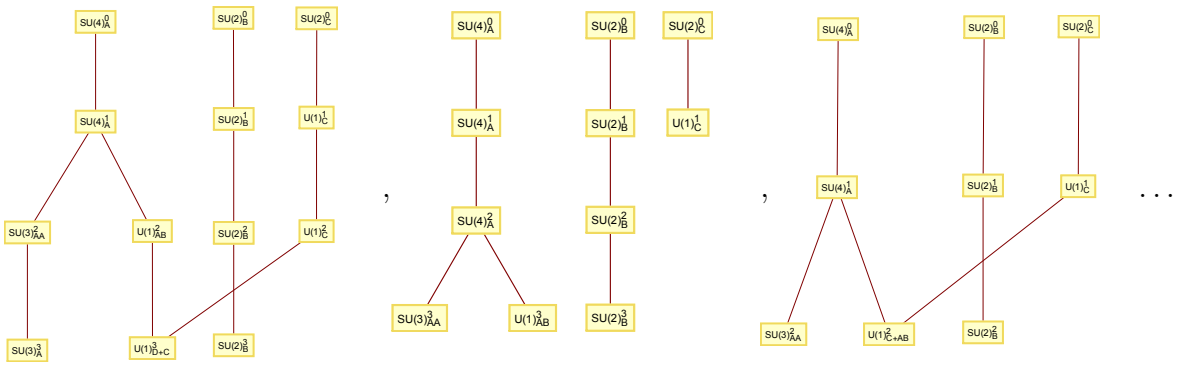

The next interesting algorithm to test is the decomposition of representations of `G` to representations of a subgroup. The representations can be taken from `Attribute[G]["Reps"]` and the subgroups from `Attribute[G]["Subgroups"]`. For simplicity we choose the representation $\{\mathbf{4},\mathbf{2},\mathbf{2}\}$ which corresponds to the identifier `(1,0,0,1,1)A3xA1xA1` and the Standard Model subgroup, which corresponds to `A2(AA)xA1(B)xU1(C+AB)[A3xA1xA1]`. Since the abelian factor of the SM group is a mix of the broken generators coming from the A_3 and the second A_1 factor (denoted by the `C+AB` label) the decomposition needs a mixing vector (see section 3.5.3), which for convenience we choose as $M = (\frac{1}{2}, \frac{1}{2})$. Hence, defining the representation, mixing vector and subgroup as

```
In[9]  := R = NewRep["(1,0,0,1,1)A3xA1xA1"]
          M = {{0.5,0.5}}
          F = NewSubgroup["A2(AA)xA1(B)xU1(C+AB)[A3xA1xA1]",M]
Out[9] := {4, 2, 2}
Out[10]:= ( 0.5 0.5 )
Out[11]:= A2(AA)xA1(B)xU1(C+AB)[A3xA1xA1]
```

the decomposition will be

```
In[12] := DecomposeReps[R, F, M]
Out[12]:= {{3, 2, 0.125},{3, 2, -0.375},{1, 2, 0.625},{1, 2, 0.125}}
```

To conclude, we demonstrate how to obtain the invariants, for the products of representations of $SU(4) \otimes SU(2) \otimes SU(2)$. For simplicity we choose the representations $\{\mathbf{4},\mathbf{2},\mathbf{2}\}$ and $\{\bar{\mathbf{4}},\mathbf{2},\mathbf{2}\}$, because they are conjugate of each other, and we choose to limit the calculation to dimension 4, as if we wanted to build a renormalisable Lagrangian. Thus we get

```
In[13] := R1 = NewRep["(1,0,0,1,1)A3xA1xA1"]
          R2 = NewRep["(0,0,1,1,1)A3xA1xA1"]
Out[13]:= {4, 2, 2}
```

```
Out[14]:= {4*, 2, 2}
In[15] := Invariants[{R1,R2},4] // TableForm
Out[15]//TableForm:=
          {4, 2, 2}   {4*, 2, 2}
          {4*, 2, 2}  {4, 2, 2}
          {4, 2, 2}   {4, 2, 2}   {4, 2, 2}   {4, 2, 2}
          {4, 2, 2}   {4, 2, 2}   {4*, 2, 2}  {4*, 2, 2}
          {4, 2, 2}   {4*, 2, 2}  {4, 2, 2}   {4*, 2, 2}
          {4, 2, 2}   {4*, 2, 2}  {4*, 2, 2}  {4, 2, 2}
          {4*, 2, 2}  {4, 2, 2}   {4, 2, 2}   {4*, 2, 2}
          {4*, 2, 2}  {4, 2, 2}   {4*, 2, 2}  {4, 2, 2}
          {4*, 2, 2}  {4*, 2, 2}  {4, 2, 2}   {4, 2, 2}
          {4*, 2, 2}  {4*, 2, 2}  {4*, 2, 2}  {4*, 2, 2}
```

As an illustrative summary of the computation capabilities of the tool, we collect the properties of the group $SU(4) \otimes SU(2) \otimes SU(2)$ in figure 3.15, and those of its representations in figure 3.16.

Group	rank	dim	id	nabelians	simple	ngroups	semisimple	Casimir
SU(4) x SU(2) x SU(2)	5	21	A3xA1xA1	0	False	3	True	{4, 2, 2}

Figure 3.15: *Properties of the group $SU(4) \otimes SU(2) \otimes SU(2)$, calculated with the computational tool.*

Rep	DynkinIndex	Group	dim	id	real	HWeight	nirreps	Casimir
{1, 1, 1}	{0, 0, 0}	A3xA1xA1	1	(0,0,0,0,0)A3xA1xA1	True	{{0, 0, 0, 0, 0}}	3	{0, 0, 0}
{1, 1, 2}	{0, 0, 0.5}	A3xA1xA1	2	(0,0,0,0,1)A3xA1xA1	True	{{0, 0, 0, 0, 1}}	3	{0, 0, 0.75}
{1, 1, 3}	{0, 0, 2}	A3xA1xA1	3	(0,0,0,0,2)A3xA1xA1	True	{{0, 0, 0, 0, 2}}	3	{0, 0, 2}
{1, 1, 4}	{0, 0, 5}	A3xA1xA1	4	(0,0,0,0,3)A3xA1xA1	True	{{0, 0, 0, 0, 3}}	3	{0, 0, 3.75}
{1, 1, 5}	{0, 0, 10}	A3xA1xA1	5	(0,0,0,0,4)A3xA1xA1	True	{{0, 0, 0, 0, 4}}	3	{0, 0, 6}
{1, 1, 6}	{0, 0, 17.5}	A3xA1xA1	6	(0,0,0,0,5)A3xA1xA1	True	{{0, 0, 0, 0, 5}}	3	{0, 0, 8.75}
{1, 1, 7}	{0, 0, 28}	A3xA1xA1	7	(0,0,0,0,6)A3xA1xA1	True	{{0, 0, 0, 0, 6}}	3	{0, 0, 12}
{1, 1, 8}	{0, 0, 42}	A3xA1xA1	8	(0,0,0,0,7)A3xA1xA1	True	{{0, 0, 0, 0, 7}}	3	{0, 0, 15.75}
{1, 1, 9}	{0, 0, 60}	A3xA1xA1	9	(0,0,0,0,8)A3xA1xA1	True	{{0, 0, 0, 0, 8}}	3	{0, 0, 20}
{1, 1, 10}	{0, 0, 82.5}	A3xA1xA1	10	(0,0,0,0,9)A3xA1xA1	True	{{0, 0, 0, 0, 9}}	3	{0, 0, 24.75}
{1, 2, 1}	{0, 0.5, 0}	A3xA1xA1	2	(0,0,0,1,0)A3xA1xA1	True	{{0, 0, 0, 1, 0}}	3	{0, 0.75, 0}
{1, 2, 2}	{0, 1, 1}	A3xA1xA1	4	(0,0,0,1,1)A3xA1xA1	True	{{0, 0, 0, 1, 1}}	3	{0, 0.75, 0.75}
{1, 2, 3}	{0, 1.5, 4}	A3xA1xA1	6	(0,0,0,1,2)A3xA1xA1	True	{{0, 0, 0, 1, 2}}	3	{0, 0.75, 2}
{1, 2, 4}	{0, 2, 10}	A3xA1xA1	8	(0,0,0,1,3)A3xA1xA1	True	{{0, 0, 0, 1, 3}}	3	{0, 0.75, 3.75}
{1, 2, 5}	{0, 2.5, 20}	A3xA1xA1	10	(0,0,0,1,4)A3xA1xA1	True	{{0, 0, 0, 1, 4}}	3	{0, 0.75, 6}
{1, 3, 1}	{0, 2, 0}	A3xA1xA1	3	(0,0,0,2,0)A3xA1xA1	True	{{0, 0, 0, 2, 0}}	3	{0, 2, 0}
{1, 3, 2}	{0, 4, 1.5}	A3xA1xA1	6	(0,0,0,2,1)A3xA1xA1	True	{{0, 0, 0, 2, 1}}	3	{0, 2, 0.75}
{1, 3, 3}	{0, 6, 6}	A3xA1xA1	9	(0,0,0,2,2)A3xA1xA1	True	{{0, 0, 0, 2, 2}}	3	{0, 2, 2}
{1, 4, 1}	{0, 5, 0}	A3xA1xA1	4	(0,0,0,3,0)A3xA1xA1	True	{{0, 0, 0, 3, 0}}	3	{0, 3.75, 0}
{1, 4, 2}	{0, 10, 2}	A3xA1xA1	8	(0,0,0,3,1)A3xA1xA1	True	{{0, 0, 0, 3, 1}}	3	{0, 3.75, 0.75}
{1, 5, 1}	{0, 10, 0}	A3xA1xA1	5	(0,0,0,4,0)A3xA1xA1	True	{{0, 0, 0, 4, 0}}	3	{0, 6, 0}
{1, 5, 2}	{0, 20, 2.5}	A3xA1xA1	10	(0,0,0,4,1)A3xA1xA1	True	{{0, 0, 0, 4, 1}}	3	{0, 6, 0.75}
{1, 6, 1}	{0, 17.5, 0}	A3xA1xA1	6	(0,0,0,5,0)A3xA1xA1	True	{{0, 0, 0, 5, 0}}	3	{0, 8.75, 0}
{1, 7, 1}	{0, 28, 0}	A3xA1xA1	7	(0,0,0,6,0)A3xA1xA1	True	{{0, 0, 0, 6, 0}}	3	{0, 12, 0}
{1, 8, 1}	{0, 42, 0}	A3xA1xA1	8	(0,0,0,7,0)A3xA1xA1	True	{{0, 0, 0, 7, 0}}	3	{0, 15.75, 0}
{1, 9, 1}	{0, 60, 0}	A3xA1xA1	9	(0,0,0,8,0)A3xA1xA1	True	{{0, 0, 0, 8, 0}}	3	{0, 20, 0}
{1, 10, 1}	{0, 82.5, 0}	A3xA1xA1	10	(0,0,0,9,0)A3xA1xA1	True	{{0, 0, 0, 9, 0}}	3	{0, 24.75, 0}
{4, 1, 1}	{0.5, 0, 0}	A3xA1xA1	4	(1,0,0,0,0)A3xA1xA1	False	{{1, 0, 0, 0, 0}}	3	{1.875, 0, 0}
{4, 1, 2}	{1, 0, 2}	A3xA1xA1	8	(1,0,0,0,1)A3xA1xA1	False	{{1, 0, 0, 0, 1}}	3	{1.875, 0, 0.75}
{4, 2, 1}	{1, 2, 0}	A3xA1xA1	8	(1,0,0,1,0)A3xA1xA1	False	{{1, 0, 0, 1, 0}}	3	{1.875, 0.75, 0}
{4*, 1, 1}	{0.5, 0, 0}	A3xA1xA1	4	(0,0,1,0,0)A3xA1xA1	False	{{0, 0, 1, 0, 0}}	3	{1.875, 0, 0}
{4*, 1, 2}	{1, 0, 2}	A3xA1xA1	8	(0,0,1,0,1)A3xA1xA1	False	{{0, 0, 1, 0, 1}}	3	{1.875, 0, 0.75}
{4*, 2, 1}	{1, 2, 0}	A3xA1xA1	8	(0,0,1,1,0)A3xA1xA1	False	{{0, 0, 1, 1, 0}}	3	{1.875, 0.75, 0}
{6, 1, 1}	{1, 0, 0}	A3xA1xA1	6	(0,1,0,0,0)A3xA1xA1	True	{{0, 1, 0, 0, 0}}	3	{2.5, 0, 0}
{10, 1, 1}	{3, 0, 0}	A3xA1xA1	10	(2,0,0,0,0)A3xA1xA1	False	{{2, 0, 0, 0, 0}}	3	{4.5, 0, 0}
{10*, 1, 1}	{3, 0, 0}	A3xA1xA1	10	(0,0,2,0,0)A3xA1xA1	False	{{0, 0, 2, 0, 0}}	3	{4.5, 0, 0}

Figure 3.16: *Properties of some of the representations of the* $SU(4) \otimes SU(2) \otimes SU(2)$ *group, up to dimension 10, calculated with the computational tool.*

4

Automated GUT Model Building

The description of Lie groups and algebras and the implementation of the group tool in section 3, has a direct application to model building in Grand Unified models. From the simple GUTs that were introduced in section 2.2 to more complicated models, the process of model building at the basic level boils down to choosing a set of symmetries, a set of representations of the groups realising those symmetries, and the symmetry breaking mechanism to the Standard Model group, $SU(3)_C \otimes SU(2)_L \otimes U(1)_Y$.

Out of the many possible choices for a unified theory, we choose $SO(10)$ as our symmetry group in the ultraviolet, because of its many interesting features, described in section 2.2.5, and the multiple possible breaking patterns and representations to choose from. $SO(10)$ models have been studied thoroughly for years, such as models with the Pati-Salam or left-right symmetry groups as intermediate steps [151, 152], models with intermediate $SU(5) \otimes U(1)$ groups, standard or flipped, [153], or even direct breaking from $SO(10)$ to the SM [154].

However, most of these attempts only deal with minimal models and to our best knowledge there has been no attempt to extend the analysis to more general cases. Therefore, our main goal in model building will be to develop a framework capable of analysing general non-minimal models that go beyond the previous approaches [211]. In order to make the analysis as general as possible we will not strive to examine the models in full detail, but we will focus on their general properties, derived from the structure of the symmetries, and on some phenomenological conditions that may constrain the scope of the models.

As a consequence of this general approach, the models obtained through this framework will not be fully determined. The focal point of the analysis will lie on the group structure, aiming to satisfy the conditions of symmetry breaking strictly from

the group properties, without realising the full scalar potential. The basic paradigm in our approach is gauge coupling unification at the $SO(10)$ breaking scale. On the other hand, we a priori allow the SUSY scale to appear at any scale between M_{EW} and M_{GUT}. This crucially departs from other analyses which usually consider SUSY scales around the TeV range. Additionally, we do not consider discrete symmetries as part of the group structure, nor do we attempt to fit the charged fermion or neutrino masses and mixing. Our analysis should therefore be considered as a starting point to demonstrate the benefits of an automated approach. It can be supplemented later with additional theoretical considerations and constraints.

Throughout this section we will describe the development of such a framework, starting with the process of generating the different models with a breaking path from $SO(10)$ and a set of representations, in section 4.1, followed by the constraints that are to imposed on those models, section 4.2. Next, we will analyse the unification of gauge couplings of the obtained models in section 4.3, including the scale of supersymmetric breaking and mixing in the abelian sector. Finally, we will conclude with a demonstration for a particular breaking chain, with the left-right symmetry group as intermediate step, where we will show the distribution of models given the theoretical and phenomenological constraints, in section 4.4.

4.1 Generating Models

The first step of model building is the identification of the symmetries. Aside from the (Super-)Poincaré group of spacetime symmetry, in this work we will focus on gauge symmetries realised by Lie Groups. Other cases, such as discrete or non-compact groups might be useful to obtain precise gauge coupling unification [146] or to provide a proper flavour structure [212], among other applications, but their inclusion goes beyond the scope of this work.

As mentioned before, our starting point will be an $SO(10)$ unified theory at high energies, which will then break down in one or more steps to the SM gauge group $\mathcal{G}_{SM} = SU(3)_C \times SU(2)_L \times U(1)_Y$. Out of all the maximal subgroups of $SO(10)$, only two of them contain $\mathcal{G}_{SM}$ as a subgroup, $SU(5) \times U(1)$ and $SU(4) \times SU(2) \times SU(2)$, hence there will be two main branches of symmetry breaking. However, as can be seen in figure 2.2, any subgroup of the maximal subgroups can be an intermediate step of the breaking chain, provided the conditions for the symmetry breaking are satisfied. There are in total 15 different possibilities, ranging from one-step breaking, path (c) in figure 2.2, to four-step breaking, taking every intermediate subgroup of

$SU(4)\times SU(2)\times SU(2)$. The possible breaking paths and the conditions they require were explained in section 2.2.5.

Given a specific breaking chain, the only remaining input needed for model building at this stage is the set of fields at every step of the chain. Starting with the fields at the highest scale M_{GUT}, the scale of $SO(10)$ symmetry breaking, one can obtain the fields at the consecutive steps by decomposing the representations of those fields, until the SM scale. As was discussed in section 2.2, the SM content can be minimally embedded into three generations of **16**-plet representations, e.g.

$$\mathbf{16} = \{u_1^c, d_1^c, d_1 u_1, \nu^c, e^c, d_2, u_2, u_2^c, d_2^c, d_3, u_3, u_3^c, d_3^c, e, \nu\}_L. \tag{4.1.1}$$

We will make the simplifying assumption that no additional fermions are present in the model, within a non-SUSY framework. Instead, we assume that all other $SO(10)$ representations present in the theory are Lorentz scalars, and in supersymmetric models the fermionic superpartners of those scalars survive only until the SUSY scale.

According to the Extended Survival Hypothesis (ESH) [213, 214], the Higgs scalars acquire a mass compatible with the pattern of symmetry breaking. This means that at every scale the only surviving scalars are those required to satisfy the remaining symmetry breaking steps, whereas the rest of scalars will be integrated out at the GUT scale or at one of the intermediate scales. However, in general, these scalar fields are allowed to live at any scale, with masses that will be obtained dynamically from the configuration of the Lagrangian and the couplings involved.

Nevertheless, at this stage of model building we do not know the configuration of the Lagrangian or its couplings, thus we will assume, a priori, that all fields have the potential to survive or be integrated out at any of the scales. This allows for a very large set of models, particularly when there are high dimensional $SO(10)$ representations present, for there are 2^n possible combinations of fields out of the n fields obtained from the decomposition of $SO(10)$ representations. In order to make the analysis more manageable, and inspired by the ESH, we will only take a small number of fields out of the large set of possible fields, at every scale.

As an example, when large representations such as **126** or **120** are involved,

which decompose into the SM subgroup as

$$\begin{aligned}
\mathbf{126} \to\ & \{\mathbf{6},\mathbf{3},\text{-}\tfrac{1}{4}\} \oplus \{\mathbf{8},\mathbf{2},\text{-}\tfrac{1}{4}\} \oplus \{\mathbf{8},\mathbf{2},\ \tfrac{1}{4}\} \oplus \{\mathbf{3},\mathbf{3},\ \tfrac{1}{4}\} \oplus \{\bar{\mathbf{6}},\mathbf{1},\text{-}\tfrac{1}{4}\} \oplus \{\bar{\mathbf{3}},\mathbf{2},\ \tfrac{1}{4}\} \\
& \oplus \{\mathbf{3},\mathbf{2},\text{-}\tfrac{3}{4}\} \oplus \{\bar{\mathbf{6}},\mathbf{1},\ \tfrac{1}{4}\} \oplus \{\bar{\mathbf{3}},\mathbf{2},\ \tfrac{3}{4}\} \oplus \{\bar{\mathbf{6}},\mathbf{1},\ \tfrac{3}{4}\} \oplus \{\mathbf{3},\mathbf{2},\text{-}\tfrac{1}{4}\} \oplus \{\bar{\mathbf{3}},\mathbf{1},\text{-}\tfrac{3}{4}\} \\
& \oplus \{\mathbf{1},\mathbf{3},\ \tfrac{3}{4}\} \oplus \{\mathbf{3},\mathbf{1},\ \tfrac{1}{4}\} \oplus \{\bar{\mathbf{3}},\mathbf{1},\text{-}\tfrac{1}{4}\} \oplus \{\bar{\mathbf{3}},\mathbf{1},\text{-}\tfrac{1}{4}\} \oplus \{\bar{\mathbf{3}},\mathbf{1},\ \tfrac{1}{4}\} \oplus \{\mathbf{1},\mathbf{2},\text{-}\tfrac{1}{4}\} \\
& \oplus \{\mathbf{1},\mathbf{2},\ \tfrac{1}{4}\} \oplus \{\mathbf{1},\mathbf{1},\text{-}\tfrac{5}{4}\} \oplus \{\mathbf{1},\mathbf{1},\text{-}\tfrac{3}{4}\} \oplus \{\mathbf{1},\mathbf{1},\text{-}\tfrac{1}{4}\},
\end{aligned}$$

$$\begin{aligned}
\mathbf{120} \to\ & \{\mathbf{8},\mathbf{2},\text{-}\tfrac{1}{4}\} \oplus \{\mathbf{8},\mathbf{2},\ \tfrac{1}{4}\} \oplus \{\mathbf{3},\mathbf{3},\ \tfrac{1}{4}\} \oplus \{\bar{\mathbf{3}},\mathbf{3},\text{-}\tfrac{1}{4}\} \oplus \{\bar{\mathbf{3}},\mathbf{2},\ \tfrac{1}{4}\} \oplus \{\mathbf{3},\mathbf{2},\text{-}\tfrac{3}{4}\} \\
& \oplus \{\bar{\mathbf{6}},\mathbf{1},\ \tfrac{1}{4}\} \oplus \{\mathbf{6},\mathbf{1},\text{-}\tfrac{1}{4}\} \oplus \{\bar{\mathbf{3}},\mathbf{2},\ \tfrac{3}{4}\} \oplus \{\mathbf{3},\mathbf{2},\text{-}\tfrac{1}{4}\} \oplus \{\mathbf{3},\mathbf{1},\text{-}\tfrac{1}{4}\} \oplus \{\bar{\mathbf{3}},\mathbf{1},\text{-}\tfrac{3}{4}\} \\
& \oplus \{\mathbf{3},\mathbf{1},\ \tfrac{1}{4}\} \oplus \{\mathbf{3},\mathbf{1},\ \tfrac{1}{4}\} \oplus \{\bar{\mathbf{3}},\mathbf{1},\text{-}\tfrac{1}{4}\} \oplus \{\bar{\mathbf{3}},\mathbf{1},\text{-}\tfrac{1}{4}\} \oplus \{\mathbf{3},\mathbf{1},\ \tfrac{3}{4}\} \oplus \{\bar{\mathbf{3}},\mathbf{1},\ \tfrac{1}{4}\} \\
& \oplus \{\mathbf{1},\mathbf{2},\text{-}\tfrac{1}{4}\} \oplus \{\mathbf{1},\mathbf{2},\text{-}\tfrac{1}{4}\} \oplus \{\mathbf{1},\mathbf{2},\ \tfrac{1}{4}\} \oplus \{\mathbf{1},\mathbf{2},\ \tfrac{1}{4}\} \oplus \{\mathbf{1},\mathbf{1},\ \tfrac{3}{4}\} \oplus \{\mathbf{1},\mathbf{1},\text{-}\tfrac{3}{4}\},
\end{aligned} \tag{4.1.2}$$

the number of fields is very high, $n = 50$, which will prompt $N = 2^{50} \sim 10^{15}$ possibilities. Therefore, whenever there is a large number of representations at a scale ($n > 10$), we will restrict to having only up to $k = 5$ representations out of the whole set, at that scale, making the process more computational accessible and including in the set the simplest models, which is what we are interested in at first. The number of possible cases is then reduced significantly, and is given by

$$N = \sum_{k=0}^{5} \begin{pmatrix} n \\ k \end{pmatrix} \sim 2.5 \times 10^6, \quad \text{for } n = 50. \tag{4.1.3}$$

Therefore, the algorithm for generating models, shown in figure 4.1, given a set of representations at the $SO(10)$ scale and a symmetry breaking chain, consists of decomposing the fields into the subsequent group in the chain and, after applying the constraints (see section 4.2 below), obtaining all possible combinations, as discussed above. Repeating this process for all scales, the outcome will be a landscape of models, where each model will be defined by the sets of representations at the different scales. For a chain $\mathcal{G} \to \mathcal{F}_1 \to \cdots \to \mathcal{F}_{m-1} \to \mathcal{G}_{SM}$, with m the number of breaking steps, the set of models will be a list of the type

$$\{\mathcal{M}\} = \left\{ \begin{pmatrix} \text{Group} \to \mathcal{G}, & \text{Chain} \to \{\mathcal{G} \ \to \cdots \to \mathcal{G}_{SM}\}, & \text{Reps} \to \{\mathcal{R}_i^{(0)}\}, \\ \text{Group} \to \mathcal{F}_1, & \text{Chain} \to \{\mathcal{F}_1 \to \cdots \to \mathcal{G}_{SM}\}, & \text{Reps} \to \{\mathcal{R}_i^{(1)}\}, \\ \quad \cdots & \quad \cdots & \quad \cdots \\ \text{Group} \to \mathcal{G}_{SM}, & \text{Chain} \to \{\mathcal{G}_{SM}\}, & \text{Reps} \to \{\mathcal{R}_i^{(m)}\} \end{pmatrix} \right\}, \tag{4.1.4}$$

where $\{\mathcal{R}_i\}$ are the representations at the $SO(10)$ scale and $\{\mathcal{R}_i^{(j)}\}$ a combination of their decompositions at the jth step.

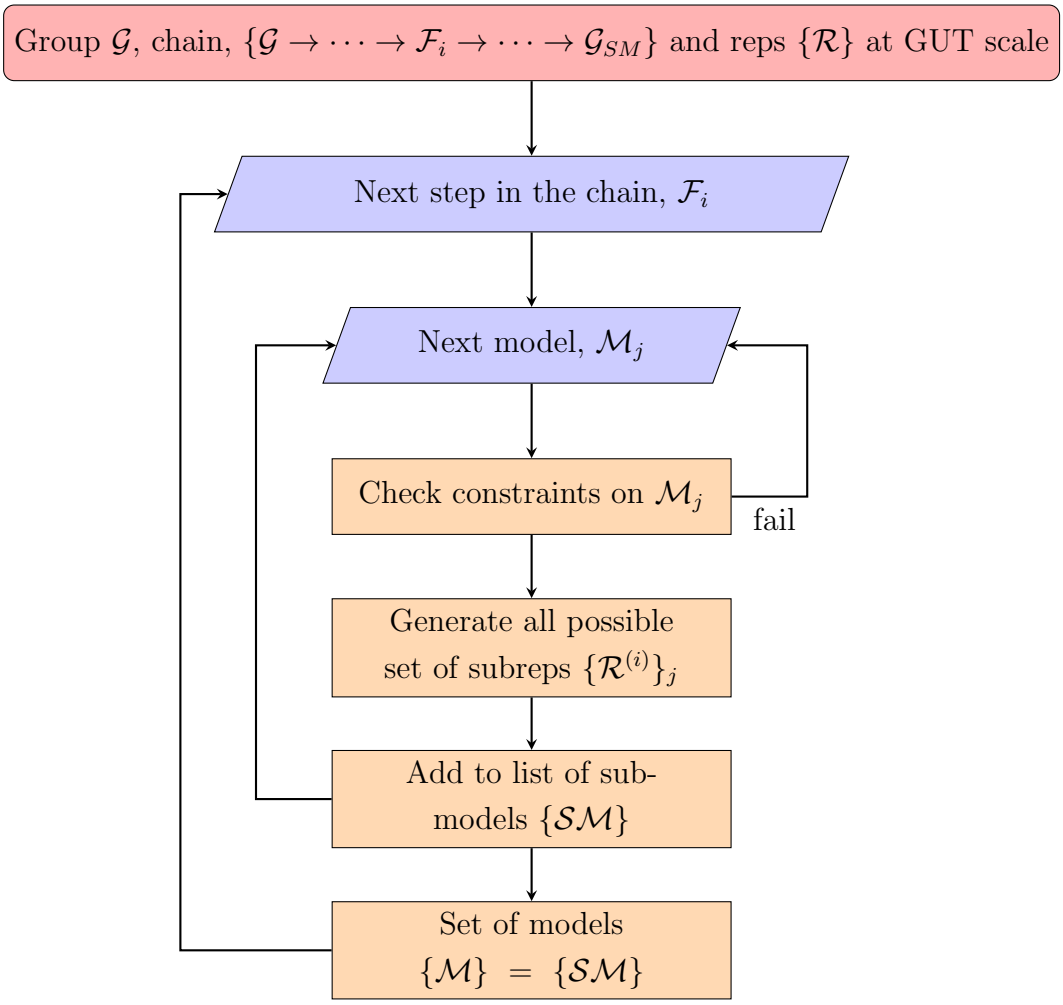

Figure 4.1: *Algorithm for generating models.*

4.2 Model Constraints

Despite the large number of models obtained via the process described above, not all of them will be valid candidates for a GUT. Each of the models, i.e. each of the combinations of fields, must satisfy a set of constraints at every step of the breaking chain, in order to be considered a successful model. We would like to stress again that we only include a basic set of constraints based on the group breaking structure and the set of representations.

4.2.1 Chirality

The first and most simple of these constraints is the condition of chirality. The gauge group of the theory, at every scale, must allow for its representations to respect the chiral structure of the SM, that left and right-handed fields transform under conjugate representations of the group[1]. As it was outlined in section 2.2, the chirality condition reduces the set of possible Lie groups that the SM can be embedded in. For simple groups this means that the group must allow complex representations which, as seen before, is satisfied by unitary groups $SU(n)$, orthogonal groups of the type $SO(2n)$ with n an odd number, and the exceptional algebra E_6.

The $SO(10)$ group is precisely one of the allowed cases for orthogonal groups, and as such it satisfies the condition as long as the SM fermions are embedded in the **16** dimensional representation. If that is the case then the chirality condition is satisfied automatically for all steps of the breaking chain, for each of the breaking patterns in figure 2.2, because they always involve unitary and semisimple subalgebras.

4.2.2 Cancellation of Anomalies

The second condition that a candidate model must meet is the cancellation of anomalies. There are several anomalies than can arise in a gauge theory, the most important of which are the Adler-Bell-Jackiw gauge anomaly [86, 87], the gravitational anomaly [215] and the Witten anomaly [216].

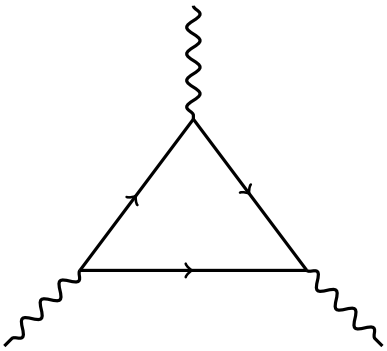

Figure 4.2: *Triangle diagram for Adler-Bell-Jackiw anomalies in gauge theories, with gauge bosons in the external legs and fermions in the loop.*

Gauge anomalies [86, 87] occur in theories with massive vector bosons, where

[1]See section 3.3 for a definition of conjugate representations.

triangle diagrams such as the one in figure 4.2 do not cancel. In such cases, the symmetry is broken at the quantum level and the theory becomes non-renormalizable [217]. The contribution of these diagrams to the anomaly is proportional to [89]

$$\mathcal{A}^i_{abc} = \mathrm{Tr}(\{T^i_a, T^i_b\}T^i_c), \tag{4.2.1}$$

where T^i_a are the generators of the group or groups associated with the gauge bosons on the external legs, written in the representation of the fermion f_i running inside the loop.

Most simple Lie algebras are automatically free of this type of anomaly and they are known as safe algebras [89], with the notable exception[2] of unitary algebras $SU(n)$ for $n \geq 3$ and the exceptional algebra E_6. In those cases, one must compute the contribution to the anomaly from all the fermions in the theory and require that their sum cancels, $\sum_i \mathcal{A}^i_{abc} = 0$.

For non-semisimple algebras, the gauge bosons in the external legs of figure 4.2 could belong to different factors of the product group. However, the properties of the generators T_a

$$\mathrm{Tr}(T_a) = 0, \quad \{T_a, T_b\} = \tfrac{1}{2}\delta_{ab}\mathbb{1}, \tag{4.2.2}$$

with δ_{ab} and $\mathbb{1}$ the identities in algebra and representation space respectively, ensure that any diagram with different non abelian gauge bosons on the external legs cancel automatically [20].

Non-supersymmetric theories without exotic fermions in non-trivial representations of the algebra are automatically anomaly free, because the fermionic matter sector, embedded in the anomaly-free **16** representation, is. However, in supersymmetric theories anomalies can easily arise from triangle diagrams with the superpartners of the various Higgs fields in the loop, so in these cases one must make sure that the contributions to the anomaly of all the representations in the theory cancel.

In the $SO(10)$ symmetric phase, all models are automatically free of gauge anomalies because $SO(10)$ is a safe algebra. For any intermediate step of the breaking chain the contribution of the gauge anomaly for every simple group factor of the gauge group at that scale, must be calculated as the sum of the contributions of each of the representations at that step. In order to calculate the contribution of each representation, we notice that the anomaly $\mathcal{A}_{abc}$ of the representation $\mathcal{R}$ can

[2]The orthogonal algebra $SO(6)$ is not safe either, since it is isomorphic to $SU(4)$, which is unitary and thus not safe.

be computed as [199]

$$\mathcal{A}_{abc}(\mathcal{R}) = \mathrm{Tr}(\{T_a, T_b\}T_c) = \mathcal{A}(\mathcal{R})d_{abc}, \tag{4.2.3}$$

where d_{abc} is the symmetrized trace of the group, defined in (3.3.21). Since d_{abc} is the same for all representations of the group $\mathcal{G}$, the value of the anomaly for a representation $\mathcal{R}$ depends only on $\mathcal{A}(\mathcal{R})$, which is obtained by using the properties [199]

$$\begin{aligned} \mathcal{A}(\overline{\mathcal{R}}) &= -\mathcal{A}(\mathcal{R}), \\ \mathcal{A}(\mathcal{R}_1 \oplus \mathcal{R}_2) &= \mathcal{A}(\mathcal{R}_1) + \mathcal{A}(\mathcal{R}_2), \\ \mathcal{A}(\mathcal{R}_1 \otimes \mathcal{R}_2) &= \dim(\mathcal{R}_1)\mathcal{A}(\mathcal{R}_2) + \dim(\mathcal{R}_2)\mathcal{A}(\mathcal{R}_1). \end{aligned} \tag{4.2.4}$$

The gravitational anomaly, which appears in theories with non-semisimple groups [215] at a scale close to the Planck scale, corresponds to triangle diagrams with two gravitons and an abelian gauge boson on the external legs, and fermions running through the loop. In this case eq. (4.2.1) boils down to $\mathcal{A} = \sum_i Q_i$, where Q_i are the abelian charges of the fermionic representations (c.f. hypercharge in the SM). For a given set of representations, the gravitational anomaly is calculated as the sum of charges for every $U(1)$, and it must cancel for each of them independently.

Lastly, the Witten anomaly has to do with the global topology of the $SU(2)$ group [216], and it requires an even number of flavours of $SU(2)$-charged fermions. Again, this condition only applies to the supersymmetric case, since the SM matter fields satisfy the constraint. If the gauge group at some scale contains one or more $SU(2)$ factors, the contribution to this anomaly from each of them is computed by counting the number of non-singlet representations of that $SU(2)$ factor, and requiring that it is even.

Those models for which the gauge, gravitational and the Witten anomaly cancel are anomaly free are considered valid in this respect. Since throughout our analysis we consider both supersymmetric and non-supersymmetric models, and the SUSY scale is allowed to slide through the scales, we will not rule out models on the basis of not being anomaly free, but rather we will tag them as such to be kept or discarded in a later stage once we have knowledge of the value of the SUSY scale. Therefore, we will extend the model in equation (4.1.4), to include the SUSY anomaly condition at every step,

$$\begin{pmatrix} \text{Group} \to \mathcal{G}, \\ \text{Chain} \to \{\mathcal{G} \to \cdots \to \mathcal{F}_m\}, \\ \text{Reps} \to \{\mathcal{R}_1, \dots\}, \\ \text{Anomaly Free} \to \text{true/false} \end{pmatrix}. \tag{4.2.5}$$

4.2.3 Symmetry Breaking

The next constraint to impose on the models is that it allows for successful symmetry breaking. Since there are one or more symmetry breaking steps throughout the chain, one needs to make sure that these can be realised by the scalar representations present in the theory. Thus, for every step, we will impose as a requirement that there is at least one field in the theory that can break the symmetry to the next step of the chain. This means that the set of representations of a step must contain a non-singlet representation that is a singlet under the subgroup, the group in the next step of the chain, but it is not a singlet under possible intermediate groups.

Of course, the existence of such a representation is not enough to trigger the breaking of the symmetry; formally one needs to make sure that there is a transition between the symmetry preserving and symmetry breaking vacua. However, this would require knowledge of the scalar potential of the theory and the parameters within, which falls out of the scope of this analysis. Therefore, we will consider as a necessary and sufficient condition for symmetry breaking that there exists a representation capable of doing so.

As a general procedure, we assume that the representation that causes the breaking acquires a mass of the order of the scale of the breaking, that is the whole multiplet, not just the singlet component that gets a vacuum expectation value, and thus we integrate it out from the possible representations at the next scale.

To give an example, we will use the breaking chain $SO(10) \to SU(5) \to SU(3) \otimes SU(2) \otimes U(1)$. In this case, the first step is satisfied if there is a scalar field in the **16** or **126** representation of $SO(10)$, because they decompose as

$$\begin{aligned} \mathbf{16} &\to \mathbf{10} \oplus \bar{\mathbf{5}} \oplus \mathbf{1}, \\ \mathbf{126} &\to \mathbf{50} \oplus \mathbf{45} \oplus \overline{\mathbf{15}} \oplus \mathbf{10} \oplus \bar{\mathbf{5}} \oplus \mathbf{1}, \end{aligned} \tag{4.2.6}$$

and both contain a singlet under $SU(5)$. The last step will then be satisfied if at the intermediate step there is a surviving field in the **24** representation, because it decomposes to $\mathcal{G}_{SM}$ as

$$\mathbf{24} \to \{\mathbf{8}, \mathbf{1}, 0\} \oplus \{\mathbf{3}, \mathbf{2}, 1\} \oplus \{\bar{\mathbf{3}}, \mathbf{2}, \text{-}1\} \oplus \{\mathbf{1}, \mathbf{3}, 0\} \oplus \{\mathbf{1}, \mathbf{1}, 0\}, \tag{4.2.7}$$

which does have a singlet under $SU(3) \otimes SU(2) \otimes U(1)$. This **24** representation comes, for example, from a **45** representation of $SO(10)$, which means that the minimum content at the $SO(10)$ scale that is able to realise this symmetry breaking pattern will be either $\mathbf{16} \oplus \mathbf{45}$ or $\mathbf{126} \oplus \mathbf{45}$.

4.2.4 Standard Model

Finally, the last (obvious) requirement that we impose on a model is that it reproduces the SM group and its particle content. The last step of the breaking chain in any realistic GUT is the SM gauge group, $SU(3)_C \otimes SU(2)_L \otimes U(1)_Y$, so one needs to ensure that at least the SM matter content is reproduced here, including the precise hypercharge assignments (modulo some overall normalisation factor). This condition must also require the existence of a Higgs doublet, so as to satisfy electroweak symmetry breaking. The minimal SM content required is

$$3 \times \left(\{\mathbf{3},\mathbf{2},\ \tfrac{1}{6}\} \oplus \{\overline{\mathbf{3}},\mathbf{1},\text{-}\tfrac{2}{3}\} \oplus \{\overline{\mathbf{3}},\mathbf{1},\ \tfrac{1}{3}\} \oplus \{\mathbf{1},\mathbf{2},\text{-}\tfrac{1}{2}\} \oplus \{\mathbf{1},\mathbf{1},\ 1\}\right) \oplus \{\mathbf{1},\mathbf{2},\text{-}\tfrac{1}{2}\}, \tag{4.2.8}$$

which includes three generations of SM fermions plus a Higgs scalar.

The fermionic content of the SM is obtained automatically, given the appropriate embedding in the 16-dimensional representation of $SO(10)$. In addition we will allow the presence of SM fermion singlets, to represent the right-handed neutrino and/or any sterile neutrino that might appear in the theory. Therefore this constraint will only affect the scalar sector, which must have a scalar field in the representation $\{\mathbf{1},\mathbf{2},\text{-}\frac{1}{2}\}$ (in addition to the three generations of lepton doublets).

Throughout this analysis we assume that the scalar fields that are integrated out at some scale, all have masses very close to that scale. Therefore, given the lack of evidence for exotic coloured states at the SM scale, we will reject models that include those states. However, since the Higgs sector of the SM is still to be fully explored and pinned down, we will allow for extra scalar fields charged under the weak and hypercharge groups, and that the known Higgs boson is just the lowest mass eigenstate of all the scalar fields in the sector. As a matter of fact this comes as a requirement for supersymmetric models, which need two Higgs doublets to cancel their gauge anomaly, and where the SM Higgs is just the lightest of all five Higgs mass eigenstates.

4.3 Unification of Gauge Couplings

Once obtained the set of valid models, with the algorithm shown in figure 4.1 and applying the constraints above, the next step is to ensure that the breaking chain is consistent with the unification of the gauge couplings for every model. The running

of the gauge couplings is given by the Renormalisation Group Equations (RGEs), which for each model depend on the representations at every scale.

The set of RGEs together with the initial condition imposed by SM couplings at the electroweak scale and by the unification condition at M_{GUT} form a stringent constraint on any GUT symmetry breaking scenario. The values of the gauge couplings at the SM scale are [4]

$$\begin{aligned} g_1(M_Z) &= 0.46235 \pm 0.00010, \\ g_2(M_Z) &= 0.65295 \pm 0.00012, \\ g_3(M_Z) &= 1.220 \pm 0.003, \end{aligned} \tag{4.3.1}$$

where 1, 2 and 3 refer to the $U(1)$, $SU(2)$ and $SU(3)$ groups, respectively.

Solving the RGEs is in general a difficult endeavour because they usually depend on the other parameters in the theory and form a system of strongly coupled differential equations. We will restrict our analysis to the one-loop level for which the gauge coupling RGEs are uncoupled and can be easily solved analytically. The one-loop RGE for the gauge coupling g of a group $\mathcal{G}$ is

$$\mu \frac{\mathrm{d}g}{\mathrm{d}\mu} = \frac{1}{16\pi^2} b g^3, \tag{4.3.2}$$

where μ is an energy scale and the slope b is calculated as [185]

$$b = \frac{2}{3} \sum_{\text{Fermions}} S(\mathcal{R}_f) + \frac{1}{3} \sum_{\text{Scalars}} S(\mathcal{R}_s) - \frac{11}{3} C_2(\mathcal{G}). \tag{4.3.3}$$

Here, $C_2(\mathcal{G})$ is the Casimir of the group $\mathcal{G}$ and $S(\mathcal{R}_{s,f})$ is the Dynkin index of the scalar $\mathcal{R}_s$ or fermionic $\mathcal{R}_f$ representation under the group $\mathcal{G}$. For abelian groups, such as the hypercharge factor in the SM, the Casimir cancels, $C_2(U(1)) = 0$, and the Dynkin index of an irrep with $U(1)$ charge Q is given by $S(Q) = Q^2$.

When a group has more than one abelian factor, there is kinetic mixing among the slopes b of both [218]. This contribution, however, is usually quite small, of the order of the two-loop correction of the RGEs [218]. Since we already neglect the two-loop correction in the analysis, we will also neglect this contribution. Another type of abelian mixing happens when the symmetry breaking reduces the rank of the group and the subgroup has an $U(1)$ factor. Though this mixing does not affect the calculation of the slopes, it affects the matching conditions at the different scales, so it will be discussed later in section 4.3.2.

Field	$\mathcal{R}$	Spin	n_f	$SU(3)_C$	$SU(2)_L$	$U(1)_Y$
Q	$\{\mathbf{3},\mathbf{2},\ \frac{1}{6}\}$	$\frac{1}{2}$	3	$\frac{1}{2}\cdot 2$	$3\cdot\frac{1}{2}$	$3\cdot 2\cdot\frac{1}{36}$
u^c	$\{\overline{\mathbf{3}},\mathbf{1},\text{-}\frac{2}{3}\}$	$\frac{1}{2}$	3	$\frac{1}{2}$	0	$3\cdot\frac{4}{9}$
d^c	$\{\overline{\mathbf{3}},\mathbf{1},\ \frac{1}{3}\}$	$\frac{1}{2}$	3	$\frac{1}{2}$	0	$3\cdot\frac{1}{9}$
L	$\{\mathbf{1},\mathbf{2},\text{-}\frac{1}{2}\}$	$\frac{1}{2}$	3	0	$\frac{1}{2}$	$\frac{1}{4}$
e^c	$\{\mathbf{1},\mathbf{1},\ 1\}$	$\frac{1}{2}$	3	0	0	1
H	$\{\mathbf{1},\mathbf{2},\text{-}\frac{1}{2}\}$	0	1	0	$\frac{1}{2}$	$\frac{1}{4}$

Table 4.1: *Standard Model particle content and associated properties: spin, number of families n_f and Dynkin index (times the number of degrees of freedom) under the groups $SU(3)_C$, $SU(2)_L$ and $U(1)_Y$.*

As an example, for the SM particle content in table 4.1, which shows the Dynkin indices of the representations, and with Casimirs $C_2(SU(3)) = 3$, $C_2(SU(2)) = 2$ and $C_2(U(1)) = 0$, one obtains the slopes[3]

$$\{b_1, b_2, b_3\} = \left\{\tfrac{41}{10}, -\tfrac{19}{6}, -7\right\}, \tag{4.3.4}$$

for the three SM gauge groups.

The gauge coupling running in supersymmetric theories is described by a special case of eq. (4.3.3), where for every fermionic Weyl degree of freedom (d.o.f) there is a complex scalar, and for every gauge boson there is a new fermion d.o.f. In this case the slope b take the form

$$b = \sum_{\text{Superfields}} S(\mathcal{R}) - 3C_2(\mathcal{G}), \tag{4.3.5}$$

where the sum runs for all chiral superfields in the theory. For the MSSM content, as shown in table 2.1 in section 2.3, the slopes are

$$\{b_1, b_2, b_3\} = \left\{\tfrac{33}{5}, 1, -3\right\}. \tag{4.3.6}$$

The RGE in eq. (4.3.2) can be conveniently rewritten in terms of the parameter $\alpha = g^2/4\pi$, also known as a fine structure constant, as

$$\mu\frac{\mathrm{d}}{\mathrm{d}\mu}\alpha^{-1} = -\frac{b}{2\pi}. \tag{4.3.7}$$

[3]This values of the slopes are calculated including the contribution from the top quark, which we will take to be approximately at the electroweak scale M_Z.

Changing the variable to $t = 1/2\pi \log(\mu/M_Z)$ and given the boundary condition $\alpha^{-1}(t_0)$ at scale t_0, it can be solved analytically as

$$\alpha^{-1}(t) - \alpha^{-1}(t_0) = -b(t - t_0). \tag{4.3.8}$$

For a breaking chain from $SO(10)$ to the SM with m steps, there are $m-1$ intermediate scales μ_i, with $t_i = 1/2\pi \log(\mu_i/M_Z)$. Starting with the unification of gauge couplings at the scale $t_m = t_{GUT} \leftrightarrow \mu_m = M_{GUT}$, the RGEs can be solved at the following scale μ_{m-1}. The new boundary conditions $\alpha(t_{m-1})$ are used to solve for subsequent scales, iterating until the SM scale, $t_0 = 0 \leftrightarrow \mu_0 = M_Z$.

In such a scenario, there are $m+1$ free parameters, the $m-1$ intermediate scales, the GUT scale M_{GUT} and the coupling at the unification scale α_{GUT}. On the other hand, the running couplings must match their values at the SM scale, in eq. (4.3.1), which leaves at least $m-2$ degrees of freedom for any GUT scenario. If further constraints are applied, e.g. if the right-handed current in left-right symmetric models would be observed, there will be fewer degrees of freedom.

Since equation (4.3.8) is linear, one can write equations for the SM couplings α_i^{-1}, with $i = 1, 2, 3$, that implement the constraint of unification at α_{GUT}^{-1} as

$$\alpha_i^{-1} = \alpha_{GUT}^{-1} + \sum_{j=1}^{m} b_j^i \Delta t_j, \tag{4.3.9}$$

where we have defined the splitting between two consecutive scales as $\Delta t_j = t_j - t_{j-1}$ with $j = 1, \ldots, m$, and b_j^i are the slopes corresponding to particular segments Δt_j of the path connecting α_{GUT}^{-1} with α_i^{-1}. One can summarize these three conditions in a matrix form as

$$\begin{pmatrix} \alpha_3^{-1} \\ \alpha_2^{-1} \\ \alpha_1^{-1} \end{pmatrix} = \begin{pmatrix} 1 & b_1^3 & b_2^3 & \cdots & b_m^3 \\ 1 & b_1^2 & b_2^2 & \cdots & b_m^2 \\ 1 & b_1^1 & b_2^1 & \cdots & b_m^1 \end{pmatrix} \begin{pmatrix} \alpha_{GUT} \\ \Delta t_1 \\ \Delta t_2 \\ \vdots \\ \Delta t_m \end{pmatrix} \equiv B_0 \cdot \Delta t. \tag{4.3.10}$$

4.3.1 Supersymmetry

In models with supersymmetry, there is an additional scale, the mass scale of the supersymmetric particles. We will assume that the SUSY spectrum can a priori appear at any point between M_{SM} and M_{GUT}. Below the SUSY scale t_{SUSY}, scalar

superpartners of the SM fermions and fermionic superpartners of any other scalar or vector boson are integrated out.

Therefore, since the spectrum changes, the slopes b_i before and after SUSY will be different. The former will use equation (4.3.5) to calculate the slopes, using the full supersymmetric spectrum, whereas the latter will use (4.3.3), using only the SM content plus scalars. Let B_{SUSY} be a matrix of slopes, analogous to B_0, but using the supersymmetric spectrum, then we can construct a matrix B, which enters equation (4.3.10) in place of B_0, that can be formed by joining the first $k+1$ columns of B_0 and the last $m-k$ columns of B_{SUSY}. To get all the possible scenarios, one naturally has to repeat this procedure over all the possible positions of the SUSY-breaking scale, i.e. over all possible values of k.

Additionally, the position of the SUSY scale helps to discard some of the many models obtained before. As was discussed in section 4.2, supersymmetric models may suffer from anomalies if the sum of the contributions of their representations do not cancel. Hence, if any of the steps with scales above the SUSY scale, $t \geq t_k$, have a non-zero anomaly, as was tagged as such in the model algorithm, eq. (4.2.5), then that model is not valid and is excluded.

4.3.2 Abelian Breaking

In a number of breaking scenarios, those where there is a rank-reducing breaking and the subgroup contains an abelian factor, the generator of the remaining $U(1)$ factor is a linear combination of the diagonal generators of the supergroup. For the simple case $U(1)_A \times U(1)_B \to U(1)_C$, the charges of a field ϕ^j under $U(1)_C$ and its gauge coupling can be calculated as

$$g_C \; Q_C^j = g_A g_B \frac{Q_A^j Q_B^v - Q_B^j Q_A^v}{\sqrt{g_A^2 (Q_A^v)^2 + g_B^2 (Q_B^v)^2}}, \tag{4.3.11}$$

where g_A and g_B are the couplings of $U(1)_A$ and $U(1)_B$, respectively, Q_A^j and Q_B^j are the charges of the field ϕ^j and Q_A^v and Q_B^v are the charges of the breaking Higgs. If any or both of the supergroups are not abelian, then the charges correspond to the eigenvalues of the diagonal generators that survive the breaking.

Though they are not defined independently, we need to use both g_C and Q_C^j separately, the former when solving the RGEs to obtain limits on the scales and the latter to obtain the slopes of the RGEs. We will then choose to define

$$g_C = g_A g_B \frac{\sqrt{(Q_A^v)^2 + (Q_B^v)^2}}{\sqrt{g_A^2 (Q_A^v)^2 + g_B^2 (Q_B^v)^2}} = \frac{g_A g_B}{\sqrt{r_A^2 g_A^2 + r_B^2 g_B^2}}, \tag{4.3.12}$$

and

$$Q_C^j = \frac{Q_A^j Q_B^v - Q_B^j Q_A^v}{\sqrt{(Q_A^v)^2 + (Q_B^v)^2}} = r_B Q_A^j - r_A Q_B^j, \tag{4.3.13}$$

with $r_{A,B} = Q_{A,B}^v / \sqrt{(Q_A^v)^2 + (Q_B^v)^2}$ such that $r_A^2 + r_B^2 = 1$.

In $SO(10)$ unified models this $2 \to 1$ abelian breaking is the only type that will appear, hence the simple analysis above is sufficient.

The $U(1)$ breaking happens at some breaking scale t_{mix}, so the model at that scale requires an extra parameter, thus extending equation (4.2.5) to

$$\begin{pmatrix} \text{Group} \to \mathcal{F}_{mix}, \\ \text{Chain} \to \{\mathcal{F}_{mix} \to \cdots \to \mathcal{F}_m\}, \\ \text{Reps} \to \{\mathcal{R}_1, \dots\}, \\ \text{Anomaly Free} \to \text{true/false}, \\ \text{Mixing} \to \{r_A, r_B\} \end{pmatrix}. \tag{4.3.14}$$

At the scale t_{mix} the boundary conditions for the gauge coupling in the broken phase α_C^{-1} is given by

$$\alpha_C^{-1}(t_{mix}) = r_A^2 \alpha_A^{-1}(t_{mix}) + r_B^2 \alpha_B^{-1}(t_{mix}). \tag{4.3.15}$$

which allows us to write α_C^{-1} at the EW scale as

$$\alpha_1^{-1} = \alpha_C^{-1}(t_0) = \alpha_{GUT}^{-1} + r_A^2 \sum_{j=mix+1}^{m} b_j^{1A} \Delta t_j + r_B^2 \sum_{j=mix+1}^{m} b_j^{1B} \Delta t_j + \sum_{j=1}^{mix} b_j^C \Delta t_j, \tag{4.3.16}$$

where the slopes b_j^{1A} and b_j^{1B} correspond to the slopes of the gauge couplings before t_{mix} and $b_j^C = b_j^1$ the slope of the remaining coupling after t_{mix}.

In terms of the matrices in equation (4.3.10), one would need three independent matrices of slopes, B_A, B_B and B_C. The first two have zeroes in every b_j^a entry for $j = 1, \dots, mix$ and the slopes b_j^{1A} and b_j^{1B} for $j = mix+1, \dots, m$. Conversely, the matrix B_C has zero entries on the right side of the mixing scale, $j > mix$ and b_j^1 on the left side, $j < mix$. Therefore, the matrix equation takes the form

$$\alpha = (r_A^2 B_A + r_B^2 B_B + B_C) \cdot \Delta t. \tag{4.3.17}$$

4.3.3 Solving the RGEs

After including supersymmetry and abelian breaking, the matrix system in eq. (4.3.10) is

$$\alpha = B \cdot \Delta t, \tag{4.3.18}$$

where Δt includes the SUSY scale and the matrix of slopes B is calculated by adding the supersymmetric slopes above t_{SUSY} and, in case of abelian mixing, the structure given in equation (4.3.17).

This system of linear equations is solvable for Δt when the number of scales m, including M_{SUSY}, is $m = 2$, which gives solutions for the intermediate and unification scales and α_{GUT}. In the case $m > 2$ the above system is underdetermined. The general solution can then be written in terms of $m - 2$ free parameters, which can be chosen to coincide with $m - 2$ of the breaking scales.

In order to maintain the order of the steps in the breaking chain, one needs to apply the constraint on the scales $\Delta t_i > 0$, for all $i = 1, \ldots, m$. This condition reduces the range of allowed values for the independent scales, which result in a set of limits on those scales. These limits then can be used to obtain equivalent limits on the dependent scales.

Therefore, for all the models obtained in section 4.1 we obtain a set of limits (or exact solution) for all scales, consistent with the unification of gauge couplings. It is worth mentioning again that we have neglected two-loop contributions to the RGEs, as well as threshold corrections and $U(1)$ mixing effects, which are all roughly of the same order. As we perform a rough scan over a large model landscape where we neglect model details (e. g. heavy states are integrated out at the exact same scale but there could be a sizeable hierarchy between different masses), these approximations are well justified for our analysis.

4.4 Results for Intermediate Left-Right Symmetry

There are many possible breaking chains form $SO(10)$, as can be seen in figure 2.2, each of which will have different properties and produce a different set of models. As a first approach to this process of model building, we will take the two-step breaking from $SO(10)$ with the left-right symmetry group $SU(3)_C \otimes SU(2)_L \otimes SU(2)_R \otimes U(1)_{B-L}$ at an intermediate scale, because some of its minimal realisations have been analysed extensively in the literature [79–82, 129–143, 145–147].

As mentioned before, the main ingredients for the start of the model building process are the gauge group, the breaking chain and the set of representations. We have already chosen our GUT gauge group to be $SO(10)$, and the gauge symmetry

breaking chain of this scenario reads

$$SO(10) \to SU(3)_C \otimes SU(2)_L \otimes SU(2)_R \otimes U(1)_{B-L} \to SU(3)_C \otimes SU(2)_L \otimes U(1)_Y. \tag{4.4.1}$$

Lastly, the set of $SO(10)$ representations need to be specified. In general most sets of representations will not produce successful models, since some of the symmetry breaking conditions require very specific representations. We therefore choose quite a large set of initial representations, partially inspired by previous works on this type of symmetry breaking [129]. The set chosen is

$$\{\mathbf{16}_F^3, \mathbf{10}, \mathbf{45}^2, \mathbf{126}, \overline{\mathbf{126}}\}, \tag{4.4.2}$$

where there are three generations of $\mathbf{16}_F$, which contain the SM fermions; a scalar **10** which will contain part of the SM Higgs boson; two **45** adjoint scalars, one required for the first step of symmetry breaking and integrated out at the $SO(10)$ scale, and the other one allowed to leak through the lower scales; and two 126-dimensional representations that will contain fields responsible for further symmetry breaking steps and other fields that can contribute to the SM Higgs boson. The right-handed neutrinos in the $SO(10)$ 16-plets will be part of $SU(2)_R$ doublets in the LR symmetric phase and thereby contribute to the RGE running. We will assume that they acquire heavy Majorana masses of the order of the LR symmetry breaking scale to potentially generate light left-handed neutrino masses of order 0.1 eV in a seesaw mechanism.

Given the large representations used, their decomposition into representations of the intermediate group $SU(3)_C \otimes SU(2)_L \otimes SU(2)_R \otimes U(1)_{BL}$ has a lot of terms. This can be seen from the decomposition of the scalar irreps

$$\begin{aligned}
\mathbf{10} &\to \{\mathbf{3},\mathbf{1},\mathbf{1},\ \tfrac{1}{2}\} \oplus \{\overline{\mathbf{3}},\mathbf{1},\mathbf{1},\text{-}\tfrac{1}{2}\} \oplus \{\mathbf{1},\mathbf{2},\mathbf{2},0\},\\
\mathbf{45} &\to \{\mathbf{3},\mathbf{2},\mathbf{2},\ \tfrac{1}{2}\} \oplus \{\overline{\mathbf{3}},\mathbf{2},\mathbf{2},\text{-}\tfrac{1}{2}\} \oplus \{\mathbf{8},\mathbf{1},\mathbf{1},\ 0\} \oplus \{\overline{\mathbf{3}},\mathbf{1},\mathbf{1},\ 1\} \oplus \{\mathbf{1},\mathbf{3},\mathbf{1},0\}\\
&\quad \oplus \{\mathbf{3},\mathbf{1},\mathbf{1},\text{-}1\} \oplus \{\mathbf{1},\mathbf{1},\mathbf{3},\ 0\} \oplus \{\mathbf{1},\mathbf{1},\mathbf{1},\ 0\},\\
\mathbf{126} &\to \{\mathbf{8},\mathbf{2},\mathbf{2},\ 0\} \oplus \{\mathbf{6},\mathbf{3},\mathbf{1},\text{-}\tfrac{1}{2}\} \oplus \{\overline{\mathbf{6}},\mathbf{1},\mathbf{3},\ \tfrac{1}{2}\} \oplus \{\overline{\mathbf{3}},\mathbf{2},\mathbf{2},\ 1\} \oplus \{\mathbf{3},\mathbf{2},\mathbf{2},\text{-}1\}\\
&\quad \oplus \{\mathbf{3},\mathbf{3},\mathbf{1},\ \tfrac{1}{2}\} \oplus \{\overline{\mathbf{3}},\mathbf{1},\mathbf{3},\text{-}\tfrac{1}{2}\} \oplus \{\mathbf{1},\mathbf{2},\mathbf{2},\ 0\} \oplus \{\mathbf{3},\mathbf{1},\mathbf{1},\ \tfrac{1}{2}\} \oplus \{\overline{\mathbf{3}},\mathbf{1},\mathbf{1},\text{-}\tfrac{1}{2}\}\\
&\quad \oplus \{\mathbf{1},\mathbf{3},\mathbf{1},\ \tfrac{3}{2}\} \oplus \{\mathbf{1},\mathbf{1},\mathbf{3},\text{-}\tfrac{3}{2}\},\\
\overline{\mathbf{126}} &\to \{\mathbf{8},\mathbf{2},\mathbf{2},\ 0\} \oplus \{\overline{\mathbf{6}},\mathbf{3},\mathbf{1},\ \tfrac{1}{2}\} \oplus \{\mathbf{6},\mathbf{1},\mathbf{3},\text{-}\tfrac{1}{2}\} \oplus \{\mathbf{3},\mathbf{2},\mathbf{2},\text{-}1\} \oplus \{\overline{\mathbf{3}},\mathbf{2},\mathbf{2},\ 1\}\\
&\quad \oplus \{\overline{\mathbf{3}},\mathbf{3},\mathbf{1},\text{-}\tfrac{1}{2}\} \oplus \{\mathbf{3},\mathbf{1},\mathbf{3},\ \tfrac{1}{2}\} \oplus \{\mathbf{1},\mathbf{2},\mathbf{2},\ 0\} \oplus \{\overline{\mathbf{3}},\mathbf{1},\mathbf{1},\text{-}\tfrac{1}{2}\} \oplus \{\mathbf{3},\mathbf{1},\mathbf{1},\ \tfrac{1}{2}\}\\
&\quad \oplus \{\mathbf{1},\mathbf{3},\mathbf{1},\text{-}\tfrac{3}{2}\} \oplus \{\mathbf{1},\mathbf{1},\mathbf{3},\ \tfrac{3}{2}\}.
\end{aligned} \tag{4.4.3}$$

There are 35 scalar representations so there will be $N = 2^{35} \sim 10^{10}$ possible combinations. As was mentioned before, in order to be able to perform a reasonable quantitative analysis, we will restrict to having up to 5 representations above the left-right (LR) scale. The number of combinations of representations is now close to 4×10^5, a more manageable amount, of which only about 2.5×10^5 models will satisfy the theoretical constraints laid out in section 4.2.

Given the large number of models that we have, even after the application of constraints, we will attempt to exclude some of them by considering their phenomenological consequences. The only information we have about the models is the set of representations and the limits on the energy scales, so there are only a few phenomenological constraints that we can apply, which will be outlined below.

4.4.1 Proton Decay

Because of the nature of GUTs, there are always exotic particles that couple to both quarks and leptons and could potentially lead to rapid proton decay through baryon and lepton number violating interactions [9]. As we briefly mentioned in section 2.2 every fully unified theory necessarily predicts proton decay.

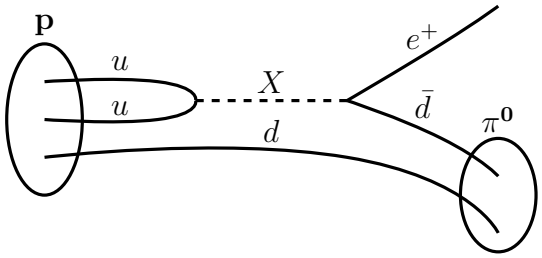

Figure 4.3: *Feynman diagram for the main decay modes of protons through a dimension 6 operator ($\bar{e}\bar{d}uu$), with a mediator of mass M_X.*

The main decay mode of protons is $p \to e^+\pi^0$ which could be mediated by gauge or scalar bosons, as can be seen in figure 4.3, coming from dimension 6 operators, suppressed by M_X^{-2}, the mass of the mediator. In the case of GUT scale gauge bosons the decay half-life can be calculated as [4]

$$\tau_p \sim \alpha_{GUT}^{-2} \frac{M_{GUT}^4}{m_p^5}, \tag{4.4.4}$$

with m_p the mass of the proton. The current experimental limit is $\tau > 1.29 \times 10^{34}$ years, set by Super-Kamiokande [105] which, for typical values of the gauge coupling

α_{GUT}, requires a GUT scale of $M_{GUT} \sim 10^{16}$. This limit excludes minimal non-supersymmetric GUTs, which typically predict a lower unification scale.

Scalar mediated proton decay is also possible via dimension 6 operators, but it depends heavily on the representation that the scalars are in [4]. For scalars in representations equivalent to those of the gauge bosons the contribution is the same and can be calculated equally with equation (4.4.4), but with the mass scale of those scalars M_X rather than the GUT scale, and their coupling to the quarks and leptons λ_X, rather than α_{GUT}. Other representations may have different contributions to the rate of decay of proton, so they need to be calculated independently.

In supersymmetric models, one expects other contributions to the decay width of the proton, coming from both dimension 4 and 5 operators. In R-parity preserving supersymmetry, however, dimension 4 operators are forbidden [181], and thus we avoid that potential source of rapid proton decay. On the other hand, dimension 5 operators are present in supersymmetric GUTs and they generate decays typically mediated by a very heavy coloured Higgsino $\tilde{X}$ [109], of the type $p \to K^+\bar{\nu}$ as can be seen in figure 4.4.

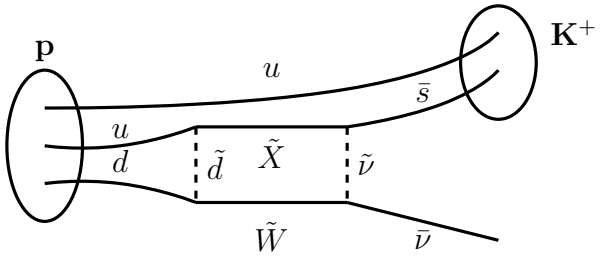

Figure 4.4: *Feynman diagram for the main decay modes of protons through dimension 5 operators ($\bar{s}u\tilde{\nu}^*\tilde{d}$ and $\bar{\nu}d\tilde{d}^*\tilde{\nu}$) in a SUSY GUT, with a Higgsino mediator $\tilde{X}$.*

We assume these dimension 5 contributions with heavy Higgsinos are equivalent to those of dimension 6 with scalars. Both coloured scalars and fermions can potentially mediate proton decay and, if supersymmetry is preserved, they have the same mass, so their contribution would be the same [219]. After the SUSY scale, the fermionic components will be integrated out, thus acquiring larger masses than their scalar partners. Hence, the contribution of dimension 5 operators after the SUSY scale is neglected with respect to dimension 6 operators.

Therefore, we will use the proton decay constraint for the left-right model, as calculated in equation (4.4.4) coming from gauge dimension 6 operators, to rule some of the models. We do not consider scalar mediated proton decay in this case,

because the computation of the amplitudes of the process in figure 4.3 lies beyond the scope of this work.

Additionally, in order to see the effect that future searches would have on the viability of models, we will use the projected bound on the proton half-life that the next generation of experiments, such as Hyper-Kamiokande, expects to reach, $\tau \gtrsim 1.3 \times 10^{35}$ y for the $p \to e^+\pi^0$ [220].

4.4.2 Direct and Indirect Detection Constraints

At the time of writing, the second run of the LHC has started and many analyses of the new data are being carried out and will soon reach public domain. One could then potentially expect the appearance of some new particle X which might be produced through resonant production. In the context of low scale left-right symmetric models, one of the most promising scenarios would be the production of a heavy right-handed gauge boson W_R, associated with the right-handed $SU(2)_R$ of the left-right symmetric gauge group. Its discovery through a charged current process would not only determine the scale of LR symmetry breaking but also the value of the corresponding gauge coupling g_R. This would provide a further constraint on GUT models in the approach considered here.

The parton level cross section for the resonant production of a heavy boson X can be approximated by a Breit-Wigner resonance

$$\sigma(Q^2) = \frac{4\pi}{9}(2J_X + 1)\frac{\Gamma(X \to q_1 q_2)}{(Q^2 - M_X^2)^2 + M_X^2\Gamma_X^2}, \tag{4.4.5}$$

with J_X being the spin of the produced boson and q_i indicating the initial partons. Integrating over the parton distribution functions (PDFs) in narrow-width approximation of the resonance (4.4.5) yields the total LHC cross section [221]

$$\sigma_{\text{LHC}} = \frac{4\pi^2}{9s}(2J_X + 1)\frac{\Gamma(X \to q_1 q_2)}{M_X} f_{q_1 q_2}\left(\frac{M_X}{\sqrt{s}}, M_X^2\right), \tag{4.4.6}$$

with the LHC center of mass energy $\sqrt{s} = 8, 13$ TeV and

$$f_{q_1 q_2}\left(r, M^2\right) = \int_{r^2}^1 \frac{dx}{x}(q_1(x, M^2)q_2(r^2/x, M^2) + q_2(x, M^2)q_1(r^2/x, M^2)). \tag{4.4.7}$$

Here, $q_i(x, Q^2)$ is the PDF of parton q_i at momentum fraction x and momentum transfer Q^2. For masses $M \approx 1 - 5$ TeV ($M \approx 3 - 9$ TeV for LHC13), this integral can be well approximated as exponential decreasing with $M/\sqrt{s}$ [221],

$$f_{q_1 q_2}\left(\frac{M}{\sqrt{s}}\right) \approx A_{q_1 q_2} \times \exp\left(-C_{q_1 q_2}\frac{M}{\sqrt{s}}\right), \tag{4.4.8}$$

where the coefficients A_{qq} and C_{qq} depend on the combination of the relevant partons q_1, q_2, ranging between $A_{\bar{u}\bar{u}} \approx 200$ to $A_{uu} \approx 4400$ and $C_{uu} \approx 26$ to $C_{\bar{d}\bar{d}} \approx 51$ [222,223].

Interestingly, even with the data collected from run I, there are excesses in various searches at the LHC with $\sqrt{s} = 8$ TeV [144,148], which could be interpreted through the production of a right-handed W_R boson with a mass of $m_{W_R} \approx 1.8 - 2.1$ TeV and a right-handed gauge coupling $g_R/g_L \approx 0.6 \pm 0.1$ [145, 224]. Using (4.4.6) the total W_R^+ and W_R^- cross section can be expressed as

$$\sigma_{\text{LHC}} = \frac{\pi}{12}\frac{g_R^2}{s}\left[f_{u\bar{d}}\left(\frac{M_{W_R}}{\sqrt{s}}\right) + f_{d\bar{u}}\left(\frac{M_{W_R}}{\sqrt{s}}\right)\right], \tag{4.4.9}$$

where we used the partial decay width $\Gamma(W_R^+ \to u\bar{d}) = 1/(16\pi)g_R^2 m_{W_R}$. The fitting parameters for the function (4.4.8) in this case are given by $A_{u\bar{d}} = 2750, C_{u\bar{d}} = 37$ and $A_{d\bar{u}} = 1065, C_{d\bar{u}} = 36$ [222, 223].

Applying such a direct collider search as a constraint or evidence in our approach would depend delicately on the process and collider details. Instead we will use the indirect bound from the measurement of the $K_L - K_S$ mass difference [134, 225–227],

$$h_K \approx \left(\frac{g_R}{g_L}\right)^2 \left(\frac{2.4 \text{ TeV}}{M_{W_R}}\right)^2 \lesssim 1. \tag{4.4.10}$$

For $g_R = g_L$ this leads to the bound $M_{W_R} \gtrsim 2.4$ TeV, whereas for $\frac{g_R}{g_L} = 0.6$ the limit weakens to $M_{W_R} \gtrsim 1.5$ TeV, compatible with the potential signal at $M_{W_R} \approx 1.9$ TeV. We will exclude all models with $h_K > 1$. Additionally, anticipating new experimental results, either by direct detection at the LHC or indirectly via the $K_L - K_S$ mass difference, we will alternatively impose a more stringent constraint $h_K < 0.06$, which corresponds to a mass of $M_W = 10$ TeV. This will highlight those models that survive if no sign of W_R is found.

Direct detection of supersymmetric particles is hoped to occur in the next run of the LHC. After the first run, no solid evidence of new physics was seen, and the limits on some of the most popular models are quite severe [14, 15]. Figures 2.4 and 2.5 show the limits for all the searches for supersymmetry done with $\sqrt{s} = 8$ TeV, where it can be seen that most of the limits lie around or below 1 TeV. So in order to represent the lack of signals for SUSY, we will impose the constraint $M_{SUSY} > 1$ TeV on the set of models. Similarly to the case of the detection of W_R, we will alternatively take the potential future limits on supersymmetry as a constraint. As with the above case we will use $M_{SUSY} > 10$ TeV as the limit for a lack of SUSY signals after Run II.

4.4.3 Model Analysis

Among the many models obtained through the procedure described above, we use one example scenario to illustrate our approach. The scalar representations of this model at M_{LR} and M_{SM} scales are

$$\begin{aligned}\{\mathcal{R}\}_{LR} &= \left\{\{\mathbf{1},\mathbf{3},\mathbf{1},\ 0\}\oplus\{\mathbf{1},\mathbf{1},\mathbf{3},\ \tfrac{49}{40}\}\oplus\{\mathbf{1},\mathbf{2},\mathbf{2},\ 0\}\oplus\{\mathbf{1},\mathbf{1},\mathbf{3},\text{-}\tfrac{49}{40}\}\right\},\\ \{\mathcal{R}\}_{SM} &= \left\{\{\mathbf{1},\mathbf{2},\ \tfrac{1}{2}\}\oplus\{\mathbf{1},\mathbf{2},\text{-}\tfrac{1}{2}\}\right\},\end{aligned} \tag{4.4.11}$$

where it can be see that this model has four representations at the LR scale and two Higgses at the SM scale, so it is a type of two Higgs doublet model (2HDM). With these representations one can calculate the gauge couplings running, as described above. The RGE running is shown in figure 4.5 for $M_{SUSY} \approx 10^4$ GeV, $M_{LR} \approx 10^{15}$ GeV and $M_{GUT} \approx 10^{16}$ GeV. As can be seen, this choice corresponds to exact gauge unification. It can be noticed also that at the LR scale the $SU(2)_R$ and $U(1)_{B-L}$ couplings (red and blue, respectively) mix to give the hypercharge α_1^{-1} coupling (purple). The slope of the $SU(2)_L$ coupling (orange) changes slightly at M_{LR}, because the representation $\{\mathbf{1},\mathbf{3},\mathbf{1},0\}$ is integrated out, whereas the $SU(3)_C$ coupling (black) remains unaffected, since there are no coloured representations at either side of M_{LR}. At the SUSY scale the slopes of the three SM gauge couplings change as a consequence of integrating out the supersymmetric degrees of freedom.

As we discussed before, for any model we can calculate the limits on the scales by imposing the unification condition, of which figure 4.5 is an example. In the supersymmetric left-right model there is one free degree of freedom, which we choose to be the SUSY scale M_{SUSY}. The limits of M_{SUSY}, M_{LR} and M_{GUT} will be affected by the phenomenological constraints that we described above, summarized in table 4.2, thereby excluding some ranges of values.

	$\tau_p(p \to e^+\pi^0)$	M_{SUSY}	h_K (M_{LR})
Current	1.29×10^{34} y	1 TeV	1 (1 TeV)
Future	1.3×10^{35} y	10 TeV	0.06 (10 TeV)

Table 4.2: *Phenomenological constraints from current and projected future experimental limits, as described in sections 4.4.1 and 4.4.2.*

Figure 4.6 shows the dependence of the scales M_{LR} (black), M_{SUSY} (blue) and M_{GUT} (red) with respect to M_{SUSY}. The dashed lines correspond to the excluded ranges by the current phenomenological constraints in table 4.2, and the solid lines the allowed values. We can notice straight away that values of M_{GUT} lower than

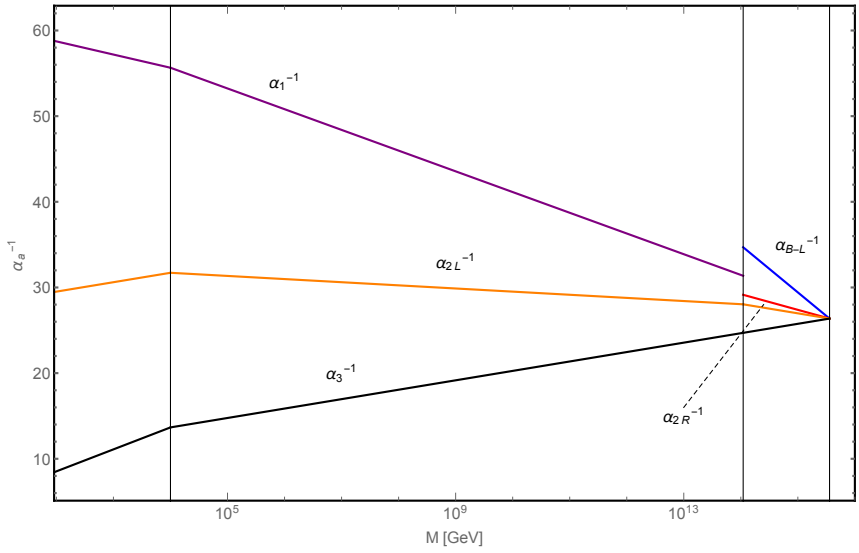

Figure 4.5: *Running of the gauge couplings in the sample model with representation content in eq.* (4.4.11)*. The scales are chosen to be* $M_{SUSY} \approx 10^4$ *GeV,* $M_{LR} \approx 10^{15}$ *GeV and* $M_{GUT} \approx 10^{16}$ *GeV. The black line corresponds to the* $SU(3)_C$ *gauge couplings, the orange line to the* $SU(2)_L$ *coupling, purple to* $U(1)_Y$*, red to* $SU(2)_R$ *and blue to* $U(1)_{B-L}$*.*

$\sim 10^{16}$ GeV are excluded, due to the proton decay constraint. Similarly, M_{SUSY} is excluded below 1 TeV, as can be seen in the bottom left corner of the figure. Lastly we notice that the LR scale decreases with the SUSY scale for $M_{LR} < M_{SUSY}$, and increases slowly for $M_{LR} > M_{SUSY}$. As a consequence this model does not allow for values of the left-right scale below $\approx 10^9$ GeV, thereby ignoring the constraint on M_{W_R}, with the minimum at $M_{LR} = M_{SUSY}$. Each constraint will correspondingly have an impact on all of the scales, in order to produce a consistently viable scenario. In the case shown in figure 4.6, the three scales would be constrained to the ranges

$$\begin{aligned} M_{SUSY} &\in \{1.0 \times 10^3, 3.48 \times 10^4\} \cup \{2.29 \times 10^{15}, 3.27 \times 10^{15}\}, \\ M_{LR} &\in \{8.03 \times 10^{13}, 2.79 \times 10^{15}\} \cup \{1.26 \times 10^{10}, 1.32 \times 10^{10}\}, \\ M_{GUT} &\in \{3.78 \times 10^{15}, 1.24 \times 10^{16}\} \cup \{3.01 \times 10^{15}, 3.28 \times 10^{15}\}, \end{aligned}$$

where the two disjoint sets correspond to when $M_{SUSY} < M_{LR}$ and $M_{SUSY} > M_{LR}$, respectively.

After having analysed a sample model, we will now attempt to study the distribution of the full set of models, trying to extract some patterns of behaviour from it and assess the consequences that the phenomenological constraints might have.

This symmetry breaking scenario has one degree of freedom, which we arbitrar-

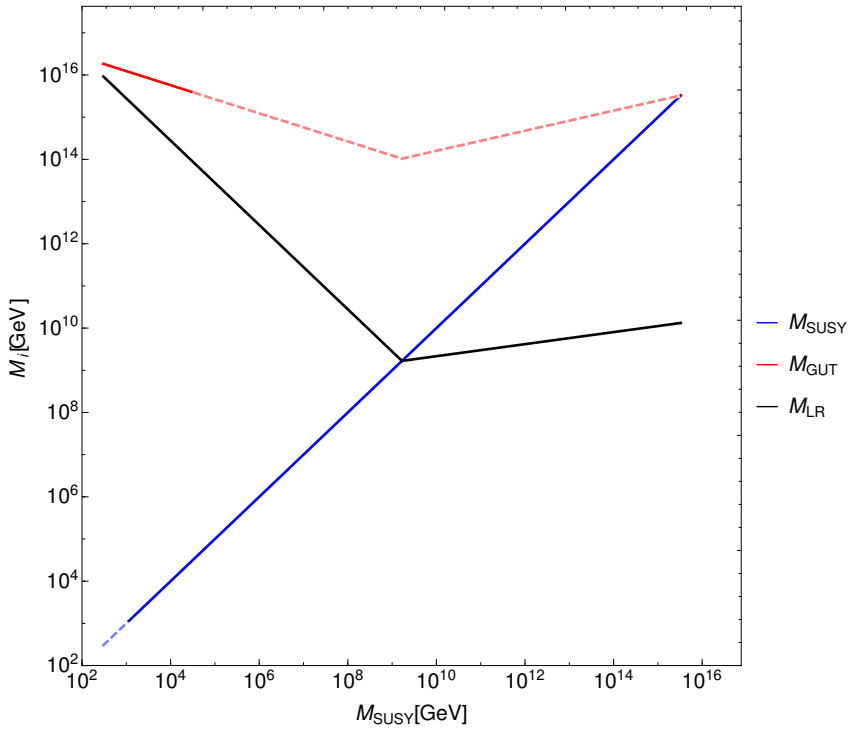

Figure 4.6: *Dependence of the scales M_{LR} (black) and M_{GUT} (red) on M_{SUSY} (blue) for a sample scenario with representation content in equation* (4.4.11)*. Dashed line refer to excluded ranges for the scale according to the current phenomenological constraints in table 4.2, and solid line to the allowed values.*

ily choose as the SUSY scale M_{SUSY}. This makes the system of equations (4.3.10) underdetermined resulting in a set of limits for the three scales rather than fixed values. This was illustrated in the example scenario discussed above. The calculated limits can be processed into histograms describing the distribution of left-right GUT models depending on the symmetry breaking scales. In other words, the height of each bin in such a histogram represents the number of models whose scale limits overlap with the bin. In figure 4.7 we can see the histograms of the distribution of models with respect to scales M_{LR}, M_{GUT} and M_{SUSY}, when no phenomenological constraints are applied [4]. The grey bars in all plots count the models with up to 3 representations at the intermediate left-right scale, the blue bars those with up to 4 representations and the red bars those with up to 5. We can notice that there is a slight preference for low values of M_{LR} and large values of M_{SUSY}, which gets more pronounced with a fewer number of representations. The GUT scale has a

[4]For convenience, we have applied the constraint $M_{GUT} > 2M_{LR}$, otherwise the two scales would be too close to each other, simulating a one-step breaking scenario, which is not our case of interest.

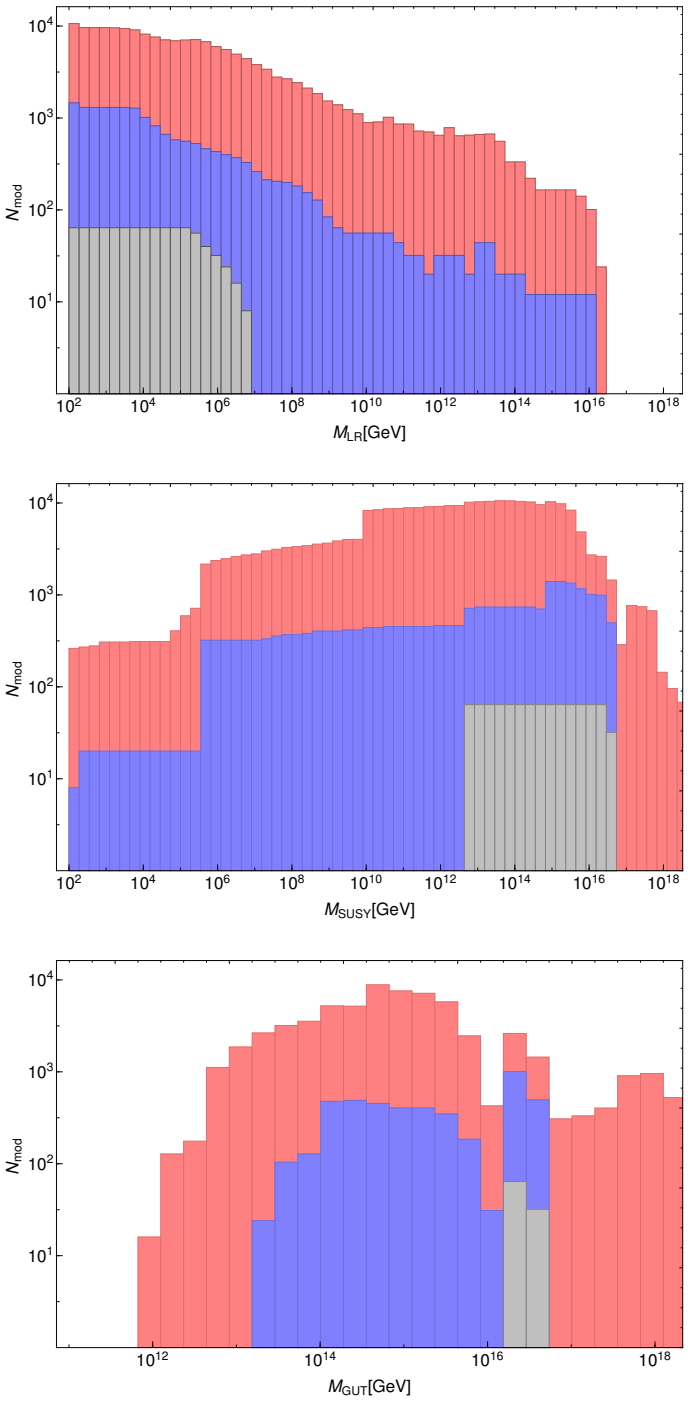

Figure 4.7: *Histograms of the distribution of SUSY models with respect to the left-right scale M_{LR} (top), unification scale M_{SUSY} (middle) and SUSY scale M_{GUT} (bottom) for the models, when no constraints are applied. Grey bars count model with up to 3 representations at the LR scale, blue bars up to 4 representations and red bars up to 5.*

preferred value between 10^{14} and 10^{16} GeV, and it shows a moderate peak slightly above 10^{16} GeV. It can be seen in the plots with M_{GUT} and M_{SUSY} that we have cut the scale at 10^{18}, roughly the Planck scale. Though there are models that have Trans-Planckian unification scales [228], we assume that non-renormalisable gravitational contributions to the gauge RGEs could potentially spoil the unification, so we eliminate those cases from our analysis.

Next we will apply the phenomenological constraints, described above in table 4.2. Figures 4.8, 4.9 and 4.10 show the histograms of models in the case of no constraints (top), current phenomenological constraints (middle), and the future phenomenological constraints (bottom), with respect to M_{LR}, M_{GUT} and M_{SUSY}, respectively. As before, grey bars count models with up to 3 reps, blue bars up to 4 and red bars up to 5. In comparison with the histograms with no constraints, we can see that the phenomenological constraints reduce severely the number of model for certain scales. The proton decay constraint has a big impact on M_{GUT} effectively excluding all models with $M_{GUT} \lesssim 10^{15-16}$. The effect of these constraints on the other two scales M_{LR} and M_{SUSY} has the consequence of reducing the number of models for intermediate values, effectively excluding the ranges $10^{12} < M_{LR} < 10^{14}$ GeV and $10^{5} < M_{SUSY} < 10^{13}$ GeV for a small number of representations.

The next generation of experiments are expected to push the limits even further, potentially excluding more models in the process. In the bottom plots of figures 4.8, 4.9 and 4.10 we show the distribution of models when a set of more stringent constraints are applied, with respect to M_{LR}, M_{GUT} and M_{SUSY}, respectively. We can easily notice that the number of models is severely reduced after the application of these constraints, the value of M_{GUT} is almost strictly above $M_{GUT} \gtrsim 10^{16}$ GeV, whereas the intermediate gap that we saw for M_{LR} and M_{SUSY} increases significantly, excluding the ranges $10^{14} < M_{LR} < 10^{15}$ GeV and $10^{8} < M_{SUSY} < 10^{11}$ GeV even for the larger number of representations.

The exclusion of models for intermediate values of M_{LR} and M_{SUSY} is quite an interesting result, and shows a correlation between the scales. In figure 4.11 we show the 2D histogram of models in the (M_{SUSY}, M_{LR}) plane with the current (left) and future (right) experimental constraints, for up to 3 (top), 4 (middle) and 5 (bottom) representations above M_{LR}. As expected from figures 4.8 and 4.9 the correlation is more evident for smaller the number representations. There is an obvious correlation between the scales, with models preferring low M_{LR} and high M_{SUSY}, or vice versa, with much lower density of models.

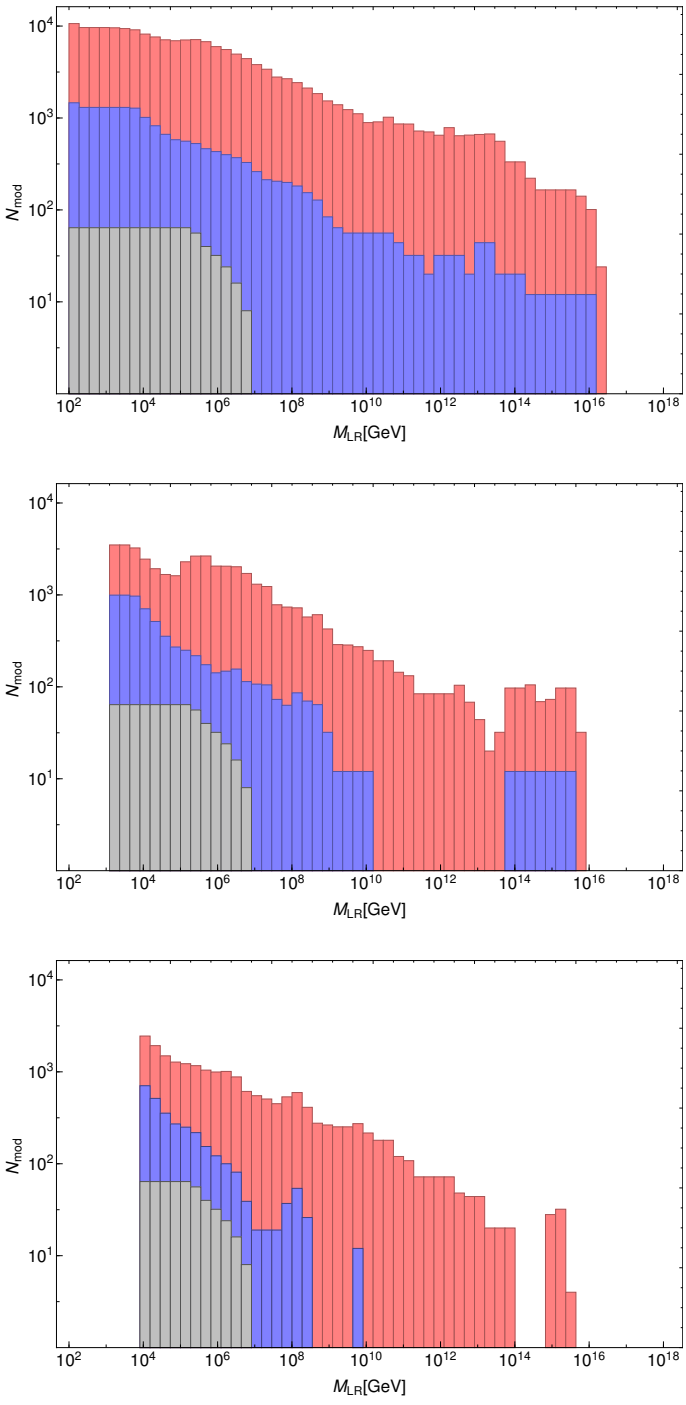

Figure 4.8: *Histograms of the distribution of SUSY models with respect to the left-right scale M_{LR}, with no constrains (top), with the current constraints $\tau_p > 10^{34}$ years, $M_{SUSY} > 1$ TeV and $h_K < 1$ (middle), and with future experimental constraints $\tau > 10^{35}$ years, $M_{SUSY} > 10$ TeV and $h_K < 0.06$ (bottom). Grey bars count model with up to 3 representations at the LR scale, blue bars 4 representations and red bars 5.*

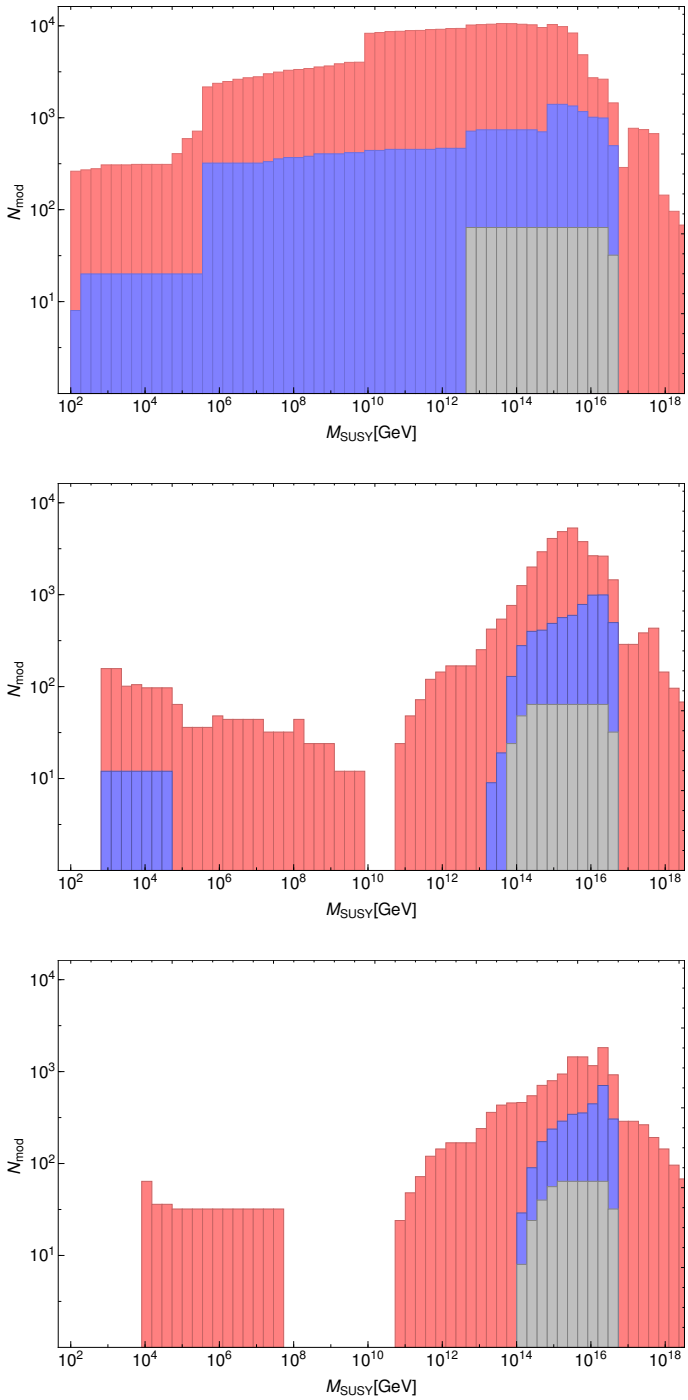

Figure 4.9: *As in figure 4.8 but with respect to* M_{SUSY}.

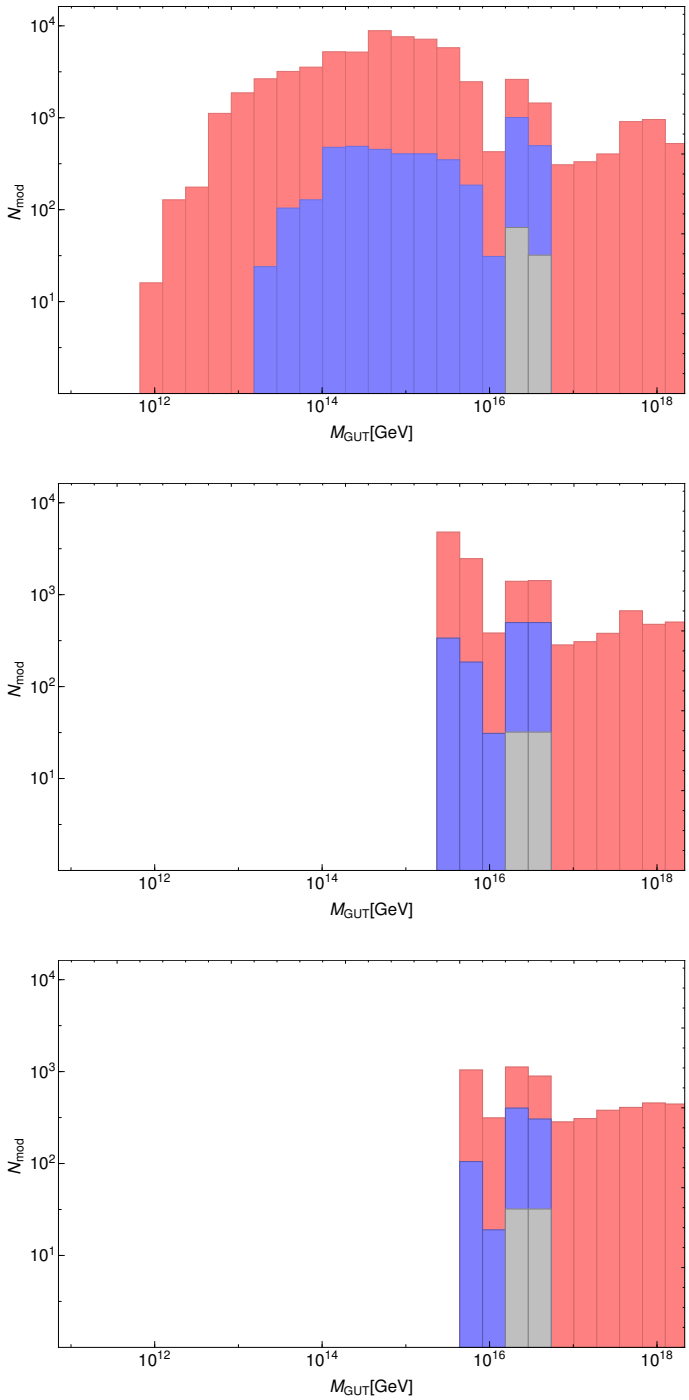

Figure 4.10: *As in figure 4.8 but with respect to* M_{GUT}.

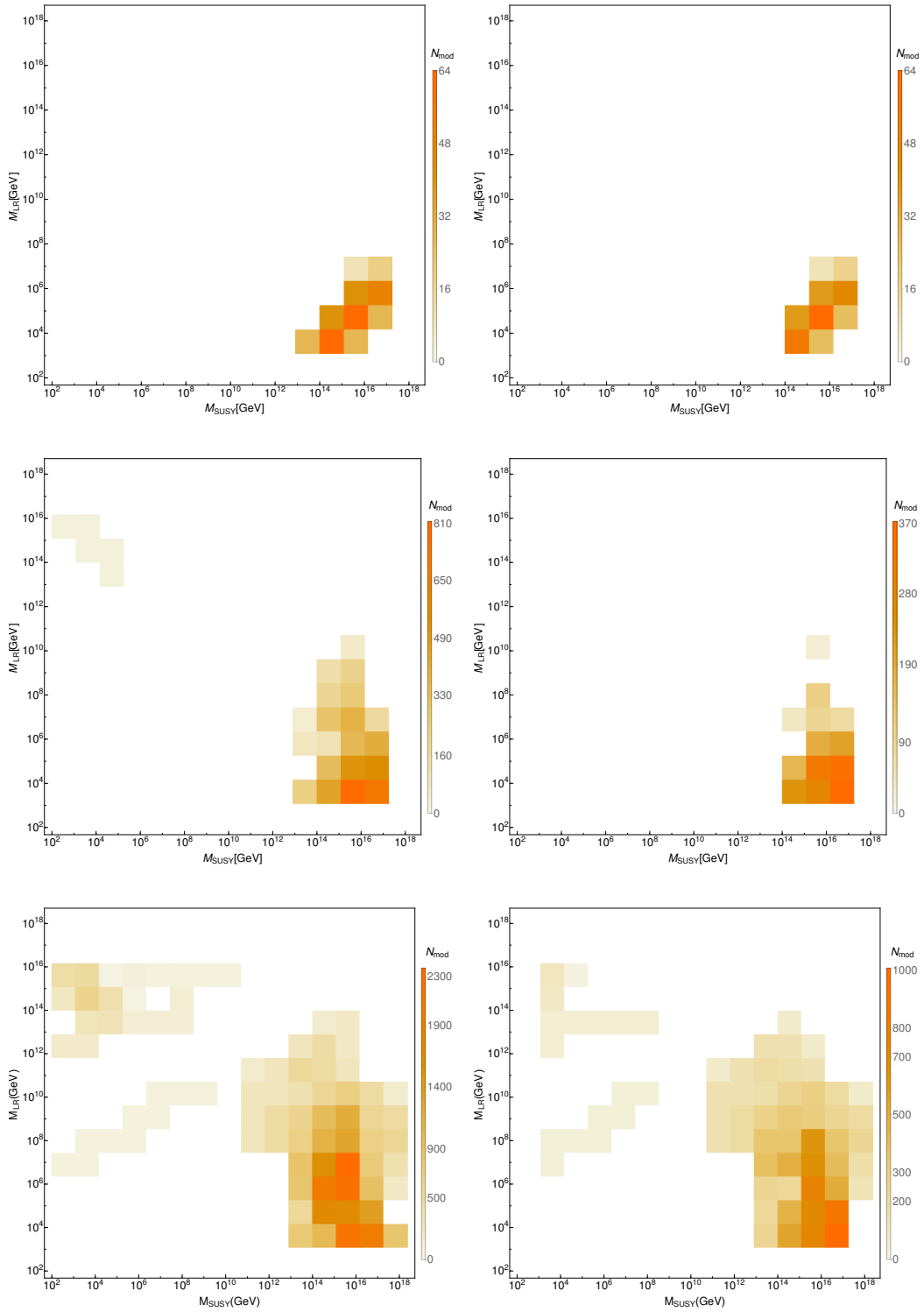

Figure 4.11: *Density histogram of the number of models in the (M_{SUSY}, M_{LR}) plane, where darker colours refer to higher density of models, for up to 3 (top), 4 (middle) and 5 (bottom) number of representations at M_{LR}. Current experimental constraints are applied on the left hand plot, $\tau_p > 10^{34}$ years, $M_{SUSY} > 1$ TeV and $h_K < 1$, and future constraints on the right hand plot, $\tau > 10^{35}$ years, $M_{SUSY} > 10$ TeV and $h_K < 0.06$, summarized in table 4.2.*

5

Aspects of GUT Phenomenology

In the previous chapter we have focused on the theoretical analysis of a great number of GUT models at the same time, focusing on the search for constraints or conditions that reduce the number and variation of the models. However, many of the interesting features and predictions of GUTs require a deeper analysis into the specific details of the models, which is beyond the scope or the power of that broad study.

This is a time during which some of the most challenging and groundbreaking experiments are being carried out. Starting with the LHC, which has surpassed all its predecessors in collision energy, reaching 8 TeV of centre of mass energy at the end of Run I and, at the time of writing, the first collisions at 13 TeV of Run II are being recorded. A lot of models and hypotheses will be put to the test in the coming years with the new data that is being collected by the ATLAS and CMS experiments at the LHC. In addition, other particle physics experiments are also pushing the boundaries of our current understanding of the field, such are neutrino oscillation experiments, e.g. Daya Bay [229], dark matter direct detection experiments, e.g. LUX [55], B-physics experiments, e.g. LHCb [53], and many more.

In particular, supersymmetric models are expected to take the first hit. The data analysed during the first run of the LHC already excluded a huge amount of the parameter space for the simplest supersymmetric models, e.g the constrained MSSM (CMSSM), as can be seen in figures 2.4 and 2.5, where they found a bound on the mass of the gluino and first and second generation squarks, $m_{\tilde{g}}, m_{\tilde{q}} \gtrsim 1$ TeV, third generation squarks $m_{\tilde{t}}, m_{\tilde{b}} \gtrsim 500$ GeV, sleptons $m_{\tilde{l}} \gtrsim 300$ GeV and gauginos $m_{\tilde{\chi}} \gtrsim 250 - 500$ GeV. In spite of these constraints, less minimal models are still very much alive and await the analysis of the new data. Thus, the coming run of the LHC may lay a final blow on low energy supersymmetry, or it may find some evidence of supersymmetric particles and revitalise the field to accommodate the

findings.

On the cosmological frontier, the Planck satellite takes the vanguard having produced the best maps of the cosmic microwave background radiation to date. The intensity and polarisation of its anisotropies have been measured with such precision, that it has revolutionised the field of observational cosmology. Among the numerous consequences of the Planck data analysis is the ability to probe a large number of models of inflation. The measurements of the spectral index of density perturbations n_s and ratio of tensor to scalar perturbations r, serve as a strong constraint on inflationary models and have managed to rule out several of them, as seen in figure 5.1, taken from [16], while the results of the BICEP2 experiment [230], may point towards a large value of r, possibly in favour of inflation. Further analysis of the Planck data, along with other forthcoming experiments such as the new phase of BICEP2, known as the Keck Array [231], is expected to set even stronger constraints on inflationary models, or could potentially confirm BICEP2's claim on the discovery of tensor modes, serving as the smoking gun of inflation.

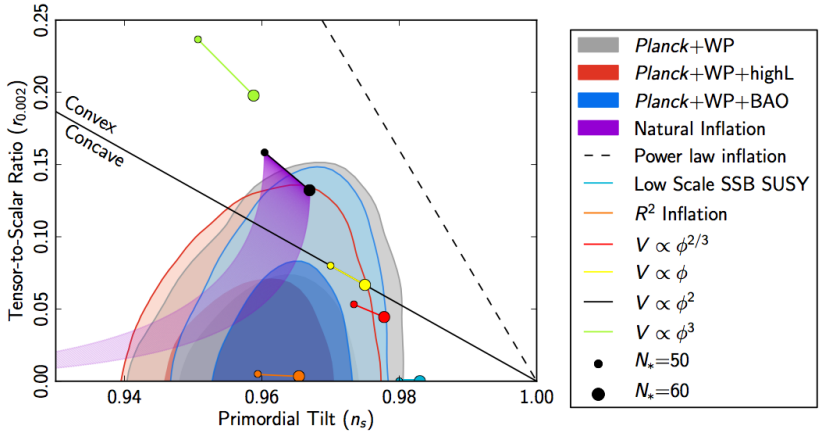

Figure 5.1: *Exclusion limits for the spectral index n_S and tensor-to-scalar ratio r from Planck, compared with predictions from some inflationary models, taken from [16]. Shaded regions indicate the 1σ (darker) and 2σ (lighter) contours using the Planck results in combination with other datasets (WMAP, high-ℓ Planck likelihood, and Baryon Acoustic Oscillation (BAO) measurements). The predictions from different inflationary models are shown for the range between 50 (small dot) and 60 (large dot) e-foldings.*

In the following, we will use an example GUT model, a supersymmetric $SO(10)$ model, in section 5.1, for which we will calculate the SUSY spectrum in detail and the phenomenological consequences at low energy for current or future colliders. This will serve as an example of the richness of GUT inspired SUSY models. We will focus on specific low energy consequences of the GUT origin beyond the broad

features covered in section 4. On the other side of the energy spectrum, in section 5.2, we will describe a flipped $SU(5) \otimes U(1)$ model, used as a basis for a scenario of hybrid inflation, which will be contrasted against the cosmological observables measured in the cosmic microwave background.

5.1 Minimal SUSY $SO(10)$

Given the lack of signals for supersymmetry in the last run of the LHC, and the severe constraints on the parameter space that the SUSY searches by ATLAS [194] and CMS [195] imposed, minimal models of low energy supersymmetry, such as the CMSSM, are in serious trouble and it is hard to reconcile their predictions with the experimental lack of evidence. Therefore, a lot of effort is going into the development and study of non-minimal models of supersymmetry, which could evade the constraints imposed by the experiments, while still making testable predictions for future searches. Such models extend the parameter space of the CMSSM in order to avoid the experimental limits, like the non-universal Higgs models (NUHM1 and NUMH2) where the soft masses of the Higgses differ from the other scalars (and among themselves in NUHM2) [186–188], or the phenomenological MSSM (pMSSM) where most of the parameters of the MSSM are a priori not related to each other [189].

Supersymmetric GUTs present a consistent and formal way to build non-minimal supersymmetric models, while still keeping a relatively low number of free parameters, unlike other phenomenological approaches like the pMSSM, because of the relations of the parameters and sparticle species at the GUT scale.

One such model is described here, a SUSY $SO(10)$ model [18] incorporating one-step breaking from $SO(10)$ down to the Standard Model gauge group at the unification scale $M_{GUT} \sim 10^{16}$ GeV, consistent with the unification of gauge couplings predicted by the MSSM. In contrast to minimal models such as the CMSSM, the scalar masses in the $SO(10)$ model are shifted by the D-terms, associated with the GUT symmetry breaking, allowing for non-universal boundary conditions and thus more degrees of freedom at the unification scale.

The description of the minimal $SO(10)$ model is laid out in section 5.1.1, with focus on an analysis of the effect that non-universality of the soft SUSY breaking (SSB) masses has on the particle spectrum, determined for the sfermion masses by the D-term splitting among the representations at the GUT scale, and for the

gaugino masses by the representation of the SUSY breaking messenger field, both cases discussed in section 5.1.2. A summary of the current state of SUSY searches and a reinterpretation of the limits given by the ATLAS collaboration is performed in section 5.1.3. Finally in section 5.1.4 the analysis of two specific scenarios with large D-terms contributions takes place, concluding with a short study of the effect of non-universal gaugino masses on the particle spectrum.

5.1.1 The Model

The field content of the minimal SUSY $SO(10)$ is set almost uniquely set by the gauge group structure. In section 2.2.5 we saw that in $SO(10)$ a generation of SM fermions, and their superpartners, is contained in a irreducible **16** representation. Also, the gauge sector is fixed, since gauge bosons need to belong to the adjoint representation of $SO(10)$, that is the **45** [18].

The Higgs sector, however, is not completely fixed and there is some freedom to choose the precise representations used in the model, according to the recipes outlined in section 2.2.5. The $SO(10)$ breaking Higgs, in particular, must be such that it satisfies the symmetry breaking requirements (c.f. figure 2.2). However, at this stage we do not concern ourselves with the particular representation it is in and we simply assume that the $SO(10)$ group is broken directly to the SM, or to any number of intermediate steps as long as they all have scales close to the unification scale. We will then neglect any further contribution of this $SO(10)$ breaking field Σ, for its effect will decouple from the theory at the GUT scale.

The embedding of the electroweak Higgs into representations of $SO(10)$ is largely fixed by the requirement that it must have Yukawa-type interactions with the SM fermions. As was discussed in section 2.2.5, the only allowed representations for this field are **10**, **120** and **126**, ignoring non-renormalisable operators. Out of the three possible options we choose the simplest of them, **10**, to contain the electroweak Higgs. This choice has the disadvantage of failing to predict the masses of all fermions, which will require several or all of the aforementioned representations to appear at the same time, as was discussed in section 2.2.5. For the sake of simplicity, and since this analysis will be focused mostly on scalar masses, rather than fermion masses, we stick to the simple **10** representation and neglect contributions from others.

With these choices, the superpotential of this minimal SUSY $SO(10)$ model

can be written as

$$W_{\mathrm{SO(10)}} = \mathbf{Y}\mathbf{16}_F\mathbf{10}_H\mathbf{16}_F + \mu_H\mathbf{10}_H\mathbf{10}_H + W(\Sigma), \tag{5.1.1}$$

where $\mathbf{Y}$ is a symmetric 3×3 matrix in generation space, the μ_H generalises the μ term in the MSSM (c.f. eq. (2.3.13)) for $SO(10)$, and the last term $W(\Sigma)$ includes all the terms that involve the Higgs field Σ responsible for $SO(10)$ symmetry breaking. Henceforth, we will neglect this term in our low energy analysis.

In this minimal $SO(10)$ model, the soft SUSY breaking sector is based on the mSUGRA scenario, defined in section 2.3.2. The unification of the MSSM fields into a matter and a Higgs multiplet, $\mathbf{16}_F$ and $\mathbf{10}_H$ respectively, implies that there are two universal scalar masses, $m^2_{16_F}$ and $m^2_{10_H}$. At some energy scale supersymmetry is broken, producing a set of soft SUSY breaking terms, similar to those of (2.3.14), which are

$$\begin{aligned}\mathcal{L}_{\mathrm{soft}} = &- m^2_{16_F}\tilde{16}^*_F\tilde{16}_F - m^2_{10_H}10^*_H10_H \\ &- \frac{1}{2}m_{1/2}\tilde{X}\tilde{X} - A_0\mathbf{Y}\tilde{16}_F\tilde{16}_F10_H - B_0\mu_H10_H10_H + c.c. \\ &+ \mathcal{L}_\Sigma,\end{aligned} \tag{5.1.2}$$

where $\tilde{16}_F$ and 10_H refer to the scalar components of $\mathbf{16}_F$ and $\mathbf{10}_H$ superfields respectively, $\tilde{X}$ represents the gaugino field, and $\mathcal{L}_\Sigma$ refers to the soft terms for the Σ field, which we do not specify, for they are irrelevant at this stage. The trilinear A_0 and bilinear B_0 terms are the supersymmetric equivalent to the Yukawa couplings and Higgs μ-term, respectively, with the boundary conditions at the GUT scale

$$A_t = A_b = A_\tau = A_0, \tag{5.1.3}$$

where A_t, A_b and A_τ are the trilinear couplings for the third generation sfermions in the MSSM.

The boundary conditions for the scalar masses m_{16_F} and m_{10_H} include an additional contribution, which does not originate from the soft-SUSY breaking sector. These so called D-terms are generated from the Kähler potential during a symmetry breaking transition that reduces the rank of the original group. A very typical example of these terms is the electroweak D-term generated in the MSSM after the SM group is broken. These introduce an extra contribution to the mass of the sfermions $\tilde{f}_L$ and $\tilde{f}_R$, as seen in equations (2.3.20) and (2.3.21), which has the form

$$\begin{aligned}\Delta m_{\tilde{f}_L} &= M_Z^2\cos(2\beta)(T_f^3 - Q_f\sin^2\theta_W), \\ \Delta m_{\tilde{f}_R} &= M_Z^2\cos(2\beta)Q_f\sin^2\theta_W.\end{aligned} \tag{5.1.4}$$

In the general case, a rank reducing symmetry breaking means that one or more of the abelian $U(1)$ factors of the group is broken. Therefore, for the case of the breaking of a single $U(1)$ group, a scalar field Φ acquires a vacuum expectation value, and right after symmetry breaking, the scalar particles ϕ^i will receive contributions to their masses [232]

$$\Delta m_i^2 = Q_i m_D^2, \qquad \text{with} \qquad m_D^2 = \frac{1}{2}\frac{m_\Phi^2}{Q_\Phi}, \tag{5.1.5}$$

with Q_i and Q_Φ the $U(1)$ charge of the scalar fields ϕ^i and Φ respectively, and m the soft mass of Φ. Interestingly, we see that the D-term mass m_D^2 is of the order of the soft masses m_Φ, rather than the GUT scale, at which the symmetry breaking occurs. For the $SO(10)$ case this means that the corresponding D-term would be proportional to the soft mass of the Σ field, responsible of symmetry breaking, $m_D^2 \propto m_\Sigma^2$, which is included in the last term of equation (5.1.2).

This contribution to the soft masses, plus the fact that there are two universal scalar masses, m_{16_F}, m_{10_H}, will change the boundary conditions at the GUT scale with respect to (2.3.24). Taking the soft masses from equation (5.1.2) to be the same for all three generations and thus proportional to the identity $\mathbb{1}$, the boundary conditions for the MSSM soft from section 2.3.3 read [18]

$$\begin{aligned}
\mathbf{m_Q^2} = \mathbf{m_u^2} = \mathbf{m_e^2} &= m_{16_F}^2 \mathbb{1} + m_D^2 \mathbb{1}, \\
\mathbf{m_L^2} = \mathbf{m_d^2} &= m_{16_F}^2 \mathbb{1} - 3m_D^2 \mathbb{1}, \\
\mathbf{m_\nu^2} &= m_{16_F}^2 \mathbb{1} + 5m_D^2 \mathbb{1}, \\
m_{H_d}^2 &= m_{10_H}^2 \ + 2m_D^2, \\
m_{H_u}^2 &= m_{10_H}^2 \ - 2m_D^2,
\end{aligned} \tag{5.1.6}$$

where $\mathbf{m}_\nu$ is the soft mass of the right-handed sneutrinos. If the right-handed neutrinos acquire a large mass through some type of see-saw mechanism (see section 2.2.3), typically of the order of 10^{14} GeV in $SO(10)$-inspired scenarios [143], so will the right-handed sneutrinos, thereby decoupling them from the low energy, TeV-scale, supersymmetric spectrum. Therefore, we will henceforth neglect the contributions of right-handed sneutrinos to the RGEs.

These set of boundary conditions exemplify the importance of the D-terms, since it induces a splitting between the particle species $\tilde{Q}$, $\tilde{u}$, $\tilde{e}$ and $\tilde{L}$, $\tilde{d}$ already at the GUT scale, which will potentially be increased through RGE running to the low scales. This D-term depends strongly on the scalar potential of the $SO(10)$ breaking sector so, in order to keep our description independent from the GUT scale physics,

we take m_D^2 to be a free parameter. The free parameters in the model are

$$\{m_{16_F}^2, m_{10_H}^2, m_D^2, m_{1/2}, A_0, \tan\beta, \text{sign}(\mu_H)\} \tag{5.1.7}$$

where $\tan\beta = v_u/v_d$, the ratio of the vevs of H_u and H_d. The value of $|\mu_H|$, as well as B_0, is fixed by imposing electroweak vacuum stability conditions. Figure 5.2 shows how the masses of the first generation of sfermions are split because of the effect of the D-terms, with the convenient definition

$$\sigma(m_D^2) = \text{sign}(m_D^2)\sqrt{|m_D^2|}, \tag{5.1.8}$$

to account for the possibility that m_D^2 can be negative. The rest of the free parameters, $m_{16_F}^2$, $m_{10_H}^2$, $m_{1/2}$, A_0 and $\tan\beta$, are taken from the benchmark scenario provided in table 1 of [187],

$$\begin{aligned} m_{16_F} = 1380 \text{ GeV}, \quad m_{10_H} = 3647i \text{ GeV}, \quad m_{1/2} = 3420 \text{ GeV}, \\ A_0 = -3140 \text{ GeV}, \quad \tan\beta = 39, \quad \text{sign}(\mu_H) = 1, \end{aligned} \tag{5.1.9}$$

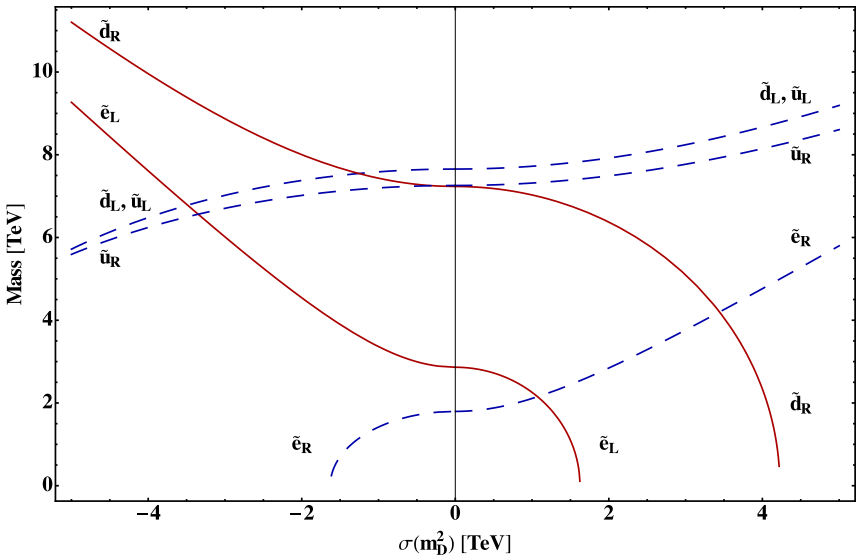

Figure 5.2: *First generation sfermion masses as a function of the $SO(10)$ D-term $\sigma(m_D^2)$ defined in the text and the rest of the parameters are fixed as in eq. (5.1.9). Solid red lines refer to those sfermion masses that grow with $m_D^2 < 0$ and dashed blue lines to those masses that grow with $m_D^2 > 0$.*

Lastly the boundary conditions for the masses of the gauginos may also differ from those of the CMSSM in (2.3.24), where they unified to a universal gaugino mass $m_{1/2}$ at the GUT scale. In general SUSY breaking mechanisms, the representation

		$M_{\rm GUT}$		$M_{\rm EW}$	
SO(10)	SU(5)	$\frac{M_1}{M_3}$	$\frac{M_2}{M_3}$	$\frac{M_1}{M_3}$	$\frac{M_2}{M_3}$
1, 54, 210, 770	**1**	1	1	$\frac{1}{6}$	$\frac{1}{3}$
54, 210, 770	**24**	$-\frac{1}{2}$	$-\frac{3}{2}$	$-\frac{1}{12}$	$-\frac{1}{2}$
210, 770	**75**	-5	3	$-\frac{5}{6}$	1
770	**200**	10	2	$\frac{5}{3}$	$\frac{2}{3}$

Table 5.1: *Ratios of gaugino masses for a SUSY breaking messenger field in different representations of $SU(5) \subset SO(10)$ [234] at the GUT and the EW scale. The EW ratios take into account the approximate effect of the RGE running on the gaugino masses.*

of the mediator field determines the matching conditions at the GUT scale. This field is required to be a SM singlet in order to preserve the SM symmetry but the same is not necessary for the GUT symmetry, $SO(10)$. The ratios of the values of M_1, M_2 and M_3, the MSSM gaugino masses, can be seen in table 5.1 for different representations of $SO(10)$ of the mediator field [233, 234].

The most common case is when the mediator field is in a singlet representation of $SO(10)$, in which case the boundary conditions are the same as in the CMSSM in equation (2.3.24)

$$M_1 = M_2 = M_3 = m_{1/2}, \tag{5.1.10}$$

but other configurations have some advantages, such as a better Yukawa coupling unification or better compatibility with the value of the anomalous magnetic moment of the muon a_μ [235].

5.1.2 Renormalisation Group Equations

As was mentioned before, the particle content of this minimal SUSY $SO(10)$ model is that of the MSSM in section 2.3.3, since all the additional gauge and scalar boson are integrated out at the GUT scale, along with the right-handed neutrinos. Thus, given the boundary conditions defined above for the soft SUSY breaking parameters, one can obtain the values at low scales by the use of the Renormalisation Group Equations of the MSSM, which are listed and solved approximately in Appendix A. In particular, the RGEs of the first and second generation of sfermions masses can be exactly solved at one loop, because the Yukawa couplings, proportional to their

fermionic masses, are negligible. These equations are given by

$$\begin{aligned}
16\pi^2\frac{d}{dt}m^2_{Q_{1,2}} &= -\frac{32}{3}g_3^2M_3^2 - 6g_2^2M_2^2 - \frac{2}{15}g_1^2M_1^2 + \frac{1}{5}g_1^2S,\\
16\pi^2\frac{d}{dt}m^2_{u_{1,2}} &= -\frac{32}{3}g_3^2M_3^2 - \frac{32}{15}g_1^2M_1^2 - \frac{4}{5}g_1^2S,\\
16\pi^2\frac{d}{dt}m^2_{d_{1,2}} &= -\frac{32}{3}g_3^2M_3^2 - \frac{8}{15}g_1^2M_1^2 + \frac{2}{3}g_1^2S,\\
16\pi^2\frac{d}{dt}m^2_{L_{1,2}} &= -6g_2^2M_2^2 - \frac{6}{5}g_1^2M_1^2 - \frac{3}{5}g_1^2S,\\
16\pi^2\frac{d}{dt}m^2_{e_{1,2}} &= -\frac{24}{5}g_1^2M_1^2 + \frac{6}{5}g_1S,
\end{aligned} \tag{5.1.11}$$

where the term S is defined as

$$S = m^2_{H_u} - m^2_{H_d} + \mathrm{Tr}\left(m_Q^2 - 2m_u^2 + m_d^2 - m_L^2 + m_e^2\right), \tag{5.1.12}$$

which, despite depending on all the scalar masses, turns out to be solvable, with a solution that depends only on the gauge couplings and the splitting of the soft masses at the GUT scale, i.e. the D-term m_D^2. With this, the solutions for the masses of the squarks and sleptons can be written as [236]

$$\begin{aligned}
m^2_{\tilde{u}_L} &= m^2_{16_F} + m_D^2\left(1 + \ 2C_1^{(1)}\right) + m_{1/2}^2\left(C_3^{(2)} + C_2^{(2)} + \frac{1}{6}C_1^{(2)}\right) + D_{u_L},\\
m^2_{\tilde{u}_R} &= m^2_{16_F} + m_D^2\left(1 - \ 8C_1^{(1)}\right) + m_{1/2}^2\left(C_3^{(2)} + \frac{8}{3}C_1^{(2)}\right) + D_{u_R},\\
m^2_{\tilde{d}_L} &= m^2_{16_F} + m_D^2\left(1 + \ 2C_1^{(1)}\right) + m_{1/2}^2\left(C_3^{(2)} + C_2^{(2)} + \frac{1}{6}C_1^{(2)}\right) + D_{d_L},\\
m^2_{\tilde{d}_R} &= m^2_{16_F} - m_D^2\left(3 - \ 4C_1^{(1)}\right) + m_{1/2}^2\left(C_3^{(2)} + \frac{2}{3}C_1^{(2)}\right) + D_{d_R},\\
m^2_{\tilde{e}_L} &= m^2_{16_F} - m_D^2\left(3 + \ 6C_1^{(1)}\right) + m_{1/2}^2\left(C_2^{(2)} + \frac{3}{2}C_1^{(2)}\right) + D_{e_L},\\
m^2_{\tilde{e}_R} &= m^2_{16_F} + m_D^2\left(1 + 12C_1^{(1)}\right) + m_{1/2}^2\left(6C_1^{(2)}\right) + D_{e_R},\\
m^2_{\tilde{\nu}_L} &= m^2_{16_F} - m_D^2\left(3 + \ 6C_1^{(1)}\right) + m_{1/2}^2\left(C_2^{(2)} + \frac{3}{2}C_1^{(2)}\right) + D_{\nu_L},
\end{aligned} \tag{5.1.13}$$

where the $C_a^{(n)}$ are constants, defined as

$$C_a^{(n)} = \frac{c_a}{b_a}\left(1 - \frac{g_a^{2n}(M_{\mathrm{SUSY}})}{g_a^{2n}(M_{\mathrm{GUT}})}\right), \quad (c_1,c_2,c_3) = \left(\frac{1}{5},\frac{3}{2},\frac{8}{3}\right), \quad (b_1,b_2,b_3) = \left(\frac{33}{5},1,-3\right), \tag{5.1.14}$$

and the electroweak D-terms D_i were defined in (2.3.21).

The masses in equation (5.1.13) depend only on the gauge couplings through the constants $C_A^{(n)}$, the soft SUSY masses $m^2_{16_F}$ and $m_{1/2}$, and the $SO(10)$ D-term

mass splitting, m_D^2. There is negligible dependence on $\tan\beta$ coming from the D_i which we ignore. One can write these masses as

$$\begin{aligned}
m^2_{\tilde{u}_L} &= m^2_{16_F} + 1.0m_D^2 + 5.3m^2_{1/2} - (53.6\text{ GeV})^2,\\
m^2_{\tilde{u}_R} &= m^2_{16_F} + 0.9m_D^2 + 4.9m^2_{1/2} - (35.8\text{ GeV})^2,\\
m^2_{\tilde{d}_L} &= m^2_{16_F} + 1.0m_D^2 + 5.3m^2_{1/2} + (59.3\text{ GeV})^2,\\
m^2_{\tilde{d}_R} &= m^2_{16_F} - 2.9m_D^2 + 4.9m^2_{1/2} + (25.3\text{ GeV})^2,\\
m^2_{\tilde{e}_L} &= m^2_{16_F} - 3.1m_D^2 + 0.5m^2_{1/2} + (47.3\text{ GeV})^2,\\
m^2_{\tilde{e}_R} &= m^2_{16_F} + 1.2m_D^2 + 0.2m^2_{1/2} + (43.9\text{ GeV})^2,\\
m^2_{\tilde{\nu}_L} &= m^2_{16_F} - 3.1m_D^2 + 0.5m^2_{1/2} - (64.5\text{ GeV})^2.
\end{aligned} \tag{5.1.15}$$

In figure 5.3 one can see the running of the first and second generation scalar masses, with the soft SUSY breaking parameters fixed to those of the benchmark point in eq. (5.1.9) with $m_D^2 = (0.7\text{ TeV})^2$ and $m^2_{10_H} = (2\text{ TeV})^2$. As expected, the running of the masses is mainly driven by the gaugino mass $m_{1/2}$, so in order to have a sizeable effect on the spectrum from the D-terms, one should have $m_D^2/m_{1/2} \gtrsim 1$.

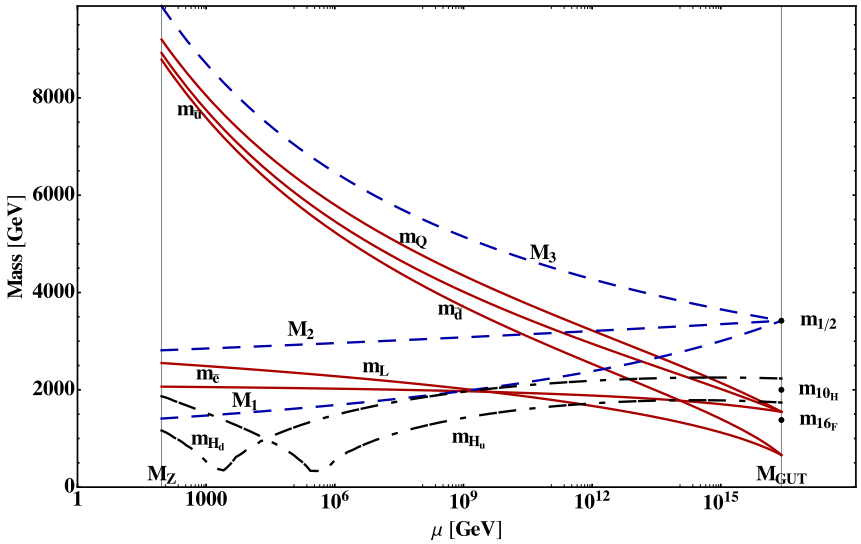

Figure 5.3: *Running of the scalar masses of the 1st generation, the gaugino masses and the Higgs doublet masses, with the soft parameters fixed as specified in the text. Solid red lines are sfermion masses, dashed blue lines gaugino masses and dash-dotted black lines are the absolute values of the Higgs mass parameters.*

It can be seen in equation (5.1.15) that the dependence on the model parameters m_{16_F}, m_D^2 and $m_{1/2}$ is quite similar for some of the scalar masses. This allows us to build linear combinations of these masses that will depend on fewer parameters.

First, for those particles with a different dependence on m_D^2, i.e. those belonging to different multiplets in the $SU(5)$ subgroup of $SO(10)$, one can eliminate the dependence on m_{16_F} and induce a large splitting between them, driven mostly by m_D^2,

$$\begin{aligned} m^2_{\tilde{d}_L} - m^2_{\tilde{d}_R} = &\quad 3.9 m_D^2 + 0.4 m_{1/2}^2 + \mathcal{O}(M_Z^2), \\ m^2_{\tilde{e}_L} - m^2_{\tilde{e}_R} = &-4.3 m_D^2 + 0.3 m_{1/2}^2 + \mathcal{O}(M_Z^2). \end{aligned} \tag{5.1.16}$$

Sparticles within the same multiplet of the $SU(5)$ subgroup of $SO(10)$ have a very similar dependence on m_D^2, the only small difference coming from the S term in equation (5.1.11), and then their splitting is basically driven by $m_{1/2}$, as it is in the CMSSM,

$$\begin{aligned} m^2_{\tilde{d}_R} - m^2_{\tilde{e}_L} = &\quad 0.2 m_D^2 + 4.4 m_{1/2}^2 + \mathcal{O}(M_Z^2), \\ m^2_{\tilde{u}_L} - m^2_{\tilde{e}_R} = &-0.2 m_D^2 + 5.1 m_{1/2}^2 + \mathcal{O}(M_Z^2), \\ m^2_{\tilde{u}_R} - m^2_{\tilde{e}_R} = &-0.3 m_D^2 + 4.7 m_{1/2}^2 + \mathcal{O}(M_Z^2). \end{aligned} \tag{5.1.17}$$

Lastly, left-handed squarks and sleptons belong to the same $SU(2)$ multiplets, and thus their only splitting comes from the contribution of the electroweak D-terms, proportional to M_Z^2,

$$\begin{aligned} m^2_{\tilde{d}_L} - m^2_{\tilde{u}_L} &= \mathcal{O}(M_Z^2), \\ m^2_{\tilde{e}_L} - m^2_{\tilde{\nu}_L} &= \mathcal{O}(M_Z^2). \end{aligned} \tag{5.1.18}$$

It is worth mentioning that the analytical solution found for the RGEs in equation (5.1.11) is only at one-loop. The second loop contribution can be approximated, from the RGEs in Appendix A, to be of the order

$$(\delta m^2_{\text{2-loop}})_{1,2} < \mathcal{O}(10^{-2})(-m^2_{16_F} - m^2_{1/2}) + \mathcal{O}(10^{-3})(-m^2_{10_H} - m^2_D), \tag{5.1.19}$$

which shows that for large values of the parameters, $m_i \gg 10^3$ GeV, their absolute contribution can be significant. Although their relative size is not that large, we will nevertheless include these approximated 2-loop contributions in the subsequent analysis.

5.1.3 Direct SUSY Searches at the LHC

At the time of writing Run II of the LHC has started but the experiments have not yet released relevant results from the newly collected data. Hence, the analyses

done during and after the first run, with ≈ 20 fb^{-1} of integrated luminosity recorded, hold the most stringent direct limits on the masses of supersymmetric particles to date. The experiments ATLAS and CMS have carried out comprehensive searches for supersymmetric signals and have analysed a great amount of data in a large number of channels and under a large number of model-agnostic approaches, aiming to exclude as much of the parameter space for supersymmetry as possible. The status of these searches at the end of Run I, in figures 2.4 and 2.5, can be summarised as follows.

The most stringent of exclusions from LHC searches are of squark and gluino masses. Searches based on multiple jets and missing energy (MET), for the decays $\tilde{q} \to q\tilde{\chi}_1^0$ or $\tilde{q} \to q(ll/l\nu/\nu\nu)\tilde{\chi}_1^0$, rule out squarks masses of the order of 2 TeV, and for gluino decays of $\tilde{g} \to q\bar{q}\tilde{\chi}_1^0$ or $\tilde{g} \to qq(W/ll/l\nu/\nu\nu)\tilde{\chi}_1^0$, the limit is of the order of 1 TeV [237,238], the precise values depending on the model that the searches are based on. These models tend to oversimplify supersymmetric spectra, for example they assume that all first and second generation squarks are degenerate in mass. This is in general not the case, and in particular for the minimal SUSY $SO(10)$ model, the splitting of the masses can be substantially large for large values of m_D^2, as can be seen from equation (5.1.16).

Stop pairs are produced at the LHC mostly through the s-channel, and the primary decay modes are $\tilde{t} \to t\tilde{\chi}^0$ and $\tilde{t} \to b\tilde{\chi}^{\pm}$. The final states studied have the signature $4j + l +$ MET. The current lower limit on the stop mass is around $m_{\tilde{t}} \gtrsim 650$ GeV [239,240]. However, if the stop is not allowed to decay to an on-shell top, $m_{\tilde{t}} < m_t + m_{\tilde{\chi}^0}$, the decay phase space is reduced and the process is suppressed which weakens the limit to $m_{\tilde{t}} \gtrsim 250$ GeV. Searches for sbottoms are similar to those for stops, with comparable production rates and complementary decays, $\tilde{b} \to b\tilde{\chi}^0$ and $\tilde{b} \to t\tilde{\chi}^{\pm}$. Consequently, the mass limits are similar, $m_{\tilde{b}} \gtrsim 650$ GeV [241–243].

Although electroweak processes at the LHC are several orders of magnitude smaller than strong processes, the precision of the measurements done by ATLAS and CMS is good enough to provide a limit of $m_{\tilde{l}} \gtrsim 300$ GeV, form the decay $\tilde{l} \to l\tilde{\chi}_1^0$ [244,245]. Similar to the sleptons, the limits on the neutralinos and charginos are considerably weaker than those of gluinos and squarks. Using purely electroweak processes such as $pp \to \tilde{\chi}_2^0\tilde{\chi}^{\pm} \to Z\tilde{\chi}^0 W^{\pm}\tilde{\chi}^0$ or $pp \to \tilde{\chi}_2^0\tilde{\chi}^{\pm} \to l\tilde{\nu}\tilde{l}l(\nu\tilde{\nu})$, both LHC experiments have currently excluded masses up to $m_{\tilde{\chi}} \gtrsim 300$ GeV [246–249]. Finally, the extra Higgs states predicted by supersymmetry have also been subject to scrutiny. However, due to the strong dependence on the parameters in the MSSM (particularly $\tan\beta$), the limits are not very strong. As of today, the limits seem to

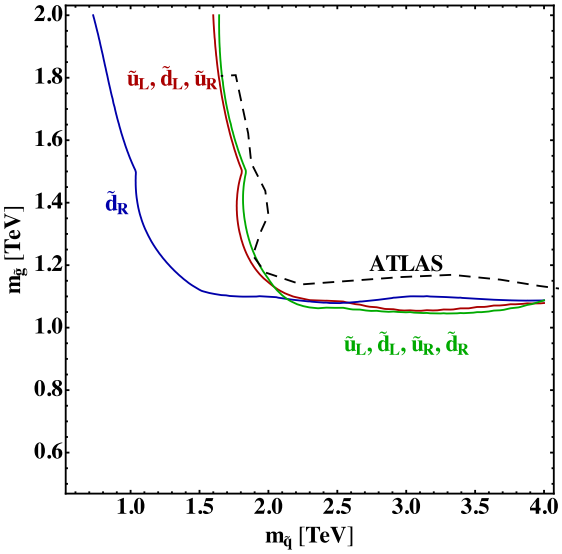

Figure 5.4: *Comparison of exclusion limits for CMSSM (green), $m_D^2 > 0$ (blue), and $m_D^2 < 0$ (red) simplified models with the ATLAS limit (dashed black).*

favour $\tan\beta \gtrsim 18$ and Higgs masses around or above that of the found Higgs state, $m_{H,A,H^\pm} \gtrsim 100$ GeV [250–253].

Because the limits discussed above on squark and gluino masses imply a series of assumptions on the SUSY spectrum, we aim to reinterpret them as a way to find a most accurate exclusion bound for models such as the minimal SUSY $SO(10)$ with non-degenerate squark masses. We start by factorizing the problem of estimating the final cross section after the cuts into two steps. First, we analytically calculate the production cross section and the branching fractions of the relevant processes for the searches. Secondly, we estimate the efficiencies of the cuts in each production mode for the jets+MET search channels reported by ATLAS using Monte Carlo simulation.

The efficiency of the cuts is calculated using a simplified model with two parameters $m_{\tilde{g}}$ and $m_{\tilde{q}}$. There are four production modes that result in jets+MET final states viz. $\tilde{g}\tilde{g}$, $\tilde{q}\tilde{q}$, $\tilde{q}\tilde{q}^*$ and $\tilde{q}\tilde{g}$. We assume each squark decays as $\tilde{q} \to q\tilde{\chi}_1^0$ and the gluino decays via either $\tilde{g} \to q\tilde{q}$ if $m_{\tilde{g}} > m_{\tilde{q}}$ or via $\tilde{g} \to q\bar{q}\tilde{\chi}_1^0$ otherwise. As a consistency check, we reproduce the ATLAS limits based on [237] for a simplified model where all squarks are degenerate and the lightest (bino-dominated) neutralino is the LSP with a mass a sixth of the gluino mass (we assume the typical CMSSM gaugino mass ratios $M_1 : M_2 : M_3 = 1 : 2 : 6$ at the electroweak scale). The comparison is shown in figure 5.4, where the CMSSM model with all squarks being degenerate

($\tilde{u}_L$, $\tilde{d}_L$, $\tilde{u}_R$, $\tilde{d}_R$) is plotted in green and the observed ATLAS limit in dashed black. The Monte-Carlo simulation was performed using Pythia 8 [254–256] with Gaussian smearing of the momenta of the jets and leptons as a theorist's detector simulation. Figure 5.4 demonstrates that we approximately reproduce the exclusion limit reported by ATLAS in our simulation.

The discrepancies with respect to the ATLAS limits for non-degenerate spectrum are studied in two scenarios. For $m_D^2 \gg 0$, the lightest of the squarks are the right-handed down-type squarks, so we take the approximation $m_{\tilde{d}_R} = m_{\tilde{s}_R} = m_{\tilde{b}_1} = m_{\tilde{q}}$, and all other squark masses are set to 10 TeV. On the other hand, for $m_D^2 \ll 0$, all the left-handed squarks and right-handed up-type quarks are light, which motivates the approximation where $m_{\tilde{q}}$ corresponds to the degenerate mass of all squarks except the right-handed down-type species. For both of these scenarios, the exclusion limits are shown in figure 5.4, where the case $m_D^2 \gg 0$ ($\tilde{d}_R$ light) is plotted in blue, and $m_D^2 \ll 0$ ($\tilde{u}_L$, $\tilde{d}_L$ and $\tilde{u}_R$ light) in red. As expected, the exclusion limit for the latter case, $m_D^2 \ll 0$, is almost identical to the fully degenerate CMSSM case, because most of the species are degenerate, whereas the former case, $m_D^2 \gg 0$, leads to a considerably weaker limit on the squark mass, $m_{\tilde{q}} \gtrsim 1$ TeV. In both cases the gluino mass limit remains unaltered at $m_{\tilde{g}} \gtrsim 1$ TeV.

In a few months, we expect new data coming from the second run of the LHC to start pushing the limits on the squark and gluino masses. Since the target integrated luminosity is about 300 fb^{-1} at 13 TeV, we expect to rule out up to $m_{\tilde{q}} \sim 3.2$ TeV for the $m_D^2 \ll 0$ case and $m_{\tilde{q}} \sim 2.8$ TeV for the $m_D^2 \gg 0$ case. The reach in gluino mass for both cases is about $m_{\tilde{g}} \sim 3.6$ TeV. Consequently, a 3-sigma discovery can be made for $m_{\tilde{q}} \sim 2.5$ TeV for the case $m_D^2 \ll 0$ and $m_{\tilde{q}} \sim 1.8$ TeV for $m_D^2 \gg 0$.

5.1.4 Phenomenological Analysis

The experimental limits discussed in section 5.1.3 constrain severely the parameter space of the minimal SUSY $SO(10)$ model. Starting with the set of free parameters, $m_{16_F}^2$, $m_{10_H}^2$, $m_{1/2}$, m_D^2, A_0, $\tan\beta$, $\text{sign}(\mu_H)$, we will look to fix or constrain some of them, focusing particularly on interesting deviations from the standard CMSSM scenario.

In the CMSSM, with a degenerate spectrum of scalar masses, the strong limits on the lightest squark $m_{\tilde{q}} \gtrsim 2$ TeV, forces the slepton masses to be heavy as well, evading experimental detection. As was seen in equation (5.1.17), one can increase the splitting between the squark and slepton masses with large $m_{1/2}$ and m_D^2.

However, very large $m_{1/2}$ values have the disadvantage of also raising the lightest neutralino, which is the preferred candidate for dark matter. Therefore, we shall fix the value of $m_{1/2}$ so as to produce a gluino with a mass around the current experimental limit, $m_{\tilde{g}} \approx 1$ TeV.

Therefore, we will seek to increase the value of m_D^2 to achieve a large splitting between squarks and sleptons. In the case that $m_D^2 \gg 0$, the lighter states that we will consider are $\tilde{e}_L$ and $\tilde{d}_R$, whereas if $m_D^2 \ll 0$, it will be $\tilde{e}_R$ and $\tilde{u}_L$. Since the value of $m_{1/2}$ is fixed to obtained the lightest possible gluino mass, and aiming to keep the mass of the lightest first generation squark ($m_{\tilde{q}}$) at the lowest allowed value, we express $m_{16_F}^2$ as a function of the other model parameters and the desired squark mass $m_{\tilde{q}}$ as

$$m_{16_F}^2 = m_{\tilde{q}}^2 - c_1 m_D^2 - c_2 m_{1/2}^2 - c_3 + \delta_2, \tag{5.1.20}$$

where the constants c_i are taken from (5.1.15) for the corresponding squark species and δ_2 is the 2-loop correction to the mass of the lightest squark, which can be significant for large $|m_D^2|$ and $m_{16_F}^2$, as discussed at the end of section 5.1.2.

Light Third Generation

The RGEs of the third generation squarks are mostly driven by the Yukawa couplings, with contributions that looks like

$$\Delta_i \approx \frac{1}{8\pi^2} y_i^2 (m_{10_H}^2 + 2m_{16_F}^2 + A_0^2), \tag{5.1.21}$$

for $i = t, b, \tau$. These terms are dominant in the third generation with respect to the gauge terms, which are the leading contribution for the first and second generation. This means that, in general, the third generation, particularly the stop squark, is lighter than the first two. Therefore, increasing the value of m_D^2 in either direction will make the stops and sbottoms very light, becoming tachyonic eventually, which enforces a maximum and minimum cut on the value of m_D^2.

Applying the conditions described above, $m_{\tilde{g}} \sim 1$ TeV, $m_{\tilde{q}} \sim 2$ TeV and equation (5.1.20), we perform a scan over m_D^2 to analyse the behaviour of the masses of the different particle species. The rest of the parameters we fix according to the benchmark scenario in eq. (5.1.9), so the full set of parameters will be

$$\begin{gathered} m_{10_H}^2 = -(3647 \text{ GeV})^2, \quad m_{1/2} = 389 \text{ GeV}, \\ A_0 = -3140 \text{ GeV}, \quad \tan\beta = 39, \quad \text{sign}(\mu_H) = 1, \\ m_{16_F}^2 \text{ such that } \min(m_{\tilde{q}}) = 2 \text{ TeV}. \end{gathered} \tag{5.1.22}$$

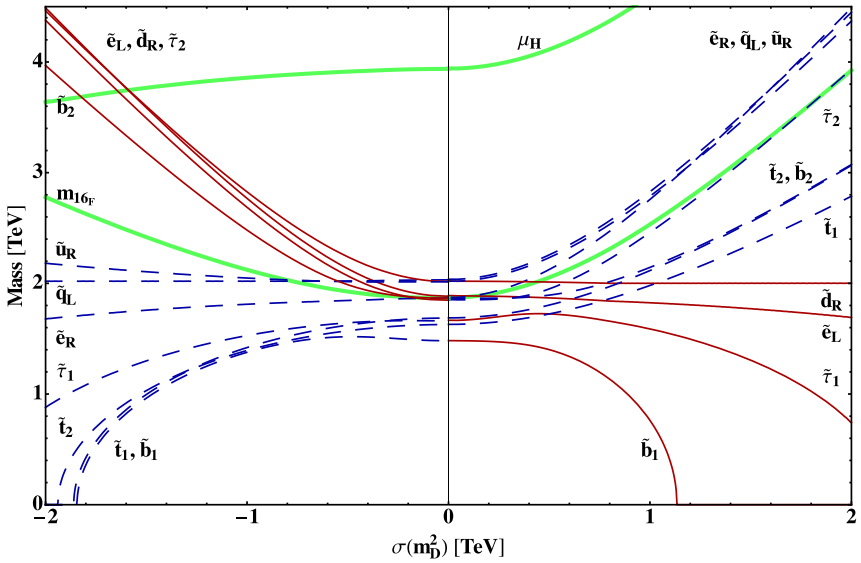

Figure 5.5: *Sparticle masses as a function of* $\sigma(m_D^2) = sign(m_D^2)\sqrt{|m_D^2|}$. *The remaining model parameters are fixed as described in eq.* (5.1.22). *As in figure 5.2, solid red lines refer to sfermion masses that grow with* $m_D^2 < 0$ *and dashed blue lines those that grow with* $m_D^2 > 0$. *Additionally, solid green lines refer to additional parameters,* m_{16_F} *and* μ_H.

In figure 5.5 we can see the dependence of the masses of all sfermions with respect to m_D^2 for both scenarios, positive and negative m_D^2, using the 2-loop RGEs described in Appendix A. In solid red we can see the particles that belong to the $\bar{\mathbf{5}}$ representation of the $SU(5)$ subgroup of $SO(10)$ and in dashed blue the ones that belong to the **10**. As expected, the splitting among these classes of sparticles increases with larger values of $|m_D^2|$, which agrees with equation (5.1.17). However, the splitting that we were aiming for, between the first generation squarks and sleptons does not get big enough for the sleptons to become appreciably lighter before the third generation stops and sbottoms become tachyonic. Therefore, the regions beyond the point at which $m_{\tilde{b}_1}$, the lightest sparticle, becomes tachyonic, which happens roughly for $m_D^2 \gtrsim (1.1 \text{ TeV})^2$ in one side and $m_D^2 \lesssim -(1.8 \text{ TeV})^2$ in the other, are non physical.

In order to have a better understanding why the third generation squarks are so light compared to their first and second generation counterparts, figure 5.6 displays the corresponding properties in the $(m_D^2, m_{1/2})$ (left) and (m_D^2, A_0) (right) parameter planes. In the plot on the left we can see that increasing $m_{1/2}$ has the effect of lowering the mass of the sleptons, as expected from eq. (5.1.17). However, the mass of the lightest neutralino increases with $m_{1/2}$, so for $m_{1/2}$ close to the upper

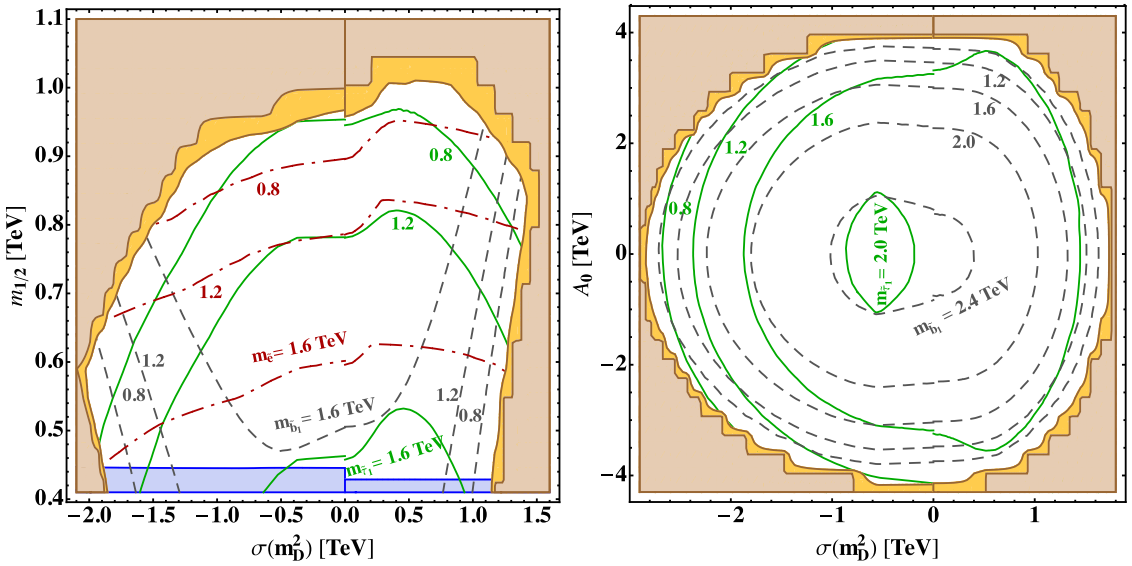

Figure 5.6: *Mass of the lightest stau $\tilde{\tau}_1$ (solid green), sbottom $\tilde{b}_1$ (dashed grey) and selectron $\tilde{e}$ (dash-dotted red) as a function of of m_D^2 and $m_{1/2}$ (left) and of m_D^2 and A_0 (right). The remaining parameters are fixed as described in eq.* (5.1.22)*. The coloured areas are excluded or disfavoured because there is at least one tachyonic state (brown), the neutralino is not the LSP (orange), the gluino mass is below the experimental limit (blue).*

limit, $m_{1/2} \approx 0.9$ TeV, either the lightest stau or selectron is the NLSP. In the plot of the right, we notice that for the sbottom and the stau, the effects of large m_D^2 and large A_0 are similar, i.e. they both push the masses down. As a matter of fact, we can actually see that the sbottom is only the lightest for large A_0 (as was the case in figure 5.5), but is heavier than the stau for small A_0, and can even be rather heavy ($m_{\tilde{b}_1} \approx 2.4$ TeV).

The spectrum obtained in this model, shown in figure 5.7 for $m_D^2 = -(1.83 \text{ TeV})^2$, belongs to a class of Split-SUSY scenarios with a compressed spectrum [257–259], with the lightest stop too light to decay into a top and the lightest neutralino. The LHC limit on the stop mass for this case is much more relaxed than in other scenarios [239, 242]. With a light stop mass just above the LHC limit for a compressed spectrum, $m_{\tilde{t}_1} \gtrsim 250$ GeV, a rough estimate of the fine tuning would be $M_{\text{SUSY}}^2/m_t^2 \approx m_{\tilde{t}_1} m_{\tilde{t}_2}/m_t^2 \approx 5$, which can potentially be consistent with naturalness and solving the hierarchy problem.

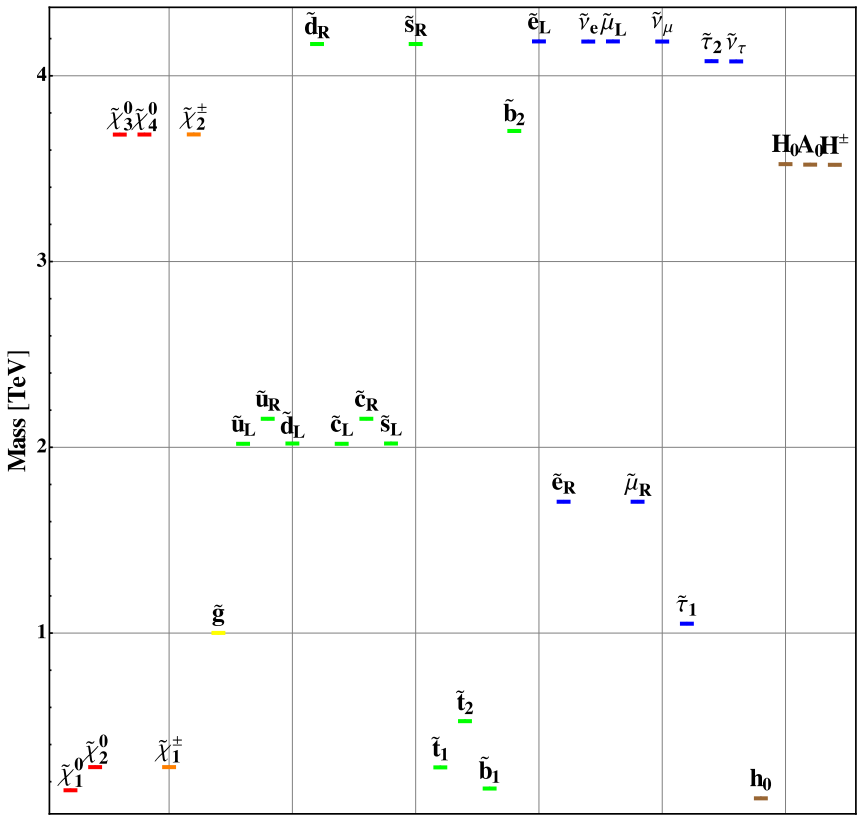

Figure 5.7: *Supersymmetric particle spectrum in the example scenario with large $SO(10)$ D-terms based on eq. (5.1.22) with $m_D^2 = -(1.83\ TeV)^2$ (light third generation).*

Light First Generation

It was mentioned before that the Yukawa couplings drive the third generation squarks to be lighter than those of the first and second generations. Then, in order to minimize the contribution of the terms proportional to the Yukawa couplings we will look into cancelling those out in the RGEs, as in eq. (5.1.21), which have the form

$$\Delta_{\tau,b,t} \propto m_{10_H}^2 + 2m_{16_F}^2 + A_0^2. \tag{5.1.23}$$

Hence, we need to compensate the increasingly large values of $m_{16_F}^2$ with equally large and opposite sign values of $m_{10_H}^2 + A_0^2$. A safe choice, keeping the trilinear couplings real, is $A_0 = 0$ and $m_{10_H}^2 = -2.1 m_{16_F}^2$, which also includes a correction for the two-loop contribution. This fine-tuned choice represents an extreme case of the more generic scenario described in the previous section. The parameters in this

model can be summarised as

$$\begin{gathered} m_{1/2} = 389 \text{ GeV}, \\ A_0 = 0, \quad \tan\beta = 39, \quad \text{sign}(\mu_H) = 1, \\ m^2_{16_F}, m^2_{10_H} = -2.1 m^2_{16_F} \text{ such that } \min(m_{\tilde{q}}) = 2 \text{ TeV}, \end{gathered} \tag{5.1.24}$$

In figure 5.8 we can see how the third generation sparticles are now made heavier

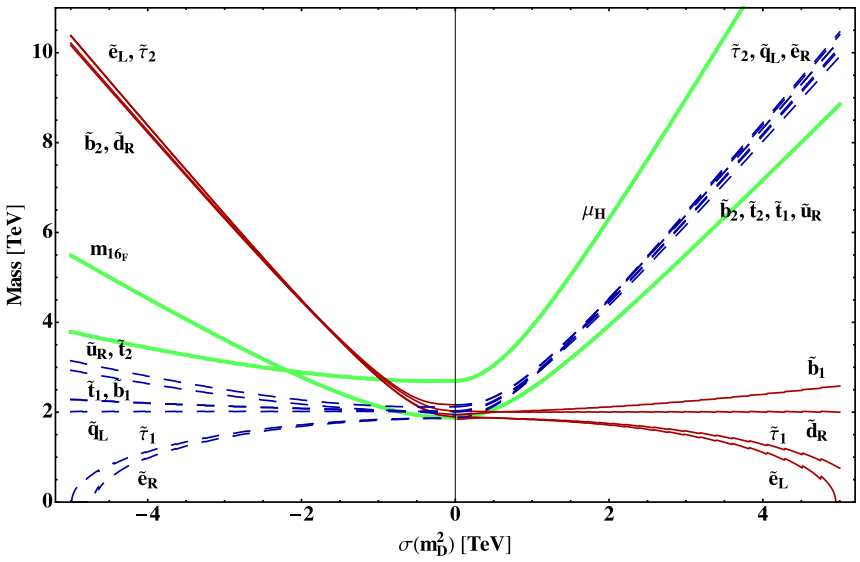

Figure 5.8: *As figure 5.5, but with the remaining model parameters fixed as described in eq.* (5.1.24)*. Colour and texture of lines are as in figure 5.5.*

than their first generation counterparts. A larger splitting between the lightest squark and slepton can be achieved here, as opposed to figure 5.5. However, in the process we have generated very heavy masses for the rest of the squarks and sleptons, which are here split off considerably, with masses up to 10 TeV.

As we did before, we display in figure 5.9 the combined dependencies of m_D^2 and either $m_{1/2}$ and A_0. We can easily notice a major difference with respect to the third generation case in the left hand side plot of figure 5.6, because now the first generation sleptons are mostly lighter than the light stau, except for small values of $|m_D^2|$. The plot on the right hand side, dependence on A_0, is rather different from the case before, since now the sbotton mass gets heavier with increasing $|m_D^2|$, but lighter with increasing A_0. This is expected as we do not compensate the effect of A_0 on the Yukawa-driven RGE contributions. As a consequence, the lightest sbottom will become the lightest sfermion for large $A_0 \gtrsim 3$ TeV.

This model presents a rather extreme scenario which is fine-tuned to cancel the Yukawa contribution of the third generation states. Nevertheless, it demonstrates

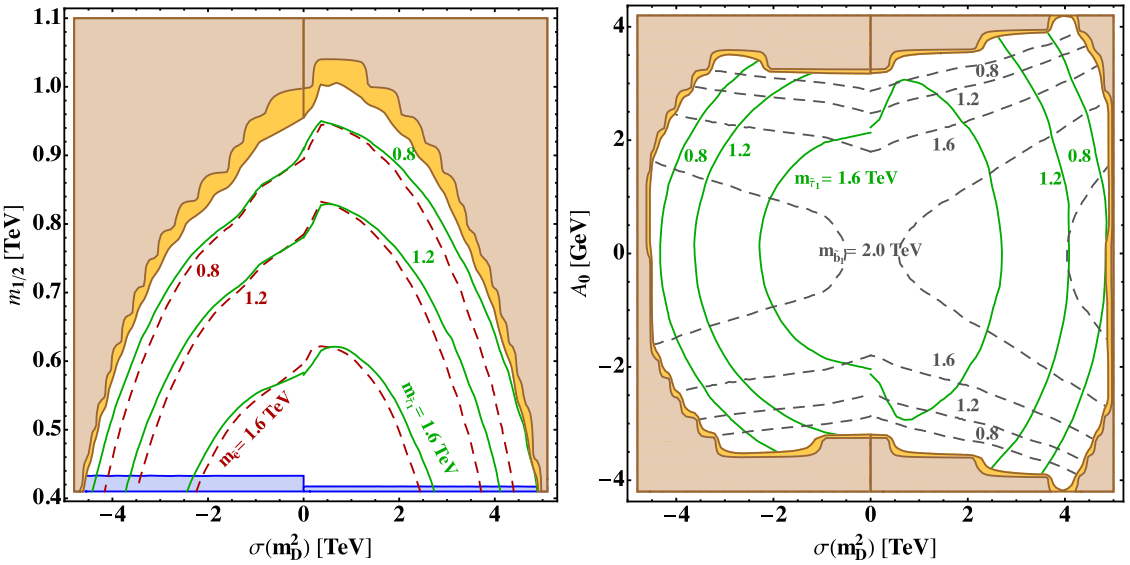

Figure 5.9: *As figure 5.6, but with the remaining model parameters fixed as described in eq.* (5.1.24).

the potential to deviate from the usual light stop/sbottom/stau case. The direct LHC limits on first and second generation slepton masses are still comparatively weak and can accommodate light sleptons $m_{\tilde{l}} \gtrsim 300$ GeV. An example spectrum for this case is shown in figure 5.10 for $m_D^2 = +(4.87 \text{ TeV})^2$, resulting in a severely split scenario, which is similar to cases of Split-SUSY [260–263], but exhibiting a three-fold splitting: Very light sleptons $\approx 0.1 - 0.2$ TeV, lightest squarks around $2 - 4$ TeV and very heavy squarks and sleptons at $9 - 10$ TeV. Consequently, there is severe fine-tuning in the model, not only by manually engineering the light selectrons, but also due to the necessary cancellations of the large contributions to the Higgs mass from the heavy stops, $M_{\text{SUSY}}^2/m_t^2 \approx m_{\tilde{t}_1} m_{\tilde{t}_2}/m_t^2 \approx 3 \times 10^3$.

Non-Universal Gauginos

Finally, we conclude the analysis of the minimal $SO(10)$ model with some remarks about the impact of non-universal gauginos at the GUT scale. We saw in section 5.1.1 that in supergravity mediated scenarios the $SO(10)$ representation of the messenger field prescribe the boundary conditions for the gaugino masses at the GUT scale. In table 5.1 we can identify three cases, corresponding to the representations **1**, **24** and **200** of the $SU(5)$ subgroup of $SO(10)$.

The simplest case is when the messenger field is a singlet, which corresponds to the approximated gaugino hierarchy $|M_1| : |M_2| : |M_3| = 1/6 : 1/3 : 1$ near the

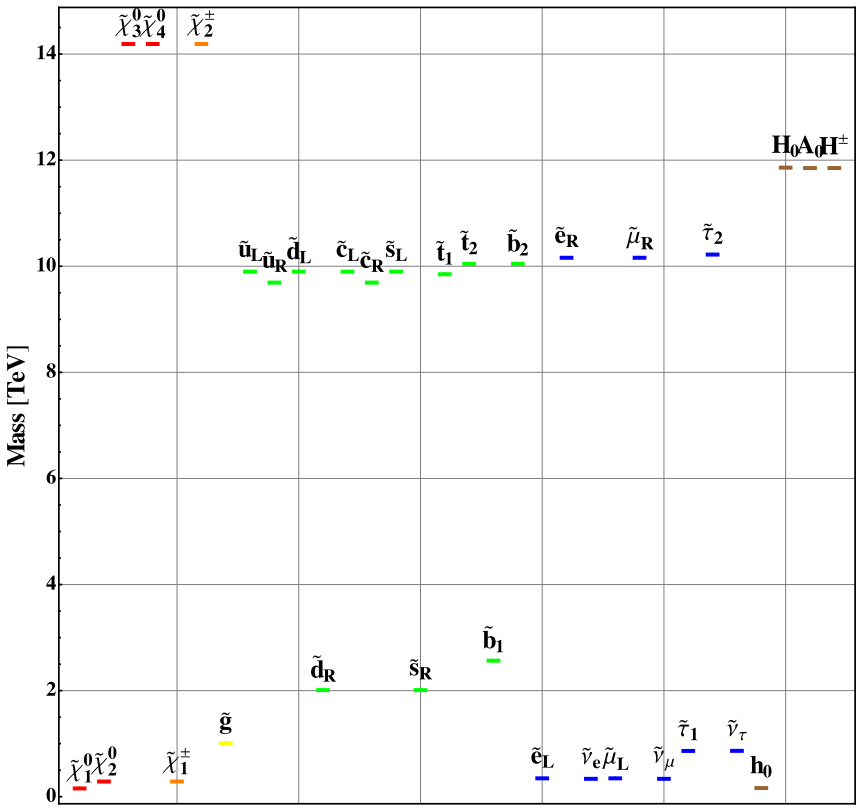

Figure 5.10: *Supersymmetric particle spectra in the example scenario with large $SO(10)$ D-terms based on eq. (5.1.24) with $m_D^2 = +(4.87\ TeV)^2$ (light first generation).*

electroweak scale. This was the case used in the above analysis and is the general prescription of the CMSSM.

If the messenger field is in the **24**-dimensional representation, the hierarchy becomes $|M_1| : |M_2| : |M_3| = 1/12 : 1/2 : 1$, which makes the bino comparatively lighter than in the CMSSM case. This modification could be phenomenologically interesting because it creates a larger splitting between the neutralino and gluino, thereby allowing for larger values of $m_{1/2}$. For example, for a gluino mass at the current limit, $m_{\tilde{g}} \approx 1.1$ TeV, the lightest neutralino could be lighter than $m_{\tilde{\chi}_1^0} \approx 100$ GeV, subject to direct search limits. On the other hand, the ratio between M_2 and M_3 is smaller than that of normal CMSSM, making the second neutralino and lightest chargino slightly heavier. Such a change will for instance suppress the SUSY contribution to the anomalous magnetic moment of the muon, because the largest contribution comes from a sneutrino-chargino loop [264], and the experimental situation would prefer both the $SU(2)$ gaugino and the sleptons to be light.

Lastly, for a messenger in the **200**-dimensional representation, we have a low energy hierarchy $|M_1| : |M_2| : |M_3| = 5/3 : 2/3 : 1$. The spectrum is rather different here, with the bino being the heaviest gaugino, heavier even than the gluino, while the mass of the wino is approximately $2/3$ of the gluino mass. Hence, the lightest neutralino would be mostly wino and would have a relatively large mass compared to the previous case.

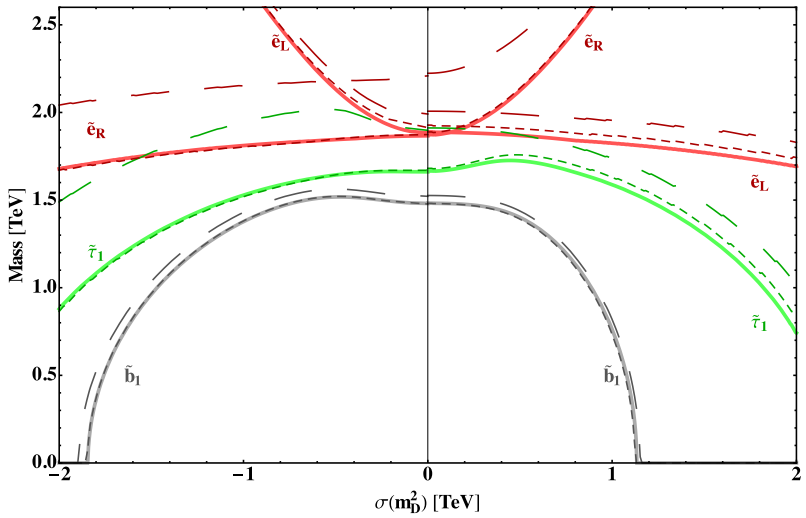

Figure 5.11: *Sparticle masses as a function of* $\sigma(m_D^2) = sign(m_D^2)\sqrt{|m_D^2|}$. *The remaining model parameters are fixed as described in eq.* (5.1.22) *for three different gaugino hierarchies at the GUT scale: (a)* $M_1 = M_2 = M_3 = m_{1/2}$ *(universality, solid); (b)* $-2M_1 = -3/2M_2 = M_3 = m_{1/2}$ *(light bino, short dashed); (c)* $10M_1 = 2M_2 = M_3 = m_{1/2}$ *(light wino, long dashed).*

Additionally, non-universal gaugino masses have an effect on the masses of the SUSY particles through RGE running. The term proportional to $m_{1/2}$ in equation (5.1.17) assumed universal masses, but if written in terms of M_1, M_2 and M_3 the RGEs generalise to

$$\begin{aligned} m^2_{\tilde{d}_R} - m^2_{\tilde{e}_L} &= \quad 0.2m_D^2 - 0.02M_1^2 - 0.5M_2^2 + 4.9M_3^2 + \mathcal{O}(M_Z^2), \\ m^2_{\tilde{u}_L} - m^2_{\tilde{e}_R} &= -0.2m_D^2 - 0.15M_1^2 + 0.5M_2^2 + 4.9M_3^2 + \mathcal{O}(M_Z^2), \\ m^2_{\tilde{u}_R} - m^2_{\tilde{e}_R} &= -0.3m_D^2 - 0.08M_1^2 \qquad\quad + 4.8M_3^2 + \mathcal{O}(M_Z^2), \end{aligned} \tag{5.1.25}$$

where we can see that the mass of the gluino has the strongest effect. Setting the gluino masses to $m_{\tilde{g}} \approx 1.1$ TeV, as we did before, we can find that gaugino non-universality induces an additional splitting between the squarks and sleptons, dominantly driven by the wino mass M_2. Figure 5.11 shows a comparison of the three cases mentioned above: universal gauginos (solid), light bino case (short dased)

and light wino case (long dashed). As expected from (5.1.25), the difference in the second case is negligible compared to the first, whereas the third scenario can have a sizeable impact on the slepton masses, especially for $m_D^2 < 0$. The negative signs in front of M_1^2 in (5.1.25) explain the larger splitting among slepton masses compared to the universal gaugino case.

5.2 Flipped GUT Inflation

For a number of years, cosmological inflation [265–268] has been thought as the solution to many of the problems in the current cosmological model of the universe, the ΛCDM model [269], such as the horizon and flatness problems [70]. The horizon problem refers to the observed homogeneity among causally disconnected regions of the universe, and the flatness problem concerns the very fine tuning of the initial conditions of the universe needed to account for the observed null curvature of spacetime. Countless numbers of models of inflation have been proposed (see [270] for a review of models) and it is currently one of the most prolific research topics in both astroparticle physics and cosmology.

Very recently, new results have been published that have shed some light into the inner workings of the universe at the very beginning. The Planck collaboration has measured the properties of the Cosmic Microwave Background (CMB) with astonishing accuracy and provided for the first time a phenomenological frontier for inflationary models [16, 17]. The measurement of the amplitude of scalar perturbations in the CMB radiation, $A_s = (2.19 \pm 0.11) \times 10^{-9}$, predicts an energy density during inflation

$$V = (2 \times 10^{16}\ \text{GeV})^4 \left(\frac{r}{0.15}\right), \tag{5.2.1}$$

where r is the ratio of tensor to scalar perturbations, which, for a value of $r \sim 0.1$ compatible with Planck's measurement, shows a remarkable coincidence between the values of $V^{1/4}$ and the value of M_{GUT} predicted by SUSY GUTs, $M_{GUT} \sim 2 \times 10^{16}$ GeV (c.f. section 2.3). Therefore, one can speculate that there might be a connection between the ideas of cosmological inflation and supersymmetric grand unification.

This intriguing connection between the scale of unification in supersymmetric theories and inflation was stimulated by the observation of the BICEP2 experiment of substantial B-mode[1] polarisation in the CMB [230]. Large B-mode polarisation can originate from gravitational waves during inflation, i.e. tensor density perturbations, which predicts a large value for the tensor-to-scalar ratio r, near the upper limit measured by Planck, motivating even further the link between the scales of unification and inflation. A follow-up analysis by the Planck collaboration [271] claims that the B-mode signal measured by BICEP2 is seriously contaminated by foreground dust pollution, thereby questioning the validity of the BICEP2 interpre-

[1] The polarisation of the CMB has two components: E-modes, for polarisation parallel or perpendicular to its direction and B-mode, for polarisation tilted 45 degrees with respect to its direction [70].

tation. Future experiments and observations, such as the Keck Array [231], may settle this issue with a very high projected sensitivity, required to measure the B-mode polarisation and thus potentially constraining GUT models of inflation.

To elucidate the potential connection between SUSY GUT models and inflationary physics we will attempt to build a supersymmetric GUT model, based on the flipped $SU(5) \otimes U(1)$ group, together with a hybrid inflation model, responsible for the GUT symmetry breaking. First, we will summarise the theory of inflation, focusing on those concepts and quantities that will be relevant for the rest of the analysis, in section 5.2.1. We will then describe the hybrid GUT inflation model, in section 5.2.2, where we find that the inflaton can be identified with the right-handed sneutrino of the flipped $SU(5) \times U(1)$ model, or with a GUT singlet, and we will analyse both cases and their consequences with respect to the cosmological observables. Finally, we will discuss in section 5.2.3 how both of these models may be embedded within the larger symmetry group $SO(10)$ and the consequences that the embedding might entail.

5.2.1 Inflation

Cosmological inflation was postulated originally to solve the flatness and horizon problems of the early universe, which were addressed by a rapid expansion of the universe, consequence of the universe decaying from a false vacuum into the current stable vacuum [265]. Though successful in its goal and in diluting away all topological defects, including domain walls and magnetic monopoles, this model was unable to reheat the universe, there was no radiation emitted to explain the initial abundance of particles in the universe. This issue was later solved by postulating the existence of a scalar field, that will cause the inflationary expansion while rolling down a potential energy hill [267, 268]. This model, known as slow-roll inflation[2], allows for a reheating phase at the end of inflation, when the scalar field, known as the inflaton, can decay into radiation [267, 268].

Slow-roll inflation

Let ϕ be a single scalar field, the inflaton. The Einstein-Hilbert action for this field can be written as [70]

$$S = \int \mathrm{d}^4x\sqrt{-g}\left(\frac{1}{2}R + \frac{1}{2}g^{\mu\nu}\partial_\mu\phi\partial_\nu\phi - V(\phi)\right), \tag{5.2.2}$$

[2]For recent encyclopedic reviews see Refs. [70, 272].

where $g^{\mu\nu}$ is the spacetime metric, g its determinant, R the scalar curvature and $V(\phi)$ the scalar potential in ϕ. Using the Friedmann-Robertson-Walker (FRW) metric $g^{\mu\nu}$ [273–276]

$$\mathrm{d}s^2 = g^{\mu\nu}\mathrm{d}x_\mu \mathrm{d}x_\nu = -\mathrm{d}t^2 + a^2(t)\left(\frac{\mathrm{d}r^2}{1-kr^2} + r^2(\mathrm{d}\theta^2 + \sin^2\theta \mathrm{d}\varphi^2)\right), \tag{5.2.3}$$

where r, θ and φ are spherical coordinates, $k = (-1, 0, +1)$ represents the curvature of space and $a(t)$ is the scale factor of the universe. The expression of the energy-momentum tensor for a perfect fluid is

$$T_{\mu\nu} = \begin{pmatrix} \rho & 0 & 0 & 0 \\ 0 & -p & 0 & 0 \\ 0 & 0 & -p & 0 \\ 0 & 0 & 0 & -p \end{pmatrix}, \tag{5.2.4}$$

with ρ and p the density and pressure of the universe. One can then find the equations of motion for the scalar field ϕ and the FRW geometry as

$$\ddot{\phi} + 3H\dot{\phi} + V' = 0, \qquad H^2 = \frac{1}{3}\left(\frac{1}{2}\dot{\phi}^2 + V(\phi)\right), \tag{5.2.5}$$

with H the Hubble parameter, $\dot{\phi} = \mathrm{d}\phi/\mathrm{d}t$, $V' = \partial V/\partial\phi$, and the equation of state of the universe in the presence of a scalar field [70]

$$\rho = wp, \quad \text{with } w = \frac{\frac{1}{2}\dot{\phi}^2 - V(\phi)}{\frac{1}{2}\dot{\phi}^2 + V(\phi)}. \tag{5.2.6}$$

If V dominates the kinetic term, then $w < 0$, the pressure is negative, from eq. (5.2.6), and the universe undergoes an accelerated expansion. The condition $\dot{\phi}^2 \ll V$ is known as the slow-roll limit [277].

In this limit, we can define the slow-roll parameters

$$\begin{aligned} \epsilon(\phi) &= \frac{M_\mathrm{P}^2}{2}\left(\frac{V'(\phi)}{V(\phi)}\right)^2, \\ \eta(\phi) &= M_\mathrm{P}^2\left(\frac{V''(\phi)}{V(\phi)}\right). \end{aligned} \tag{5.2.7}$$

where M_P is the Planck mass. The slow-roll condition is satisfied if $\epsilon(\phi), \eta(\phi) \ll 1$, and in that case the equations of motion reduce to

$$\dot{\phi} \approx -\frac{V'}{3H}, \qquad H^2 \approx \frac{1}{3}V(\phi). \tag{5.2.8}$$

With this we can define the number of e-folding from a time where the value of the field is ϕ until the end of inflation as

$$N_{tot} = \int_t^{t_{end}} H \mathrm{d}t = \int_\phi^{\phi_{end}} \frac{H}{\dot{\phi}} \mathrm{d}\phi \approx \int_{\phi_{end}}^{\phi} \frac{V}{V'} \mathrm{d}\phi$$
$$\approx \frac{1}{M_{\mathrm{P}}} \int_{\phi_{\mathrm{end}}}^{\phi} \frac{\mathrm{d}\phi}{\sqrt{2\epsilon(\phi)}}, \tag{5.2.9}$$

where ϕ_{end} is the value of ϕ when the slow-roll limit becomes invalid, corresponding to the end of inflation. Typically, one needs a long period of inflation, over 60 e-foldings of inflation, in order to solve the flatness and horizon problems [70].

The density fluctuations observed in the CMB occur between 40 - 60 e-folds before the end of inflation [70]. We can then find the value of the field ϕ^* when the CMB modes leave the event horizon during inflation as

$$N_e \approx \frac{1}{M_{\mathrm{P}}} \int_{\phi_{\mathrm{end}}}^{\phi^*} \frac{\mathrm{d}\phi}{\sqrt{2\epsilon(\phi)}} \approx 40 - 60. \tag{5.2.10}$$

As we have mentioned, the earliest information we have of the universe comes from the recombination era, when the CMB is produced. Fortunately, quantum fluctuations over the scalar field or the metric at the time of inflation are imprinted as anisotropies in the CMB [70]. The power spectrum of scalar and tensor perturbations can be parametrised as [16, 70]

$$\mathcal{P}_s = A_s \left(\frac{k}{k_*}\right)^{n_s - 1 + \frac{1}{2}\alpha_s(k_*)\ln(k/k_*)}, \tag{5.2.11}$$

$$\mathcal{P}_t = A_t \left(\frac{k}{k_*}\right)^{n_t}, \tag{5.2.12}$$

where $A_s(A_t)$ is the scalar (tensor) amplitude, $n_s(n_t)$ are the scalar (tensor) spectral index, α_s the running of the scalar spectral index and k_* is a reference pivot scale. The scalar amplitude A_s and the scalar spectral index n_s, together with the ratio of tensor perturbations to scalar perturbations, $r = \mathcal{P}_t/\mathcal{P}_s$, are among the most important cosmological observables, since they have an big significance in inflationary models.

In the context of the slow-roll approximation, for a singlet field inflation, the scalar and tensor power spectrum can be calculated as [70]

$$\mathcal{P}_s = \frac{H_\star^2}{(2\pi)^2} \frac{H_\star^2}{(\dot{\phi}^\star)^2}, \tag{5.2.13}$$

$$\mathcal{P}_t = \frac{2}{\pi^2} \frac{H_\star^2}{M_p^2}, \tag{5.2.14}$$

which, using equations (5.2.5) and (5.2.7), give equations for the observables A_s, n_s and r in terms of the energy density and slow-roll parameters as

$$\begin{aligned} A_s &= \frac{V(\phi^*)}{24\pi^2 M_{\rm P}^4 \epsilon(\phi^*)}, \\ n_s &= 1 - 6\epsilon(\phi^*) + 2\eta(\phi^*), \\ r &= 16\epsilon(\phi^*), \end{aligned} \tag{5.2.15}$$

and their experimental values, recently measured by the Planck collaboration, can be seen in table 5.2.

A_s	n_s	r
$(2.19 \pm 0.11) \times 10^{-9}$	0.9603 ± 0.0073	< 0.16

Table 5.2: *Experimental constraints for the amplitude of scalar perturbations A_s, the spectral index n_s and tensor-to-scalar ratio r, from [16, 17].*

The apparent observation of B-mode polarisation of the CMB at BICEP2 [230] would suggest a relatively larger value $r = 0.20^{+0.07}_{-0.05}$ in the absence of dust, with respect to the one used in table 5.2. The BICEP2 collaboration estimated the possible reduction in r implied by dust contamination, but a recent Planck study of the galactic dust emission [271] suggests that this may be more important than estimated by BICEP2. It could be that the polarized galactic dust emission accounts for most of the BICEP2 signal, although further study is needed to settle this issue. To be conservative, the value shown in table 5.2 is a compromise between the BICEP2 results and the limit set by Planck $r < 0.16$ at the 95% CL [16].

Hybrid Inflation

Among the many models of inflation in the literature, hybrid inflation is one of the most popular, for it provides a natural setup for the end of inflation as a second order phase transition of another scalar field [278–287].

Let ϕ be the scalar inflaton field and h another scalar field, responsible for the breaking of some symmetry, with a scalar potential

$$V(\phi, h) = \frac{m^2}{2}\phi^2 + \frac{g^2}{2}\phi^2 h^2 + \frac{1}{4\lambda}(M^2 - \lambda h^2)^2, \tag{5.2.16}$$

where m^2, g^2, λ and M^2 are real parameters. As can be seen in figure 5.12, this potential has a minimum at $h = 0$ for a large value of the field $\phi > \phi_c = M/g$,

so it can be assumed that the universe was stable at this minimum at the start of inflation. The potential during this era is just

$$V(\phi, h = 0) = \frac{m^2}{2}\phi^2, \tag{5.2.17}$$

and thus it can be expected that the field ϕ will slow-roll down its potential, inflating the universe.

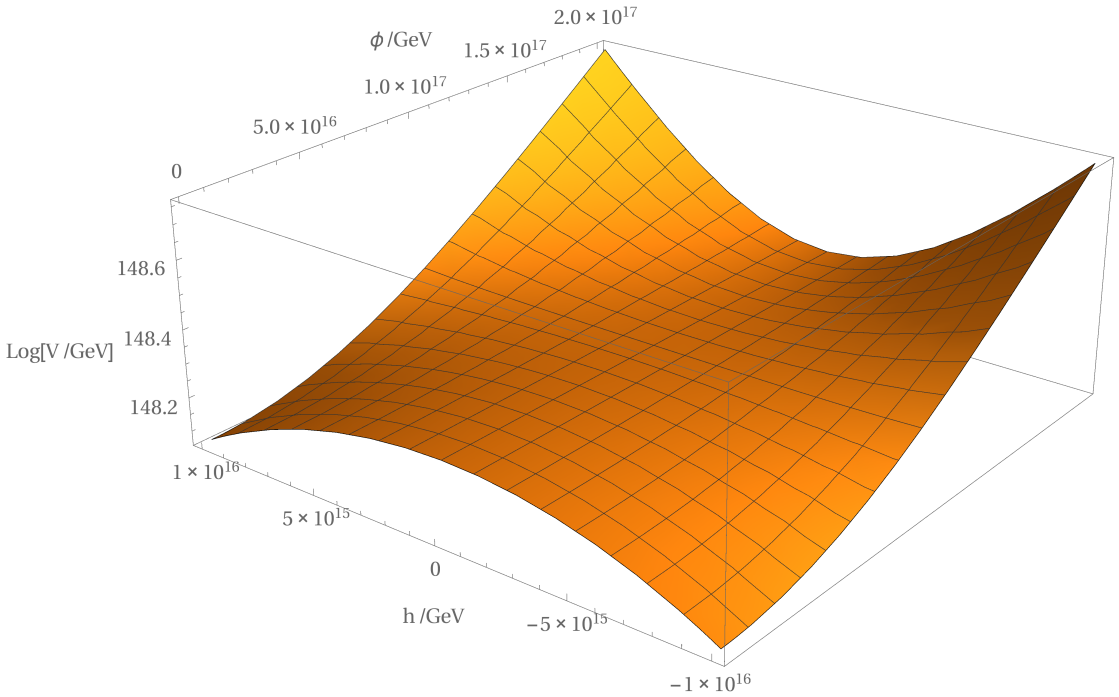

Figure 5.12: *Scalar potential for the hybrid inflation model.*

After a number of e-foldings of inflation, the value of the field will drop below $\phi_c = M/g$. This makes the potential in h unstable at $h = 0$, because the curvature of the potential at that point is given by

$$\left.\frac{\partial^2 V}{\partial h^2}\right|_{h=0} = g^2\phi^2 - M^2, \tag{5.2.18}$$

which becomes negative for $\phi < \phi_c$. The system will then suffer a second-order phase transition, with h moving to the new minimum $h \neq 0$, as can be seen in figure 5.12, breaking the symmetry.

In the process of decaying to its new vacuum, the field h drags the inflaton ϕ with it. The slow-roll approximation is no longer valid after ϕ_c because of the non-vanishing vacuum expectation value of h, and inflation ends.

Therefore, as soon as the field $\phi < \phi_c$, the end of inflation and breaking of the symmetry happen simultaneously, and both fields will roll, "waterfall", quickly down the slope of their potential to their true minimum, which corresponds to $\phi = 0$, $h = M/\sqrt{\lambda}$.

The measurement of the scalar amplitude A_s and tensor-to-scalar ration r in table 5.2, predict the energy density to be at the unification scale. From the expressions for A_s and r in the slow-roll approximation, eq. (5.2.15), we have that the energy density can be written as

$$V = \frac{3}{2} M_P^4 \pi^2 r A_s \approx (2 \times 10^{16} \text{ GeV})^4 \left(\frac{r}{0.15}\right), \tag{5.2.19}$$

as in eq. (5.2.1). Thus, hybrid inflation models have become quite popular because they provide a mechanism to link the end of the inflationary era with the symmetry breaking required to happen at the unification scale [19, 288].

5.2.2 Minimal GUT Inflation

A common prediction of GUTs is the emergence of magnetic monopoles at an early stage of the universe [10, 289], which can overclose the universe if their density is too large [265]. As mentioned before, inflation has a way of avoiding the monopole problem. If any monopoles are present before the inflationary epoch, their density will be diluted away after the expansion, thus avoiding detection and not contributing to the overall energy density of the universe. Therefore, to develop a monopole free GUT model, one must impose that the GUT symmetry breaking happens prior to inflation, thus washing away any monopoles that emerged before.

In the context of hybrid inflation, as was described above, the symmetry breaking happens right at the end of the inflationary era and so it cannot benefit from the rapid expansion to dilute the density of monopoles. An interesting way to circumvent this problem is to have the unified group to be non-semisimple, for which the magnetic monopole flux cancels, provided that the abelian electromagnetic $U(1)$ factor is not entirely contained in the semisimple subalgebra [10]. One such model is the flipped $SU(5) \otimes U(1)$ model, which was described in section 2.2.2 as it satisfies all the above requirements: it is consistent with the unification of gauge couplings at $M_{GUT} \sim 10^{16}$ and the SM hypercharge is a linear combination of the abelian generator T_{24} in the $SU(5)$ simple group and the charge X of the external $U(1)$

$$Y = -\frac{1}{5} T_{24} + \frac{1}{5} X, \tag{5.2.20}$$

thus cancelling the flux of magnetic monopoles [10].

With the field content of the flipped $SU(5)\otimes U(1)$ model, described in section 2.2.2, we can construct the most general superpotential as

$$\begin{aligned} W = \; & y_u \hat{10}_F \hat{10}_F \hat{5}_{H_u} + y_d \hat{10}_F \hat{\bar{5}}_F \hat{\bar{5}}_{H_d} + y_e \hat{\bar{5}}_F \hat{1}_F \hat{5}_{H_u} \\ & + \lambda_u \hat{10}_H \hat{10}_H \hat{5}_{H_u} + \lambda'_u \hat{10}_F \hat{10}_H \hat{5}_{H_u} + \lambda_d \hat{\overline{10}}_H \hat{\overline{10}}_H \hat{\bar{5}}_{H_d} + \lambda'_d \hat{10}_H \hat{\bar{5}}_F \hat{\bar{5}}_{H_d} \\ & + \lambda_F \hat{10}_F \hat{\overline{10}}_H \hat{1}_S + \lambda_5 \hat{5}_{H_u} \hat{\bar{5}}_{H_d} \hat{1}_S + \lambda_{10} \hat{10}_H \hat{\overline{10}}_H \hat{1}_S + \lambda_S \hat{1}_S \hat{1}_S \hat{1}_S \\ & + \mu_F \hat{10}_F \hat{\overline{10}}_H + \mu_5 \hat{5}_{H_u} \hat{\bar{5}}_{H_d} + \mu_{10} \hat{10}_H \hat{\overline{10}}_H + \mu_S \hat{1}_S \hat{1}_S + M_S^2 \hat{1}_S \,, \end{aligned} \tag{5.2.21}$$

where $\hat{10}_F$ and $\hat{\bar{5}}_F$ contains the SM fermions, $\hat{1}_F$ the right-handed neutrino, $\hat{5}_{H_u}$ and $\hat{\bar{5}}_{H_d}$ the MSSM Higgses, $\hat{\overline{10}}_H$ and $\hat{10}_H$ the unification group breaking Higgses, and $\hat{1}_S$ is a group singlet. The couplings y_i, λ_i and λ'_i are dimensionless Yukawa-like couplings, whereas the couplings μ_i have dimension one and are equivalent to the μ terms in the MSSM. The linear coupling M_S^2 has also dimension one and it sets the energy scale of the potential, since $V \sim M_S^4$.

Additionally, soft SUSY breaking terms for the scalar fields need to be added to the model. Provided supersymmetry is broken above the GUT scale as in supergravity models [172, 290], we obtain soft SUSY breaking terms, c.f. eq. (2.3.10), such as

$$V_{SSB} = \; (A_{ijk} y_{ijk} \phi^i \phi^j \phi^k + B_{ij} \mu_{ij} \phi^i \phi^j + c.c.) + m_i^2 |\phi^i|^2 \tag{5.2.22}$$

at some high renormalisation scale $\mu > M_{GUT}$. Through RGE evolution, the soft masses for the $SU(5) \otimes U(1)$ breaking Higgses, $m^2_{10_H}$ and $m^2_{\overline{10}_H}$, may become tachyonic at some $\mu \sim M_{GUT}$, and thus trigger the symmetry breaking $SU(5) \otimes U(1) \to SU(3)_c \otimes SU(2)_L \otimes U(1)_Y$ [76, 77].

There are two fields in the superpotential above that can act as the inflaton, the right-handed sneutrino $\tilde{\nu}^c$ embedded in $\hat{10}_F$, or the singlet S in $\hat{1}_S$. Although sneutrino inflation has been studied extensively [291–299], to the best of our knowledge no study of sneutrino-driven inflation in a flipped $SU(5)\otimes U(1)$ model has been performed, though it was suggested in [300].

Sneutrino Inflation

From the superpotential 5.2.21, the only relevant terms for this model of sneutrino inflation are

$$W \supset \; \lambda_F \hat{10}_F \hat{\overline{10}}_H \hat{1}_S + \mu_F \hat{10}_F \hat{\overline{10}}_H + \mu_{10} \hat{10}_H \hat{\overline{10}}_H + \lambda_{10} \hat{10}_H \hat{\overline{10}}_H \hat{1}_S \,, \tag{5.2.23}$$

whereas the rest of the terms in (5.2.21) include other superfields that we do not consider for inflation, such as the antisymmetric coupling $\hat{10}_F\hat{10}_H\hat{\bar{5}}_{H_u}$, which includes components of fields other than ν^c, ν^c_H and $\bar{\nu}^c_H$.

It was discussed in [301], in the context of a Wess-Zumino model, that in order to realise a model of inflation with a cubic or quartic scalar potential, one needs couplings of the order $\lambda \sim 10^{-7} - 10^{-8}$. The main sources of high powers of the inflaton in our model are the D-terms, but their couplings are of the order of the gauge couplings, i.e. $g \sim 0.1 - 1$, which will not be able to reproduce the cosmological observables [288]. Therefore, in order to cancel the contributions from the D-terms, we introduce another field $\hat{\bar{10}}_F$, with the couplings

$$W \supset \bar{\lambda}_F\hat{\bar{10}}_F\hat{10}_H\hat{1}_S + \bar{\mu}_F\hat{\bar{10}}_F\hat{10}_H\,, \tag{5.2.24}$$

and for the same reason, to avoid quartic couplings, we do not consider terms like $\hat{\bar{10}}_F\hat{10}_F$ or $\hat{\bar{10}}_F\hat{10}_F\hat{1}_S$.

With the redefinitions $h = \nu^c_H$, $\bar{h} = \bar{\nu}^c_H$, $\phi = \nu^c$ and $\bar{\phi} = \bar{\nu}^c$, then one can calculate the F-term scalar potential, defined in chapter 2.3, as

$$\begin{aligned} V_F = \; & 4(\mu_{10}^2 + \bar{\mu}_F^2)h^2 + 4(\mu_{10}^2 + \mu_F^2)\bar{h}^2 + 4\lambda_{10}^2 h^2\bar{h}^2 \\ & + 4(2\lambda_{10}h\bar{h})(\lambda_F\bar{h}\phi + \bar{\lambda}_F h\bar{\phi}) + 8\mu_{10}(\mu_F h\phi + \bar{\mu}_F\bar{h}\bar{\phi}) \\ & + 4(\bar{\lambda}_F h\bar{\phi} + \lambda_F\bar{h}\phi)^2 + 4\mu_F^2\phi^2 + 4\bar{\mu}_F^2\bar{\phi}^2, \end{aligned} \tag{5.2.25}$$

and the D-term scalar potential has the form

$$V_D \propto (\phi^2 - \bar{\phi}^2 + h^2 - \bar{h}^2)^2, \tag{5.2.26}$$

whose contribution proportional to ϕ and $\bar{\phi}$ cancels during inflation if $\phi = \bar{\phi}$. In order to achieve this, it is enough to consider that $\phi^* = \bar{\phi}^*$ at the start of the inflationary phase [3] and that their evolution is the same, which is obtained by imposing the constraint $\mu_F = \bar{\mu}_F$.

We will assume that all soft SUSY breaking parameters are of the order of the SUSY scale, typically at the TeV scale. We will neglect these, except those for h and $\bar{h}$, because they are needed to trigger $SU(5) \otimes U(1)$ symmetry breaking, and they will have the form

$$V_{SSB} = -m_h^2|h|^2 - m_{\bar{h}}^2|\bar{h}|^2\,, \tag{5.2.27}$$

where $m_h^2, m_{\bar{h}}^2 > 0$.

[3] The superscript $*$ refers to the time of horizon crossing.

Before the inflationary epoch, the symmetry $SU(5) \otimes U(1)$ is unbroken, and so we would expect the fields h and $\bar{h}$ to be stable at zero. However, that is not the case for the general potential $V = V_F + V_D + V_{SSB}$, which does not have a minimum at the origin, unless $\mu_{10} = 0$. In that case, the scalar potential during inflation, while the symmetry is preserved, reads

$$V_\phi = 4\mu_F^2\phi^2 + 4\bar{\mu}_F^2\bar{\phi}^2. \tag{5.2.28}$$

As mentioned before, cancellation of ϕ^4 contribution from the D-terms happens if $\phi = \bar{\phi}$ and $\mu_F = \bar{\mu}_F$ during inflation. Hence, this inflationary potential is quadratic in ϕ, and all isocurvature perturbations cancel.

Therefore, the only free parameter is μ_F, so we will attempt to constrain it using the cosmological observables, A_s, n_s and r, whose experimental values can be seen in table 5.2, and the expressions in terms of the parameters in the potential can be seen in (5.2.15).

Figure 5.13 shows the allowed parameter space in the plane (μ_F, N_e), with N_e the number of e-foldings, in accordance with the cosmological observables. It can be easily noticed that the strongest constraint comes from the scalar amplitude A_s (blue), whereas the spectral index n_s (pink) and tensor-to-scalar ration r (green) set a upper and lower bound, respectively, on the number of e-foldings.

From figure 5.13 we pick out an example scenario, shown in table 5.3, that is consistent with all three observables and which we will use for the the rest of the analysis.

N_e	μ_F (GeV)	ϕ^* (GeV)	A_s	n_s	r
55	5.75×10^{12}	2.55×10^{19}	2.28×10^{-9}	0.9636	0.145

Table 5.3: *Sample scenario taken from the allowed region in figure 5.13.*

At some point close to the end of inflation, the fields h and/or $\bar{h}$ become unstable at the origin, thus triggering the symmetry breaking of $SU(5) \otimes U(1)$. All four fields, ϕ, $\bar{\phi}$, h and $\bar{h}$ will fall to the true minimum of the potential. For this to happen, the fields ϕ and $\bar{\phi}$ must have reached the critical values

$$\phi_c^2 = \frac{\frac{1}{2}m_h^2 - \mu_F^2}{\bar{\lambda}_F^2}, \quad \bar{\phi}_c^2 = \frac{\frac{1}{2}m_{\bar{h}}^2 - \mu_F^2}{\lambda_F^2}, \tag{5.2.29}$$

for which the origin $h = \bar{h} = 0$ becomes a local maximum, which is satisfied by the conditions $m_h^2 \gg 2\mu_F^2$ and $m_{\bar{h}}^2 \gg 2\mu_F^2$.

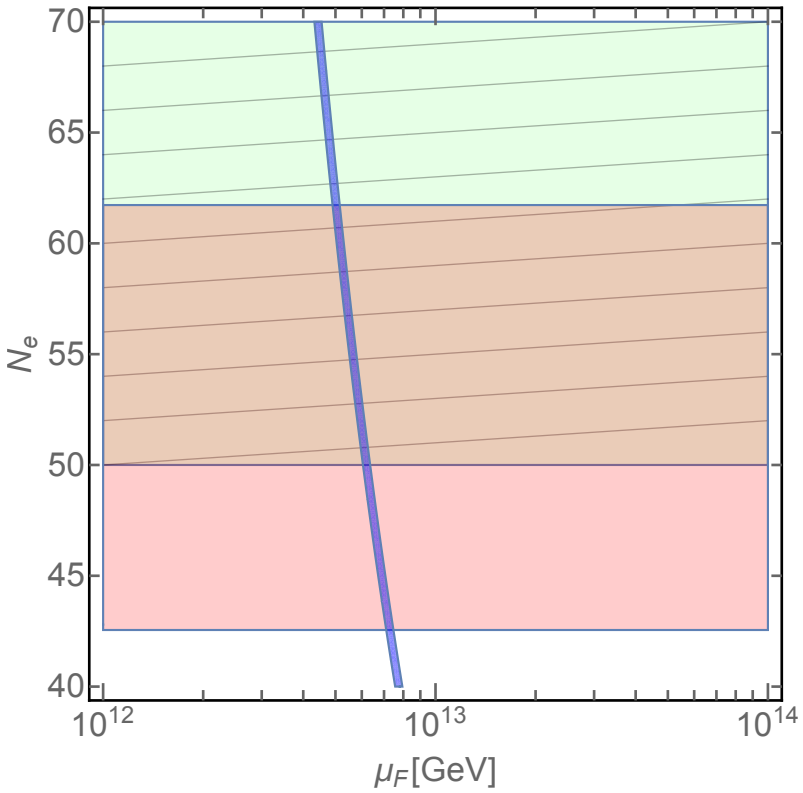

Figure 5.13: *Region plot in the* $(\mu_F = \bar{\mu}_F, N_e)$ *plane, with the allowed regions by the cosmological observables* A_s *(blue curve), spectral tilt* n_s *(pink region), and tensor-to-scalar ratio,* r *(green hatched region).*

Further, we need to ensure that the inflaton ϕ does not acquire a vacuum expectation value at the end of inflation, i.e. we need that $\langle\phi\rangle = 0$. Otherwise, since it is a sneutrino, it would generate a large mass term for the corresponding lepton and Higgsino, which would make them near-degenerate, and would also violate R-parity, losing the supersymmetric dark matter candidate.

Unfortunately, there are no solutions that allow $\langle\phi\rangle = 0$ while at the same time $\langle h\rangle = \langle\bar{h}\rangle \neq 0$, required so as to break the $SU(5) \otimes U(1)$ symmetry. However, there are four solutions with $\langle\phi\rangle = \langle\bar{\phi}\rangle = 0$ and either h or $\bar{h}$ acquiring a vacuum expectation value,

$$\begin{aligned}
\langle h\rangle &= \pm\sqrt{\frac{5}{6}}\frac{\sqrt{m_h^2 - 2\mu_F^2}}{g}, \quad \langle\bar{h}\rangle = 0, \quad \langle\phi\rangle = 0, \quad \langle\bar{\phi}\rangle = 0 \\
\langle\bar{h}\rangle &= \pm\sqrt{\frac{5}{6}}\frac{\sqrt{m_h^2 - 2\mu_F^2}}{g}, \quad \langle h\rangle = 0, \quad \langle\phi\rangle = 0, \quad \langle\bar{\phi}\rangle = 0,
\end{aligned} \tag{5.2.30}$$

so if we choose one of them, $\langle\bar{h}\rangle = 0$ for example, the inflation field will not acquire

a v.e.v. and the GUT symmetry will be broken. In this case $\bar{h}$ must be stable at its minimum $\bar{h} = 0$ for all values of ϕ and $\bar{\phi}$, which will happen if $2\mu_F^2 \gg m_{\bar{h}}^2$. Without loss of generality and knowing the value of μ_F from table 5.3, we can choose a value for $m_{\bar{h}}$ compatible with this constraint, $m_{\bar{h}} \sim 10^{12}$.

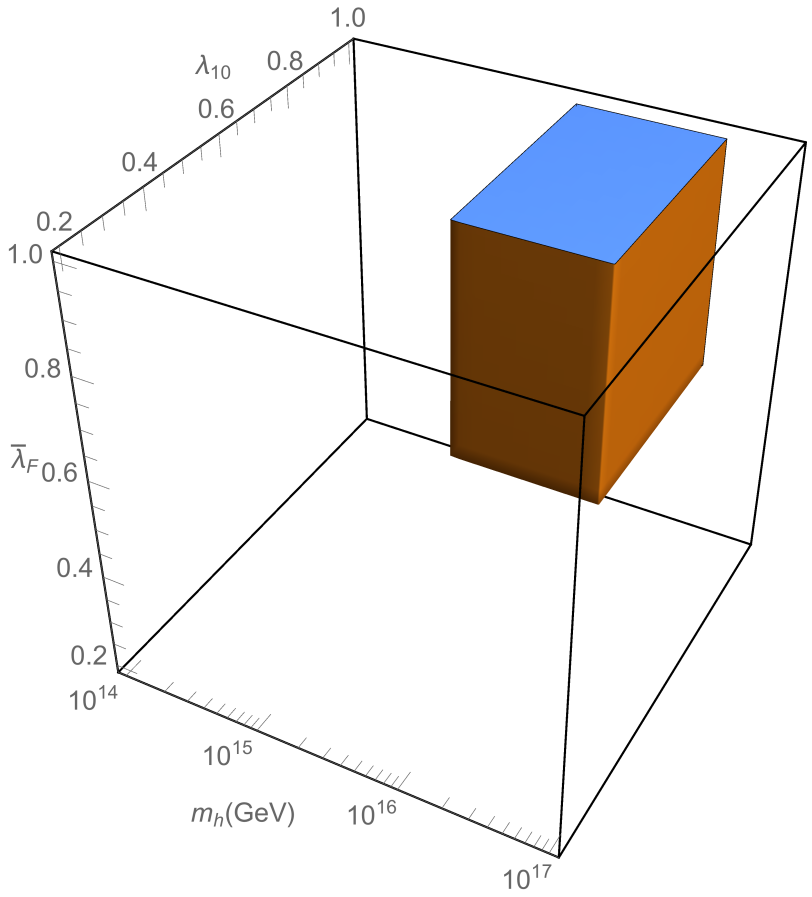

Figure 5.14: *Allowed region in the m_h, $\bar{\lambda}_F$ and λ_{10} parameter space for which $\langle h \rangle \sim 10^{16}$ GeV and the system is in its true minimum. We have $3.89 \times 10^{15} \leq m_h \leq 3.89 \times 10^{16}$ GeV, $0.56 \leq \bar{\lambda}_F$, $\lambda_{10} \leq 4\pi$, where the upper bound on $\bar{\lambda}_F$ and λ_{10} results from the perturbativity limit.*

The remaining parameters of the model are m_h, $\bar{\lambda}_F$ and λ_{10}, since the coupling λ_F drops out from all equations because of the minimum condition $\bar{h} = 0$. Imposing that the system falls to its true minimum, with $\langle h \rangle \sim 10^{16}$, required by unification, we can find constraints on these parameters, whose allowed region of parameter space is shown in figure 5.14. We can see that only high values of m_h, close to the GUT scale, are allowed, as was expected. Further, values of the couplings $\bar{\lambda}_F$ and λ_{10} must be large, $\bar{\lambda}_F, \lambda_{10} \in (0.5, 4\pi)$, but obviously below the perturbativity limit.

Singlet Inflation

The other candidate that we will consider as inflaton in the superpotential in (5.2.21) is the singlet $\hat{1}_S$. The relevant terms for this case, with the redefinition $\varphi = \hat{1}_S$, are

$$W(\varphi, h, \bar{h}) = M_S^2\ \varphi - \mu_S\ \varphi^2 + \lambda_S\ \varphi^3 - 2\lambda_{10}\ h\bar{h}\varphi + 2\mu_{10}\ h\bar{h}\,. \tag{5.2.31}$$

Along the lines of the analysis in the previous case, we focus here on quadratic inflation only, thus we set $\lambda_S = 0$, cancelling the cubic term in φ. Hence the F-term scalar potential is

$$\begin{aligned} V_F = \ & M_S^4 + 4\mu_{10}^2(h^2 + \bar{h}^2) - 4\lambda_{10}^2 h^2\bar{h}^2 - 4\lambda_{10}M_S^2 h\bar{h} \\ & - 8\lambda_{10}\mu_{10}(h^2 + \bar{h}^2)\varphi + 8\lambda_{10}\mu_S h\bar{h}\varphi + 4\lambda_{10}^2(h^2 + \bar{h}^2)\varphi \\ & - 4\mu_S M_S^2\varphi + 4\mu_S^2\varphi^2\,. \end{aligned} \tag{5.2.32}$$

The only other contributions to the scalar potential in this scenario come from the symmetry breaking Higgses, h and $\bar{h}$, from their SSB masses, the same as for the sneutrino case in eq. (5.2.27), and their D-terms. The contribution from the D-terms cancels for φ, because it is a singlet. As before, we assume the SSB mass of the inflaton to be negligible compare to those of h and $\bar{h}$.

It is straightforward to see that the potential in equation (5.2.32) has a stable minimum for $h = \bar{h} = 0$, so during inflation it reduces to

$$V_\varphi = \left(M_S^2 + 2\mu_S\varphi\right)^2\,. \tag{5.2.33}$$

Once again, using the cosmological parameters in (5.2.15) - (5.2.10), we perform an analysis to constrain the couplings in (5.2.33). Since there are now two parameters M_S and μ_S, we present corresponding results for different numbers of e-foldings $N_e = 40, 50, 60$ in figure 5.15.

Similar to the sneutrino case explored in section 5.2.2, the strongest constraint in figure 5.15, as expected, comes from the scalar amplitude A_s. It can be seen that for $N_e = 40$, only a small region of parameter space is compatible with the observables, and this could disappear entirely with a stronger upper limit on r. For $N_e = 50 - 60$, however, the parameter space becomes less constrained since the bounds on n_s and r are less restrictive for a larger number of e-foldings. However, when $N_e = 60$, the upper limit on M_S drops slightly. Curiously, we do not find a lower bound on M_S, so a value of $M_S = 0$ would be perfectly valid without disturbing the observables. If that were the case, then we recover from figure 5.13, since the inflationary potential in (5.2.33) is the same as in (5.2.28) with $\varphi^2 = \phi^2 + \bar{\phi}^2$.

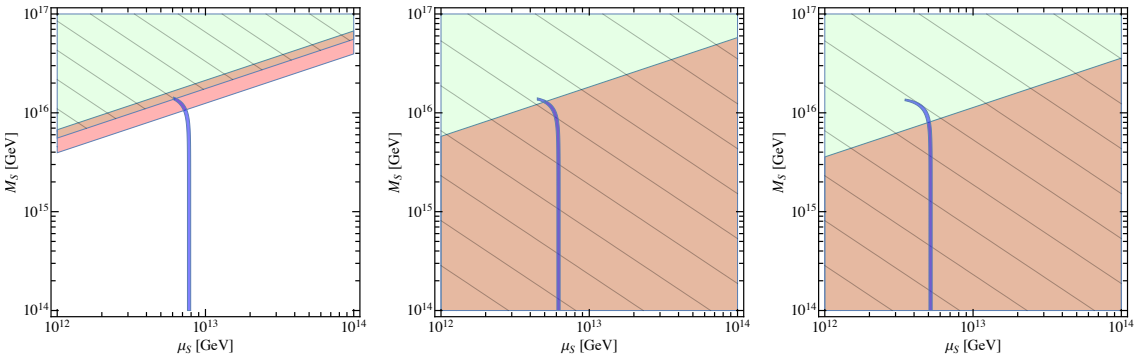

Figure 5.15: *Allowed regions of the (μ_S, M_S) parameter space according to the scalar amplitude A_s (blue curved), the tensor-to-scalar ratio r (green hatched region) and the spectral tilt n_s (pink region), for $N_e = 40$ e-foldings (left), $N_e = 50$ (centre) and $N_e = 60$ (right).*

A example scenario is shown in table 5.4, with $N_e = 50$ and $M_S = 6.03 \times 10^{15}$ GeV, close to the GUT scale.

N_e	μ_S (GeV)	M_S (GeV)	φ^* (GeV)	A_s	n_s	r
50	6.17×10^{12}	6.03×10^{15}	3.16×10^{19}	2.20×10^{-9}	0.9603	0.159

Table 5.4: *Sample scenario taken from the allowed region in figure 5.15 for $N_e = 50$.*

The waterfall fields, h and $\bar{h}$, become unstable at $h = \bar{h} = 0$ near to the end of the inflationary era, for the values of the inflaton

$$\varphi_c = \frac{\frac{1}{2}m_h - \mu_{10}}{2\lambda_{10}}, \quad \varphi_c = \frac{\frac{1}{2}m_{\bar{h}} - \mu_{10}}{2\lambda_{10}}, \tag{5.2.34}$$

which we will assume to be equal, thus $m_{\bar{h}} = m_h$, so that h and $\bar{h}$ move simultaneously away from the origin and to the true minimum. The $SU(5) \otimes U(1)$ is broken at this stage, since h and $\bar{h}$ acquire a non zero v.e.v. at the true minimum $\langle h \rangle = \langle \bar{h} \rangle \neq 0$.

Since φ is a singlet, it is free to acquire an expectation value, so there is no problem finding a solution for which both $\langle h \rangle = \langle \bar{h} \rangle \neq 0$, regardless of the value of $\langle \varphi \rangle$. The remaining parameters of the model, m_h, μ_{10} and λ_{10} can be constrained by requiring that $\langle h \rangle \sim \langle \bar{h} \rangle \sim 10^{16}$ GeV and that the system falls to the true minimum, as can be seen in figure 5.16. In comparison to figure 5.14, we find that the allowed region of parameter space is much larger. The value of μ_{10} is roughly unconstrained, whereas the lower limit of the value of λ_{10} depends on m_h, with $\lambda_{10} \gtrsim 0.1$ for $m_h \gtrsim 10^{16}$.

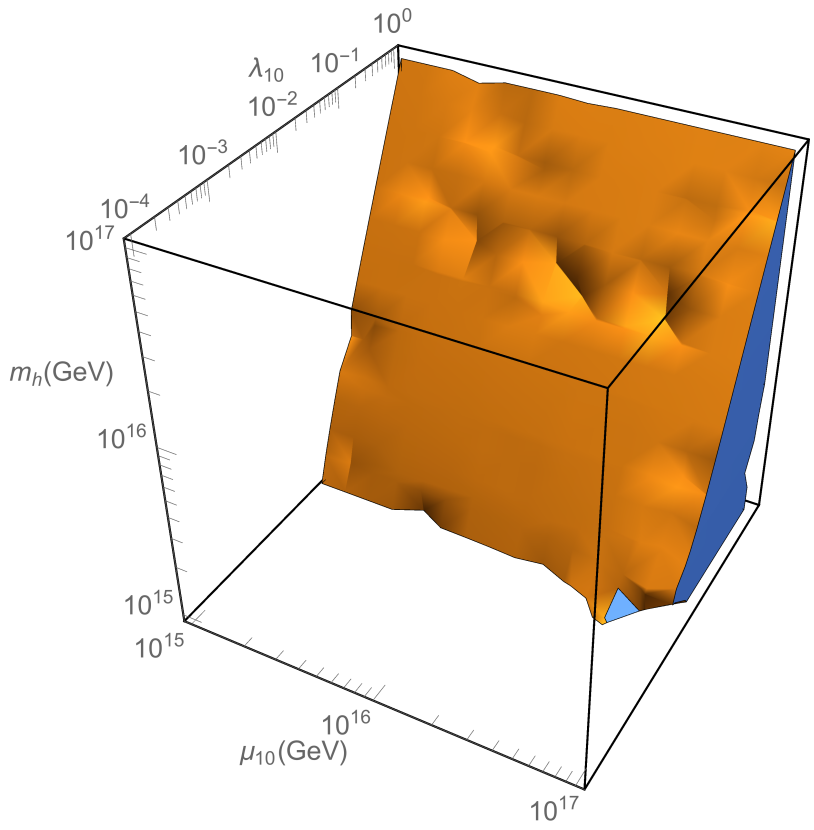

Figure 5.16: *Region of the* $(\mu_{10}, \lambda_{10}, m_h)$ *parameter space that allows vevs for* h *and* $\bar{h}$*:* $\langle h\rangle = \langle \bar{h}\rangle \sim 10^{16}$ *GeV.*

5.2.3 Embedding in SO(10)

The superpotentials for both the above inflation scenarios, with a sneutrino inflaton and a singlet inflaton, are

$$\begin{aligned} W_{\phi\in\hat{1}\hat{0}_F} &= \mu_F(\hat{1}\hat{0}_F\hat{\bar{1}}\hat{0}_H + \hat{\bar{1}}\hat{0}_F\hat{1}\hat{0}_H) + \bar{\lambda}_F\hat{\bar{1}}\hat{0}_F\hat{1}\hat{0}_H\hat{1}_S + \lambda_{10}\hat{1}\hat{0}_H\hat{\bar{1}}\hat{0}_H\hat{1}_S, \\ W_{\varphi\in\hat{1}_S} &= M_S^2\ \hat{1}_S + \mu_S\hat{1}_S\hat{1}_S + \mu_{10}\hat{1}\hat{0}_H\hat{\bar{1}}\hat{0}_H + \lambda_{10}\hat{1}\hat{0}_H\hat{\bar{1}}\hat{0}_H\hat{1}_S\,, \end{aligned} \tag{5.2.35}$$

respectively. They contain one or more dimensionful parameters, namely μ_F in the scenario of sneutrino inflation and μ_S and μ_{10} for the singlet case. However, above the $SU(5)\otimes U(1)$ breaking scale, the only real scale in the model is the Planck scale, but according to the constraints found for these parameters, c.f. figures 5.13, 5.15 and 5.16, their values are considerably lower than the Planck scale.

Therefore, we could postulate a pre-inflationary era during which there is a prior phase transition when some larger group breaks down to $SU(5)\otimes U(1)$. The dimensionful parameters at the intermediate scale may then be obtained via the expectation values of the scalar field(s) breaking the larger symmetry.

The simplest and most straightforward candidate would be the group $SO(10)$. The 10-dimensional $SU(5)$ representations can be embedded into 16-dimensional representations of $SO(10)$, and the singlet can be taken either as a singlet of $SO(10)$ or as a component of the adjoint 45-dimensional representation of $SO(10)$. Here we choose it to be in the adjoint representation, $\hat{45}_H$, which is also needed to break $SO(10)$ into $SU(5)\otimes U(1)$. In the unbroken $SO(10)$ phase, the superpotentials are given by

$$\begin{aligned} W_{\phi\in\hat{16}_F} &= \lambda_{45}(\hat{16}_F\hat{\bar{16}}_H + \hat{\bar{16}}_F\hat{16}_H)\hat{45}_H + \bar{\lambda}_F\hat{\bar{16}}_F\hat{16}_H\hat{45}_H + \lambda_{10}\hat{16}_H\hat{\bar{16}}_H\hat{45}_H, \\ W_{\varphi\in\hat{1}_S} &= \lambda_{45}\hat{45}_H\hat{45}_H\hat{45}_H + \lambda'_{45}\hat{16}_H\hat{\bar{16}}_H\hat{45}_H + \lambda_{10}\hat{16}_H\hat{\bar{16}}_H\hat{45}_H. \end{aligned} \tag{5.2.36}$$

When the $SO(10)$ group is broken, the $\hat{45}_H$ acquires a v.e.v. with the little group $SU(5)\otimes U(1)$, $\langle\hat{45}_H\rangle = v$. The $SO(10)$ representations are then broken, and give rise to (among others) the terms in (5.2.35), which allows for the following identifications of the couplings

$$\begin{aligned} &\mu_F = v\lambda_{45}, \\ &M_S^2 = v^2\lambda_{45}, \quad \mu_S = v\lambda_{45}, \quad \mu_{10} = v\lambda'_{45}. \end{aligned} \tag{5.2.37}$$

Since the $SO(10)$ breaking happens above the GUT scale, $v \gtrsim 10^{16}$ GeV, we can see that for the reference scenarios in tables 5.3 and 5.4, for which $\mu_F \sim \mu_S \lesssim 10^{13}$ GeV, we find that $\lambda_{45} \lesssim 10^{-3}$. This is consistent with the fact that we have taken $M_S \neq 0$ in section 5.2.2, as we find now that $M_S = v\sqrt{\lambda_{45}} \sim 10^{15}$ GeV, which roughly matches and motivates our choice in table 5.4.

Although this embedding into $SO(10)$ seems reasonable and provides a suitable superpotential prior to inflation, it looses the ultraviolet connection with weakly-coupled string theory. This is because it is, in general, not possible to obtain such large representations as $\hat{45}_H$ from a manifold compactification of string theory [172, 290]. One possible alternative would be to consider *flipped* $SO(10)\otimes U(1)$ as the pre-inflationary GUT symmetry group. This differs from the usual $SO(10)$ in that the SM matter content is not fully embedded in a 16-dimensional representation, but in the direct sum $16_1 \oplus 10_{-2} \oplus 1_4$. This kind of model could in principle be derived from string compactification, since it no longer requires large field representations: the symmetry breaking $SO(10)\otimes U(1) \to SU(5)\otimes U(1)$ can be realised by a pair of representations $16_1 \oplus \overline{16}_{-1}$. However, the only way to obtain superpotentials such as (5.2.35) would be with non-renormalisable terms involving four 16-dimensional representations.

6

Conclusions and Outlook

The discovery of the Higgs boson by the ATLAS and CMS collaborations agrees with the predictions of the Standard Model, thereby confirming the success of gauge theories. The mechanism of spontaneous symmetry breaking has been verified by the presence of the Higgs boson, responsible for triggering the phase transition. This fact, along with the known issues of the SM, such as charge quantisation or neutrino masses, among others, strongly motivates the extension to GUTs.

GUTs are very powerful theories, with many of their properties dictated by the mathematical group structure. They reproduce the successes of the SM, and provide a solution to many of its problems. Arguably the most popular of them are supersymmetric GUTs, which bring together the unified picture of GUTs with the predictive power of SUSY.

However, the lack of signs for SUSY in current experiments puts many of the minimal SUSY GUT models under pressure. Therefore, it is of paramount importance to extend the study beyond minimal GUT models, in a systematic fashion, in order to satisfy the current experimental constraints and prepare for the upcoming results from current or future experiments.

Throughout this thesis we have discussed the development of a framework capable of performing a systematic and general study of unified theories, and we have given some examples of its use. The first piece of this framework is the group theory tool, whose algorithms and implementation are detailed in chapter 3. This tool deals with the mathematical properties of Lie algebras and their representations, in terms of their roots and weights, and through its interface allows the calculation of properties needed for the model building phase, such as the breaking chains, decomposition of representations and calculation of invariants.

The second stage of the tool is the model building itself, described in chapter

4, which, by using the group theory tool is able to obtain a large collection of GUT models. Given the input: a gauge group, a breaking chain and a set of representations at the unification scale, this framework calculates all the possible models consistent with theoretical constraints: chirality, anomaly cancellation, successful symmetry breaking and reproduction of the SM representations. For each of these models, we then solve the unification conditions, to obtain the allowed values for the energy scales.

There exists a very pronounced connection between GUTs and supersymmetry, motivated partially by of the unification of gauge couplings in the MSSM, as in figure 1.2. Although SUSY is preferred at low energies, recent searches have set stringent constraints on SUSY light states, thereby encouraging the analysis of models where supersymmetry lives at higher scales. Therefore, the GUT models calculated using the model building framework allow for a sliding SUSY scale, i.e. the value or limits of the SUSY breaking scale would only be constrained by the unification of gauge couplings, not by the need to have a low supersymmetric spectrum. We thereby implicitly disregard the hierarchy problem as a theoretical issue and assume that it is solved in a different fashion or that it is irrelevant.

As an example we applied the tool to the case of a $SO(10)$ GUT with a specific set of representations and a symmetry breaking chain with the left-right symmetry group $SU(3)_C \otimes SU(2)_L \otimes SU(2)_R \otimes U(1)_{B-L}$ at an intermediate step. We find that, for up to five exotic scalar states above the left-right symmetric scale, there are over 250,000 models allowed by the theoretical constraints. We noticed that there is an overall preference for low values of the left-right scale and high values of the SUSY breaking scale, which is more pronounced for minimal cases, with fewer number of representations.

GUT models with intermediate left-right symmetric make additional predictions that can be compared with experimental observations. We imposed phenomenological constraints on the set of models, such as consistency with the current SUSY searches, discarding models with $M_{SUSY} < 1$ TeV, stability of the proton longer than the measured half-life $\tau_p > 10^{34}$ years, and agreement with the bound on the mass of the W_R, coming from the mass difference of the $K_S - K_L$ system. Alternatively, we imposed more stringent constraints, according to the projected limits of future experiments.

These constraints reduced the number of models significantly and they enhanced the preference for low M_{LR} and high M_{SUSY}, showing a correlation between the left-right and SUSY scales, where if either one of them has a value close the

the electroweak scale, the other one must be close to the GUT scale. The GUT scale M_{GUT} is required to be larger than 10^{16} in order to satisfy the proton decay constraint.

The current limits on the masses of supersymmetric particles impose very strong constraints on SUSY and GUT models. In section 5.1 we analysed a SUSY $SO(10)$ model, which deviates from the usual mSUGRA scenario by assuming different boundary conditions at the GUT scale for the soft SUSY breaking masses. These deviations were due to the contribution of $SO(10)$ D-terms to scalar masses and the effect of the $SO(10)$ representation of the SUSY breaking messenger on the gaugino masses. We calculated the spectrum of supersymmetric particles and we found two interesting cases. One of them has light third generation squarks, so light in fact that they are nearly degenerate with the LSP. This scenario falls into the category of "compressed" SUSY, evading the current LHC constraints on stop searches. The other scenario has a lighter first and second generation of sfermions and predicts light sleptons, close to the current limit.

On the other side of the energy spectrum, the measurements of the amplitude of scalar and tensor perturbations in the CMB by the Planck and BICEP2 collaborations has shown hints of a correlation between the scales of inflation and unification. We have therefore built, in section 5.2, a flipped $SU(5) \otimes U(1)$ model in which inflation and GUT symmetry breaking happen around the same energy scale. The scenario offers two possible candidates for the inflaton: the sneutrino, embedded in the $\hat{10}_F$ representation of the unified group along with the other sfermions; and the singlet, in a $\hat{1}_S$ representation. For both cases we find the limits on the parameters of the model, by reproducing the measurements of the scalar amplitude A_s, spectral index n_s and tensor-to-scalar ratio r measured by the Planck collaboration.

Throughout this thesis we have asserted that GUTs are very powerful and promising extensions of the SM, either by generating a multitude of models, showing the flexibility of GUTs, or by performing analyses of GUT models on the two sides of the energy spectrum: SUSY phenomenology and cosmological inflation. This work is, however, not complete, for there are many versions or variations of GUT models that we have not yet considered and that are equally likely candidates for BSM theories, given the status of experimental observations to date.

Therefore, one could speculate on the directions to extend the above work. A rather obvious one is to implement an extension of the group theory tool, able to deal with groups of symmetries other than Lie groups, such as discrete groups, which are often present in the literature, e.g. Z_2 left-right symmetry or S_4 flavour symmetry.

In the model building phase there are many roads for improvement: starting from a more specific analysis of the symmetry breaking mechanism, by studying the scalar potential of the theory, rather than simply requiring the right representation content; or by performing a similar analysis for other initial conditions, increasing the set of representations at the GUT scale, choosing different breaking paths or starting with another gauge group e.g. E_6, $SO(12)$ or E_8, which have been considered in the literature due to their relation to superstring models.

Phenomenological analyses of the obtained models could also be a potential way forward. There is a plethora of computational tools available dedicated to calculating observable quantities, aimed to either reproduce or predict experimental observables. One could, therefore, build a link between this model building framework and some of those tools, allowing a direct connection between high energy GUT models and direct low energy predictions.

Finally, it is worth mentioning that the rapid advances on the experimental frontier might bring GUTs into the spotlight very soon. At the moment of writing the experiments of the LHC are collecting data during Run II, many analyses are on their way which could potentially find hints of unified theories, for example, a right-handed gauge boson at 2 TeV. Many other experiments could also have important relevance for GUTs in many different fronts: cosmological observation, dark matter detection, proton decay measurements, neutrino experiments, $g-2$ experiments and many more. It is a very exciting time for BSM theories, in particular for GUTs, since in the coming few years we could start detecting signs of new physics, which could prove or falsify many of the models in the literature. Perhaps more interesting, we could find something totally unexpected and new, thereby opening the field of theoretical particle physics to new ideas.

A

MSSM RGEs

We here list the RGEs for the MSSM at one and two loop level [185]. In cases where the equations are analytically solvable, we provide the exact solution. Otherwise, we provide an analytical approximation. The scale parameter t is defined as $t = \log \mu$ for an energy scale μ.

A.1 Gauge Couplings

The β-functions for the gauge couplings at 1-loop are:

$$\frac{1}{16\pi^2}\beta_{g_a} = \frac{dg_a}{dt} = \frac{b_a}{16\pi^2} g_a^3, \qquad (b_1, b_2, b_3) = (\tfrac{33}{5}, 1, -3), \tag{A.1.1}$$

They are exactly solvable at 1-loop with solution ($\alpha_a = g_a^2/4\pi$):

$$\alpha_a(\mu) = \frac{\alpha(M_{\rm GUT})}{1 - \frac{b_a}{2\pi}\alpha(M_{\rm GUT}) \log \frac{\mu}{M_{\rm GUT}}}. \tag{A.1.2}$$

A.2 Yukawa Couplings

Neglecting the Yukawa couplings of the first two generations, the β-functions for the 3rd generation Yukawa couplings are at 1-loop level:

$$\begin{aligned}
\frac{1}{16\pi^2}\beta_{y_t} &= \frac{dy_t}{dt} = \frac{y_t}{16\pi^2}\left(6y_t^2 + y_b^2 - \frac{16}{3}g_3^2 - 3g_2^2 - \frac{13}{15}g_1^2\right), \\
\frac{1}{16\pi^2}\beta_{y_b} &= \frac{dy_b}{dt} = \frac{y_b}{16\pi^2}\left(6y_b^2 + y_t^2 + y_\tau^2 - \frac{16}{3}g_3^2 - 3g_2^2 - \frac{7}{15}g_1^2\right), \\
\frac{1}{16\pi^2}\beta_{y_\tau} &= \frac{dy_\tau}{dt} = \frac{y_\tau}{16\pi^2}\left(4y_\tau^2 + 3y_b^2 - 3g_2^2 - \frac{9}{5}g_1^2\right).
\end{aligned} \tag{A.2.1}$$

These equations are not analytically solvable, so we will make the approximation that the γ_i's are constant and equal to their value at the electroweak scale. The approximate solutions are therefore

$$\begin{aligned} y_t(\mu) &= \sqrt{2}\frac{m_t}{v_u}\left(\frac{\mu}{M_Z}\right)^{\gamma_t}, \\ y_b(\mu) &= \sqrt{2}\frac{m_b}{v_d}\left(\frac{\mu}{M_Z}\right)^{\gamma_b}, \\ y_\tau(\mu) &= \sqrt{2}\frac{m_\tau}{v_d}\left(\frac{\mu}{M_Z}\right)^{\gamma_\tau}, \end{aligned} \tag{A.2.2}$$

with

$$\begin{aligned} \gamma_t &= \frac{1}{16\pi^2}\left(12\frac{m_t^2}{v_u^2} + 2\frac{m_b^2}{v_d^2} - \frac{16}{3}g_3(M_Z)^2 - 3g_2(M_Z)^2 - \frac{13}{15}g_1(M_Z)^2\right), \\ \gamma_b &= \frac{1}{16\pi^2}\left(12\frac{m_b^2}{v_u^2} + 2\frac{m_t^2}{v_d^2} + 2\frac{m_\tau}{v_d^2} - \frac{16}{3}g_3(M_Z)^2 - 3g_2(M_Z)^2 - \frac{7}{15}g_1(M_Z)^2\right), \\ \gamma_t &= \frac{1}{16\pi^2}\left(8\frac{m_\tau^2}{v_d^2} + 6\frac{m_b^2}{v_d^2} - 3g_2(M_Z)^2 - \frac{9}{5}g_1(M_Z)^2\right). \end{aligned} \tag{A.2.3}$$

A.3 Gaugino Masses

The RGEs for the gauginos are very similar to the gauge couplings, and can therefore be solved analytically at 1-loop. The β-functions are

$$\beta_{M_a} = 16\pi^2\frac{dM_a}{dt} = 2b_a g_a^2 M_a, \tag{A.3.1}$$

and the solution can be expressed in terms of the gauge couplings as

$$\frac{M_a(\mu)}{M_a(M_{\rm GUT})} = \frac{g_a^2(\mu)}{g_a^2(M_{\rm GUT})}. \tag{A.3.2}$$

A.4 Trilinear Couplings

As for the Yukawa couplings, we only consider the 3rd generation trilinear couplings. Their RGEs are:

$$\begin{aligned} \frac{1}{16\pi^2}\beta_{A_t} &= \frac{dA_t}{dt} = \frac{1}{16\pi^2}\left(12y_t^2A_t + 2y_b^2A_b + \frac{32}{3}g_3^2M_3 + 6g_2^2M_2 + \frac{26}{15}g_1^2M_1\right), \\ \frac{1}{16\pi^2}\beta_{A_b} &= \frac{dA_b}{dt} = \frac{1}{16\pi^2}\left(12y_b^2A_b + 2y_t^2A_t + 2y_\tau^2A_\tau + \frac{32}{3}g_3^2M_3 + 6g_2^2M_2 + \frac{14}{15}g_1^2M_1\right), \\ \frac{1}{16\pi^2}\beta_{A_\tau} &= \frac{dA_\tau}{dt} = \frac{1}{16\pi^2}\left(8y_\tau^2A_\tau + 6y_b^2A_b + 6g_2^2M_2 + \frac{18}{5}g_1^2M_1\right). \end{aligned} \tag{A.4.1}$$

The terms proportional to the Yukawa and trilinear couplings are not exactly solvable, thus we will make the approximation that A_i is roughly constant and equal to its value at the GUT scale, A_0, and we solve for the Yukawa part using the approximated solution obtained above. This gives

$$\begin{aligned}
A_t(\mu) &= A_0 - \frac{A_0}{8\pi^2}\left(6\delta_t + \delta_b)\right) - \left(\frac{16}{3}C_3^{(1)}(\mu) + 3C_2^{(1)}(\mu) + \frac{13}{15}C_1^{(1)}(\mu)\right) m_{1/2}, \\
A_b(\mu) &= A_0 - \frac{A_0}{8\pi^2}\left(\delta_t + 6\delta_b + \delta_\tau\right) - \left(\frac{16}{3}C_3^{(1)}(\mu) + 3C_2^{(1)}(\mu) + \frac{7}{15}C_1^{(1)}(\mu)\right) m_{1/2}, \\
A_\tau(\mu) &= A_0 - \frac{A_0}{8\pi^2}\left(4\delta_\tau + 3\delta_b\right) - \left(3C_2^{(1)}(\mu) + \frac{9}{5}C_1^{(1)}(\mu)\right) m_{1/2},
\end{aligned} \tag{A.4.2}$$

where $\delta_i = \frac{1}{2\gamma_i}(y_i^2(M_{\rm GUT}) - y_i^2(\mu))$ and

$$C_a^{(n)}(\mu) = \frac{1}{b_a}\left(1 - \frac{g_a^{2n}(\mu)}{g_a^{2n}(M_{\rm GUT})}\right). \tag{A.4.3}$$

A.5 Scalar Masses

The β-functions for the matter sfermion masses are

$$\begin{aligned}
\frac{1}{16\pi^2}\beta_{\mathbf{m}_Q^2} &= \frac{d}{dt}\mathbf{m}_Q^2 = \frac{1}{16\pi^2}\left(\mathbf{X}_u + \mathbf{X}_d - \frac{32}{3}g_3^2M_3^2 - 6g_2^2M_2^2 - \frac{2}{15}g_1^2M_1^2 + \frac{1}{5}g_1^2S\right), \\
\frac{1}{16\pi^2}\beta_{\mathbf{m}_u^2} &= \frac{d}{dt}\mathbf{m}_u^2 = \frac{1}{16\pi^2}\left(2\mathbf{X}_u - \frac{32}{3}g_3^2M_3^2 - \frac{32}{15}g_1^2M_1^2 - \frac{4}{5}g_1^2S\right), \\
\frac{1}{16\pi^2}\beta_{\mathbf{m}_d^2} &= \frac{d}{dt}\mathbf{m}_d^2 = \frac{1}{16\pi^2}\left(2\mathbf{X}_d - \frac{32}{3}g_3^2M_3^2 - \frac{8}{15}g_1^2M_1^2 + \frac{2}{3}g_1^2S\right), \\
\frac{1}{16\pi^2}\beta_{\mathbf{m}_L^2} &= \frac{d}{dt}\mathbf{m}_L^2 = \frac{1}{16\pi^2}\left(\mathbf{X}_e - 6g_2^2M_2^2 - \frac{6}{5}g_1^2M_1^2 - \frac{3}{5}g_1^2S\right), \\
\frac{1}{16\pi^2}\beta_{\mathbf{m}_e^2} &= \frac{d}{dt}\mathbf{m}_e^2 = \frac{1}{16\pi^2}\left(2\mathbf{X}_e - \frac{24}{5}g_1^2M_1^2 + \frac{6}{5}g_1S\right),
\end{aligned} \tag{A.5.1}$$

where $\mathbf{X}_i$ are 3×3 matrices proportional to the 3×3 Yukawa matrices and

$$S = m_{H_u}^2 - m_{H_d}^2 + \mathrm{Tr}\left(\mathbf{m}_Q^2 - \mathbf{m}_L^2 - 2\mathbf{m}_u^2 + \mathbf{m}_d^2 + \mathbf{m}_e^2\right). \tag{A.5.2}$$

Neglecting the Yukawa couplings for the first and second generations, the (3,3) components of the $\mathbf{X}_i$ can be written as

$$\begin{aligned}
X_t &= 2y_t^2\left(m_{H_u}^2 + m_{Q_3}^2 + m_{u_3}^2 + A_t^2\right), \\
X_b &= 2y_b^2\left(m_{H_d}^2 + m_{Q_3}^2 + m_{d_3}^2 + A_b^2\right), \\
X_\tau &= 2y_\tau^2\left(m_{H_d}^2 + m_{L_3}^2 + m_{e_3}^2 + A_\tau^2\right).
\end{aligned} \tag{A.5.3}$$

The gauge components are exactly solvable, as is the dependence on S. Hence, for the first two generations it is possible to arrive at an exact analytical solution at 1-loop:

$$\begin{aligned}
m^2_{Q_{1,2}} &= m^2_{16_F} + \left(1 + \frac{2}{5}C_1^{(1)}\right) m_D^2 + \left(\frac{8}{3}C_3^{(2)} + \frac{3}{2}C_2^{(2)} + \frac{1}{30}C_1^{(2)}\right) m^2_{1/2}, \\
m^2_{u_{1,2}} &= m^2_{16_F} + \left(1 - \frac{8}{5}C_1^{(1)}\right) m_D^2 + \left(\frac{8}{3}C_3^{(2)} + \frac{8}{15}C_1^{(2)}\right) m^2_{1/2}, \\
m^2_{d_{1,2}} &= m^2_{16_F} + \left(-3 + \frac{4}{5}C_1^{(1)}\right) m_D^2 + \left(\frac{8}{3}C_3^{(2)} + \frac{2}{15}C_1^{(2)}\right) m^2_{1/2}, \\
m^2_{L_{1,2}} &= m^2_{16_F} + \left(-3 - \frac{6}{5}C_1^{(1)}\right) m_D^2 + \left(\frac{3}{2}C_2^{(2)} + \frac{3}{10}C_1^{(2)}\right) m^2_{1/2}, \\
m^2_{e_{1,2}} &= m^2_{16_F} + \left(1 + \frac{12}{5}C_1^{(1)}\right) m_D^2 + \frac{6}{5}C_1^{(2)} m^2_{1/2},
\end{aligned} \tag{A.5.4}$$

where the dependence on μ is implied. The third sfermion generations have an extra dependence on the Yukawa and trilinear couplings via the terms X_t, X_b, X_τ. Their RGEs cannot be solved analytically. We approximate the dependence on the scalar masses and trilinear couplings by taking them constant with values given by the geometrical average of their values at the GUT scale and the SUSY scale. Using the approximate solution for the Yukawa couplings, this gives

$$\begin{aligned}
m^2_{Q_3} &= m^2_{Q_{1,2}} - \Delta_t - \Delta_b, \\
m^2_{\bar{u}_3} &= m^2_{\bar{u}_{1,2}} - 2\Delta_t, \\
m^2_{\bar{d}_3} &= m^2_{\bar{d}_{1,2}} - 2\Delta_b, \\
m^2_{L_3} &= m^2_{L_{1,2}} - \Delta_\tau, \\
m^2_{\bar{e}_3} &= m^2_{\bar{e}_{1,2}} - 2\Delta_\tau,
\end{aligned} \tag{A.5.5}$$

with

$$\begin{aligned}
\Delta_t &= \frac{1}{8\pi^2}\delta_t \left(m^2_{10_H} + 2|m_{16_F}|\tilde{M} + A_0 A_t(\tilde{M})\right), \\
\Delta_b &= \frac{1}{8\pi^2}\delta_b \left(m^2_{10_H} + 2|m_{16_F}|\tilde{M} + A_0 A_b(\tilde{M})\right), \\
\Delta_\tau &= \frac{1}{8\pi^2}\delta_\tau \left(m^2_{10_H} + 2|m_{16_F}|\tilde{M} + A_0 A_\tau(\tilde{M})\right).
\end{aligned} \tag{A.5.6}$$

Finally, the Higgs doublet soft masses have similar RGEs to the other scalars,

$$\begin{aligned}
\frac{1}{16\pi^2}\beta_{m^2_{H_u}} &= \frac{d}{dt}m^2_{H_u} = \frac{1}{16\pi^2}\left(3X_t - 6g_2^2M_2^2 - \frac{6}{5}g_1^2M_1^2 + \frac{3}{5}g_1^2 S\right), \\
\frac{1}{16\pi^2}\beta_{m_{H_d}} &= \frac{d}{dt}m_{H_d} = \frac{1}{16\pi^2}\left(3X_b + X_\tau - 6g_2^2M_2^2 - \frac{6}{5}g_1^2M_1^2 - \frac{3}{5}g_1^2 S\right),
\end{aligned} \tag{A.5.7}$$

and can be solved using the same approximation yielding

$$m_{H_u}^2 = m_{10_H}^2 + \left(-2 + \frac{6}{5}C_1^{(1)}\right) m_D^2 + \left(\frac{3}{2}C_2^{(2)} + \frac{3}{10}C_1^{(2)}\right) m_{1/2}^2 - 3\Delta_t,$$
$$m_{H_d}^2 = m_{10_H}^2 + \left(2 - \frac{6}{5}C_1^{(1)}\right) m_D^2 + \left(\frac{3}{2}C_2^{(2)} + \frac{3}{10}C_1^{(2)}\right) m_{1/2}^2 - 3\Delta_b - \Delta_\tau. \quad \text{(A.5.8)}$$

A.6 μ_H and B Terms

Both μ_H and B can be fixed at the electroweak scale by requiring successful electroweak symmetry breaking. Therefore we will use the electroweak scale (M_Z) as the reference point to solve the RGEs. The RGEs are

$$\frac{1}{16\pi^2}\beta_{\mu_H} = \frac{d\mu_H}{dt} = \frac{\mu_H}{16\pi^2}\left(3y_t^2 + 3y_b^2 + y_\tau^2 - 3g_2^2 - \frac{3}{5}g_1^2\right),$$
$$\frac{1}{16\pi^2}\beta_B = \frac{dB}{dt} = \frac{1}{16\pi^2}\left(3A_t y_t^2 + 6A_b y_b^2 + 2A_\tau y_\tau^2 + 6g_2^2 M_2 + \frac{6}{5}g_1^2 M_1\right). \quad \text{(A.6.1)}$$

The solution is calculated using the analogous approximations we used for the Yukawa couplings and the trilinear terms, respectively,

$$\mu_H(\mu) = \mu_H(M_Z)\left(\frac{\mu}{M_Z}\right)^{\gamma_{\mu_H}},$$
$$B(\mu) = B(M_Z) - \frac{A_0}{8\pi^2}(6\delta_t' + 6\delta_b' + \delta_\tau') - \left(3C'^{(1)}_2 - \frac{3}{5}C'^{(1)}_1\right) m_{1/2}, \quad \text{(A.6.2)}$$

where δ_i' and $C'^{(1)}_a$ are the same as δ_i and $C_a^{(1)}$ defined before but with M_Z as a reference scale instead of $M_{\rm GUT}$, and

$$\gamma_{\mu_H} = \frac{1}{16\pi^2}\left(6\frac{m_t^2}{v_u^2} + 6\frac{m_b^2}{v_d^2} + 2\frac{m_\tau^2}{v_d^2} - 3g_2(M_Z)^2 - \frac{3}{5}g_1(M_Z)^2\right). \quad \text{(A.6.3)}$$

The values of μ_H and B at the EW scale are given at 1-loop by ($t_\beta \equiv \tan\beta$) [184]

$$\mu_{H,\rm tree}^2 = -\frac{m_{H_d}^2}{1-t_\beta^2} - \frac{m_{H_u}^2}{1-t_\beta^{-2}} - \frac{1}{8}(g_2^2 + \frac{3}{5}g_1^2)(v_d^2 + v_u^2),$$
$$B_{\rm tree}^2 = \frac{1}{\mu_{H,tree}}\left(\frac{m_{H_d}^2 - m_{H_u}^2}{t_\beta - t_\beta^{-1}} - \frac{1}{4}(g_2^2 + \tfrac{3}{5}g_1^2)v_u v_d\right),$$
$$\mu_H^2(M_Z) = \mu_{H,\rm tree}^2 - \frac{3y_t^2}{32\pi^2(1-t_\beta^2)}\frac{\mu_{H,\rm tree}(\mu_{H,\rm tree} - A_t)t_\beta}{m_{\tilde t_1}^2 - m_{\tilde t_2}^2}\left(f(m_{\tilde t_1}^2) - f(m_{\tilde t_2}^2)\right) + \frac{3y_t^2}{32\pi^2}\frac{t_\beta^2}{1-t_\beta^{-2}}$$
$$\times\left(f(m_{\tilde t_1}^2) + f(m_{\tilde t_2}^2) - 2f(m_t^2) + \frac{A_t(A_t - \mu_{H,\rm tree}t_\beta^{-1})}{m_{\tilde t_1}^2 - m_{\tilde t_2}^2}\left(f(m_{\tilde t_1}^2) - f(m_{\tilde t_2}^2)\right)\right), \quad \text{(A.6.4)}$$

with the stop mass eigenvalues $m_{\tilde{t}_{1,2}}$ and the function

$$f(x) = 2x\left(\log\frac{x}{M_{\text{SUSY}}^2} - 1\right). \tag{A.6.5}$$

A.7 Two-Loop Corrections

We employ two loop corrections only for the scalar masses, because for large m_D^2 and consequently large m_{16_F} their contribution can be sizable. The relevant 2-loop beta functions, in which we neglect the Yukawa couplings of the first two generations, are given by [185]

$$\begin{aligned}
\beta^{(2)}_{m_Q^2} =& -20(m_Q^2 + m_{H_u}^2 + m_u^2)y_u^4 - 20(m_Q^2 + m_{H_d}^2 + m_d^2)y_d^4 \\
&- 2(m_Q^2 + m_L^2 + 2m_{H_d}^2 + m_d^2 + m_e^2)y_d^2 y_e^2 \\
&- 40A_t^2 y_u^2 - 40A_b^2 y_d^2 - 2y_d^2 y_e^2 (A_b + A_\tau)^2 \\
&+ \frac{2}{5}g_1^2\left\{4(m_Q^2 + m_{H_u}^2 + m_u^2 + A_t^2 - (M_1 + M_1^*)A_t + 2|M_1|^2)y_u^2\right. \\
&\left.+ 2(m_Q^2 + m_{H_d}^2 + m_d^2 + A_b^2 - (M_1 + M_1^*)A_b + 2|M_1|^2)y_d^2\right\} \\
&- \frac{128}{3}g_3^4|M_3|^2 + 32g_3^2 g_2^2(|M_3|^2 + |M_2|^2 + \Re[M_2 M_3^*]) \\
&+ \frac{32}{45}g_3^2 g_1^2(|M_3|^2 + |M_1|^2 + \Re[M_1 M_3^*]) + 33g_2^4|M_2|^2 \\
&+ \frac{2}{5}g_2^2 g_1^2(|M_2|^2 + |M_1|^2 + \Re[M_1 M_2^*]) + \frac{199}{75}g_1^4|M_1|^2 + \frac{16}{3}g_3^2\sigma_3 \\
&+ 3g_2^2\sigma_2 + \frac{1}{15}g_1^2\sigma_1 + \frac{2}{5}g_1^2 S',
\end{aligned} \tag{A.7.1}$$

$$\begin{aligned}
\beta^{(2)}_{m_L^2} =& -12(m_L^2 + m_{H_d}^2 + m_e^2)y_e^4 \\
&- 6(m_Q^2 + m_L^2 + 2m_{H_d}^2 + m_d^2 + m_u^2)y_d^2 y_e^2 \\
&- 24A_\tau^2 y_e^4 - 6y_d^2 y_e^2 (A_b + A_\tau)^2 \\
&+ \frac{12}{5}g_1^2\left\{m_L^2 + m_{H_d}^2 + m_e^2 + A_\tau^2 - (M_1 + M_1^*)A_\tau + 2|M_1|^2\right\}y_e^2 \\
&+ 33g_2^4|M_2|^2 + \frac{18}{5}g_2^2 g_1^2(|M_2|^2 + |M_1|^2 + \Re[M_1 M_2^*]) + \frac{621}{25}g_1^4|M_1|^2 \\
&+ 3g_2^2\sigma_2 + \frac{3}{5}g_1^2\sigma_1 - \frac{6}{5}g_1^2 S',
\end{aligned} \tag{A.7.2}$$

$$\begin{aligned}\beta^{(2)}_{m_u^2} =& -32(m_u^2+m_{H_u}^2+m_Q^2)y_u^4\\ &-4(m_u^2+2m_Q^2+m_d^2+m_{H_u}^2+m_{H_d}^2)y_u^2y_d^2\\ &-64A_t^2y_u^4-4y_u^2y_d^2(A_t+A_b)^2\\ &+\left[12g_2^2-\frac{4}{5}g_1^2\right]\left\{m_u^2+m_Q^2+m_{H_u}^2+A_t^2\right\}y_u^2\\ &+12g_2^2\left\{2|M_2|^2-(M_2+M_2^*)A_t\right\}y_u^2-\frac{4}{5}\left\{2|M_1|^2-(M_1+M_1^*)A_t\right\}y_u^2\\ &-\frac{128}{3}g_3^4|M_3|^2+\frac{512}{45}g_3^2g_1^2(|M_3|^2+|M_1|^2+\Re[M_1M_3^*])+\frac{3424}{75}g_1^4|M_1|^2\\ &+\frac{16}{3}g_3^2\sigma_3+\frac{16}{15}g_1^2\sigma_1-\frac{8}{5}g_1^2S',\end{aligned} \tag{A.7.3}$$

$$\begin{aligned}\beta^{(2)}_{m_d^2} =& -32(m_d^2+m_{H_d}^2+m_Q^2)y_d^4\\ &-4(m_d^2+2m_Q^2+m_u^2+m_{H_u}^2+m_{H_d}^2)y_u^2y_d^2-8(m_L^2+m_e^2)y_d^2y_e^2\\ &-64A_b^2y_d^4-4y_d^2y_u^2(A_t+A_b)^2-4y_d^2y_e^2(A_b+A_\tau)^2\\ &+\left[12g_2^2+\frac{4}{5}g_1^2\right]\left\{m_d^2+m_{H_d}^2+m_Q^2+A_b^2\right\}y_d^2\\ &+12g_2^2\left\{2|M_2|^2-(M_2+M_2^*)A_b\right\}y_d^2+\frac{4}{5}g_1^2\left\{2|M_1|^2-(M_1+M_1^*)A_b\right\}y_d^2\\ &-\frac{128}{3}g_3^4|M_3|^2+\frac{128}{45}g_3^2g_1^2(|M_3|^2+|M_1|^2+\Re[M_1M_3^*])+\frac{808}{75}g_1^4|M_1|^2\\ &+\frac{16}{3}g_3^2\sigma_3+\frac{4}{15}g_1^2\sigma_1+\frac{4}{5}g_1^2S',\end{aligned} \tag{A.7.4}$$

$$\begin{aligned}\beta^{(2)}_{m_e^2} =& -16(m_e^2+m_{H_d}^2+m_L^2)y_e^2-12(m_e^2+m_L^2+m_d^2+2m_{H_d}^2)y_d^2y_e^2\\ &-32A_\tau y_e^4-4y_e^2y_d^2(A_\tau+A_d)^2+(12g_2^2+\frac{12}{5}g_1^2)\left\{m_e^2+m_L^2+m_{H_d}^2+A_\tau^2\right\}y_e^2\\ &+12g_2^2\left\{2|M_2|^2-(M_2+M_2^*)A_\tau\right\}y_e^2-\frac{12}{5}\left\{2|M_1|^2-(M_1+M_1^*)A_\tau\right\}y_e^2\\ &+\frac{2808}{25}g1_4|M_1|^2+\frac{12}{5}g_1^2\sigma_1+\frac{12}{5}g_1^2S',\end{aligned} \tag{A.7.5}$$

$$\begin{aligned}\beta^{(2)}_{m_{H_u}^2} =& -36(m_{H_u}^2+m_Q^2+m_u^2)y_u^4-6(m_{H_u}^2+m_{H_d}^2+2m_Q^2+m_u^2+m_d^2)y_u^2y_d^2\\ &-72A_t^2y_u^4-6y_u^2y_d^2(A_u+A_d)^2+\left[32g_3^2+\frac{8}{5}g_1^2\right]\left\{m_{H_u}^2+m_Q^2+m_u^2+A_t^2\right\}y_u^2\\ &+32g_3^2\left\{2|M_3|^2-(M_3+M_3^*)A_t\right\}y_u^2+\frac{8}{5}g_1^2\left\{2|M_1|^2-(M_1+M_1^*)A_t\right\}y_u^2\\ &+33g_2^4|M_2|^2+\frac{18}{5}g_2^2g_1^2(|M_2|^2+|M_1|^2+\Re[M_1M_2^*])+\frac{621}{25}g_1^4|M_1|^2\\ &+3g_2^2\sigma_2+\frac{3}{5}g_1^2\sigma_1-+\frac{6}{5}g_1^2S',\end{aligned} \tag{A.7.6}$$

$$
\begin{aligned}
\beta^{(2)}_{m^2_{H_d}} =& -36(m^2_{H_d}+m^2_Q+m^2_d)y^4_d - 6(m^2_{H_u}+m^2_{H_d}+2m^2_Q+m^2_u+m^2_d)y^2_u y^2_d \\
&- 12(m^2_{H_d}+m^2_L+m^2_e)y^4_e - 72A^2_b y^4_d - 6y^2_u y^2_d (A_t+A_b)^2 - 24A^2_\tau y^4_e \\
&+ \left[33g^2_3 - \frac{4}{5}g^2_1\right]\left\{m^2_{H_d}+m^2_Q+m^2_d+A^2_b\right\}y^2_d \\
&+ 32g^2_3\left\{2|M_3|^2-(M_3+M^*_3)A^2_b\right\}y^2_d - \frac{4}{5}g^2_1\left\{2|M_1|^2-(M_1+M^*_1)A^2_b\right\}y^2_d \\
&+ \frac{12}{5}g^2_1\left\{m^2_{H_d}+m^2_L+m^2_e+A^2_\tau+2|M_1|^2-(M_1+M^*_1)A_\tau\right\}y^2_e \\
&+ 33g^4_2|M_2|^2 + \frac{18}{5}g^2_2g^2_1(|M_2|^2+|M_1|^2+\Re[M_1M^*_2]) + \frac{621}{25}g^4_1|M_1|^2 \\
&+ 3g^2_2\sigma_2 + \frac{3}{5}g^2_1\sigma_1 - \frac{6}{5}g^2_1 S'. \qquad \text{(A.7.7)}
\end{aligned}
$$

In the above equations, the following definitions apply:

$$
\begin{aligned}
S' =& -(3m^2_{H_u}+m^2_Q-4m^2_u)y^2_u + (3m^2_{H_d}-m^2_Q-2m^2_d)y^2_d + (m^2_{H_d}+m^2_L-m^2_e)y^2_e \\
&+ \left[\frac{3}{2}g^2_2+\frac{3}{10}g^2_1\right]\left\{m^2_{H_u}-m^2_{H_d}+\mathrm{Tr}(m^2_L)\right\} + \left[\frac{8}{3}g^2_3+\frac{3}{2}g^2_2+\frac{1}{30}g^2_1\right]\mathrm{Tr}(m^2_Q) \\
&- \left[\frac{16}{3}g^2_3+\frac{16}{15}g^2_1\right]\mathrm{Tr}(m^2_u) + \left[\frac{8}{3}g^2_3+\frac{2}{15}g^2_1\right]\mathrm{Tr}(m^2_d) + \frac{6}{5}g^2_1\mathrm{Tr}(m^2_e), \\
\sigma_1 =& \frac{1}{5}g^2_1\left\{3(m^2_{H_u}+m^2_{H_d}) + \mathrm{Tr}(m^2_Q+3m^2_L+8m^2_u+2m^2_d+6m^2_e)\right\}, \\
\sigma_2 =& g^2_2\left\{m^2_{H_u}+m^2_{H_d}+\mathrm{Tr}(3m^2_Q+m^2_L)\right\}, \\
\sigma_3 =& g^2_3\mathrm{Tr}(2m^2_Q+m^2_u+m^2_d). \qquad \text{(A.7.8)}
\end{aligned}
$$

The approximate solutions of this second loop correction are obtained by taking the value of the beta functions as constant and equal to the values at the GUT scale, using the 1-loop solutions, and integrating over scales,

$$
m^2_{i,\text{2-loop}} = m^2_{i,\text{1-loop}} - \frac{1}{(16\pi^2)^2}\beta^{(2)}_{m^2_{i,\text{1-loop}}}(M_{\text{GUT}})\log\frac{M_{\text{GUT}}}{M_{\text{SUSY}}}. \qquad \text{(A.7.9)}
$$

Bibliography

[1] S. Glashow, Nucl. Phys. **22** (1961).

[2] S. Weinberg, Phys. Rev. Lett. **19** (1967).

[3] A. Salam, Conf. Proc. C **680519** (1968).

[4] Particle Data Group, K. A. Olive *et al.*, Chin. Phys. **C38**, 090001 (2014).

[5] ATLAS, G. Aad *et al.*, Phys.Lett. **B716**, 1 (2012), [1207.7214].

[6] CMS, S. Chatrchyan *et al.*, Phys.Lett. **B716**, 30 (2012), [1207.7235].

[7] H. Georgi and S. L. Glashow, Phys. Rev. Lett. **32** (1974).

[8] R. N. Mohapatra and G. Senjanovic, Phys.Rev.Lett. **44**, 912 (1980).

[9] M. Gell-Mann, P. Ramond and R. Slansky, Conf. Proc. **C790927**, 315 (1979), [1306.4669].

[10] G. 't Hooft, Nucl. Phys. **B79**, 276 (1974).

[11] J. Wess and B. Zumino, Nucl.Phys. **B70**, 39 (1974).

[12] S. Weinberg, Phys.Rev. **D13**, 974 (1976).

[13] J. R. Ellis, S. Kelley and D. V. Nanopoulos, Phys.Lett. **B260**, 131 (1991).

[14] ATLAS, G. Aad *et al.*, JHEP **1409**, 176 (2014), [1405.7875].

[15] CMS, V. Khachatryan *et al.*, JHEP **1505**, 078 (2015), [1502.04358].

[16] Planck, P. Ade *et al.*, Astron.Astrophys. **571**, A22 (2014), [1303.5082].

[17] Planck, P. A. R. Ade *et al.*, [1502.02114].

[18] F. F. Deppisch, N. Desai and T. E. Gonzalo, Front. Phys. **2**, 00027 (2014), [1403.2312].

[19] J. Ellis, T. E. Gonzalo, J. Harz and W.-C. Huang, JCAP **1503**, 039 (2015), [1412.1460].

[20] M. E. Peskin and D. V. Schroeder, *An Introduction to quantum field theory* (Reading, USA: Addison-Wesley (1995) 842 p, 1995).

[21] P. Dirac, Proc.Roy.Soc.Lond. **A113**, 621 (1927).

[22] C.-N. Yang and R. L. Mills, Phys.Rev. **96**, 191 (1954).

[23] Y. Nambu, Phys.Rev. **117**, 648 (1960).

[24] J. Goldstone, Nuovo Cim. **19**, 154 (1961).

[25] P. W. Higgs, Phys.Lett. **12**, 132 (1964).
[26] P. W. Higgs, Phys.Rev.Lett. **13**, 508 (1964).
[27] F. Englert and R. Brout, Phys.Rev.Lett. **13**, 321 (1964).
[28] E. Noether, Gott. Nachr. **1918**, 235 (1918), [physics/0503066], [Transp. Theory Statist. Phys.1,186(1971)].
[29] E. Fermi, Nuovo Cim. **11**, 1 (1934).
[30] S. Glashow, J. Iliopoulos and L. Maiani, Phys.Rev. **D2**, 1285 (1970).
[31] C. Wu, E. Ambler, R. Hayward, D. Hoppes and R. Hudson, Phys.Rev. **105**, 1413 (1957).
[32] N. Cabibbo, Phys.Rev.Lett. **10**, 531 (1963).
[33] M. Kobayashi and T. Maskawa, Prog.Theor.Phys. **49**, 652 (1973).
[34] J. Christenson, J. Cronin, V. Fitch and R. Turlay, Phys.Rev.Lett. **13**, 138 (1964).
[35] SLAC-SP-017, J. Augustin *et al.*, Phys.Rev.Lett. **33**, 1406 (1974).
[36] E598, J. Aubert *et al.*, Phys.Rev.Lett. **33**, 1404 (1974).
[37] PLUTO, C. Berger *et al.*, Phys.Lett. **B82**, 449 (1979).
[38] PLUTO, C. Berger *et al.*, Z.Phys. **C8**, 101 (1981).
[39] UA1, G. Arnison *et al.*, Phys.Lett. **B126**, 398 (1983).
[40] UA1, G. Arnison *et al.*, Phys.Lett. **B122**, 103 (1983).
[41] UA2, P. Bagnaia *et al.*, Phys.Lett. **B129**, 130 (1983).
[42] UA2, M. Banner *et al.*, Phys.Lett. **B122**, 476 (1983).
[43] CDF, F. Abe *et al.*, Phys.Rev.Lett. **74**, 2626 (1995), [hep-ex/9503002].
[44] D0, S. Abachi *et al.*, Phys.Rev.Lett. **74**, 2632 (1995), [hep-ex/9503003].
[45] E. Gildener, Phys.Rev. **D14**, 1667 (1976).
[46] L. Susskind, Phys.Rev. **D20**, 2619 (1979).
[47] Super-Kamiokande, Y. Fukuda *et al.*, Phys.Rev.Lett. **81**, 1562 (1998), [hep-ex/9807003].
[48] SNO, Q. Ahmad *et al.*, Phys.Rev.Lett. **87**, 071301 (2001), [nucl-ex/0106015].
[49] RENO, J. Ahn *et al.*, Phys.Rev.Lett. **108**, 191802 (2012), [1204.0626].
[50] Planck, P. Ade *et al.*, Astron.Astrophys. **571**, A16 (2014), [1303.5076].
[51] Planck, P. A. R. Ade *et al.*, [1502.01589].
[52] Muon g-2, G. Bennett *et al.*, Phys.Rev. **D73**, 072003 (2006), [hep-ex/0602035].
[53] CMS, LHCb, V. Khachatryan *et al.*, Nature (2015), [1411.4413].
[54] XENON100, E. Aprile *et al.*, Phys.Rev.Lett. **109**, 181301 (2012), [1207.5988].
[55] LUX, D. Akerib *et al.*, Phys.Rev.Lett. **112**, 091303 (2014), [1310.8214].
[56] CoGeNT, C. Aalseth *et al.*, Phys.Rev. **D88**, 012002 (2013), [1208.5737].
[57] Super-Kamiokande, T. Tanaka *et al.*, Astrophys.J. **742**, 78 (2011), [1108.3384].

[58] IceCube, R. Abbasi *et al.*, Phys.Rev. **D85**, 042002 (2012), [1112.1840].
[59] IceCube, M. Aartsen *et al.*, Phys.Rev.Lett. **110**, 131302 (2013), [1212.4097].
[60] R. Peccei and H. R. Quinn, Phys.Rev. **D16**, 1791 (1977).
[61] R. Peccei and H. R. Quinn, Phys.Rev.Lett. **38**, 1440 (1977).
[62] S. Weinberg, Phys.Rev.Lett. **40**, 223 (1978).
[63] F. Wilczek, Phys.Rev.Lett. **40**, 279 (1978).
[64] A. Kusenko, Phys.Rept. **481**, 1 (2009), [0906.2968].
[65] H. Goldberg, Phys.Rev.Lett. **50**, 1419 (1983).
[66] J. R. Ellis, J. Hagelin, D. V. Nanopoulos, K. A. Olive and M. Srednicki, Nucl.Phys. **B238**, 453 (1984).
[67] A. Sakharov, Pisma Zh.Eksp.Teor.Fiz. **5**, 32 (1967).
[68] Supernova Search Team, A. G. Riess *et al.*, Astron.J. **116**, 1009 (1998), [astro-ph/9805201].
[69] Supernova Cosmology Project, S. Perlmutter *et al.*, Astrophys.J. **517**, 565 (1999), [astro-ph/9812133].
[70] D. Baumann, 0907.5424.
[71] H. Fritzsch and P. Minkowski, Annals Phys. **93** (1975).
[72] H. Georgi, AIP Conf.Proc. **23**, 575 (1975).
[73] A. De Rújula, H. Georgi and S. Glashow, Phys.Rev.Lett. **45**, 413 (1980).
[74] S. M. Barr, Phys.Lett. **B112**, 219 (1982).
[75] J. Derendinger, J. E. Kim and D. V. Nanopoulos, Phys.Lett. **B139**, 170 (1984).
[76] I. Antoniadis, J. R. Ellis, J. Hagelin and D. V. Nanopoulos, Phys.Lett. **B194**, 231 (1987).
[77] J. R. Ellis, J. Hagelin, S. Kelley and D. V. Nanopoulos, Nucl.Phys. **B311**, 1 (1988).
[78] J. Pati and A. Salam, Phys. Rev. D **10** (1974).
[79] R. Mohapatra and J. C. Pati, Phys.Rev. **D11**, 2558 (1975).
[80] R. N. Mohapatra and J. C. Pati, Phys.Rev. **D11**, 566 (1975).
[81] G. Senjanovic and R. N. Mohapatra, Phys.Rev. **D12**, 1502 (1975).
[82] G. Senjanovic, Nucl.Phys. **B153**, 334 (1979).
[83] F. Gursey, P. Ramond and P. Sikivie, Phys. Lett. B **60** (1976).
[84] E. Witten, Nucl. Phys. B **258** (1985).
[85] F. Buccella and G. Miele, Phys. Lett. B **189** (1987).
[86] S. L. Adler, Phys. Rev. **177** (1969).
[87] J. Bell and R. Jackiw, Nuovo Cim. **A60**, 47 (1969).
[88] L. Di Luzio, Aspects of symmetry breaking in Grand Unified Theories, 2011.

[89] H. Georgi and S. L. Glashow, Phys. Rev. D **6** (1972).
[90] G. Branco *et al.*, Phys.Rept. **516**, 1 (2012), [1106.0034].
[91] A. Giveon, L. J. Hall and U. Sarid, Phys.Lett. **B271**, 138 (1991).
[92] S. Dimopoulos and H. Georgi, Nucl.Phys. **B193**, 150 (1981).
[93] E. Witten, Phys.Lett. **B105**, 267 (1981).
[94] A. Masiero, D. V. Nanopoulos, K. Tamvakis and T. Yanagida, Phys.Lett. **B115**, 380 (1982).
[95] D. V. Nanopoulos and K. Tamvakis, Phys.Lett. **B113**, 151 (1982).
[96] S. Dimopoulos and H. Georgi, Phys.Lett. **B117**, 287 (1982).
[97] B. Grinstein, Nucl.Phys. **B206**, 387 (1982).
[98] K. Babu and C. F. Kolda, Phys.Lett. **B451**, 77 (1999), [hep-ph/9811308].
[99] A. Buras, J. R. Ellis, M. Gaillard and D. V. Nanopoulos, Nucl.Phys. **B135**, 66 (1978).
[100] H. Georgi and C. Jarlskog, Phys.Lett. **B86**, 297 (1979).
[101] J. R. Ellis and M. K. Gaillard, Phys.Lett. **B88**, 315 (1979).
[102] I. Dorsner and P. Fileviez Perez, Nucl.Phys. **B723**, 53 (2005), [hep-ph/0504276].
[103] B. Bajc and G. Senjanovic, JHEP **0708**, 014 (2007), [hep-ph/0612029].
[104] L. J. Hall and M. Suzuki, Nucl.Phys. **B231**, 419 (1984).
[105] Super-Kamiokande, H. Nishino *et al.*, Phys. Rev. **D85**, 112001 (2012), [1203.4030].
[106] P. Langacker, Phys.Rept. **72**, 185 (1981).
[107] P. Nath and P. Fileviez Perez, Phys.Rept. **441**, 191 (2007), [hep-ph/0601023].
[108] G. Senjanovic, AIP Conf.Proc. **1200**, 131 (2010), [0912.5375].
[109] N. Sakai and T. Yanagida, Nucl.Phys. **B197**, 533 (1982).
[110] D. Emmanuel-Costa and S. Wiesenfeldt, Nucl.Phys. **B661**, 62 (2003), [hep-ph/0302272].
[111] B. Bajc, P. Fileviez Perez and G. Senjanovic, Phys.Rev. **D66**, 075005 (2002), [hep-ph/0204311].
[112] W. Martens, L. Mihaila, J. Salomon and M. Steinhauser, Phys.Rev. **D82**, 095013 (2010), [1008.3070].
[113] J. Hisano, H. Murayama and T. Yanagida, Nucl.Phys. **B402**, 46 (1993), [hep-ph/9207279].
[114] B. Bajc, P. Fileviez Perez and G. Senjanovic, [hep-ph/0210374].
[115] B. Kyae and Q. Shafi, Phys.Lett. **B635**, 247 (2006), [hep-ph/0510105].
[116] B. Campbell, J. R. Ellis, J. Hagelin, D. V. Nanopoulos and R. Ticciati, Phys.Lett. **B198**, 200 (1987).

[117] I. Antoniadis, J. R. Ellis, J. Hagelin and D. V. Nanopoulos, Phys.Lett. **B205**, 459 (1988).

[118] I. Antoniadis, J. R. Ellis, J. S. Hagelin and D. V. Nanopoulos, Phys.Lett. **B208**, 209 (1988).

[119] I. Antoniadis, J. R. Ellis, J. Hagelin and D. V. Nanopoulos, Phys.Lett. **B231**, 65 (1989).

[120] C. S. Aulakh, B. Bajc, A. Melfo, A. Rasin and G. Senjanovic, Nucl. Phys. **B597**, 89 (2001), [hep-ph/0004031].

[121] S. Weinberg, Phys.Rev.Lett. **43**, 1566 (1979).

[122] P. Minkowski, Phys.Lett. **B67**, 421 (1977).

[123] S. Glashow, NATO Sci.Ser.B **59**, 687 (1980).

[124] M. Magg and C. Wetterich, Phys.Lett. **B94**, 61 (1980).

[125] J. Schechter and J. Valle, Phys.Rev. **D22**, 2227 (1980).

[126] R. N. Mohapatra and G. Senjanovic, Phys.Rev. **D23**, 165 (1981).

[127] R. Foot, H. Lew, X. He and G. C. Joshi, Z.Phys. **C44**, 441 (1989).

[128] R. N. Mohapatra and R. Marshak, Phys.Rev.Lett. **44**, 1316 (1980).

[129] C. Arbeláez, M. Hirsch, M. Malinský and J. C. Romo, Phys.Rev. **D89**, 035002 (2014), [1311.3228].

[130] N. Deshpande, J. Gunion, B. Kayser and F. I. Olness, Phys.Rev. **D44**, 837 (1991).

[131] C. S. Aulakh, K. Benakli and G. Senjanovic, Phys.Rev.Lett. **79**, 2188 (1997), [hep-ph/9703434].

[132] C. S. Aulakh, A. Melfo, A. Rasin and G. Senjanovic, Phys.Rev. **D58**, 115007 (1998), [hep-ph/9712551].

[133] P. Duka, J. Gluza and M. Zralek, Annals Phys. **280**, 336 (2000), [hep-ph/9910279].

[134] Y. Zhang, H. An, X. Ji and R. N. Mohapatra, Nucl.Phys. **B802**, 247 (2008), [0712.4218].

[135] B. Brahmachari, U. Sarkar and K. Sridhar, Phys.Lett. **B297**, 105 (1992).

[136] B. Brahmachari, E. Ma and U. Sarkar, Phys.Rev.Lett. **91**, 011801 (2003), [hep-ph/0301041].

[137] F. Siringo, Phys.Part.Nucl.Lett. **10**, 94 (2013), [1208.3599].

[138] M. Lindner and M. Weiser, Phys.Lett. **B383**, 405 (1996), [hep-ph/9605353].

[139] R. Mohapatra and J. Valle, Phys.Rev. **D34**, 1642 (1986).

[140] S. Das, F. Deppisch, O. Kittel and J. Valle, Phys.Rev. **D86**, 055006 (2012), [1206.0256].

[141] C.-H. Lee, P. Bhupal Dev and R. Mohapatra, Phys.Rev. **D88**, 093010 (2013),

[1309.0774].
[142] M. Duerr, P. Fileviez Perez and M. Lindner, Phys.Rev. **D88**, 051701 (2013), [1306.0568].
[143] F. F. Deppisch, P. S. B. Dev and A. Pilaftsis, New J. Phys. **17**, 075019 (2015), [1502.06541].
[144] CMS, V. Khachatryan *et al.*, Eur.Phys.J. **C74**, 3149 (2014), [1407.3683].
[145] F. F. Deppisch, T. E. Gonzalo, S. Patra, N. Sahu and U. Sarkar, Phys.Rev. **D90**, 053014 (2014), [1407.5384].
[146] F. F. Deppisch, T. E. Gonzalo, S. Patra, N. Sahu and U. Sarkar, Phys.Rev. **D91**, 015018 (2015), [1410.6427].
[147] W. Dekens, [1505.06599].
[148] ATLAS, G. Aad *et al.*, [1506.00962].
[149] Alp Deniz Özer, SO(10)-Grand Unification and Fermion Masses, 2005.
[150] R. N. Mohapatra and B. Sakita, Phys. Rev. **D21**, 1062 (1980).
[151] C. Aulakh and R. N. Mohapatra, Phys.Rev. **D28**, 217 (1983).
[152] C. S. Aulakh and A. Girdhar, Int.J.Mod.Phys. **A20**, 865 (2005), [hep-ph/0204097].
[153] G. Anastaze, J. Derendinger and F. Buccella, Z.Phys. **C20**, 269 (1983).
[154] T. Clark, T.-K. Kuo and N. Nakagawa, Phys.Lett. **B115**, 26 (1982).
[155] S. P. Martin, *A Supersymmetry Primer*, in *Perspectives on Supersymmetry II*, edited by G. L. Kane, pp. 1–153, 1997, [hep-ph/9709356].
[156] P. Ramond, Phys.Rev. **D3**, 2415 (1971).
[157] A. Neveu and J. Schwarz, Nucl.Phys. **B31**, 86 (1971).
[158] J.-L. Gervais and B. Sakita, Nucl.Phys. **B34**, 632 (1971).
[159] Y. Golfand and E. Likhtman, JETP Lett. **13**, 323 (1971).
[160] D. Volkov and V. Akulov, Phys.Lett. **B46**, 109 (1973).
[161] R. Haag, J. T. Lopuszanski and M. Sohnius, Nucl.Phys. **B88**, 257 (1975).
[162] S. R. Coleman and J. Mandula, Phys. Rev. **159** (1967).
[163] D. Bailin and A. Love, *Supersymmetric gauge field theory and string theory* (Bristol, UK: IOP (1994) 322 p. (Graduate student series in physics), 1994).
[164] S. Weinberg, Phys.Rev. **135**, B1049 (1964).
[165] M. T. Grisaru and H. Pendleton, Phys.Lett. **B67**, 323 (1977).
[166] A. H. Chamseddine, R. L. Arnowitt and P. Nath, Phys.Rev.Lett. **49**, 970 (1982).
[167] R. Barbieri, S. Ferrara and C. A. Savoy, Phys.Lett. **B119**, 343 (1982).
[168] L. E. Ibanez, Phys.Lett. **B118**, 73 (1982).
[169] L. J. Hall, J. D. Lykken and S. Weinberg, Phys.Rev. **D27**, 2359 (1983).

[170] J. R. Ellis, D. V. Nanopoulos and K. Tamvakis, Phys.Lett. **B121**, 123 (1983).
[171] L. Alvarez-Gaume, J. Polchinski and M. B. Wise, Nucl.Phys. **B221**, 495 (1983).
[172] H. P. Nilles, Phys. Rept. **110**, 1 (1984).
[173] M. Dine and W. Fischler, Phys.Lett. **B110**, 227 (1982).
[174] C. R. Nappi and B. A. Ovrut, Phys.Lett. **B113**, 175 (1982).
[175] L. Alvarez-Gaume, M. Claudson and M. B. Wise, Nucl.Phys. **B207**, 96 (1982).
[176] M. Dine and A. E. Nelson, Phys.Rev. **D48**, 1277 (1993), [hep-ph/9303230].
[177] M. Dine, A. E. Nelson and Y. Shirman, Phys.Rev. **D51**, 1362 (1995), [hep-ph/9408384].
[178] M. Dine, A. E. Nelson, Y. Nir and Y. Shirman, Phys.Rev. **D53**, 2658 (1996), [hep-ph/9507378].
[179] L. Randall and R. Sundrum, Nucl.Phys. **B557**, 79 (1999), [hep-th/9810155].
[180] G. F. Giudice, M. A. Luty, H. Murayama and R. Rattazzi, JHEP **9812**, 027 (1998), [hep-ph/9810442].
[181] H. K. Dreiner, Adv.Ser.Direct.High Energy Phys. **21**, 565 (2010), [hep-ph/9707435].
[182] L. E. Ibanez and G. G. Ross, Phys.Lett. **B110**, 215 (1982).
[183] S. Heinemeyer, Int. J. Mod. Phys. **A21**, 2659 (2006), [hep-ph/0407244].
[184] M. Drees, R. Godbole and P. Roy, *Theory and phenomenology of sparticles: An account of four-dimensional N=1 supersymmetry in high energy physics* (Hackensack, USA: World Scientific (2004) 555 p, 2004).
[185] S. P. Martin and M. T. Vaughn, Phys. Rev. D **50** (1994), [hep-ph/9311340v4].
[186] O. Buchmueller *et al.*, Eur.Phys.J. **C72**, 2243 (2012), [1207.7315].
[187] O. Buchmueller *et al.*, Eur.Phys.J. **C74**, 2922 (2014), [1312.5250].
[188] O. Buchmueller *et al.*, Eur.Phys.J. **C74**, 3212 (2014), [1408.4060].
[189] K. de Vries *et al.*, 1504.03260.
[190] A. G. Cohen, D. Kaplan and A. Nelson, Phys.Lett. **B388**, 588 (1996), [hep-ph/9607394].
[191] J. L. Feng and K. T. Matchev, Phys.Rev. **D63**, 095003 (2001), [hep-ph/0011356].
[192] S. P. Martin, Phys.Rev. **D75**, 115005 (2007), [hep-ph/0703097].
[193] C. Csaki, Y. Grossman and B. Heidenreich, Phys.Rev. **D85**, 095009 (2012), [1111.1239].
[194] ATLAS Collaboration, ATLAS Supersymmetry (SUSY) Searches, 2015, https://twiki.cern.ch/twiki/bin/view/AtlasPublic/SupersymmetryPublicResults.
[195] CMS Collaboration, CMS Supersymmetry Physics Results, 2015,

https://twiki.cern.ch/twiki/bin/view/CMSPublic/PhysicsResultsSUS.
[196] N. Bohr, Phil.Mag. **26**, 1 (1913).
[197] B. Hall, *Lie Groups, Lie Algebras, and Representations* (Springer, 2003).
[198] H. Osborn, Symmetries and groups, Lecture notes, Cambridge University, 2008.
[199] H. Georgi, *Lie Algebras in Particle Physics* (Perseus Books, 1999).
[200] E. Cartan, *Sur la structure des groupes de transformations finis et continus* (Nony, 1894).
[201] J. Gutowski, Classification of semi-simple algebras, Lecture notes, Cambridge University, 2007.
[202] E. B. Dynkin, Uspehi Matem. Nauk, (N.S.) (in Russian) **2**, 59 (1947).
[203] R. Slansky, Phys.Rept. **79**, 1 (1981).
[204] R. Feger and T. W. Kephart, Comput.Phys.Commun. **192**, 166 (2015), [1206.6379].
[205] E. Moore, Bulletin of the American Mathematical Society **26**, 394.
[206] R. Penrose, Proc. Cambridge Phil. Soc. **51**, 406 (1955).
[207] T. E. Gonzalo, (in preparation).
[208] T. Hahn, Computer Physics Communications **183**, 460 (2012), [1107.4379].
[209] R. M. Fonseca, Comput.Phys.Commun. **183**, 2298 (2012), [1106.5016].
[210] Standard ECMA-404: The JSON Data Interchange Format, 2013.
[211] F. F. Deppisch, T. E. Gonzalo and L. Graf, (in preparation).
[212] S. F. King, JHEP **08**, 130 (2014), [1406.7005].
[213] H. Georgi, Nucl. Phys. **B156**, 126 (1979).
[214] F. del Aguila and L. E. Ibanez, Nucl. Phys. **B177**, 60 (1981).
[215] L. Alvarez-Gaume and E. Witten, Nucl. Phys. **B234**, 269 (1984).
[216] E. Witten, Phys. Lett. **B117**, 324 (1982).
[217] D. J. Gross and R. Jackiw, Phys. Rev. D **6** (1972).
[218] R. M. Fonseca, M. Malinsky, W. Porod and F. Staub, Nucl. Phys. **B854**, 28 (2012), [1107.2670].
[219] J. R. Ellis, D. V. Nanopoulos and S. Rudaz, Nucl. Phys. **B202**, 43 (1982).
[220] Hyper-Kamiokande Proto-Collaboration, K. Abe *et al.*, PTEP **2015**, 053C02 (2015), [1502.05199].
[221] A. Leike, Phys. Rept. **317**, 143 (1999), [hep-ph/9805494].
[222] F. F. Deppisch, J. Harz and M. Hirsch, Phys. Rev. Lett. **112**, 221601 (2014), [1312.4447].
[223] A. D. Martin, W. J. Stirling, R. S. Thorne and G. Watt, Eur. Phys. J. **C63**, 189 (2009), [0901.0002].

[224] J. Brehmer, J. Hewett, J. Kopp, T. Rizzo and J. Tattersall, 1507.00013.
[225] G. Beall, M. Bander and A. Soni, Phys. Rev. Lett. **48**, 848 (1982).
[226] A. Maiezza, M. Nemevsek, F. Nesti and G. Senjanovic, Phys. Rev. **D82**, 055022 (2010), [1005.5160].
[227] S. Bertolini, A. Maiezza and F. Nesti, Phys. Rev. **D89**, 095028 (2014), [1403.7112].
[228] L. Calibbi, L. Ferretti, A. Romanino and R. Ziegler, Phys. Lett. **B672**, 152 (2009), [0812.0342].
[229] Daya Bay, F. P. An *et al.*, Phys. Rev. Lett. **108**, 171803 (2012), [1203.1669].
[230] BICEP2, P. A. R. Ade *et al.*, Phys. Rev. Lett. **112**, 241101 (2014), [1403.3985].
[231] BICEP2, Planck, P. Ade *et al.*, Phys. Rev. Lett. **114**, 101301 (2015), [1502.00612].
[232] C. F. Kolda and S. P. Martin, Phys. Rev. D **53** (1996), [hep-ph/9503445v2].
[233] J. R. Ellis, K. Enqvist, D. V. Nanopoulos and K. Tamvakis, Phys. Lett. **B155**, 381 (1985).
[234] S. P. Martin, Phys. Rev. D **79** (2009), [0903.3568v2].
[235] M. Badziak, Mod. Phys. Lett. **A27**, 1230020 (2012), [1205.6232].
[236] D. J. Miller, A. P. Morais and P. N. Pandita, Phys. Rev. **D87**, 015007 (2013), [1208.5906].
[237] ATLAS collaboration, CERN Report No. ATLAS-CONF-2013-047, 2013 (unpublished).
[238] CMS Collaboration, S. Chatrchyan *et al.*, 1402.4770.
[239] ATLAS Collaboration, CERN Report No. ATLAS-CONF-2013-024, ATLAS-CONF-2013-037, ATLAS-CONF-2013-048, ATLAS-CONF-2013-065, ATLAS-CONF-2013-068, 2013 (unpublished).
[240] CMS Collaboration, CERN Report No. CMS-PAS-SUS-13-008, 2013 (unpublished).
[241] ATLAS, G. Aad *et al.*, JHEP **1310**, 189 (2013), [1308.2631].
[242] CMS Collaboration, S. Chatrchyan *et al.*, Eur.Phys.J. **C73**, 2677 (2013), [1308.1586].
[243] CMS Collaboration, S. Chatrchyan *et al.*, Eur.Phys.J. **C73**, 2568 (2013), [1303.2985].
[244] ATLAS, G. Aad *et al.*, JHEP **05**, 071 (2014), [1403.5294].
[245] CMS, V. Khachatryan *et al.*, Eur. Phys. J. **C74**, 3036 (2014), [1405.7570].
[246] ATLAS Collaboration, CERN Report No. ATLAS-CONF-2013-028,ATLAS-CONF-2013-035, 2013 (unpublished).
[247] ATLAS Collaboration, CERN Report No. ATLAS-CONF-2013-049, 2013 (un-

published).
[248] CMS Collaboration, CERN Report No. CMS-PAS-SUS-13-006, 2013 (unpublished).
[249] CMS Collaboration, CERN Report No. CMS-PAS-SUS-13-017, 2013 (unpublished).
[250] ATLAS Collaboration, G. Aad *et al.*, JHEP **1302**, 095 (2013), [1211.6956].
[251] CERN Report No. ATLAS-CONF-2013-090, 2013 (unpublished).
[252] CMS Collaboration, S. Chatrchyan *et al.*, JHEP **1207**, 143 (2012), [1205.5736].
[253] CMS Collaboration, CERN Report No. CMS-PAS-HIG-13-021, 2013 (unpublished).
[254] T. Sjostrand, S. Mrenna and P. Z. Skands, JHEP **0605**, 026 (2006), [hep-ph/0603175].
[255] T. Sjostrand, S. Mrenna and P. Z. Skands, Comput.Phys.Commun. **178**, 852 (2008), [0710.3820].
[256] N. Desai and P. Z. Skands, Eur.Phys.J. **C72**, 2238 (2012), [1109.5852].
[257] J. Alwall, M.-P. Le, M. Lisanti and J. G. Wacker, Phys.Lett. **B666**, 34 (2008), [0803.0019].
[258] T. J. LeCompte and S. P. Martin, Phys.Rev. **D84**, 015004 (2011), [1105.4304].
[259] F. Brummer, S. Kraml, S. Kulkarni and C. Smith, [1402.4024].
[260] N. Arkani-Hamed and S. Dimopoulos, JHEP **0506**, 073 (2005), [hep-th/0405159].
[261] G. Giudice and A. Romanino, Nucl.Phys. **B699**, 65 (2004), [hep-ph/0406088].
[262] N. Arkani-Hamed, A. Gupta, D. E. Kaplan, N. Weiner and T. Zorawski, [1212.6971].
[263] A. Arvanitaki, N. Craig, S. Dimopoulos and G. Villadoro, JHEP **1302**, 126 (2013), [1210.0555].
[264] M. Endo, K. Hamaguchi, S. Iwamoto and T. Yoshinaga, JHEP **1401**, 123 (2014), [1303.4256].
[265] A. H. Guth, Phys. Rev. **D23**, 347 (1981).
[266] A. A. Starobinsky, Phys. Lett. **B91**, 99 (1980).
[267] A. D. Linde, Phys. Lett. **B108**, 389 (1982).
[268] A. Albrecht and P. J. Steinhardt, Phys. Rev. Lett. **48**, 1220 (1982).
[269] S. Weinberg, *Cosmology* (Oxford, UK: Oxford Univ. Pr. (2008) 593 p, 2008).
[270] J. Martin, C. Ringeval, R. Trotta and V. Vennin, JCAP **1403**, 039 (2014), [1312.3529].
[271] Planck, R. Adam *et al.*, 1409.5738.
[272] J. Martin, C. Ringeval and V. Vennin, Phys.Dark Univ. **5-6**, 75235 (2014),

[1303.3787].
[273] A. Friedmann, Z. Phys. **21**, 326 (1924), [Gen. Rel. Grav.31,2001(1999)].
[274] H. P. Robertson, Astrophys. J. **82**, 284 (1935).
[275] G. Lemaitre, Gen. Rel. Grav. **29**, 641 (1933), [Annales Soc. Sci. Brux. Ser. I Sci. Math. Astron. Phys. A53, 51 (1933)].
[276] A. G. Walker, Proc. London Math. Soc. **42**, 90 (1937).
[277] A. R. Liddle, P. Parsons and J. D. Barrow, Phys. Rev. **D50**, 7222 (1994), [astro-ph/9408015].
[278] A. D. Linde, Phys. Lett. **B259**, 38 (1991).
[279] A. R. Liddle and D. H. Lyth, Phys. Rept. **231**, 1 (1993), [astro-ph/9303019].
[280] A. D. Linde, Phys. Rev. **D49**, 748 (1994), [astro-ph/9307002].
[281] E. J. Copeland, A. R. Liddle, D. H. Lyth, E. D. Stewart and D. Wands, Phys. Rev. **D49**, 6410 (1994), [astro-ph/9401011].
[282] E. D. Stewart, Phys. Lett. **B345**, 414 (1995), [astro-ph/9407040].
[283] L. Randall, M. Soljacic and A. H. Guth, Nucl. Phys. **B472**, 377 (1996), [hep-ph/9512439].
[284] L. Randall, M. Soljacic and A. H. Guth, [hep-ph/9601296].
[285] J. Garcia-Bellido, A. D. Linde and D. Wands, Phys. Rev. **D54**, 6040 (1996), [astro-ph/9605094].
[286] D. H. Lyth, JCAP **1205**, 022 (2012), [1201.4312].
[287] A. H. Guth and E. I. Sfakianakis, [1210.8128].
[288] M. P. Hertzberg and F. Wilczek, [1407.6010].
[289] A. M. Polyakov, JETP Lett. **20**, 194 (1974), [Pisma Zh. Eksp. Teor. Fiz. 20, 430 (1974)].
[290] A. Brignole, L. E. Ibanez and C. Munoz, Adv. Ser. Direct. High Energy Phys. **21**, 244 (2010), [hep-ph/9707209].
[291] H. Murayama, H. Suzuki, T. Yanagida and J. Yokoyama, Phys. Rev. Lett. **70**, 1912 (1993).
[292] J. R. Ellis, M. Raidal and T. Yanagida, Phys. Lett. **B581**, 9 (2004), [hep-ph/0303242].
[293] S. Antusch, M. Bastero-Gil, S. F. King and Q. Shafi, Phys. Rev. **D71**, 083519 (2005), [hep-ph/0411298].
[294] C.-M. Lin and J. McDonald, Phys. Rev. **D74**, 063510 (2006), [hep-ph/0604245].
[295] F. Deppisch and A. Pilaftsis, JHEP **10**, 080 (2008), [0808.0490].
[296] S. Antusch *et al.*, JHEP **08**, 100 (2010), [1003.3233].
[297] S. Antusch, J. P. Baumann, V. F. Domcke and P. M. Kostka, JCAP **1010**,

006 (2010), [1007.0708].

[298] J. Ellis, M. Fairbairn and M. Sueiro, JCAP **1402**, 044 (2014), [1312.1353].

[299] H. Murayama, K. Nakayama, F. Takahashi and T. T. Yanagida, Phys. Lett. **B738**, 196 (2014), [1404.3857].

[300] J. Ellis, D. V. Nanopoulos and K. A. Olive, Phys. Rev. **D89**, 043502 (2014), [1310.4770].

[301] D. Croon, J. Ellis and N. E. Mavromatos, Phys.Lett. **B724**, 165 (2013), [1303.6253].